

Université de Montréal

**Diffusion de solutés dans des solutions
et gels de polymère étudiée par spectroscopie RMN**

par

Laurent Masaro

Département de chimie

Faculté des arts et des sciences

Thèse présentée à la Faculté des études supérieures
en vue de l'obtention du grade de
Philosophiæ Doctor (Ph.D.)
en chimie

Février, 1999

© Laurent Masaro, 1999



Université de Montréal

Faculté des études supérieures

Cette thèse intitulée:

**Diffusion de solutés dans des solutions
et gels de polymère étudiée par spectroscopie RMN**

présentée par:

Laurent Masaro

a été évaluée par un jury composé des personnes suivantes:

Professeur J. Prud'homme	Président Rapporteur
Professeur T. Ellis	Membre du Jury
Professeur J. Zhu	Directeur de recherche
Professeure M. Auger	Examinatrice externe
Professeur P. Carreau	Représentant du Doyen

Thèse acceptée le: 99.05.27

à Fabienne,
à mes Parents.

Sommaire

Afin de mieux comprendre les phénomènes de diffusion dans les solutions et gels de polymères, il est nécessaire de procéder à l'étude de la diffusion de petites molécules et macromolécules dans ces systèmes. Les mesures de diffusion peuvent être faites en utilisant la résonance magnétique nucléaire (RMN). La séquence RMN d'écho de spin à gradient de champ pulsé est très appropriée pour mesurer les coefficients d'auto-diffusion de solutés dans les réseaux polymères. Les données ainsi obtenues permettent de caractériser la diffusion par le biais de modèles théoriques. Les plus pertinents ont été testés.

L'étude de la diffusion de deux séries de solutés, ou diffusants, dans les solutions et gels d'alcool polyvinylique (PVA) par spectroscopie RMN a été menée. Une série de diffusants de taille croissante, variant de l'éthylène glycol au poly(éthylène glycol) (PEG) de masse molaire 10 000, a servi à analyser l'influence de la taille du soluté sur la diffusion. La diffusion diminue lorsque la taille du soluté augmente. Il en est de même avec la concentration en polymère. Les données expérimentales ont été testées avec le modèle décrit par Petit *et al.* Une bonne corrélation entre les données et la théorie a été observée. Une énergie d'activation de 21.1, 30.0, 36.5 et 39.0 kJ/mol a été obtenue pour le *tert*-butanol, l'éthylène glycol, le PEG-600 et le PEG-2000, respectivement. Les mêmes données expérimentales ont été utilisées pour vérifier la validité des modèles décrits par Mackie et Meares, Ogston *et al.*, Yasuda *et al.*, de Gennes, Phillies, et Amsden. Parmi ces modèles seuls ceux de Phillies et Amsden ont reproduit fidèlement les données expérimentales. Par ailleurs, une série de diffusants avec des groupes terminaux modifiés a été utilisée pour analyser l'importance de la géométrie du soluté sur la diffusion. En comparant deux diffusants dont les masses molaires sont voisines, nous avons constaté que le diffusant le plus volumineux restreignait plus la diffusion. L'utilisation de modèles théoriques

de diffusion a permis de montrer que les modèles de Phillis, Amsden et Petit *et al.* reproduisent fidèlement les données expérimentales. L'analyse des paramètres spécifiques de chacun des modèles a montré que seuls ceux définis par Petit *et al.* ont une signification physique.

L'influence de la matrice polymère a également été examinée en mesurant la diffusion du solvant et d'un soluté dans plusieurs systèmes polymères, à savoir des PVA avec des masses molaires et des taux d'hydrolyse différents, des hydroxypropyl méthyl celluloses (HPMC), le poly(*N,N*-diéthyl acrylamide) et le poly(*N*-isopropyl acrylamide). L'utilisation des modèles de diffusion de Yasuda *et al.*, Phillis et Amsden a permis de confirmer leurs limites. L'application du modèle de diffusion proposé par Petit *et al.* a montré que ce modèle est applicable pour de tels systèmes.

Le PVA est un polymère ayant de nombreux groupements hydroxyles qui peuvent former des ponts hydrogène avec des molécules comme l'éthylène glycol. Les techniques RMN peuvent être utilisées pour prouver l'existence des ces interactions. Le pontage hydrogène induit un nouveau déplacement chimique pour la molécule d'éthylène glycol liée au polymère, laquelle possède un coefficient d'auto-diffusion différent de la molécule d'éthylène glycol libre. De plus, les molécules d'éthylène glycol libres et liées possèdent des temps de relaxation spin-réseau et spin-spin différents. Une constante d'équilibre de $1.7 \times 10^3 \text{ M}^{-1}$ a pu être mesurée pour cette association.

Table des matières

Sommaire.....	iii
Liste des tableaux.....	xii
Liste des figures.....	xv
Liste des abréviations.....	xxi
Remerciements	xxiv
Partie I. Introduction générale	1
1. Diffusion et libération contrôlée	2
2. Les objectifs de cette étude	3
3. Présentation des travaux	5
4. Références	6
Chapitre 1. Physical models of diffusion for polymer solutions, gels and solids	7
1.1. Abstract	9
1.2. Introduction.....	11
1.2.1. Fickian diffusion	12
1.2.2. Non-Fickian diffusion	13
1.2.3. Self-diffusion and mutual diffusion coefficients	14
1.2.4. Diffusion in polymers.....	15
1.3. Theories and physical models of diffusion.....	16
1.3.1. Diffusion models based on obstruction effects.....	16
1.3.1.1. The Maxwell-Fricke model.....	16

1.3.1.2. The model of Mackie and Meares.....	20
1.3.1.3. The model of Ogston <i>et al.</i>	21
1.3.1.4. The hard sphere theory.....	22
1.3.1.5. Summary.....	24
1.3.2. Hydrodynamic theories.....	27
1.3.2.1. Cukier's model.....	27
1.3.2.2. The model of Altenberger <i>et al.</i>	30
1.3.2.3. Phillis' model.....	31
1.3.2.4. The reptation and reptation plus scaling models.....	37
1.3.2.5. The model of Gao and Fagerness.....	40
1.3.2.6. Summary.....	46
1.3.3. Diffusion models based on the free volume theory.....	48
1.3.3.1. Fujita's model.....	48
1.3.3.2. The model of Yasuda <i>et al.</i>	50
1.3.3.3. The model of Vrentas and Duda.....	52
1.3.3.4. The model of Peppas and Reinhart.....	56
1.3.3.5. Summary.....	59
1.3.4. Other physical models of diffusion.....	60
1.3.4.1. Arrhenius' theory.....	60
1.3.4.2. The modified Enskog theory.....	64
1.3.4.3. The model of Petit <i>et al.</i>	65
1.3.4.4. Amsden's model.....	71
1.3.4.5. Summary.....	73
1.4. Concluding remarks.....	73
1.5. Symbols and abbreviations.....	74
1.6. Acknowledgment.....	75
1.7. References.....	76

Chapitre 2. Pulsed field gradient NMR spectroscopy in the study of self-diffusion in polymer systems.....	86
--	-----------

2.1. Abstract	87
2.2. Introduction	87
2.3. The PGSE NMR technique	88
2.4. Calibration of the gradient strength	92
2.5. Temperature calibration	95
2.6. The study of diffusion in polymer systems	96
2.7. <i>J</i> -modulation effects	97
2.8. Spin-spin relaxation time and eddy currents problems	97
2.9. Signal overlapping	100
2.10. Non-homogenous or anomalous diffusion	102
2.11. Restricted diffusion	105
2.12. Concluding remarks	106
2.13. Acknowledgment	106
2.13. References	106
Partie II. L'influence de la taille du soluté sur la diffusion.....	110
Chapitre 3. Self-diffusion of oligo- and poly(ethylene glycol)s in poly(vinyl alcohol) aqueous solutions as studied by pulsed gradient NMR spectroscopy	111
3.1. Abstract	112
3.2. Introduction	112
3.3. Experimental	115
3.4. Results and discussion	117
3.4.1. Effect of polymer concentration	119
3.4.2. Effect of molecular size of the diffusant	120
3.4.3. Effect of temperature	124
3.4.4. Correspondence with the new diffusion model	124
3.5. Concluding remarks	128
3.6. Acknowledgment	128

3.7. References and notes.....	128
Chapitre 4. Study of the self-diffusion of poly(ethylene glycol)s in poly(vinyl alcohol) aqueous systems	131
4.1. Abstract.....	132
4.2. Introduction.....	132
4.3. Theoretical models of diffusion	133
4.3.1. Models based on obstruction effect.....	133
4.3.2. Free volume models.....	134
4.3.3. Hydrodynamic models	135
4.3.4. Combined theory	136
4.4. Experimental.....	137
4.5. Results and discussion.....	138
4.5.1. The obstruction models	138
4.5.2. The free volume model	141
4.5.3. The hydrodynamic models	141
4.5.4. Amsden's model	144
4.6. Concluding remarks	149
4.7. Acknowledgment	149
4.8. References	150
Partie III. L'influence de la géométrie du soluté sur la diffusion	152
Chapitre 5. Self-diffusion of end-capped(ethylene glycol)s in poly(vinyl alcohol)aqueous solutions and gels	153
5.1. Abstract.....	154
5.2. Introduction.....	154
5.3. Experimental section.....	155
5.3.1. Materials	155
5.3.2. NMR measurements	158

5.3.3. Rheological measurements.....	158
5.4. Results and discussion.....	158
5.4.1. The model of Petit <i>et al</i>	159
5.4.2. The model of Phillies	165
5.4.3. The model of Yasuda <i>et al</i>	169
5.4.4. The model of Mackie and Meares	170
5.4.5. The model of Ogston <i>et al</i>	171
5.4.6. The model of Amsden.....	174
5.5. Concluding remarks	176
5.6. Acknowledgment	177
5.7. References and notes.....	177
Partie IV. L'influence du réseau polymère sur la diffusion.....	180
Chapitre 6. Self-diffusion of water and poly(ethylene glycol) in solutions and gels of selected hydrophilic polymers	181
6.1. Abstract	182
6.2. Introduction.....	182
6.3. Theoretical background.....	183
6.4. Experimental section	185
6.4.1. Materials	185
6.4.2. Synthesis of polymers	186
6.4.3. Molecular weight determination.....	186
6.4.4. Pulsed-gradient spin-echo (PGSE) NMR Measurements.....	187
6.5. Results and discussion.....	187
6.5.1. Characterization of polymers	187
6.5.2. Analysis of the diffusion data with the model of Yasuda <i>et al</i>	190
6.5.3. Analysis of the diffusion data with the model of Phillies.	192
6.5.4. Analysis of the diffusion data with the model of Petit <i>et al</i>	196
6.6. Concluding remarks	202

6.7. Acknowledgments.....	204
6.8. References and notes.....	204
Partie V. L'influence des interactions soluté-polymère sur la diffusion.....	208
Chapitre 7. Interaction of ethylene glycol with poly(vinyl alcohol) in aqueous systems as studied by NMR spectroscopy.....	209
7.1. Abstract	210
7.2. Introduction.....	210
7.3. Experimental section	212
7.4. Results and discussion.....	213
7.4.1. Chemical shift (δ).....	213
7.4.2. PGSE NMR measurements.....	217
7.4.3. Measurements of NMR relaxation times (T_1 and T_2).....	223
7.5. Concluding remarks	225
7.6. Acknowledgment	225
7.7. References and notes.....	225
Partie VI. Conclusion générale	228
8.1. L'effet de la taille et de la géométrie du soluté.....	229
8.2. L'effet du réseau polymère.....	229
8.3. L'effet de la température.....	230
8.4. Les interactions dans les systèmes aqueux	230
8.5. Les modèles physique de diffusion.....	231
8.6. Travaux futurs	232
Partie VII. Annexe	234
Annexe A. Résultats expérimentaux.....	235

Annexe B. Autres articles publiés ou en préparation..... 255

Liste des tableaux

Table 1.1. Summary of the diffusion models based on obstruction effect	26
Table 1.2. List of the parameters found in the literature for the hydrodynamic equations in the form of $D = D_0 \exp(-\alpha c^v)$	29
Table 1.3. Dependence of parameter α on the hydrodynamic radius of the diffusant obtained in the literature for Phillies' diffusion model.....	35
Table 1.4. Experimental values obtained for the dependence on the molecular weight (M) of the diffusant and polymer concentration (c) in de Gennes' reptation models.....	41
Table 1.5. Summary of the diffusion models based on hydrodynamic theories.....	47
Table 1.6. Summary of the diffusion models based on the free volume theories	61
Table 1.7. Example of activation energy (E_a) studies based on Arrhenius equation found in the literature	63
Table 2.1. List of standards with known self-diffusion coefficients that can be used for the gradient strength calibration	94

Table 2.2. Example of chemical shift difference between the CH ₂ and OH groups for ethylene glycol and the CH ₃ and OH groups for methanol at 29, 30 and 31 °C	96
Table 3.1. Number- and weight-average molecular weights (M_n and M_w) of OEG and PEG samples used in the diffusion studies as determined by SEC.....	116
Table 3.2. Hydrodynamic radii, self-diffusion coefficients and fitting parameters $k\beta^2$ and ν obtained for the diffusants in aqueous PVA systems	121
Table 4.1. Hydrodynamic radii, measured self-diffusion coefficients and fitting parameters D_0 , α and ν obtained for the diffusants in aqueous PVA systems	139
Table 5.1. The structure and molecular weight of the end-capped oligo-(ethylene glycol)s	156
Table 5.2. Measured D_0 values, calculated hydrodynamic radius and D_0 , α and ν obtained as free parameters from fits to eq 5.4	162
Table 5.3. Measured D_0 values and the D_0 , $k\beta^2$ and ν values obtained as free parameters from fits to eq 5.6 and the D_0 and $k\beta^2$ values obtained from fits to eq 5.6 with ν fixed to 0.58.....	166
Table 5.4. The parameters D_0 , r_f and k_1 obtained by fitting the diffusion data to eq 5.8 while fixing r_s to the R_h values reported in Table 5.2.....	176
Table 6.1. The physical characteristics of the polymer used	190
Table 6.2. D_0 and B_s/f_w as free parameters obtained from the fits to eq 6.4 with the experimental data.....	192

Table 6.3. D_0 , α and ν as free parameters obtained from the fits to eq 6.2 with the experimental data.....	195
Table 6.4. D_0 , $k\beta^2$ and ν as free parameters obtained from the fits to eq 6.3 with the experimental data.....	198
Table 7.1. Chemical shift, D_0 , α , ν and R_h for free and bound EG	223

Liste des figures

Figure 1. (A) Représentation des différents systèmes polymères utilisés pour la libération contrôlée de médicaments, (B) profil de la concentration en médicament en fonction du temps 4

Figure 1.1. Semi-logarithmic plot of solvent self-diffusion coefficient as a function of the polymer concentration. The predictions of the Maxwell-Fricke model and the model of Mackie-Mearns are represented by solid lines 18

Figure 1.2. Normalized self-diffusion coefficient of fluorescein dye as a function of the polymer volume fraction..... 19

Figure 1.3. Simulation of D/D_0 versus the polymer volume fraction for particles with 5 Å, 12 Å, 20 Å and 30 Å. The solid lines are predictions with the hard sphere theory..... 25

Figure 1.4. Representation of the dilute, semi-dilute and concentrated regimes of polymer solutions as well as the correlation length in the concentrated regime 33

Figure 1.5. Logarithmic plots of the self-diffusion coefficients of PS in dibutyl phthalate as a function of the molecular weight of PS at various polymer concentrations 36

Figure 1.6. Plot of the self-diffusion coefficients of adinazolam as a function of the VIA concentration. Fits are obtained by the use of eq 1.32..... 43

Figure 1.7. Plot of the self-diffusion coefficients of adinazolam as a function of HPMC concentrations. Fits are obtained with the use of eq 1.32	44
Figure 1.8. Semi-logarithmic plot of the normalized self-diffusion coefficients of various diffusants as a function of $1(1-\phi_p)$. The dotted lines are fits to the free volume model of Yasuda <i>et al.</i> (eq 1.40)	53
Figure 1.9. Semi-logarithmic plot of the self-diffusion coefficient of ethylbenzene in PS as a function of the mass fraction of the solvent. The solid lines are fit to the model of Vrentas-Duda (eq 1.41).....	57
Figure 1.10. The self-diffusion of methyl red plotted as a function of PVME concentration in toluene.....	66
Figure 1.11. Representation of the polymer solution of a network of mesh size ξ , and potential E for the diffusion process of a diffusant in a polymer network.....	67
Figure 1.12. The logarithm plots of the self-diffusion coefficients of a linear PS (A) and a star-PS (B) as a function of the PVME concentration.....	70
Figure 2.1. Illustrations of a uniform magnetic field and of a magnetic field with gradient.....	90
Figure 2.2. Pulsed-gradient spin-echo NMR sequence and representation of the motion of the spins with respect to the r.f. pulses and gradient pulses.....	91
Figure 2.3. Example of ^1H PGSE NMR spectra of PEG-600 in a PVA-water binary mixture and the corresponding semi-logarithmic plot of the signal intensities as a function of $\delta^2(\Delta-\delta/3)$	93

Figure 2.4. The compensation of the eddy current effect caused by the first gradient pulse (δ) by the addition of a correction (ϵ) to the second gradient pulse.....	99
Figure 2.5. The stimulated echo NMR sequence, and the longitudinal eddy-current delay NMR sequence.....	101
Figure 2.6. Plot of the echo attenuation versus $X = (\gamma\delta G)^2(\Delta-\delta/3)$ for ethylene glycol in poly(vinyl alcohol)-water system	104
Figure 3.1. ^1H PGSE-NMR spectra of the PVA-water-PEG-2000 system, and semi-logarithmic plot of the signal intensities as a function of $\delta^2(\Delta-\delta/3)$ for PVA, PEG-2000 and water proton signals.....	118
Figure 3.2. Self-diffusion coefficients of the solute probes plotted as a function of PVA concentration at 23 °C	122
Figure 3.3. Self-diffusion coefficients of PEG-600 plotted as a function of PVA concentration at four different temperatures.....	123
Figure 3.4. Semi-logarithmic plot of $k\beta^2$ and plot of the parameter ν as a function of the hydrodynamic radius, R_h	126
Figure 3.5. Logarithm of the parameter $k\beta^2$ plotted as a function of reciprocal temperature. The potential energy barriers can be calculated from the slopes of these lines.....	127
Figure 4.1. Plot of the normalized self-diffusion coefficient of selected diffusants as a function of the volume fraction of PVA. Dashed line is fit to eq 4.1.....	140

Figure 4.2. Semi-logarithmic plot of the normalized self-diffusion coefficient of selected diffusants as a function of the volume fraction of PVA. Dashed lines are fits to eq 4.3	142
Figure 4.3. Self-diffusion coefficients of selected PEGs plotted as a function of PVA concentration. Self-diffusion coefficients of PEG-600 plotted as a function of the PVA concentration at four temperatures. Dashed lines are fits to eq 4.4.....	145
Figure 4.4. Plot of the hydrodynamic radius, R_h , as a function of molecular weight M of the PEG diffusants	146
Figure 4.5. Semilogarithmic plot of the self-diffusion coefficients D_0 as a function of the reciprocal temperature for selected diffusant	147
Figure 4.6. Plot of the normalized self-diffusion coefficient of selected diffusants as a function of the volume fraction of PVA. Dashed lines are fits to eq 4.5	148
Figure 5.1. Chemical structure of the diffusants 18-crown-6 and 2-[3-(6-Methyl-2-pyridyl)-propoxy]ethanol (MPPE) used in this study.....	157
Figure 5.2. Plot of the self-diffusion coefficient of (A) ethylene glycol and its end-capped derivatives, (B) end-capped di(ethylene glycol) and (C) other end-capped oligo(ethylene glycol)s. Dashed lines are fits to eq 5.1	163
Figure 5.3. Semi-logarithmic plot of the parameter $k\beta^2$ as a function of (A) the hydrodynamic radius and (B) the molecular weight of the diffusants	164
Figure 5.4. Plot of the self-diffusion coefficient of (A) ethylene glycol and its end-capped derivatives, (B) end-capped di(ethylene glycol) and (C) other end-capped oligo(ethylene glycol)s. Dashed lines are fits to eq 5.4.....	167

Figure 5.5. (A) Plot of the parameter α as a function of the hydrodynamic radius of the diffusants, (B) plot of ν as a function of the molecular weight of the diffusants.....	168
Figure 5.6. Plot of the logarithmic self-diffusion coefficient of selected diffusants as a function of $\phi/(1-\phi)$, and plot of the parameter B_s/f_w as a function of the hydrodynamic radius of the diffusants.....	172
Figure 5.7. Plot of the normalized self-diffusion coefficient of selected diffusants as a function of the volume fraction of PVA. Dotted line and dashed lines are fits to eq 5.6 and 5.7, respectively.....	173
Figure 5.8. Plot of the normalized self-diffusion coefficient of selected diffusants as a function of the volume fraction of PVA. Dashed lines are fits to eq 5.8	175
Figure 6.1. Size exclusion chromatograms obtained for PVA-4, (A) dissolved in an aqueous solution of NaSCN (salt/polymer weight ratio = 1.5:1), (B) dissolved in water and injected three days after preparation, and (C) the same water solution as B but injected after seven days	189
Figure 6.2. Semi-logarithmic plot of the self-diffusion coefficient of water and PEG-600 in PVA-2 as a function of $\phi/(1-\phi)$. Dashed lines are the best fits to eq 6.4.....	193
Figure 6.3. Plot of the self-diffusion coefficient of water (A) and PEG-600 (B) as a function of the PVA concentration for various PVA matrices at 25 °C. Dashed lines are fits to eq 6.2.....	194

Figure 6.4. Plot of the self-diffusion coefficient of water (A) and PEG-600 (B) as a function of the PVA concentration for various PVA matrices at 25 °C. Dashed lines are fits to eq 6.3	200
Figure 6.5. Plot of the self-diffusion coefficient of water (A) and PEG-600 (B) as a function of the HPMC concentration for the two HPMC matrices at 25 °C. Dashed lines are fits to eq 6.3	201
Figure 6.6. Plot of the self-diffusion coefficient of water (A) and PEG-600 (B) as a function of the polymer (PNNDEA and PNIPA) concentration for at 25 °C. Dashed lines are fits to eq 6.3	203
Figure 7.1. ¹ H NMR spectra of EG in PVA-D ₂ O solution at different PVA concentrations	215
Figure 7.2. Plot of the fractions of free and bound EG as a function of the PVA concentration.....	216
Figure 7.3. ¹ H PGSE NMR spectra of EG in PVA-D ₂ O solution and the plot of the NMR signal intensity according to eq 7.1	218
Figure 7.4. Plot of the self-diffusion coefficient for free and bound EG as a function of PVA concentration	219
Figure 7.5. Semi-logarithmic plot of the NMR signal intensity as a function of $(\gamma G \delta)^2 (\Delta - \delta/3)$ for ethylene glycol in PVA-water system.....	221
Figure 7.6. Plot of T_1 and T_2 relaxation times for free and bound EG as a function of PVA concentration	224

Liste des symboles et abréviations

1. Symboles et abréviations utilisés pour les produits chimiques

18-crown-6	Éther couronne 18-6
DEG-Me	Di(éthylène glycol) méthyl éther
DEG-Et	Di(éthylène glycol) éthyl éther
DEG-tBuOH	Di(éthylène glycol) <i>tert</i> -butyl méthyl éther
EG	Éthylène glycol
(EG) _x	Oligo(éthylène glycol) ayant x motifs éthylène glycol
EG-Me	Éthylène glycol méthyl éther
EG-Me ₂	Éthylène glycol diméthyl éther
EG-tBuOH	Éthylène glycol <i>tert</i> -butyl méthyl éther
HPMC	Hydroxypropylmethylcellulose
MPPE	2-[3-(6-Méthyl-2-pyridyl)-propoxyl]éthanol
OEG	Oligo(éthylène glycol)
PEG	Poly(éthylène glycol)
PEG-x	Poly(éthylène glycol) de poids moléculaire x
PMA	Poly(acrylate de méthyle)
PMMA	Poly(méthacrylate de méthyle)
PNIPA	Poly(<i>N,N</i> -isopropyl acrylamide)
PNNDEA	Poly(<i>N,N</i> -diéthyl acrylamide)
PS	Polystyrène
PVA	Poly(alcool vinylique)
<i>t</i> BuOH	<i>tert</i> -butanol
TEG-Me	Tri(éthylène glycol) méthyl éther
TEG-2Me	Tri(éthylène glycol) diméthyl éther

2. Symboles et abréviations utilisés pour les différents modèles physique de diffusion

α	Paramètre du modèle de diffusion décrit par Phillies
a	Paramètre du modèle de diffusion décrit par Petit <i>et al.</i>
Å	Angström (10^{-10} m)
β	Constante dépendant de la température
c	Concentration de polymère (g/mL)
c^*	Concentration critique, ou concentration de chevauchement des chaînes de polymère (g/mL)
E_a	Énergie d'activation d'un processus dynamique en solution (kJ/mol)
η	Viscosité d'une solution de polymère (Pas.s)
η_0	Viscosité du solvant (Pas.s)
k	Fréquence de saut d'une molécule
k_B	Constante de Boltzmann (1.380658×10^{-23} JK ⁻¹)
M	Masse moléculaire, utilisé dans le modèle de diffusion proposé par de Gennes
M_n	Masse moléculaire en nombre d'un polymère (g/mol), généralement obtenu par chromatographie d'exclusion stérique (SEC)
M_w	Masse moléculaire en poids d'un polymère (g/mol), généralement obtenu par chromatographie d'exclusion stérique (SEC)
v	Paramètre du modèle de diffusion de Phillies et de Petit <i>et al.</i>
ρ	Rayon du polymère ou de la fibre (Å) (modèle de Ogston <i>et al.</i>)
r_f	Rayon hydrodynamique de la fibre ou polymère (Å) (modèle de Amsden)
r_s	Rayon hydrodynamique du diffusant (Å) (modèle de Amsden et Ogston <i>et al.</i>)
R	Constante des gaz parfaits (8.31451 Lmol ⁻¹ K ⁻¹)
R_h	Rayon hydrodynamique (Å)
SEC	Size exclusion chromatographie, ou encore chromatographie d'exclusion stérique
T	Température (°C ou K)
ξ	Longueur de corrélation d'une solution polymère semidiluée

3. Symboles et abréviations utilisés en résonance magnétique nucléaire

$A_{(\delta)}$ ou $I_{(\delta)}$	Intensité du signal RMN en présence de gradient
$A_{(0)}$ ou $I_{(0)}$	Intensité du signal RMN en absence de gradient
δ	Temps d'application du gradient magnétique (ms)
Δ	Temps entre deux gradients (ms)
D	Coefficient d'auto diffusion dans une solution polymère (m^2/s)
D_0	Coefficient d'auto diffusion dans le solvant pur (m^2/s)
γ	Rapport gyromagnétique du proton ($2.6752 \times 10^8 \text{ rad.s}^{-1}.\text{T}^{-1}$)
G	Intensité du gradient de champ magnétique (T/m)
NMR	Nuclear magnetic resonance (voir RMN)
PGSE	Pulsed-gradient spin-echo (écho de spin à gradient de champ pulsé)
RMN	Résonance magnétique nucléaire
STE	Stimulated echo (écho stimulé)
T_1	Temps de relaxation spin-réseau
T_2	Temps de relaxation spin-spin
90_i	Impulsion de 90° selon l'axe i
180_i	Impulsion de 180° selon l'axe i

Remerciements

Ce travail a été réalisé au département de chimie de l'Université de Montréal sous la direction du Professeur Julian X.X. Zhu que je tiens à remercier vivement pour m'avoir donné l'opportunité de réaliser ce projet de doctorat, pour son appui constant, son soutien sans faille, et pour son optimisme permanent durant toutes ces années.

Je souhaite remercier le Docteur Minh Tan Phan Viet, Directeur du Laboratoire Régional de RMN, pour son aide ainsi que Sylvie et Robert pour leur gentillesse et leur grande disponibilité.

Je tiens également à remercier le Professeur P.M. Macdonald de l'Université de Toronto, ainsi que ses étudiants, pour avoir mis à notre disposition leur équipement RMN nécessaire à la réalisation d'une partie de ce projet ainsi que pour leur aide et leur accueil. De même que Paul-André Lavoie, et les étudiants du groupe de recherche du Professeur P. Carreau de l'École Polytechnique de Montréal, pour leur aide précieuse et leurs conseils judicieux dans les études rhéologiques.

Mes remerciements s'adressent aussi à mes collègues de laboratoire (Aline, Amina, Damien, David, Eider, Huiyou, Karima, Marcela, Mohand, Mu, Sebastien, Sumitra, Wilms, Yuehua et Zhengzi) avec qui il fût un plaisir de travailler, de même qu'aux étudiantes du groupe du Prof. Michel Lafleur avec qui j'ai partagé le temps d'utilisation de l'appareil RMN. Enfin j'aimerais remercier à titre personnel Jean-Michel Petit et le Professeur F. Brisse.

La réalisation de ce projet a été rendue possible grâce à l'appui financier des fonds de recherche du CRSNG et du FCAR. Les déplacements à Mississauga ont été financés par un fonds de coopération Québec-Ontario provenant du Ministère de l'éducation du Québec.

Partie I

Introduction générale

Les études de diffusion dans les solutions et gels de polymères sont très importantes car elles génèrent de nombreuses applications dans plusieurs domaines. Par exemple, les études de diffusion peuvent être utiles pour analyser la miscibilité de deux polymères [1]. Il est également possible de mesurer la diffusion d'un plastifiant dans un polymère [2], la diffusion d'ions dans des polyélectrolytes [3] ou la diffusion d'un gaz dans une membrane polymère [4]. Les propriétés de diffusion des matériaux sont également importantes dans le domaine de l'agriculture [5], dans le domaine biomédical [6], et dans le domaine de l'alimentation [7]. Au cours de la dernière décennie, l'application la plus importante concernant les mesures de diffusion a été la libération contrôlée de médicaments. Il existe aussi un intérêt théorique dans les études de diffusion. Plusieurs modèles théoriques de diffusion ont été proposés [8–21], mais l'utilisation de ces modèles est souvent limitée [22–25]. Ces modèles méritent donc d'être testés afin de mieux cerner leur domaine d'application.

1. Diffusion et libération contrôlée

Un des grands défis de la chimie moderne est de concevoir des matériaux biocompatibles qui puissent libérer des substances actives sur une période de temps préétablie pour des applications pharmaceutiques. En effet, la libération contrôlée de médicaments est le sujet d'intenses recherches qui nécessitent une grande connaissance des matériaux polymères. Parmi ces matériaux, les hydrogels sont des matériaux très prometteurs car ils absorbent de grandes quantités d'eau, ce qui les rendent généralement biocompatibles. De plus, les hydrogels sont des matériaux qui peuvent être réticulés chimiquement ou physiquement, dont les propriétés physico-chimiques se situent entre celles d'un solide et d'un liquide. Cette caractéristique les rend encore plus intéressants. Cependant, pour relever ce défi, il est primordial de comprendre le mécanisme de diffusion dans ces matériaux polymères.

Pour véhiculer les molécules lors de la libération contrôlée de médicaments, les matériaux polymères peuvent être utilisés selon deux concepts distincts (Figure 1A). Premièrement, les matériaux polymères sont mélangés avec la substance active à l'état

sec. Au contact du liquide biologique, le polymère gonfle, ses chaînes forment un réseau tridimensionnel dans lequel les solutés peuvent diffuser. Donc, la perméabilité du réseau va influencer leur déplacement, de même que la taille des diffusants. L'existence éventuelle d'interactions entre le soluté et le polymère influencerait également le procédé de diffusion. Une variante de ce système est l'utilisation de polymères biodégradables. En plus du gonflement du polymère et de la diffusion, il y a érosion du réseau polymère. Le deuxième concept est l'utilisation d'un polymère sous forme de membrane pour former un réservoir à partir duquel le médicament diffuse. L'utilisation de tels matériaux permet d'améliorer l'efficacité de certains médicaments dont l'action est reliée principalement à la concentration dans l'organisme. En effet, l'action spécifique de certains médicaments est évaluée par leur concentration, que l'on nomme zone efficace tel qu'illustré sur la Figure 1B. Au dessus de cette zone, le médicament devient toxique. En dessous, le médicament perd de son efficacité. Dans les traitements conventionnels, pour garder le médicament en concentration efficace dans l'organisme, il doit être appliqué périodiquement. Cette procédure est fastidieuse pour le patient et multiplie le risque de surdose.

2. Les objectifs de cette étude

Au cours des dernières décennies, la spectroscopie RMN a connu un développement technique et un essor fulgurant qui en fait aujourd'hui une méthode d'analyse de pointe pour la mesure des coefficients d'auto-diffusion dans les solutions et gels de polymères. La technique d'écho de spin à gradient de champ pulsé (PGSE) et l'imagerie RMN en sont les exemples les plus probants.

Le but de ce travail est d'étudier la diffusion de solutés dans les solutions et gels de polymères, par RMN PGSE, afin de mieux comprendre les procédés de diffusion dans les systèmes polymères. Ce phénomène est fortement associé aux propriétés physico-chimiques ainsi qu'à la dynamique de la molécule diffusante et celle du système polymère.

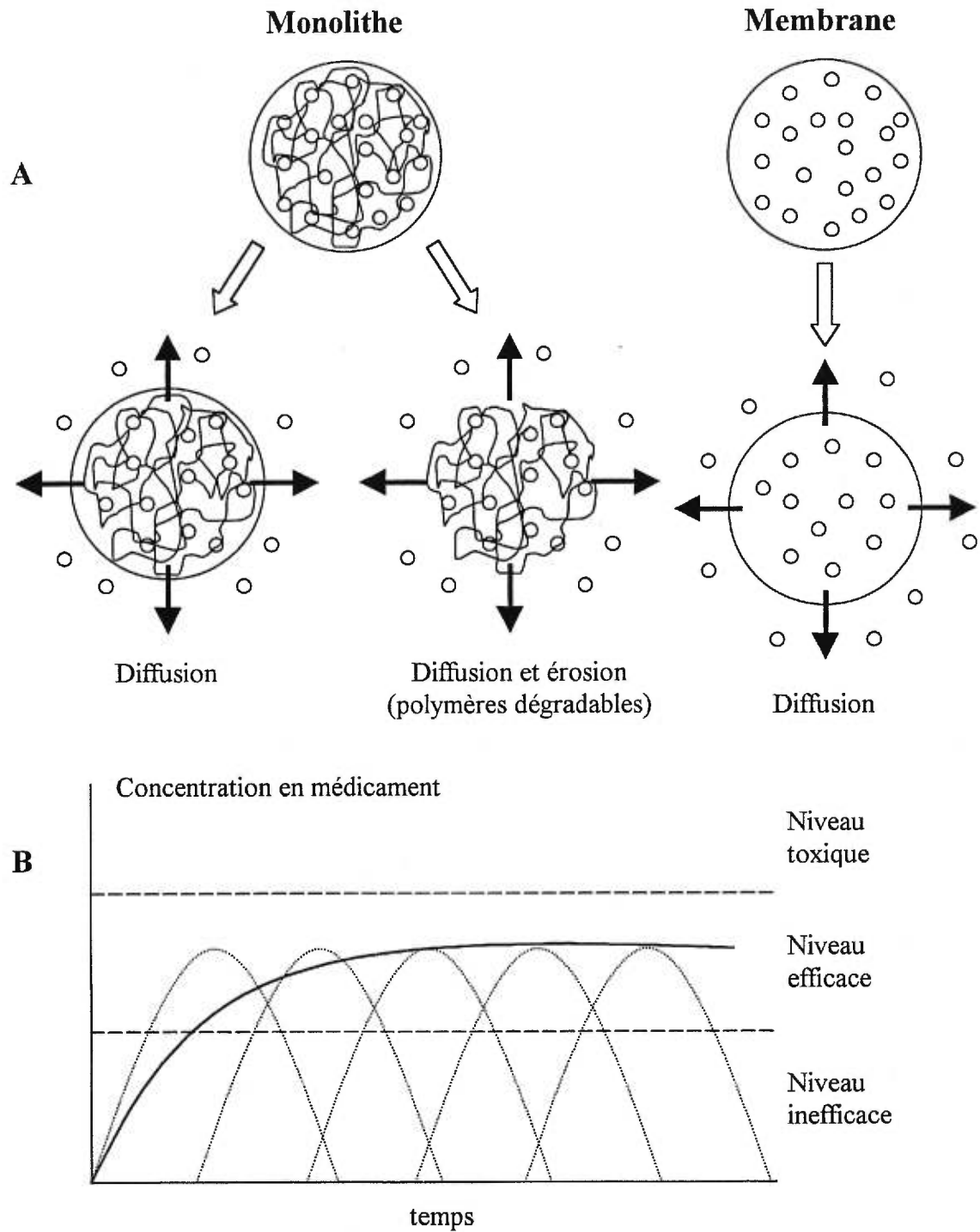


Figure 1: (A) Représentation de différents systèmes polymères utilisés pour la libération contrôlée de médicaments, (B) profil de la concentration en médicament en fonction du temps. Les pointillés représentent des injections successives d'un médicament traditionnel et le trait plein l'injection d'un médicament à libération contrôlée.

Beaucoup de modèles théoriques de diffusion ont été proposés dans la littérature. Ces modèles sont généralement divisés en trois catégories qui correspondent à trois concepts physiques de diffusion: l'effet d'obstruction [8–11], les interactions hydrodynamiques [12–16] et la théorie du volume libre [17–21]. Les modèles les plus importants de chacune de ces catégories sont décrits dans le premier chapitre. L'accent a été mis sur la caractérisation du domaine d'application de chaque modèle en se basant sur les nombreux exemples trouvés dans la littérature. En plus de ces modèles, nous avons également analysé deux nouveaux modèles physiques de diffusion qui ont été définis récemment par Petit *et al.* [26] et Amsden [22]. L'objectif de cette thèse est d'appliquer les modèles de diffusion les plus pertinents au plus grand nombre possible de systèmes soluté-polymère afin de mieux les caractériser et mieux comprendre les procédés de diffusion dans les polymères. Les mesures des coefficients d'auto-diffusion ont été réalisées par RMN PGSE, dont les détails sont décrits dans le deuxième chapitre.

3. Présentation des travaux

Dans un premier temps, nous avons étudié comment la taille du soluté influence la diffusion. Des solutés, aussi dénommées diffusants, linéaires et de taille croissante, basées sur l'éthylène glycol ont été utilisées. La diffusion de ces solutés dans les solutions et gels d'alcool polyvinylique (PVA) a été mesurée. Le choix du PVA est justifié par le fait que ce polymère est beaucoup utilisé pour des applications pharmaceutiques et biomédicales. Les données expérimentales ont été traitées avec le modèle de diffusion décrit par Petit *et al.* [26] (chapitre 3), ainsi qu'avec les modèles de diffusion de Mackie et Meares [9], Ogston *et al.* [10], Yasuda *et al.* [18], de Gennes [14], Phillies [16] et Amsden [22] (chapitre 4). Le choix des modèles de diffusions se fait selon deux critères: (i) les propriétés physico-chimiques des solutés étudiés; et (ii) le domaine d'application des modèles.

L'effet de la géométrie du soluté sur la diffusion a également été examiné. Des solutés basées sur l'éthylène glycol mais ayant des groupes terminaux différents ont été utilisées. Les groupements terminaux incluent des groupements linéaires (méthyle, éthyle, hexyle, etc.) et des groupements sphériques rigides (*tert*-butyle, pyridinium, groupement cyclique, etc.). Les modèles de diffusion de Mackie-Meares [9], Ogston *et al.* [10], Yasuda *et al.* [18], Phillies [16], Petit *et al.* [26] et Amsden [22] ont été

testés avec les données expérimentales (chapitre 5). Les paramètres employés dans ces modèles ont été corrélés avec les rayons hydrodynamiques des solutés ainsi qu'avec leurs masses molaires.

Nous avons aussi analysé l'impact du réseau polymère sur la diffusion. Plusieurs polymères ont été utilisés, notamment des PVA avec des masses molaires et des taux d'hydrolyse différents, des hydroxypropyl méthyl celluloses, le poly(*N,N*-diéthylacrylamide) et le poly(*N*-isopropyl acrylamide). La diffusion du solvant (l'eau) et d'un soluté (PEG-600) dans les différents systèmes a été mesurée. Les modèles de diffusion de Yasuda *et al.* [18], Phillies [16], Amsden [22] ainsi que le modèle de Petit *et al.* [26] ont été utilisés (chapitre 6).

Nous avons démontré qu'il existe des interactions sous forme de liaisons hydrogène entre certains diffusants et le polymère (chapitre 7). Cette association a été caractérisée par diverses techniques RMN, comme l'étude du déplacement chimique, l'étude du coefficient d'auto-diffusion, et par l'étude des temps de relaxation spin-réseau et spin-spin. L'existence de liaisons diffusant-polymère influence beaucoup les procédés de diffusion dans les solutions et gels de polymères.

4. Références

- [1] Hoerner, P.; Riess, G.; Rittig, F.; Fleischer G. *Macromol. Chem. Phys.* **1998**, *199*, 343.
- [2] Waggoner, A.; Blum, F.D. *J. Coatings Technol.* **1989**, *61*, 768.
- [3] Clericuzio, M.; Parker, W.O.; Soprani, M.; Andrei, M. *Solid States Ionic* **1995**, *77*, 685.
- [4] Hariharan, D.; Peppas, N.A. *J. Contr. Release* **1993**, *23*, 123.
- [5] Paul, B.K.; Moulik, S.P. *J. Dispersion Sci. Technol.* **1997**, *18*, 301.
- [6] Gao, P.; Fagerness, P.E. *Pharm. Res.* **1995**, *12*, 955.
- [7] Rosca, I.D.; Vergnaud J.D. *J. Appl. Polym. Sci.* **1997**, *66*, 1291.
- [8] Fricke, H. *Phys. Rev.* **1924**, *24*, 575.
- [9] Mackie, J.S.; Meares, P. *Proc. R. Soc. Lond., A* **1955**, *232*, 498.

- [10] Ogston, A.G.; Preston, B.N.; Wells, J.D. *Proc. R. Soc. Lond., A* **1973**, *333*, 297.
- [11] Johansson, L.; Elvingson, C.; Löfroth, J.-E., *Macromolecules* **1991**, *24*, 6024.
- [12] Cukier, R.I. *Macromolecules* **1984**, *17*, 252.
- [13] Altenberger, A.R.; Tirrell, M. *J. Chem. Phys.* **1984**, *80*, 2208.
- [14] de Gennes, P.G. *J. Phys. Chem.* **1971**, *55*, 572.
- [15] de Gennes, P.-G. *Scaling Concepts in Polymer Physics*, Cornell University Press: Ithaca, New-York, 1979.
- [16] Phillies, G.D.J. *Macromolecules* **1986**, *19*, 2367.
- [17] Fujita, H. *Adv. Polym. Sci.* **1961**, *3*, 1.
- [18] Yasuda, H.; Lamaze, C.E.; Ikenberry, L.D. *Makromol. Chem.* **1968**, *118*, 19.
- [19] Peppas, N.A.; Lustig, S.R. *Hydrogels in medicine and pharmacy, Vol. I*, CRC Press, Boca Raton (1987).
- [20] Vrentas, J.S.; Duda, J.L. *J. Polym. Sci., Polym. Phys. Ed.* **1977**, *15*, 403.
- [21] Vrentas, J.S.; Duda, J.L. *J. Polym. Sci., Polym. Phys. Ed.* **1977**, *15*, 417.
- [22] Amsden, B. *Polym. Gels Networks* **1998**, *6*, 13.
- [23] Muhr, H.; Blanshard, M.V. *Polymer* **1982**, *23*, 1012.
- [24] Waggoner, R.A.; Blum, F.D.; MacElroy, J.M.D. *Macromolecules* **1993**, *26*, 6848.
- [25] Petit, J.-M.; Zhu, X.X.; Macdonald, P.M.; *Macromolecules* **1996**, *29*, 70.
- [26] Petit, J.-M.; Roux, B.; Zhu, X.X.; Macdonald, P.M. *Macromolecules* **1996**, *29*, 6031.

Chapitre 1

Physical Models of Diffusion for Polymer Solutions, Gels and Solids

Masaro, L.; Zhu, X.X.
Progress in Polymer Science

1999, soumis.

1.1. Abstract

Diffusion in polymer solutions and gels has been studied by various techniques such as gravimetry, membrane permeation, fluorescence and radioactive labeling. These studies have led to a better knowledge on polymer morphology, transport phenomena, polymer melt and controlled release of drugs from polymer carriers. Various theoretical descriptions of the diffusion processes have been proposed. The theoretical models are based on different physical concepts such as obstruction effects, free volume effects and hydrodynamic interactions. With the availability of pulsed field gradient NMR techniques and others modern experimental methods, the study of diffusion has become much easier and data on diffusion in polymers have become more available. This review article summarizes the different physical models and theories of diffusion and their uses in describing the diffusion in polymer solutions, gels and even solids. Comparisons of the models and theories are made in an attempt to illustrate the applicability of the physical concepts. Examples in the literature are used to illustrate the application and applicability of the models in the treatment of diffusion data in various systems.

CONTENTS

1.1. Abstract	9
1.2. Introduction	11
1.2.1. Fickian diffusion	12
1.2.2. Non-Fickian diffusion	13
1.2.3. Self-diffusion and mutual diffusion coefficients	14
1.2.4. Diffusion in polymers	15
1.3. Theories and physical models of diffusion	16
1.3.1. Diffusion models based on obstruction effects	16
1.3.1.1. The Maxwell-Fricke model	16
1.3.1.2. The model of Mackie and Meares	20
1.3.1.3. The model of Ogston <i>et al.</i>	21
1.3.1.4. The hard sphere theory	22
1.3.1.5. Summary	24
1.3.2. Hydrodynamic theories	27
1.3.2.1. Cukier's model	27
1.3.2.2. The model of Altenberger <i>et al.</i>	30
1.3.2.3. Phillis' model	31
1.3.2.4. The reptation and reptation plus scaling models	37
1.3.2.5. The model of Gao and Fagerness	40
1.3.2.6. Summary	46
1.3.3. Diffusion models based on the free volume theory	48
1.3.3.1. Fujita's model	48
1.3.3.2. The model of Yasuda <i>et al.</i>	50
1.3.3.3. The model of Vrentas and Duda	52
1.3.3.4. The model of Peppas and Reinhart	56
1.3.3.5. Summary	59
1.3.4. Other physical models of diffusion	60
1.3.4.1. Arrhenius' theory	60
1.3.4.2. The modified Enskog theory	64
1.3.4.3. The model of Petit <i>et al.</i>	65
1.3.4.4. Amsden's model	71
1.3.4.5. Summary	73
1.4. Concluding remarks	73
1.5. Symbols and abbreviations	74
1.6. Acknowledgment	75
1.7. References	76

1.2. Introduction

Diffusion is the process responsible for the movement of matter from one part of a system to another,¹ and it is mainly due to random molecular motions. In gases, diffusion processes are fast (10 cm/min) whereas they are much slower in liquids (0.05 cm/min) and solids (0.00001 cm/min).² According to Cussler,² diffusion in both gases and liquids can be successfully predicted by theories. Diffusion is known to depend on temperature, pressure, solute size and viscosity. Diffusion has a much larger range of values in solids, where diffusion coefficients can differ by more than a factor of 10^{10} . Therefore, diffusion in solids is difficult to estimate with theoretical models.² Diffusion in polymers is complex and the diffusion rates should lie between those in liquids and in solids. It depends strongly on the concentration and degree of swelling of polymers. Consequently, it remains a challenge to understand, predict and control the diffusion of small and large molecules in polymer systems. The theories and physical models of diffusion may help to realize these goals.

The first mathematical treatment of diffusion was established by Fick³ who developed a law for convection in one dimension:

$$J = -A j = -AD \frac{\partial c}{\partial z} \quad (1.1)$$

where J is the flux, j the flux per unit area, A the area across which diffusion occurs, D the diffusion coefficient, c the concentration, z the distance and $\partial c/\partial z$ the gradient of the concentration along the z axis. This equation is also known as Fick's first law. In the case of diffusion without convection and a unitary area, Eq 1.1 can be written as

$$J = -D \frac{\partial c}{\partial z} \quad (1.2)$$

Eq 1.2 is the starting point of numerous models of diffusion in polymer systems.

In the study of solvent diffusion in polymers, different behaviors have been observed. It is known that the diffusion of the solvent is linked to the physical properties of the polymer network and the interactions between the polymer and the solvent itself. Alfrey *et al.*⁴ proposed a classification according to the solvent

diffusion rate and the polymer relaxation rate: Fickian (Case I) and non-Fickian (Case II and anomalous) diffusions. The amount of solvent absorbed per unit area of polymer at time t , M_t , is represented by

$$M_t = k t^n \quad (1.3)$$

where k is a constant and n a parameter related to the diffusion mechanism, the value of which lies between $\frac{1}{2}$ and 1. Eq 1.3 can be used to describe solvent diffusional behaviors for any polymer-penetrant system whatever the temperature and the penetrant activity.

1.2.1. Fickian diffusion

Fickian diffusion (Case I) is often observed in polymer networks when the temperature is well above the glass transition temperature of the polymer (T_g). When the polymer is in the rubbery state, the polymer chains have a higher mobility that allows an easier penetration of the solvent.⁵ Therefore, Fickian diffusion is characterized by a solvent diffusion rate, R_{diff} , slower than the polymer relaxation rate, R_{relax} ($R_{\text{diff}} \ll R_{\text{relax}}$). A large gradient of solvent penetration is observed in the system. The solvent concentration profile shows an exponential decrease from the completely swollen region to the core of the polymer. The solvent penetration front is proportional to the square-root of time⁶

$$M_t = k t^{1/2} \quad (1.4)$$

Few examples of Fickian diffusion in polymer systems are reported in the literature, since solvent absorption studies have been often carried out at ambient temperature which is often below T_g . Nevertheless, Fickian diffusion can be observed in polymer systems below T_g with the addition of a plasticizer. Grinsted *et al.*⁵ studied the diffusion of methanol in poly(methyl methacrylate) (PMMA) as a function of water concentration by NMR imaging. They found that the diffusion rate of methanol increased with increasing water concentration. In addition, the diffusion of methanol changed from Case II (see Section 1.2.2) to Fickian when the water content was increased. This change in methanol diffusional behavior was explained by the presence of water that acted as a plasticizer. Ercken *et al.*⁷ also reported studies of

methanol diffusion in PMMA. They showed that methanol diffusion followed Case II behavior at ambient temperature, whereas Fickian behavior was observed at higher temperatures.

1.2.2. Non-Fickian diffusion

Non-Fickian diffusion processes are mainly observed in glassy polymers, i.e., when the temperature of study is below T_g . At a specific temperature below T_g , the polymer chains are not sufficiently mobile to permit immediate penetration of the solvent in the polymer core.⁵ Two kinds of non-Fickian diffusion were defined: Case II diffusion and anomalous diffusion. The main difference between these two diffusion categories concerns the solvent diffusion rate. In Case II diffusion, the solvent diffusion rate is faster than the polymer relaxation process ($R_{diff} \gg R_{relax}$), whereas in anomalous diffusion the solvent diffusion rate and the polymer relaxation are about the same order of magnitude ($R_{diff} \sim R_{relax}$).⁴

In general, Case II diffusion is observed when solvents have high penetrative activities.⁸ The characteristics of Case II diffusion are the following: (1) a rapid increase in the solvent concentration in the swollen region which leads to a sharp solvent penetration front between the swollen region and the inner polymer core; (2) the solvent concentration is quite constant in the swollen region behind the solvent penetration front; (3) the solvent penetration front is sharp and advances at a constant rate, thus the diffusion distance is directly proportional to time

$$M_t = k t \quad (1.5)$$

(4) There is an induction time of Fickian concentration profile which precedes the solvent penetration front into the glassy polymer core.⁹⁻¹³

Fickian and Case II diffusions are considered as limiting types of transport processes. Anomalous diffusion lies in between and is characterized by the following equation:

$$M_t = k t^n \text{ and } \frac{1}{2} < n < 1 \quad (1.6)$$

Examples of Case II diffusion with polymer/solvent systems are abundant in the literature. For example, Weisenberger and Koenig¹⁴ showed that methanol

diffusion in PMMA obeys Eq 1.5 (Case II). Dioxane in polystyrene (PS),¹⁵ acetone in poly(vinyl chloride)¹⁶ and in polycarbonate⁶ have the same diffusional behavior.

1.2.3. Self-diffusion and mutual diffusion coefficients

According to Fick's first law (Eq 1.1), the diffusion coefficient is defined as the rate of transfer of the diffusant across the diffusion section divided by the space gradient concentration at this specific section. If we consider the mixing of two pure species, A and B, without volume variation, then an equal quantity of each component will be transferred in the opposite direction. From a diffusion point of view, we obtain one diffusion coefficient related to both species, referred to as the **mutual diffusion coefficient**.^{1,17} However, it is important to note that the mutual-diffusion coefficient, D_m , can be expressed as the sum of two **intrinsic diffusion coefficients** related to each individual component.¹⁷

$$D_m = V_A C_A (D_B - D_A) + D_A \quad (1.7)$$

where C_A is the amount of component A contained in the system, V_A the constant volume of component A and D_i the intrinsic diffusion coefficient of component i .

In already equilibrated systems such as polymer solutions and gels, there is no volume variation and no mass transfer. Nevertheless, the molecules are in motion and diffusion occurs without the presence of a concentration gradient. In this case the diffusion is defined by the **self-diffusion coefficient**. This diffusion coefficient can be related to the intrinsic diffusion coefficient (thus indirectly related to the mutual diffusion coefficient) by¹⁷

$$D_A = D C_A \frac{\partial \mu_A}{\partial C_A} = RT D \frac{\partial \ln a_A}{\partial \ln C_A} \quad (1.8)$$

where D is the self-diffusion coefficient of component A, μ_A the chemical potential and a_A the thermodynamic activity of component A.

Generally speaking, self-diffusion occurs in systems composed of chemical species in the same phase such as polymer solutions. When the concentration of the studied species is very small, the self-diffusion of the species is also called **tracer diffusion**. Tracer diffusion also includes the diffusion of chemical species in different

physical states, for example, the diffusion of water vapor in a polymer thin film, which involves the diffusion of a gas in a solid.²

Most diffusion studies have been carried out by measuring the self-diffusion coefficient as it is more convenient to study the already equilibrated systems. In this review article, the applicability of the diffusion models in tracer and self-diffusion will be discussed as described in the literature.

1.2.4. Diffusion in polymers

Diffusion in polymer solutions and gels have been studied for decades by the use of various techniques such as gravimetry,¹⁸ membrane permeation,¹⁹ fluorescence²⁰ and dynamic light scattering.²¹ The studies have resulted in a better knowledge on polymer morphology and structure,²² transport phenomena²³ and, more recently, the controlled release of drugs from polymer carriers.²⁴ In addition, these studies have led to theoretical descriptions of the diffusion of solvents and/or solutes in polymer solutions, gels and even solids.²⁵⁻²⁷ These physical models are based on different physical concepts (the obstruction effects, the hydrodynamic interactions and the free volume theory) and their applicability varies.²⁸ With the development of modern techniques such as the pulsed-gradient nuclear magnetic resonance (NMR) spectroscopy,²⁹ the study of diffusion has become much easier than with the other techniques mentioned above.³⁰ With the availability of the diffusion data, several new models of diffusion, concepts, as well as modifications or improvements of the existing theories have appeared in the literature in the last decade.^{28,31-33} Limitations in the use of many of these models have been observed in the literature.^{28,31,34-59} Review articles have been published by Murh and Blanshard,⁶⁰ von Meerwall^{61,62} and Tirrell.⁶³ It is the intention of this article to review the various theoretical models, the recent development and the use of the models in the interpretation of the experimental results of diffusion in polymers.

1.3. Theories and physical models of diffusion

We intend to use homogeneous notations in the text, but the physical significance of the symbols may still differ, which will be indicated.

1.3.1. Diffusion models based on obstruction effects

In the diffusion models based on obstruction effects, polymer chains are regarded as motionless relative to the diffusing molecules, i.e., solvents and/or solutes. This approximation is based on the assumption that the polymer self-diffusion coefficient is much smaller than that of the diffusant. Thus the polymer is represented as fixed and impenetrable segments immersed in a solution. The presence of the motionless polymer chains leads to an increase in the mean path length of the diffusing molecules between two points in the system.

1.3.1.1. The Maxwell-Fricke model

The obstruction concept was first introduced by Fricke²⁵ in 1924 who studied electric conductivity and capacity of spheroids dispersed in dog blood medium. In this study, the author considered different geometries of spheroids (oblates and prolates) and the best results were obtained with spheres. The following equation was given³⁶

$$\frac{D(1-\varphi)}{D_0} = \frac{1-\varphi'}{1+\varphi'/\chi} \quad (1.9)$$

where D is the diffusion coefficient, D_0 is the diffusion coefficient in pure solvent, φ is the volume fraction of the polymer, φ' is the volume fraction of the polymer plus non-diffusing solvent bound to the polymer, and χ is a factor depending on the solvent shape (ranging from 1.5 for rods to 2.0 for spheres). This model was called the Maxwell model^{64,65} or the Maxwell-Fricke model.^{36,37}

Langdon and Thomas⁶⁶ studied mutual diffusion coefficient of small diffusants such as anions ($^{36}\text{Cl}^-$, $^{131}\text{I}^-$) and a cation ($^{22}\text{Na}^+$) in agar gels of composition ranging from 0.67 to 4 wt %, by radioactive labeling (soft β emitters). They found a linear dependence of the self-diffusion coefficient on the gel composition, when the

electrolyte concentration was below 0.1 M. Their analysis in regard to the Maxwell-Fricke model suggested that the hindrance to diffusion was due to the hydration of the agar molecules. According to Cheever *et al.*,⁶⁴ diffusion of water in a suspension of latex at low concentrations was predicted correctly by the Maxwell-Fricke model. Griffith *et al.*³⁷ reported that the diffusion of water in a suspension of impenetrable spherical particles which showed no hydration effect was closely predicted by this model. Therefore, the Maxwell-Fricke model seems to provide good results for small diffusing particles in dilute polymer solutions. Waggoner *et al.*³⁶ showed that this model overestimates the diffusion coefficient at higher polymer concentrations. They studied the self-diffusion of solvents (toluene, ethylbenzene, cumene, *tert*-butyl acetate, chloroform and methyl ethyl ketone) in PS and PMMA systems. The polymer concentration ranged from 0 up to 50 wt %. From their data, it is clear that the Maxwell-Fricke model did not fit well the experimental data even for low polymer concentrations, as shown in Figure 1.1. The same results were observed by Mustafa *et al.*,³⁵ who studied the self-diffusion coefficient of fluorescein dye in dilute and concentrated aqueous hydroxypropyl cellulose gels (ϕ_{HPC} ranging for 0 to 0.65), as illustrated in Figure 1.2.

The Maxwell-Fricke equation gives a dependence of the self-diffusion coefficient on the polymer volume fraction and on the solvent shape, ϕ and χ , respectively. However, the diffusion is closely linked to the size of the diffusant. For example, variation of the self-diffusion coefficient between a small molecule such as water ($D = 2.77 \times 10^{-9} \text{ m}^2/\text{s}$) and a macromolecule such as poly(ethylene glycol) with a molecular weight of 2000 ($D = 1.73 \times 10^{-10} \text{ m}^2/\text{s}$) in the same poly(vinyl alcohol) (PVA) system ($[\text{PVA}] = 0.03 \text{ g/mL}$, $T = 43 \text{ }^\circ\text{C}$) is more than one order of magnitude and far from being identical.⁶⁷

Therefore, this model can be used in the study of small-sized molecules such as solvents³⁶ in dilute polymer solutions³⁷ and/or gas diffusion in highly swollen membranes, for which the difference of self-diffusion coefficients is insignificant for the different diffusants.

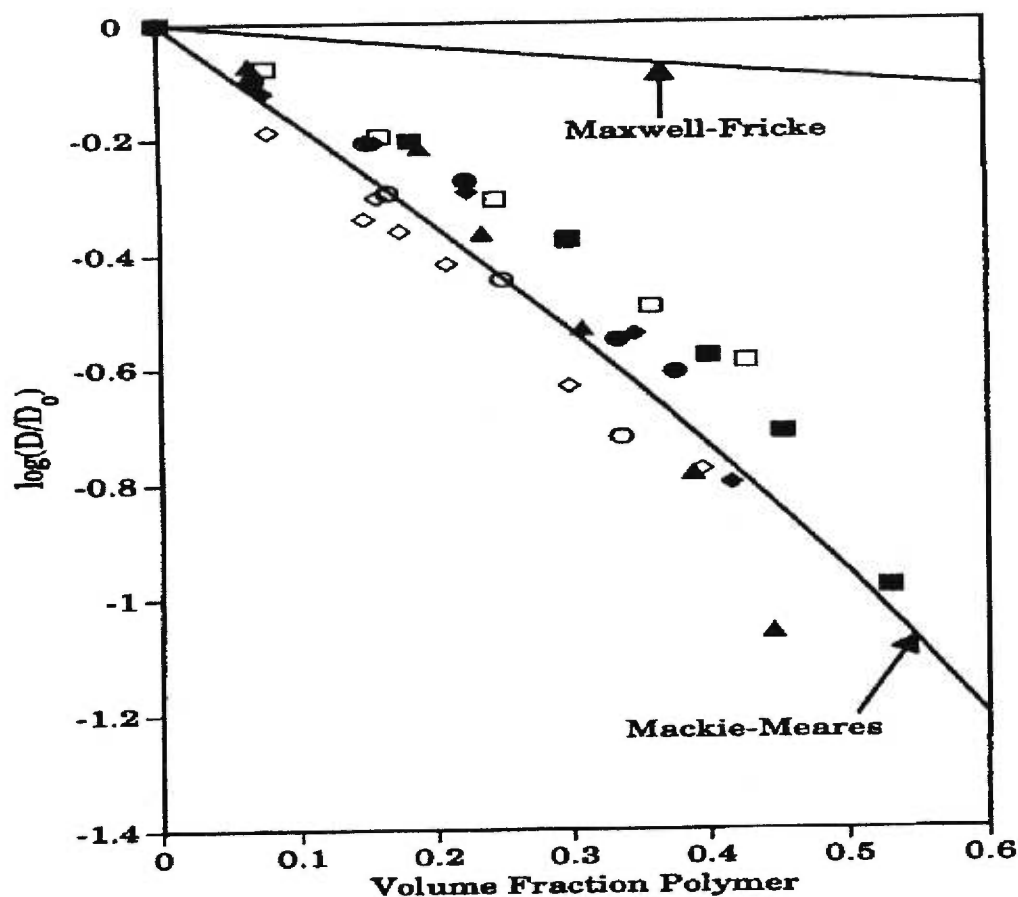


Figure 1.1. Semilogarithmic plot of solvent self-diffusion coefficient as a function of the polymer concentration: closed diamonds, toluene-PS; closed triangles, *tert*-butyl acetate-PS; closed circles, ethylbenzene-PS; open circles, cumene-PS; closed squares, chloroform-PS; open triangles, methyl-methacrylate-PMMA; and open squares, methyl ethyl ketone. The prediction of the Maxwell-Fricke model (Eq 1.9) and the model of Mackie and Meares (Eq 1.10) are represented by solid lines. Reproduced with permission from ACS Publications (Waggoner, A. R. *et al.*, *Macromolecules* 1993, 26, 6841).³⁶

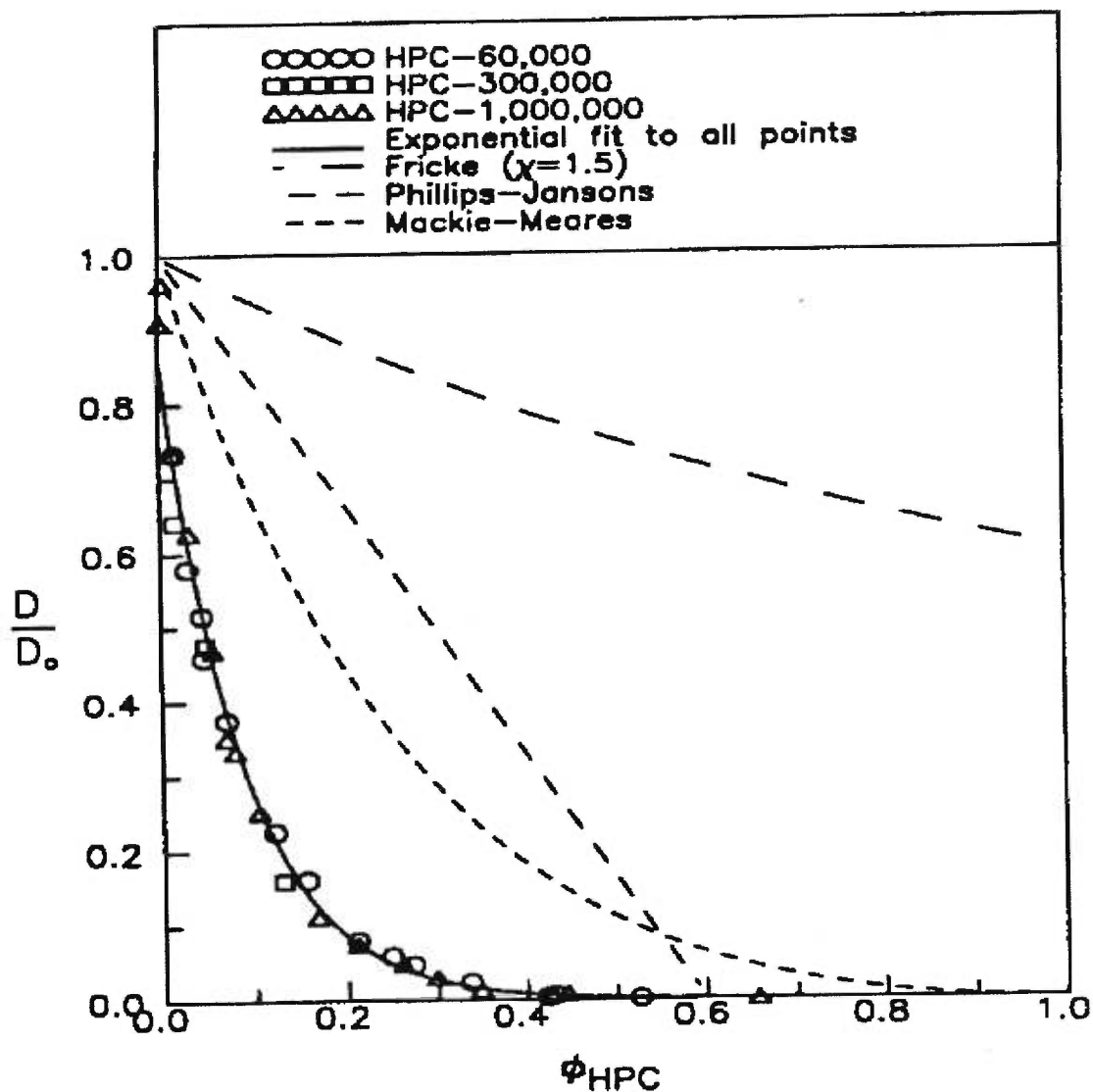


Figure 1.2. Normalized self-diffusion coefficient of fluorescein dye as a function of the polymer volume fraction. Reproduced with permission from ACS Publications (Mustafa, M. B. *et al.*, *Macromolecules* 1993, **26**, 370).³⁵

Remarque: dans le carré au dessus du graphe, il faut lire Phillips-Jansons et non Phillips-Jansons.

1.3.1.2. The model of Mackie and Meares

In 1955, Mackie and Meares⁶⁸ employed the physical concept proposed by Fick to describe the diffusion of electrolytes in a resin membrane, assuming that the polymer mobility is less important than the mobility of ions or water, so that sites occupied by the polymer are permanently unavailable to ions or water. Thus, the motionless polymer chains impose a tortuosity or an increase in the path length for the molecules in motion. The diffusion coefficient of a small molecule, equal in size to the monomer segment in the polymer, is given by the following equation:

$$\frac{D}{D_0} = \left[\frac{1-\phi}{1+\phi} \right]^2 \quad (1.10)$$

where D , D_0 and ϕ are the same as defined for Eq 1.9.

This model provided satisfactory results over a wide range of concentrations (up to 60 wt % of cellulose) as shown by Brown and coworkers.⁶⁹⁻⁷¹ Their work was based upon a series of diffusants with increasing size: water, *tert*-butanol, dioxane,⁶⁹ ethylene glycol, poly(ethylene glycol), oligosaccharides and poly(hydric alcohol).⁷⁰ In each case, they analyzed the data in regard to the model of Mackie and Meares. These studies led to the conclusion that the diffusion of small-sized diffusants can be described by this obstruction model, while for oligomers and polymers they observed a weaker correlation between the experimental data and the theory. The authors attributed this divergence to the interactions between the larger diffusants and the polymer chains. In a later work, Brown *et al.*⁷¹ studied the diffusion of diffusants with increasing size such as ethylene glycol and 15-crown-5 ether in cellulose gels. The results were analyzed with the model of Mackie and Meares and another similar model defined by Wang:⁷²

$$\frac{D}{D_0} = 1 - \alpha\phi \quad (1.11)$$

where α is a parameter depending on the diffusant geometry (1.5 for prolate and 3 for oblate ellipsoids). This model is also based on the obstruction effect and is generally used to describe diffusion in microemulsion systems.^{35,73} Despite the introduction of a diffusant shape parameter, comparison between these two models led to the

conclusion that Wang's model was valid only for small diffusants in the dilute regime, whereas the model of Mackie and Meares was valid for regimes slightly more concentrated.⁷¹ However, their results showed that neither model is in good agreement with the data in the concentrated regions. The divergence is smaller with the model of Mackie and Meares in semi-dilute regime but keeps on increasing with higher polymer concentration.⁷¹

The model of Mackie and Meares has provided satisfactory results for the diffusion of molecules of various sizes in cellulose networks with polymer concentration up to 60 wt % as well as for the diffusion of organic solvents in PS and PMMA, as shown in Figure 1.1. However, this model showed significant deviations from the experimental data with large diffusants in polymer solutions as demonstrated by several researchers.^{34-36,65} An example is provided in Figure 1.2. In addition, Eq 1.10 does not provide diffusant size or shape dependence either, as in the case of Eq 1.9 discussed in Section 2.1.1.

1.3.1.3. The model of Ogston *et al.*

In order to provide a theoretical explanation for the empirical equation of Laurent and coworkers,^{74,75} which relates the sedimentation of proteins in hyaluronic acid solutions, Ogston *et al.*⁷⁶ developed an approach for the diffusion of larger diffusants. The authors considered the polymer as barriers formed by a random distribution of long molecular fibers. Consequently, the self-diffusion coefficient for a given diffusant molecule depends both on the size of the obstacle present in the solution and on the size of the diffusant, as shown in the following equation

$$\frac{D}{D_0} = \exp\left[-\frac{R_h + \rho}{\rho} \phi^{1/2}\right] \quad (1.12)$$

where ϕ represents the volume fraction of the polymer, R_h the hydrodynamic radius of the diffusing molecule and ρ defines the effective cylindrical radius of the fiber. Diffusing molecules are considered as non-perturbing for the network. Therefore, this model should be applicable to polymer solutions and gels. Nevertheless, their data showed different results depending on the polymers employed (dextran and hyaluronic

acid).⁷⁷ They attributed these differences to the morphology of the polymers, i.e., the rigidity and/or thickness of the polymer chains.

According to Johansson *et al.*,⁷⁷ the differences observed by Ogston and coworkers were due to differences in the flexibility of the polymer chains. In a companion paper, they showed that the phenomenological approach of Ogston *et al.*⁷⁶ did not give consistent explanation in regard to their experimental results.³¹ They demonstrated that the model of Ogston *et al.* remained valid for dilute or semi-dilute polymer solutions. This conclusion is in agreement with several other studies.^{26,38,78} For example, Petit⁷⁸ showed that the model of Ogston *et al.* did not provide satisfactory results for large molecules despite the introduction of parameters related to the sizes of both the solute and the polymer. The deviation is more pronounced for concentrated polymer solutions.

1.3.1.4. The hard sphere theory

In order to expand the approach of Ogston *et al.*⁷⁶ to flexible polymers, Johansson and coworkers^{31,79} elaborated a new diffusion model for spherical solutes in polymer solutions and gels. This model was based upon three main assumptions: (1) steric hindrance is the cause of the reduction of solute diffusion, and hydrodynamic interactions are negligible in the polymer solutions and gels; (2) the steric hindrance is caused by the static network, not by the interaction with diffusing species; (3) the structure of the network is decomposed into a set of cylindrical cells and the contribution from each cell to the diffusion coefficient is determined by the distribution of spaces in the network.³¹

In this model, the hindrance due to the polymer chains is considered to depend not only on the size of the diffusant and the amount of polymer but also on the properties of the polymer chains, i.e., their thickness and stiffness.³¹ Basically, they regarded the diffusion quotient, D/D_0 , as the result of local flows in microscopic subsystems. Consequently, in order to quantify the hindrance of the polymer chains, the authors evaluated by the use of computational methods the closest distance (R)

between a point in the network and the fiber, which is represented as a cylindrical cell. According to the computational modeling, the diffusion coefficient is given by

$$\frac{D}{D_0} = e^{-\alpha} + \alpha^2 e^{\alpha} E_1(2\alpha) \quad (1.13)$$

where α is a parameter related to the physical properties of both the polymer and the diffusant:

$$\alpha = \varphi \frac{(R_h + \rho)^2}{\rho^2} \quad (1.14)$$

where φ is the volume fraction of the network, ρ is the polymer radius and R_h the hydrodynamic radius of the diffusant. In Eq 1.13, E_1 is an exponential integral:

$$E_1(x) = \int_x^{\infty} \frac{e^{-u}}{u} du \quad (1.15)$$

Application of this model provided good results for the diffusion of albumin, $M \cong 69\,000$ dalton,⁸⁰ in hyaluronic acid and dextran solutions and gels, $\varphi = 0.004$ and 0.006 , respectively.³¹ Several simulations⁸¹⁻⁸³ of the hard sphere theory were made and limitations of the model were shown. For example, the theory failed when the authors attempted to simulate the self-diffusion coefficients of diffusants with increasing radius (5–30 Å) for a fixed polymer radius of 5 Å and a given persistence length of 200 Å.⁸¹ In fact, Eq 1.13 does not fit Brownian dynamic simulations of spheres when the diffusant radius was above 20 Å (Figure 1.3). Moreover, the authors were unable to provide an interpretation concerning the parameter α (Eq 1.14), which depends on the volume fraction and radius of the polymer as well as the hydrodynamic radius of the diffusant. The correlation between the theory and the simulation is good for low α , but discrepancy appears especially for higher values of α which correspond to large-sized diffusants.⁸¹ The model also failed for nonionic micelles systems in ionic polymers.⁸³

Zhang and Lindman⁸⁴ reported the application of the obstruction model of Johansson and coworkers^{31,79} for the diffusion of micelles in cellulose solutions ($\varphi < 2$ wt %). The obstruction due to the polymer was predicted correctly by the model. This diffusion study was carried out only in very dilute polymer concentrations. Bu

and Russo³⁹ tried to interpret their diffusion data of dextran in 1 wt % hydroxypropyl cellulose solutions with the hard sphere theory. They found that the model of Johansson *et al.*^{31,79} underestimated the diffusion coefficient at larger R_h . They concluded that the diffusants were structurally too complex to agree with Eq 1.13. Other discrepancies with the hard sphere theory were also found in the literature.^{28,85}

1.3.1.5. Summary

It appears that all the obstruction effect models can fit self-diffusion coefficient data of small molecules in dilute or semi-dilute polymer solutions. We would like to point out that other theories, such as the models of Laurent *et al.*,⁸⁶ Jönsson *et al.*,⁸⁷ Hanai⁸⁸ and Phillips and Janssons⁸⁹ (see Figure 1.2 for example) were also proposed. Their applicability is similar to those described in this section.^{37,64,90} The uses and constraints for the models described in this section are summarized in Table 1.1.

Several self-diffusion studies in polymer solutions and gels have led to similar conclusions concerning the model of Mackie and Meares and the Maxwell-Fricke model.^{35,36,65} The phenomenological approach of Ogston *et al.*⁷⁶ for larger molecules and the hard sphere theory failed at high polymer concentrations when hydrodynamic interactions became non-negligible.²⁸ In a study of self-diffusion in aqueous solutions of PVA, Petit *et al.*³⁴ demonstrated that the diffusion behavior of very small molecules such as water and methanol can be described by the obstruction models. But the same study showed that the theoretical prediction by the model of Mackie and Meares⁶⁸ deviates progressively from the experimental data with increasing diffusant size. Even for small diffusants, problems arose when the polymer concentration was high.

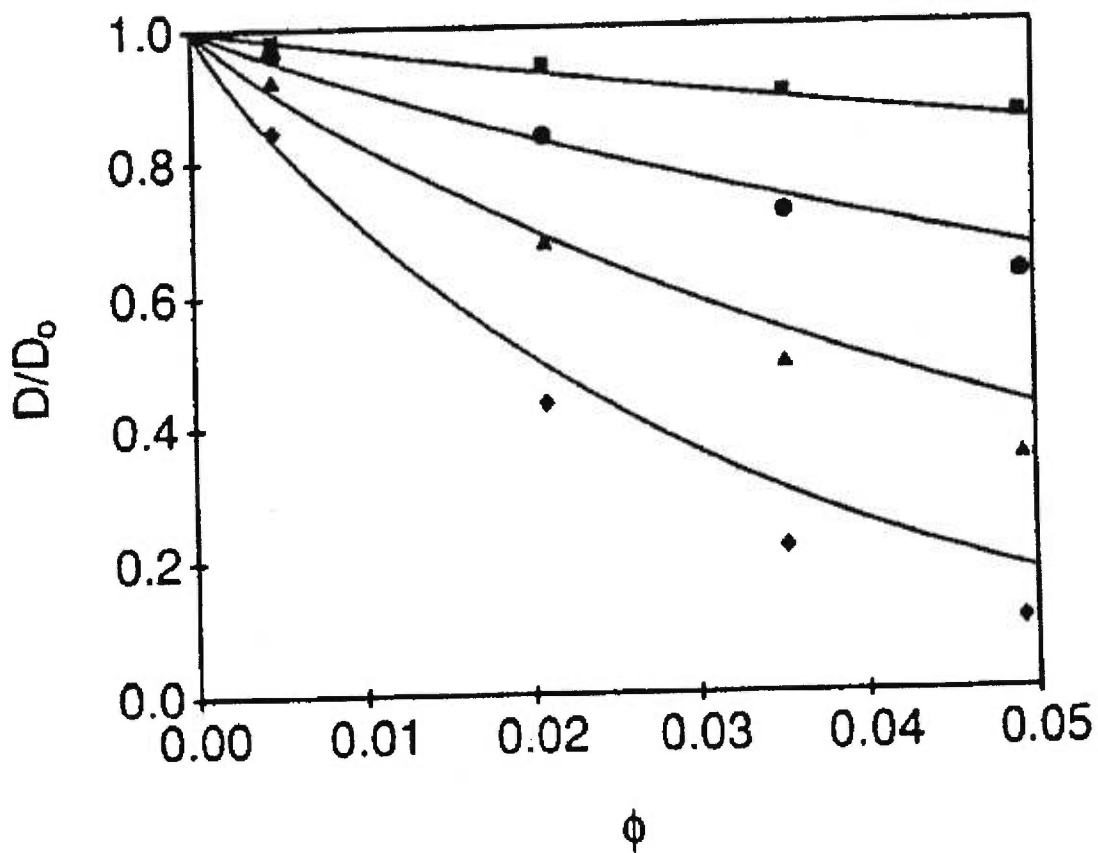


Figure 1.3. Simulation of D/D_0 versus the polymer volume fraction for particles with 5 Å (squares), 12 Å (circles), 20 Å (triangles) and 30 Å (diamonds). The solid lines are the predictions with the hard sphere theory (Eq 1.13). Reproduced with permission from Johansson, L. & Löfroth, J.-E., "Diffusion and interaction in gels and solutions. 4. Hard sphere Brownian dynamics simulations", *Journal of Chemical Physics* **98**(9) May 1, 1993, pp.7471-7479. Copyright 1993 American Institute of Physics.⁸²

Table 1.1. Summary of the diffusion models based on obstruction effect (Section 1.3.1) with their applicability and restraints.

Author(s)	Ref(s).	Application(s)	Limitation(s)
Maxwell-Fricke	25	- Solvents and small-sized diffusants - Very dilute polymer solutions	- Large diffusants - Semi-dilute and concentrated polymer solutions
Mackie and Meares	68	- Solvents and small-sized diffusants - Semi-dilute polymer solutions	- Large diffusants - Concentrated polymer solutions
Ogston <i>et al.</i>	76	- Solvents and small-sized diffusants - Semi-dilute polymer solutions	- Large diffusants - Concentrated polymer solutions
Hard sphere Theory	31, 79	- Solvents and small-sized diffusants - Semi-dilute polymer solutions	- Diffusant with $R_h > 20 \text{ \AA}$ - Concentrated polymer solutions

1.3.2. Hydrodynamic theories

The hydrodynamic theories take into account the hydrodynamic interactions present in the whole system. These interactions include frictional interactions between the solute and the polymer, likely the most important ones, between the solute and the solvent, and also between the solvent and the polymer. Such considerations allow the description of the diffusion process in more concentrated regimes when the polymer chains start to overlap, which seemed difficult with the obstruction models.

1.3.2.1. Cukier's model

In 1984, Cukier²⁶ developed an equation to describe the diffusion of Brownian spheres in semi-dilute polymer solutions based upon hydrodynamic interactions. In this theory, the semi-dilute solution was considered as a homogeneous monomer unit environment as the polymer coils overlap, in comparison to the dilute solutions where the polymer chains do not interact with each other (Figures 1.4A). In fact, the whole semi-dilute solution was viewed as a uniform solvent-polymer mixture. The dilute solution was considered as an inhomogeneous system composed of both polymer-solvent and pure solvent domains.²⁶ This semi-dilute solution of the polymer was approximated as motionless relative to the diffusing solvent, and represented by randomly distributed spheres immersed in an incompressible Navier-Stokes fluid. Thus, the diffusant was considered to undergo screening effects due to the overlapping of the polymer chains, and its diffusion coefficient follows

$$D = D_0 \exp(-\kappa R_h) \quad (1.16)$$

where κ represents the screening hydrodynamic interactions between the polymer and the solute in a semi-dilute polymer solution, and R_h is the hydrodynamic radius of the diffusing sphere. The screening parameter relates the resistance of the polymer network to the diffusion of the remaining molecules, i.e., solvent(s) and diffusant particle(s). For dilute polymer solutions, assuming that screening remains dominated by hydrodynamic interactions, Eq 1.16 can be rewritten as

$$\frac{D}{D_0} = 1 - \kappa R_h \quad (1.17)$$

Cukier compared screening effects between rod and coil polymer solutions for the diffusion of Brownian spheres of radius R , but basically no difference was found. In the case of rod-like polymer molecules, the screening parameter was found to have the following relationship

$$\kappa_L^2 = \frac{\xi_L n_L}{\eta} \quad (1.18)$$

where ξ_L is the friction coefficient for one rod, n_L the number density of rod-like polymer molecules and η the solution viscosity. The rod friction coefficient depends on the length and diameter of the rod (L and b , respectively, with $L \gg b$):

$$\xi_L = \frac{6\pi\eta(L/2)}{\ln(L/b)} \quad (1.19)$$

Similar to Eq 1.18, the dependence of the screening parameter for coil-like polymer molecules can be written as

$$\kappa_D^2 = \frac{\xi n_a^*}{\eta} = 6\pi n_a^* a \quad (1.20)$$

where n_a^* is the monomer number density and a the monomer radius.

In semi-dilute solutions and with small-sized diffusants (R_h smaller), a dependence was found with the polymer concentration: $\kappa \sim c^\nu$ with $\nu = 1/2$, but not with the geometric factors of the polymer.

This model was initially elaborated with theoretical considerations and calculations. It was employed often in the literature.^{40,91,92} Mel'nichenko *et al.*⁹¹ studied tracer self-diffusion of water in moderately concentrated hydrogels. The results were found to be in agreement with the theory. More recently, the same research group presented evidence that Cukier's model remained valid for water self-diffusion in polyacrylamide (PA) and silica gels.⁹² These studies showed clearly the validity domain of Cukier's model: diffusion of small diffusants in semi-dilute networks, i.e., semi-dilute polymer solutions and slightly cross-linked gels. Limitations were shown when the model was used for large-sized diffusants such as

polymers or proteins. For example, Park *et al.*⁴⁰ showed that Eq 1.16 is not applicable for protein diffusion in PA gels. This conclusion was corroborated by the work of Lodge and coworkers^{41,42} who studied the diffusion of linear and star-branched polystyrene in poly(vinyl methyl ether) (PVME) gels and by Johansson and co-workers,^{31,79} who studied diffusion of albumin in hyaluronic acid and dextran gels.

The screening parameter which was found to depend with the polymer concentration (c^v), have been shown to vary in different studies^{93,94} as noted by Cukier.²⁶ Freed and Edwards⁹³ obtained an exponent equal to 1 for c for an ideal chain, defined as a polymer chain in an undiluted polymer solution without entanglements. This result was re-examined by de Gennes,⁹⁴ who described the stochastic motion of long flexible chains in good solvents and concluded that in such systems the diffusion coefficient should scale with $c^{3/4}$. Other works listed in Table 1.2 reported values between 0.5 and 1.

Table 1.2. List of the parameters found in the literature for the hydrodynamic equations in the form of $D = D_0 \exp(-\alpha c^v)$.

Author(s)	Ref.	α	v
Cukier	26	$\propto R_h^{-1}$	0.5
Laurent <i>et al.</i>	95	$\propto R_h^{-1}$	0.5
Freed and Edwards	93	$\propto R_h^{-1}$	1
Brown and Stilbs	96	$\propto R_h^{-1}$	1
De Gennes	94	$\propto R_h^{-1}$	0.75
Altenberger <i>et al.</i>	97	$\propto R_h^0$	0.5
Ogston <i>et al.</i>	76	$\propto (R_h + \rho)/\rho$	0.5
Matsukawa and Ando	98	—	0.71

All the studies showed that the self-diffusion coefficient of a diffusant in a polymer solution is closely related to the polymer concentration. However, the exponent of the polymer concentration dependence is not a simple constant value and disagreement remains.

1.3.2.2. The model of Altenberger *et al.*

Altenberger *et al.*⁹⁷ described the rigid body of the polymer as immobilized points randomly distributed in a solution. The solvent is considered as an incompressible Newtonian fluid, filling the space between these points. A small molecule present in the solvent will interact with these points which represent the network. Thus, the hydrodynamic interactions are represented by the friction with the stationary points. The mobility of a diffusant will depend on the concentration of the obstacle, i.e., the polymer. At low concentrations (dilute or semi-dilute regimes) the interactions are weak and the diffusion coefficient is given by

$$D = D_0 \exp(-\alpha c^{1/2}) \quad (1.21)$$

where α is a parameter depending on the diffusing particle, and c represents the number concentration of obstacle (the polymer). Eq 1.21 is a generalization of a previous prediction elaborated by the same research group also based on hydrodynamic interactions⁹⁹

$$\frac{D}{D_0} = 1 - A c^{1/2} - B c + \dots \quad (1.22)$$

where A is proportional to the diffusant radius, and B defines a constant that relates to the interactions between the polymer network and the diffusant particle.

These two equations (Eqs 1.21 and 1.22) bear resemblance to the equations defined by Cukier (Eqs 1.16 and 1.17). Kosar and Phillips¹⁰⁰ demonstrated that Eqs 1.16 and 1.21 are mathematically equivalent, although derived differently. But the authors predicted a larger validity domain than that of Cukier's (*higher obstacle concentration and/or for particles which interact strongly with the solvent*). Several studies showed that this model had similar limitations in its applications.⁴⁰⁻⁴² Petit *et al.*³⁴ also showed that these models were less satisfactory in the interpretation of

diffusion data of large molecules such as PEG-4000 in PVA solutions. The motion of larger diffusants can happen on the same scale as the motion of the polymer networks.⁷⁸ The applicability of these two models seems to be limited to small molecules as in the case of the obstruction models (Section 2.1)

1.3.2.3. Phillies' model

A more phenomenological approach was used by Phillies^{52,101,102} to describe the self-diffusion behavior of macromolecules (polymer and protein) over a wide range of concentrations. The stretched exponential equation was proposed based upon numerous experimental data from his own research as well as those from the literature.⁵² According to his observations, the polymer self-diffusion coefficient obeys a scaling law

$$D = D_0 \exp(-\alpha c^\nu) \quad (1.23)$$

where α and ν represent the scaling parameters which should depend on the molecular weight of the diffusant polymer. Experimentally, α was found to depend on the diffusant molecular weight ($\alpha \sim M^{0.9 \pm 0.1}$) for macromolecules, whereas α depends on the diffusant hydrodynamic radius ($\alpha \sim R_h$) for smaller molecules.^{102,104,105} The scaling parameter ν should scale between 1 for low molecular weight diffusant and 0.5 for high molecular weight diffusant.¹⁰¹ Inside these limits $\nu \sim M^{-1/4}$.¹⁰¹ Phillies considered the three regimes of concentrations (Figure 1.4) defined for reptation theories, i.e., dilute solution where polymer chains move independently, semi-dilute solutions where polymer chains start to overlap, and concentrated solutions where diffusion is dominated by polymer friction. These regimes can be regarded as close to the polymer solutions regimes examined by Cukier (Section 1.3.2.1), where forces in solution were defined as predominantly hydrodynamic for the last two regimes (Figures 1.4B and 1.4C). Nevertheless, an important difference between this model and the former ones is that the polymer chains are regarded here as mobile and are described as spheres joined by rods that can rotate as defined by Kirkwood and Riseman.¹⁰³

In his following publications, Phillies developed theoretical arguments for Eq 1.23.^{101,102} The stretched exponential equation is based on the following assumptions: (1) *the self-similar effect of infinitesimal concentration increment on D* ; (2) *the functional form for hydrodynamic interactions between mobile polymer chains*; (3) *the dependence of chain extension on polymer concentration*.¹⁰¹

The first assumption means that an infinitesimal increase of the concentration dc increases the drag coefficient of the diffusant from f to $f+Kdc$ (K may be concentration dependent). This assumption is based on the fact that the polymer self-diffusion coefficient is related to its drag coefficient, f , by the Einstein relation

$$D = \frac{k_B T}{f} \quad (1.24)$$

where k_B is the Boltzmann constant and T the temperature. The polymer should retard the diffusant and increase the drag. The drag coefficient of the solution that already exerts a retard on the diffusant particle should be more important. The second assumption considers that the polymer-polymer interactions are mainly in hydrodynamic modes rather than in entanglement modes. Nevertheless, Eq 1.23 does not provide a screening effect parameter because the polymer chains were regarded as mobile, thus no fixed sources of frictional interactions were present in the solution. In fact, polymer chains in solution will reduce both the flow rate and the molecular diffusion as the chains rotate. Moreover, the polymer chains will create an echo phenomenon responsible for fluctuation on the whole polymer system. The final approximation, based on Daoud law¹⁰⁶ for a large polymer in semi-dilute regimes, stipulates that the polymer chains contract under the overlap concentration: $R_g^2 \approx M c^{-x}$ where x is a parameter. As results of these presumptions, ν should range between $\frac{1}{2}$ for large polymers to 1 for small polymers, and inside these limits, $\nu \sim M^{-1/4}$ for a given diffusant.¹⁰¹ Macromolecular self-diffusion coefficient can be described by the stretched exponential equation (Eq 1.23) with $\alpha \sim M$ and ν as stipulated above.¹⁰¹

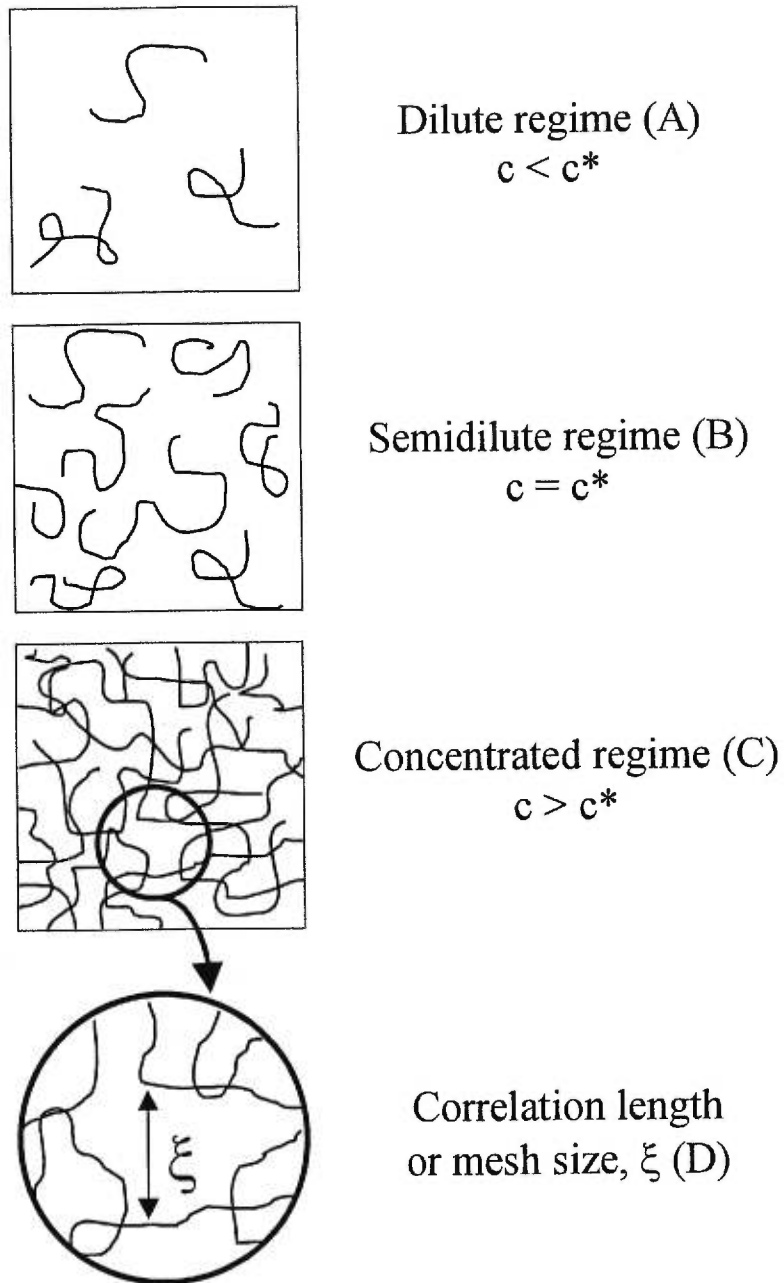


Figure 1.4. Representation of the dilute (A) semi-dilute (B) and concentrated (C) regimes of polymer solution as well as the correlation length in the concentrated regime (D).

Such an equation has already been employed to describe other physical transport phenomena such as sedimentation of large colloidal particles through a semi-dilute polymer solution,¹⁰⁷ electrophoretic mobility⁴³ and viscosity.¹⁰⁸ Thus, Eq 1.23 can be considered as a “universal” equation, as named by Phillies, because it can be employed for different physical transport phenomena. This equation is very flexible in nature. Walderhaug *et al.*⁴⁴ and Wheeler and Lodge⁴⁵ pointed out that it should be regarded as an empirical equation.

Phillies investigated the applications of the universal equation to numerous experimental data from the literature and found good agreements of the equation with the data for various polymer systems.^{101,109,110} Similarly, several publications showed excellent fits of the experimental data with Eq 1.23.^{40,45-48,111,112} These articles reported the diffusion of large diffusants in dextran gels,^{46,47} PA gels,⁴⁰ associative polymers,^{48,112} and the diffusion of linear and star branched PS in PVME gels^{45,111} over large ranges of concentrations. In addition, this equation was also employed successfully to describe self-diffusion data of small diffusants in PA gels⁴⁰ and in PVA solutions and gels.³⁴ However, Won *et al.*⁴⁹ reported deviations from the equation for PS sphere tracer diffusion in PVME solutions at higher polymer concentrations.

It was argued, however, that the physical meaning of the parameters α and ν in the various systems remains vague, and the lack of theoretical justifications was underlined in the literature.^{34,40,43-51} Phillies suggested that α varies with R_h/a_0 for the polymer diffusant, where R_h is the hydrodynamic radius of the diffusant and a_0 is defined as the distance of closest approach between the solute and the polymer bead.¹⁰⁴ Other estimations of α led to slightly different results as shown in Table 1.3. Masaro *et al.*¹¹⁶ used Eq 1.23 to analyze the diffusion data of PEG in PVA solutions and gels. Eq 1.23 provided good fits to the experimental data, but attempts to relate the scaling parameters with the physical properties of the system (such as diffusant size) were not successful. These results are corroborated by several reports in the literature.^{34,40,43-51} In addition, analyses of variable temperature diffusion data showed that the scaling parameters are not temperature-dependent. An Arrhenius dependence

of D_0 on the temperature was found. The results are different from the temperature dependence of the scaling parameters found by Phillis.

Recently, Phillis *et al.*^{105,117} reported on the applicability of this hydrodynamic scaling model for high molecular weight polymers over small and large concentrations. From these studies, it seems clear that the stretched exponential form can fit easily diffusion data in solution-like systems whereas a power law is more appropriate to fit diffusion data in melt-like systems, which correspond to very concentrated polymer solutions. The boundary between solution-like to melt-like systems was estimated to be in the order of $M \approx 10^6$ g/mol in the case of polystyrene (Figure 1.5).¹¹⁷

Table 1.3. Dependence of parameter α on the hydrodynamic radius of the diffusant obtained in the literature for Phillis' diffusion model (Section 1.3.2.3)

$$D = D_0 \exp(-\alpha c^\nu)$$

Author(s)	Ref(s).	α	δ
Phillis	52,101,102	R_h^δ	0 ± 0.2
Phillis	104	R_h^δ / a_0	1
Park <i>et al.</i>	40	$3.03 \times R_h^\delta$	0.59
Gibbs and Johnsson	113	$3.2 \times R_h^\delta$	0.53
Russo <i>et al.</i>	114	R_h^δ	0
Yang <i>et al.</i>	115	$R_h^\delta M^{0.76}$	0
Furukawa <i>et al.</i>	46	$MP^{1/2}$	–

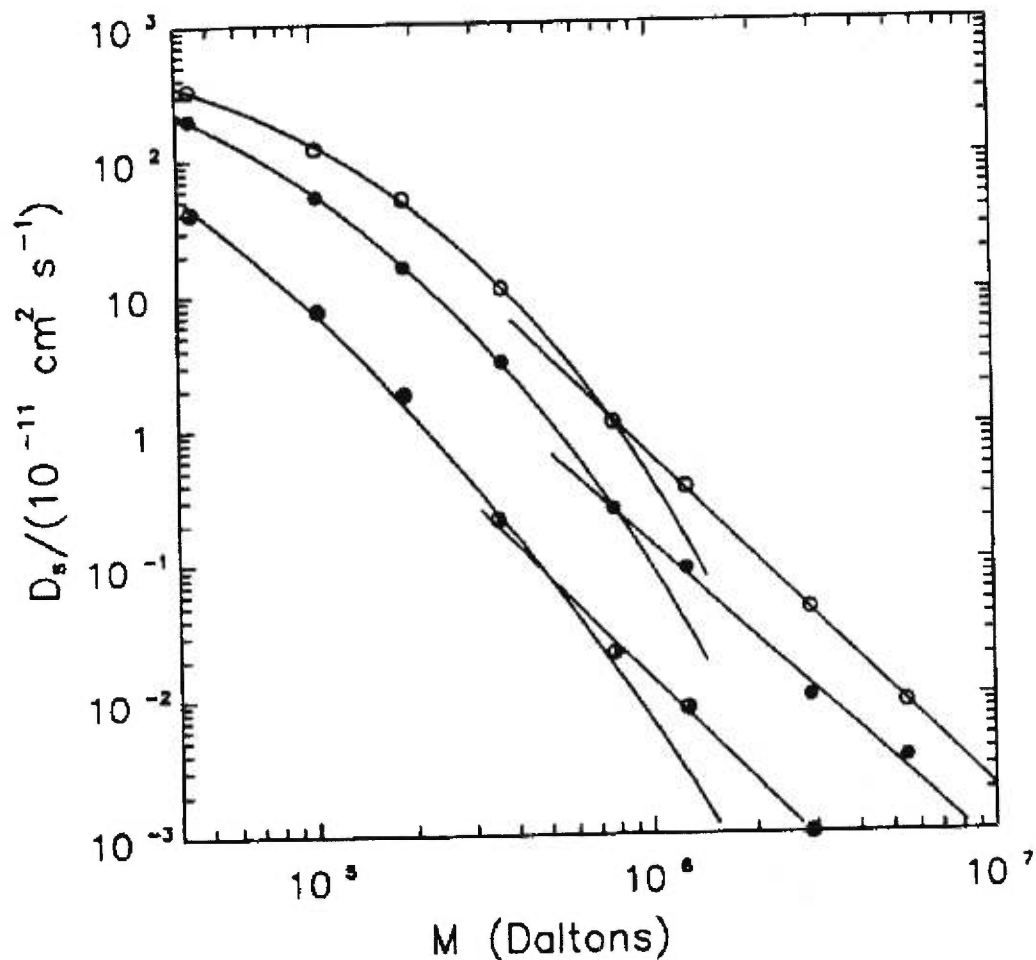


Figure 1.5. Logarithmic plots of self-diffusion coefficients of PS in dibutyl phthalate as a function of the molecular weight of PS at various polymer concentrations: 13 g % (open circles), 18 g % (filled circles) and 40.6 g % (half-filled circles). Curved lines represent fits to the stretched exponential equation (Eq 1.23) while straight lines correspond to power laws. Reproduced with permission from ACS Publications (Phillies, G. D. J., *J. Phys. Chem.* 1992, **96**, 10061).¹¹⁷

1.3.2.4. The reptation and reptation plus scaling models

The reptation theory was first introduced by de Gennes¹¹⁸ who discussed the self-diffusion of a polymer chain of molecular weight M moving inside a three-dimensional network of polymer chains of molecular weight P , which is considered as a gel. This theory was complementary to the works of Rouse¹¹⁹ and Zimm,¹²⁰ who had studied the stochastic motion of a single polymeric chain dissolved in a solvent of low molecular weight.¹¹⁸

In the reptation theory, the diffusing polymer chain is regarded as constrained by fixed obstacles that represent the gel chains. As the polymer chain is surrounded, the leading motions of the polymer chain are feasible only at the extremities. Thus, the motion of the central part of the polymer chain takes place when the extremity enters inside a new tube. Consequently, the central part of the polymer chain remains confined between the same fixed obstacles for a longer time in comparison to the extremity of the polymer chain. Thus, this part of the polymer chain is said to remain in a tube formed by the neighboring polymer chains.¹²¹ Therefore, only “tubular” motion is conceivable and lateral motion is not considered, as long as the diffusant polymer is enveloped by the network. Brownian motion for high molecular weight polymers in the tube was predicted to depend on their molecular weight:¹¹⁸

$$D \sim M^{-2} \quad (1.25)$$

The diffusion of a high molecular weight polymer in an unentangled system, or a diluted solution, is described by the Rouse model:¹¹⁹

$$D \sim M^{-1} \quad (1.26)$$

Several years later, de Gennes¹²² reexamined the reptation theory in order to introduce the scaling concepts. He took into account of the effect of the matrix on the self-diffusion coefficient of the diffusant. This reexamination led to a new model, the *reptation plus scaling* concept, which is defined by the following equation^{122,123}

$$D \sim M^{-2} c^{(2-\nu)/(1-3\nu)} \quad (1.27)$$

where M is the molecular weight of the diffusant, c the polymer matrix concentration and ν the Flory exponent for the excluded volume.

Eq 1.27 leads to two distinct equations for diffusion in the semi-dilute regime, one for good solvents ($\nu = 3/5$),

$$D \sim M^{-2} c^{-1.75} \quad (1.28)$$

and the second for θ solvents ($\nu = 1/2$):

$$D \sim M^{-2} c^{-3} \quad (1.29)$$

The θ solvent regime corresponds to an exact cancellation between steric repulsion and van der Waals attraction between monomers.¹²³ Thus, the polymer chains do not overlap in θ solvents. This regime corresponds to $c < c^*$ (Figure 4B), where c^* is defined as the critical overlap concentration. In the good solvent regime, the polymer chains tend to swell. Therefore, the polymer chains are densely packed and start to overlap, which corresponds to the concentrated regime, $c > c^*$ (Figure 4C).

Applications of de Gennes' diffusion models are numerous in the literature. Léger *et al.*¹²¹ showed that the dynamics of a linear chain could be described by simple reptation (Eq 1.25). The same correlation was reported by Gent *et al.*,^{124,125} who studied diffusion of *cis*-1,4-polyisoprene into *cis*-polyisoprene networks, and by Antonietti and Sillescu,¹²⁶ who studied PS self-diffusion in bulk PS network by holographic grating technique. Previously, Léger *et al.*¹²⁷ had studied the self-diffusion of labeled PS chains in unlabeled PS chains of the same molecular weight in benzene by forced Raleigh scattering and found reasonable agreement with Eq 1.28. Similar results were obtained by Kim *et al.*¹²⁸ who studied the diffusion of styrene-acrylonitrile copolymers by recoil spectrometry, Pajavic *et al.*¹²⁹ who studied the diffusion of linear polyelectrolyte in gels by dynamic light scattering and von Meerwall *et al.*¹³⁰ who studied PS self-diffusion in tetrahydrofurane by NMR for a concentration above the entanglement concentration and after correction for local frictions. Recently, this model was also employed to explain the disentanglement of polymeric chains during dissolution which led to the definition of a mathematical model for polymer dissolutions.^{131,132} The reptation theory was also used for the electrophoretic separation of DNA in gels.^{38,133-135} The theoretical treatments of the motion of DNA through gels are mainly based on the reptation model. The DNA is pictured as

moving through an impenetrable tube defined by the surrounding gel obstruction, with the motion mediated by a snake-like reptation of the polymer ends.¹³³

Phillies⁵² pointed out that the use of Eqs 1.25 and 1.26 to describe diffusion does not allow an exponential decrease of the diffusant self-diffusion coefficient with respect to the polymer concentration which was frequently observed.^{34,36,65,136} The reptation model led to two distinct regions as shown by Eqs 1.28 and 1.29, one for each concentration regime: $c > c^*$ and $c < c^*$ (Figures 1.4C and 1.4B). The original reptation model of de Gennes considers that the entanglement of the polymer chains occurs at the critical overlap concentration c^* . However, Kavassalis and Noolandi^{137,138} have predicted that the entanglement concentration, c_e , is about 10 times higher than the overlap concentration. In the work of Cosgrove *et al.*,^{53,54} the reptative dependence M^{-2} (Eq 1.25) was not found even for high polymer concentrations but the spin-spin NMR relaxation time and viscosity measurements showed the presence of chain entanglements. Nemoto *et al.*⁵⁵ reported studies of concentrated solutions of linear PS self-diffusion in dibutyl phthalate (M_w from 6 180 to 2 890 000). They interpreted their data by the use of the reptation model (Eqs 1.25 and 1.26) and found good agreement with the model of Rouse (M^{-1}) for low concentrations whereas a power law of $M^{-2.6}$ was found for concentrated solutions instead of M^{-2} . In the study of linear PS (M_w from 32 000 to 1 050 000) diffusion in PVME gels, Rotstein and Lodge⁴¹ reported a power law of $M^{-2.8}$. Yu and coworkers^{56,57} studied diffusion of labeled PS chains (M_w from 32 000 to 360 000) in unlabeled PS-THF systems (with $P = M$), and diffusion of labeled PS chains (M_w from 10 000 to 1 800 000) in PS-toluene systems (with $P/M \geq 3.5$). In both cases, the authors did not observe any concentration scaling. The results from the use of de Gennes' models are summarized in Table 1.4. In a recent work, Cheng *et al.*¹⁴⁹ studied self-diffusion of poly(ethylene oxide) in the melt as a function of the temperature. They showed that the power dependence for high molecular weight diffusants varied between $M^{-2.24}$ (353.7 K) and $M^{-2.75}$ (413.7 K). These values are not in good agreement with the prediction of de Gennes (Eq 1.25) and indicate that de Gennes' reptation model cannot be used to describe the temperature dependence of the diffusion in polymer systems. In addition,

Wheeler and Lodge⁴⁵ studied linear and branched PS diffusion in PVME/*o*-fluorotoluene solutions and observed a large variation of the scaling exponent varying from $M^{-0.56}$ to $M^{-2.3}$ with changes in the matrix concentration, which demonstrate that a simple power law equation is not sufficient to describe the diffusion process. In the same study, Wheeler and Lodge have studied the concentration effect. In concentrated polymer solutions they observed a power dependence of $c^{-3.3}$, close to the predicted value of c^{-3} , whereas in semi-dilute solutions the predicated $c^{-1.75}$ scaling was not observed. Marmonier and Léger¹⁴⁸ noticed that the diffusion coefficient depends on P when the factor P/M is greater than 5.

The limitations in the application of the reptation model were discussed in several publications by Phillies.^{52,101,102} The main conclusion was that *reptation is probably not important for polymer self-diffusion in solution*.¹⁰¹ However, de Gennes' model succeeded in the interpretation of results of diffusion of linear and branched polymers in concentrated polymer matrix solutions,^{45,111} DNA diffusion,³⁸ polymer dissolution,¹³² etc. Nevertheless, some important points should be addressed since no comprehensive illustration based on a molecular theory explains the entanglement phenomenon (the nature of an entanglement and the criteria for the onset of entanglement effects are not established), and no clear explanation concerning the reptation of a single linear chain in dilute solution has been provided yet.^{42,150}

1.3.2.5. The model of Gao and Fagerness

This model is based on measurements of drug (adinazolam) and water diffusion in hydroxypropyl methyl cellulose (HPMC) gels studied by NMR spectroscopy.³² The authors did not elaborate on hydrodynamic arguments, but the form of the equation is very similar to the form of the equations based on hydrodynamic theories.

Table 1.4. Experimental values obtained for the dependence on the molecular weight (M) of the diffusant and polymer concentration (c) in de Gennes' reptation models (Section 1.3.2.4)

Author(s)	Ref(s).	Description	Result
<i>Reptation model: $D \sim M^{-2}$ and $D \sim M^{-1}$</i>			
Klein	139	Polyethylene in bulk	$D \sim M^{-2}$
Bartels <i>et al.</i>	140	Polybutadiene in bulk	$D \sim M^{-2}$
Fleischer ^(a)	141	PS self-diffusion by NMR	$D \sim M^{-2}$
Kumagai <i>et al.</i>	142	PS in bulk	$D \sim M^{-2.7}$
Smith <i>et al.</i>	142	poly(propylene oxides) by fluorescence photobleaching	$D \sim M^{-1.7}$
Antonietti <i>et al.</i>	144	PS by forced Rayleigh scattering	$D \sim M^{-2.2}$
Wheeler and Lodge	45	PS in PVME/o-fluorotoluene	$D \sim M^{-0.56-2.3}$
Yu <i>et al.</i>	56,57	PS in THF	$D \sim M^{-2}$
		PS in toluene (no concentration scaling)	$D \sim M^{-3}$
<i>Reptation plus scaling model: $D \sim M^{-2} c^{-1.75}$ and $D \sim M^{-2} c^{-3}$</i>			
Léger <i>et al.</i>	127	PS in benzene	$D \sim M^{-2} c^{-1.75}$
Schaefer <i>et al.</i>	145	Marginal solvent	$D \sim M^{-2} c^{-2.5}$
Wheeler and Lodge	45	PS in PVME/o-fluorotoluene	$D \sim c^{-3.3}$
von Meerwall <i>et al.</i>	130	PS in THF Without correction for local friction	$D \sim M^{-1.5} c^{-1.75}$
Cosgrove <i>et al.</i>	53	PS in CCl ₄	$D \sim c^{-2.25}$
Callaghan and Pinder	146	PS in CCl ₄	$D \sim M^{-1.4} c^{-1.75}$
Manz and Callaghan	147	PS in cyclohexane	$D \sim c^{-2}$

(a) also valid for molecular weight less than the critical molecular weight, M_c , observed in the melt viscosity.

Gao and Fagerness³² observed exponential decrease of both adinazolam and water diffusion with increasing HPMC concentration. Furthermore, using different HPMC gels with different viscosity grades (100, 4,000 and 15,000 cps), i.e, different molecular weights, they did not observe any effect on the diffusion process. Diffusion measurements in HPMC gels were also carried out in the presence of glucose, or lactose, or maltoheptaose (monomer, dimer and oligomer of the HPMC, respectively), which were defined as viscosity-inducing agent (VIA).³² A significant decrease in the adinazolam self-diffusion coefficient was reported with increasing the size of the VIA in the adinazolam-water-VIA ternary solutions.

Thus, the self-diffusion coefficient of adinazolam was found to depend on the nature of the VIA present in solution as well as on its concentration as illustrated in Figure 1.6. This dependence can be described by an exponential function of the VIA concentration

$$D = D_0 \exp(-K_i c_i) \quad (1.30)$$

where D is the self-diffusion coefficient of adinazolam, i represents the VIA, K_i is a proportionality constant and c_i the concentration of VIA. K_i values for adinazolam were obtained by a linear least square fit of the diffusion data from binary systems. For example, $K_{glucose}$ ($i = \text{glucose}$) is obtain from the diffusion data of glucose-water binary solution.

Gao and Fagerness³² examined also adinazolam diffusion in VIA mixtures. Their results indicated that the diffusivity of this drug in a multi-component system (HPMC and lactose) was influenced by all the components present in the system: VIA, polymer and even the drug concentration (Figure 1.7). This result led to a re-examination of Eq 1.30

$$D = D_0 \exp(-K_H c_H - K_L c_L - K_A c_A) \quad (1.31)$$

where c_H , c_L and c_A are the concentrations of HPMC, lactose and the drug (adinazolam), respectively.

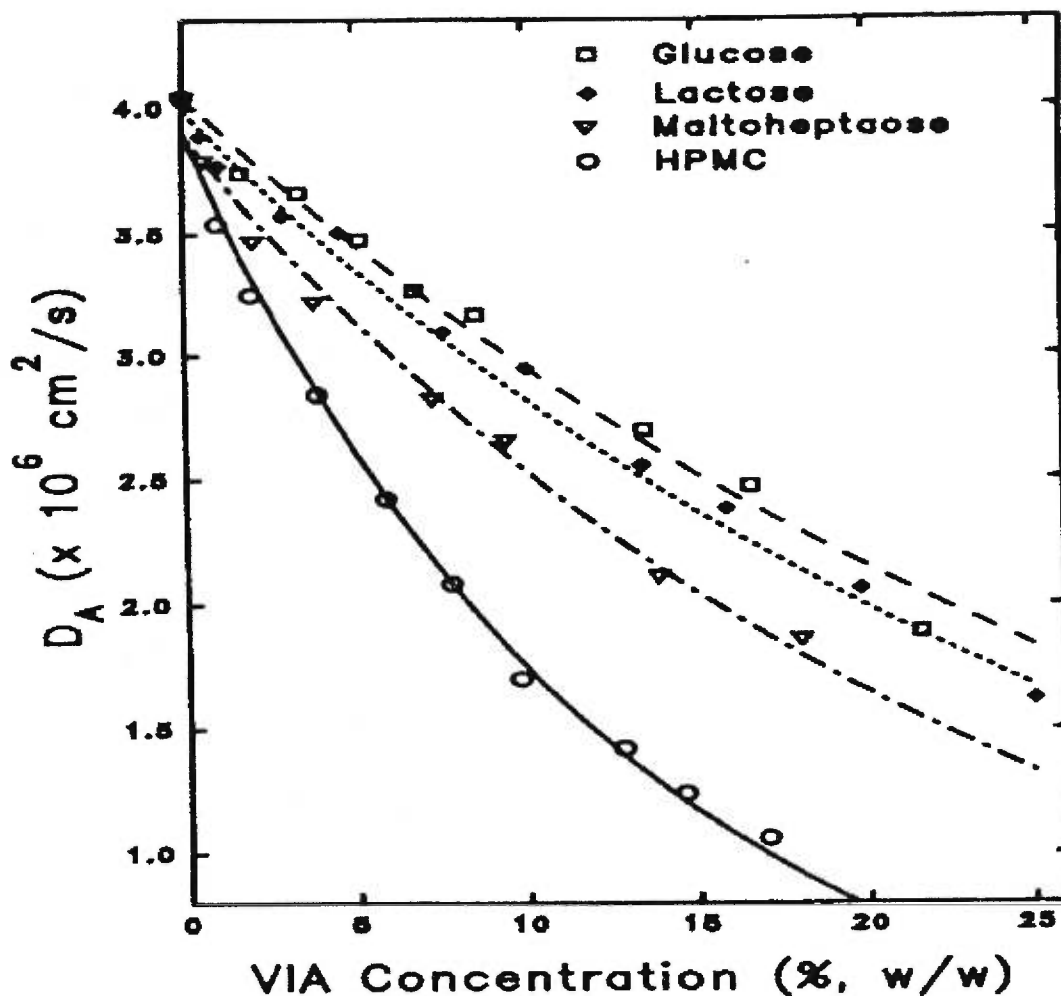


Figure 1.6. Plot of the self-diffusion coefficients of adinazolam as a function of the VIA concentration (w/w, %). The adinazolam concentration is kept constant for each series. Squares, 0.5 % Adinazolam plus x % glucose; diamonds, 0.5 % Adinazolam plus x % lactose; triangles, 0.5 % Adinazolam plus x % maltoheptaose; and circles, 0.5 % Adinazolam plus x % HPMC (4,000 cps). Fits are obtained by the use of Eq 1.30. Reproduced with permission from Plenum Publication Corporation (Gao, P. and Fagerness, P. E., *Pharmaceutical Research* 1995, 12, 955).³²

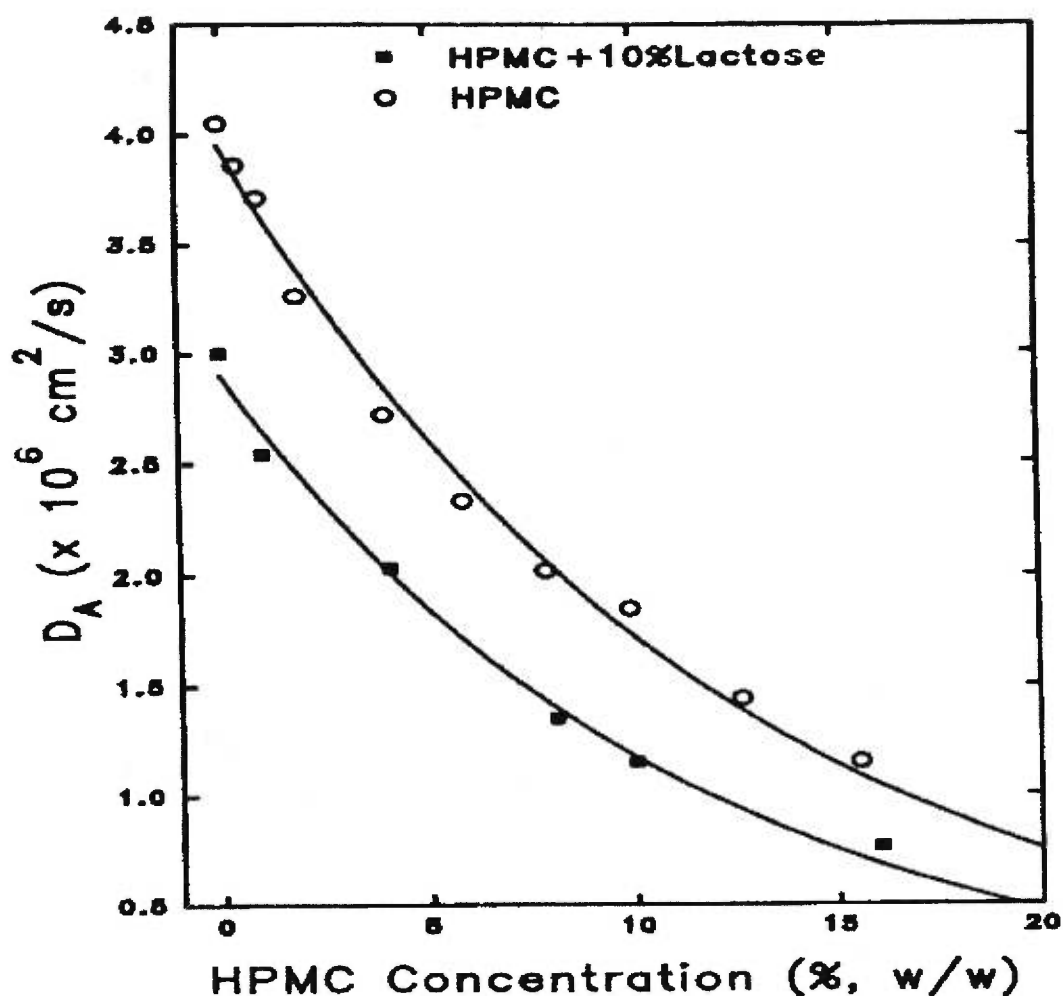


Figure 1.7. Plot of the self-diffusion coefficients of adinazolam as a function of HPMC (10,000 cps) concentration (w/w, %). Open symbols represent the data for 0.5 % Adinazolam plus x % HPMC, and filled symbols represent the data for 0.5 % Adinazolam plus 10 % lactose and x % HPMC. Fits are obtained by the use of Eq 1.31. Reproduced with permission from Plenum Publication Corporation (Gao, P. and Fagerness, P. E., *Pharmaceutical Research* 1995, **12**, 955).³²

Good agreement was found between the measured and the calculated self-diffusion coefficients over a wide range of HPMC concentrations (0–30 wt %). The self-diffusion coefficient dependence on the VIA concentration was also determined successfully. These results lead to the final form of the model³²

$$D = D_0 \exp(-\sum K_i c_i) \quad (1.32)$$

Variable temperature experiments were done between 10 and 50 °C. The activation energy of drug diffusion, E_a , was determined in each of the solutions with a fixed concentration of VIA. The same Arrhenius behavior was observed in these cases, leading to a similar E_a . A comparable result was obtained with water diffusion over the same temperature range.³²

If we consider the specific case of a ternary solution of low concentration of the diffusant ($c_A \ll c_H$) plus solvent and HPMC, the self-diffusion coefficient of the drug will depend only on the polymer concentration, according to this model. Thus the self-diffusion coefficient of the drug can be written as

$$D = D_0 \exp(-K_H c_H) \quad (1.33)$$

which is similar to the equation defined by Freed and Edwards⁹³ for an ideal chain, with $K_H \sim R_h$

$$D = D_0 \exp(-R_h c) \quad (1.34)$$

Moreover, Eq 1.33 represents also a particular circumstance of Phillies' stretched exponential equation with $\nu = 1$ (Section 1.3.2.4).

This model provided good agreements for the diffusion of small molecules such as a drug and water in multi-component systems over a wide range of concentrations at different temperatures. However, the authors did not explain the magnitude of the proportionality constant, K_i , neither its physical meaning nor its dependence on the polymer molecular weight and/or diffusant size. In addition, no relationship between the diffusion coefficient of the drug and the temperature was provided.

In a companion paper, Gao *et al.*¹⁵¹ tried to make predictions of drug release rates in polymer tablets. To reach this goal, they used the Higuchi equation¹⁵² in which they introduced their diffusion model (Eq 1.32) by assuming that *the*

formulations exhibit identical swelling kinetics (medium penetration rate, matrix swelling and erosion) and that the concentration of drug and VIA in the gel layer are proportional to their respective weight concentration in the dry tablet. However, no good agreement was found between the experimental results and the theoretical prediction, although the agreement was good in the previous self-diffusion study.³² This work demonstrated that diffusion in swollen and equilibrated gel is quite different from the drug release from a dry tablet. The self-diffusion studies of already equilibrated systems may be quite different from real time situations such as the release of drugs. It is important to establish correlations between these two diffusion processes.

1.3.2.6. Summary

The major advantages and constraints for the models described in this section are summarized in Table 1.5.

The models of Cukier²⁶ and Altenberger *et al.*,⁷⁷ where the polymer chains are regarded as motionless, can be used to describe the diffusion of small-sized diffusant in semi-dilute polymer solutions. These models cannot be employed to describe solute diffusion in concentrated polymer solutions.

The universal equation proposed by Phillies is a useful equation (simple form, good correlation with experimental data) to fit diffusion data of both small-sized diffusants and macromolecules in all concentration regimes, excepted for melt-like region. This model has a simple equation which generally provides good fits to the experimental data. Further improvements were reported by Phillies and coworkers on the effect of temperature,¹⁵³ glass transition temperature dependence,¹⁵⁴ diffusion under θ and good solvent conditions,¹⁵⁵ a reanalysis of the stretched exponential equation¹⁵⁶ and justifications.¹⁵⁷⁻¹⁵⁹ However, some applications of the model remained obscure. Temperature variation was not supported and the interpretations of the scaling parameters was sometimes contested, even though complementary justifications have been published recently.¹⁶⁰

Table 1.5. Summary of the diffusion models based on hydrodynamic theories (Section 1.3.2) with their applicability and restraints.

Author(s)	Ref(s).	Application(s)	Limitation(s)
Cukier	26	- Solvents and small-sized diffusants - Semi-dilute polymer solutions and highly swollen gels	- Large diffusants - Concentrated polymer solutions
Altenberger <i>et al.</i>	97	- Solvents and small-sized diffusants - Semi-dilute polymer solutions	- Large diffusants - Concentrated polymer solutions
Phillies	52 101 102	- Solvents, small-sized diffusants and macromolecules - Diffusion in solution-like regimes	- Significance of the scaling parameters - Diffusion in melt-like regime ($M > 10^6$)
de Gennes	122 123	- Diffusion of macromolecules in gels and concentrated polymer solutions	- Molecular significance of entanglements - Theoretical prediction not observed even for $c > c^*$
Gao and Fagerness	32	- Diffusion of small-sized diffusants in multi-component systems	- Significance of the main parameters

The reptation model was first introduced to describe diffusion in gels but can also be used in some cases for polymer solutions.¹²⁵⁻¹²⁸ It seems that its application is successful in cross-linked gels, concentrated polymer solutions and melts. It cannot be used in semi-dilute polymer solutions, especially when the entanglement concentration is not reached.¹¹⁶ The use of the reptation equations (Eqs 1.25, 1.26 and eqs 1.27, 1.28) to describe diffusion with respect to the polymer concentration does not reproduce the exponential dependence observed experimentally. In addition, the model cannot describe the temperature dependence, and discrepancy was underlined concerning the power dependence of M and c and the theoretical predictions, as shown in Table 1.4.

The main advantage of the model of Gao and Fagerness³² is that the diffusant concentration is also taken into account. The physical significance of the parameters in this model needs to be elucidated. No other application of the model was found in the literature due to novelty of the model.

1.3.3. Diffusion models based on the free volume theory

The free volume concept in polymer science is well known. The free volume was defined as the volume not occupied by the matter. More generally, the free volume can be specified as the volume of a given system at the temperature of study minus the volume of the same system at 0 K. Thus, rearrangement of the free volume creates holes through which diffusing particles are able to pass through. The free volume is contributed by all the species present in the system, solvent, solute(s) and polymer. The free volume theories are based on the assumption that the free volume is the major factor controlling the diffusion rate of molecules.

1.3.3.1. Fujita's model

The first diffusion model based on free volume theory was proposed by Fujita.²⁷ The measurements were carried out in a ternary system including a solvent, a polymer and a penetrating molecule (a plasticizer). The concentration of the plasticizer was kept low, in comparison with the polymer concentration, thus the

system could be approximated as a pseudo-binary system. Therefore, the average free volume in such a system was contributed by the polymer and the solvent. In order to estimate the free volume, Fujita used the concept of Cohen and Turnbull¹⁶¹ which defines the probability, $P(v^*)$, to find holes of size v^* in a liquid of identical molecules

$$P(v^*) = A \exp\left(-\frac{bv^*}{f_v}\right) \quad (1.35)$$

where A is constant, b a numerical factor of the order of unity and f_v is the average free volume per molecule. The product bv^* is interpreted as the measure of the minimum hole size required for diffusant displacement, B . The diffusion model is based on several assumptions: (1) the diffusion process occurs because of the redistribution of the free volume within the matrix; (2) the redistribution of the free volume does not require energy change; (3) the diffusion process is enabled when the free volume exceeds holes of size v^* ; (4) the self-diffusion coefficient is directly proportional to the probability, $P(v^*)$, of finding a hole of volume v^* or larger adjacent to the diffusant molecule.¹⁶¹

Fujita assumed that Eq 1.35 was valid also in the case of a binary system. Further, the probability that the molecule found in its surrounding a hole large enough to permit displacement is closely linked to the diffusant mobility, m_d

$$m_d = A \exp\left(-\frac{B}{f_v}\right) \quad (1.36)$$

where A is a proportionality factor and B depends only on the particle size but not on the temperature or on the polymer concentration. The definition of the mobility is given by

$$D = RT m_d \quad (1.37)$$

where D is the self-diffusion coefficient of the molecule, T is the temperature and R the gas constant. Finally, substituting Eq 1.36 into Eq 1.37, we have

$$D = ART \exp\left(-\frac{B}{f_v}\right) \quad (1.38)$$

The application of Fujita's free volume theory showed successful correlations between the model and the data in the case of the diffusion of small molecules in semi-

crystalline polymers.¹⁶² Stern and coworkers^{163,164} used Eq 1.38 to fit their data of gas diffusion in polyethylene membranes and concluded that Fujita's model was applicable when the penetrant volume fraction was less than 0.20. Zhu *et al.*^{165,166} showed that self-diffusion of ketone and ester solvents of various sizes and shapes in PMMA solutions can be well described by Fujita's free volume model. Similar results of solvent or tracer diffusion in polymer solutions and gels have appeared in the literature.^{46,163,164,169}

According to Fujita²⁷ and others authors,^{164,170} the free volume theory provided a good agreement with polymer-organic solvent systems whereas polymer-water systems failed because of the numerous interactions between the molecules. Recently, Matsukawa and Ando⁹⁸ studied PEG diffusion in poly(*N,N*-diethylacrylamide)-water system. They showed that Fujita's equation fitted well water diffusion data, whereas for macromolecules such as PEG, the diffusion data was better described by de Gennes' reptation theory. In addition, Xia and Wang¹⁶⁷ showed that Fujita's model is valid only for low polymer volume fractions. Thus, Fujita's free volume model seems to be adequate in the description of the diffusion of small-sized diffusants in dilute and semi-dilute polymer solutions and gels, mostly organic systems.

1.3.3.2. The model of Yasuda *et al.*

Yasuda *et al.*¹⁷¹ examined the free volume theory of diffusion assuming that the free volume of a binary system, as proposed by Fujita,²⁷ mostly depends on the volume fraction of the solvent. This assumption was based on the fact that: (1) the polymer is less mobile than the solvent; (2) the effective free volume was considered mainly as a contribution from the solvent; (3) in practice, the solvent diffusion decreases with increasing polymer concentration. Therefore, the total free volume may be written as

$$f_V = \varphi_S f_S + \varphi_P f_P \approx \varphi_S f_S = (1 - \varphi_P) f_S \quad (1.39)$$

where f_V is the total free volume, f_S the free volume contribution from the solvent, f_P the free volume contribution from the polymer, ϕ_S the volume fraction of the solvent and ϕ_P the volume fraction of the polymer.

Substituting Eq 1.39 into Eq 1.38, and assuming that there is no interaction between the polymer and the diffusing molecule, we can obtain

$$\frac{D}{D_0} = \exp \left[\frac{B}{f_V^*} \left(1 - \frac{1}{1 - \phi_P} \right) \right] \quad (1.40)$$

where f_V^* is the solvent free volume in the polymer solution.

Yasuda *et al.*¹⁷¹ used the free volume theory to treat electrolyte (NaCl) diffusion in polymer systems. They used several swellable polymers derived from methacrylate, such as methyl, hydroxypropyl and hydroxyethyl methacrylate as well as cellulose in different solvents (dioxane, acetone, ethylene glycol, and water mixed with formic acid). The dependence of the diffusion coefficient on the volume fraction of water can be described by this model.¹⁷¹ Matsukawa and Ando¹⁷² studied water diffusion and used this model with success. Other sources of agreement were found in the work by Chen and Lostritto¹⁷³ who studied drug diffusion (benzocaine, with size smaller than the gel mesh size) in highly swollen poly(ethylene-co-vinyl acetate) membranes. Gilbert *et al.*¹⁷⁴ studied protein diffusion (lysozyme, ovalbumin, bovine serum albumin and carbonic anhydrase) in collagen membranes with glass diffusion cells and obtained results in good agreement with the model of Yasuda *et al.*

Petit *et al.*^{34,78} who studied diffusion of various diffusants in PVA-water systems demonstrated that this model works well for small diffusants but gradually deteriorates with increasing molecular size of the diffusants (from oligomers to polymers) especially at high polymer concentrations (Figure 1.8). Similar results were reported by Amsden.²⁸ Hennink and coworkers⁵⁸ studied protein diffusion in derivatized dextran hydrogels (chemically cross-linked). Their results showed disagreement between the data and the theory when the diffusant size is close to the hydrogel mesh size. In this case, screening effects started to occur which are not taken into account by the free volume concept. Therefore, the model of Yasuda *et*

al.¹⁷¹ can be used to analyze the diffusion data of relatively small-sized diffusants in dilute and semi-dilute polymer systems.

1.3.3.3 The model of Vrentas and Duda

A major contribution to the development of free volume theory was made by Vrentas and Duda¹⁷⁵⁻¹⁷⁸ and coworkers¹⁷⁹⁻¹⁸¹ who re-examined and improved the free volume model over the years. They extended the free volume theory to a wide range of temperatures and polymer concentrations.¹⁸² The free volume contributions from both the solvent and the polymer are taken into account. Therefore, Fujita's free volume model²⁷ appeared as a special case of the newer model of Vrentas and Duda.¹⁸² With these numerous improvements, this free volume theory takes into account several physical parameters such as the temperature, the activation energy, the polymer concentration, the solvent size, and the molecular weight of the diffusant. In the case of a binary system (solvent diffusion in a polymer network) the model of Vrentas and Duda is expressed by the following equation

$$D = D_{01} \exp\left[-\frac{E}{RT}\right] \exp\left[-\frac{\omega_1 \hat{V}_1^* + \omega_2 \xi \hat{V}_2^*}{K_{11} \omega_1 (K_{21} - T_{g1} + T)/\gamma_1 + K_{12} \omega_2 (K_{22} - T_{g2} + T)/\gamma_2}\right] \quad (1.41)$$

where D_{01} is the solvent self-diffusion coefficient in the absence of polymer or a constant pre-exponential factor, E is the activation energy for a solvent jump, ω_i is the weight fraction of component i , \hat{V}_i^* is the specific volume needed for one jumping unit of component i , ξ is the ratio of the volume of solvent jumping unit to that of the polymer jumping unit, γ_i represents the overlap factor for the free volume for pure component i , T_{gi} is the glass transition temperature of component i , K_{11} and K_{21} are free volume parameters for the solvent and K_{21} and K_{22} are free volume parameters for the polymer. The free volume parameters K_{11} and K_{21} were defined as follow

$$K_{11} = \hat{V}_1^0 T_{g1} \left[\alpha_1 - (1 - f_{H1}^G) \alpha_{c1} \right] \quad (1.42)$$

$$K_{21} = \frac{f_{H1}^G}{\alpha_1 - (1 - f_{H1}^G) \alpha_{c1}} \quad (1.43)$$

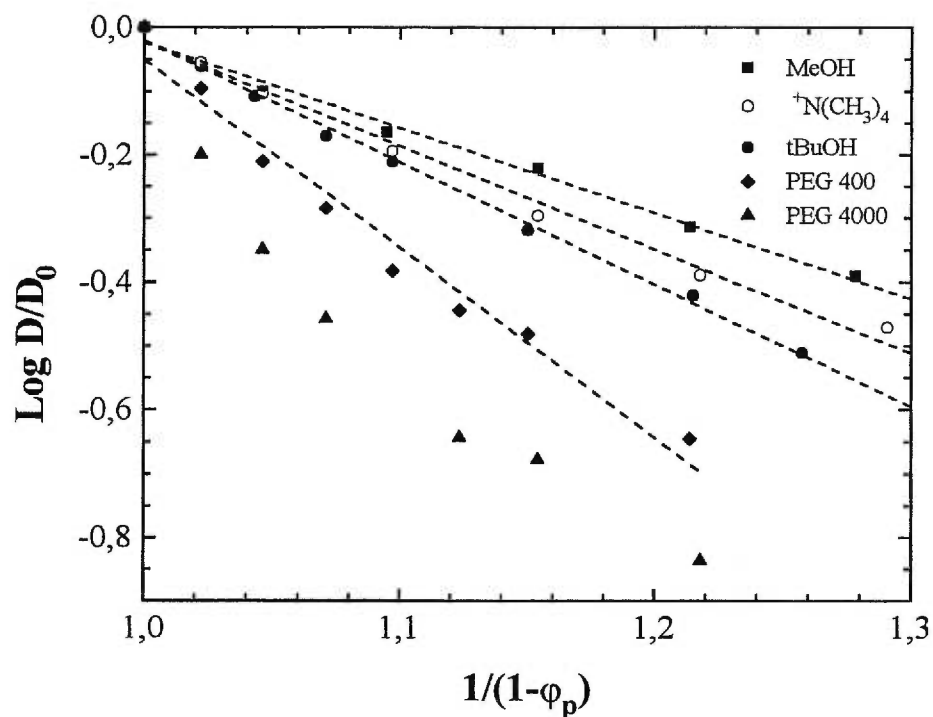


Figure 1.8. Semilogarithmic plot of the normalized self-diffusion coefficient of various diffusants as a function of $1/(1-\phi_p)$, ϕ_p being the polymer volume fraction. The dotted lines are fits to Yasuda's free volume model (Eq 1.40). Reproduced with permission from ACS Publications (Petit, J.-M. *et al.*, *Macromolecules* 1996, **29**, 70).³⁴

where α_1 is the thermal expansion coefficient of the solvent, α_{c1} is the thermal expansion coefficient for the sum of the specific occupied volume and the specific interstitial free volume, \hat{V}_1^0 is the free volume occupied by the solvent at 0 K, and f_{H1}^G is the average fractional hole free volume.

The approach of Vrentas and Duda is based on the following assumptions: (1) the mixing of the polymer and solvent partial specific volumes does not lead to volume change; (2) the polymer thermal expansion coefficients α_2 and α_{c2} are approximated to the average values over the temperature interval of interest; (3) the total hole free volume of the system is computed by using the free volume parameters K_{11}/γ_1 and K_{21}/γ_2 , which are determined from pure component data for solvent and polymer; (4) the activation energy for the solvent jump, E , depends on the polymer concentration since the energy per mole needed by the solvent molecule to overcome attractive forces depends on its neighbors. The transition from the energy in the concentrated region to the region near the pure solvent limit is assumed to be smooth as ω_1 approaches unity.¹⁸³

Eq 1.41 can be simplified in the special case of pure solvent or very low polymer concentrations:

$$\log\left(\frac{D}{D_0}\right) = \frac{-\xi V_2 \omega_2}{2.303 K_{11} (K_{21} - T_{g1} + T) / \gamma} \quad (1.44)$$

The parameters K_{ij} , γ and T_{g1} are available in the literature for many common organic solvents and polymers.^{20,179,184,185}

Eqs 1.41 and 1.44, though complicated in their forms, were used successfully to fit experimental data of diffusion. For example, Lodge *et al.*¹⁸⁶ used the forced Raleigh scattering technique to measure tracer diffusion in poly(vinyl acetate)-toluene system. Agreement between the model of Vrentas and Duda, or Fujita's model, and the experimental data was good over the entire range of polymer concentrations (0-96 wt %). Similar results were published by Zielinski *et al.*¹⁸⁷ who studied diffusion in PS solutions by static field gradient NMR, and Wisnudel and Torkelson²⁰ who studied small molecule diffusion in PS by the Taylor dispersion technique. Other studies have also demonstrated good agreement with this model.^{136,188,189} However, several papers

reported problems that occurred below the glass transition temperature.^{65,168,184,187} Correlation with the data was achieved only with negative values for the polymer free volume parameter, which is physically impossible.^{65,184,187} This problem was overcome recently by Vrentas and Vrentas who introduced a specific hole free volume, \hat{V}_{2g}^0 , of the glassy polymer at any temperature below T_{gm} (glass transition temperature of the polymer-solvent mixture) at a particular temperature.^{176,184}

Despite the re-examination of the model by Vrentas and Vrentas^{183,190} in order to provide a better agreement with diffusion data over a large temperature range and below the glass transition temperature, certain failures have been demonstrated. For example, Waggoner *et al.*³⁶ showed that this model cannot fit the data in the low polymer concentration region. Similar conclusions were also made by Hong *et al.*¹⁹¹ Wisnudel and Torkelson²⁰ pointed out that the diffusion model of Vrentas and Duda did not take into account the flexibility of the diffusant, as they noticed poorer agreement with flexible diffusants than with rigid ones. Zielinski and Duda¹⁸⁵ expected that the model of Vrentas and Duda will deviate from experimental observations at high temperatures (150 °C above T_g) because the diffusion will be no longer limited by the free volume. Energy effects will become dominant.

Some papers compared the free volume models of Vrentas and Duda with the original free volume theory of Fujita. According to Landry *et al.*,¹⁹² the application of both models had no difference. The same conclusion was drawn by Lodge *et al.*,¹⁸⁶ but they also concluded that the model of Vrentas and Duda is successful as a predictive theory over the complete range of polymer concentrations, and over a substantial range of temperatures (above the glass transition temperature), whereas Fujita's model cannot be used to predict or examine the temperature dependence.

Zielinski and Duda¹⁸⁵ used the free volume model of Vrentas and Duda to estimate the diffusion of organic solvents in polymer systems. Their work seemed to be among the first attempts in diffusion prediction reported in the literature. First, they reviewed the literature to evaluate the independent parameters necessary to apply the model. Then, they estimated the diffusion of solvents (toluene, ethylbenzene, chloroform, methyl acetate, and tetrahydrofuran) in polymer systems (PS, PVAc,

PMA, and PMMA). They obtained fairly good correlations with the experimental data (Figure 1.9). Guo *et al.*⁵⁹ tried to predict the diffusion coefficients of benzene, *o*-xylene, ethylbenzene, and chloroform in natural rubber membranes using the approach of Zielinski and Duda.¹⁸⁵ They did not find good agreements and suggested that the parameters proposed by Zielinski and Duda¹⁸⁵ did not yield acceptable predictions of the diffusion coefficients.

An important point to be underlined is that the model of Vrentas and Duda needs numerous parameters. For example, Duda and coworkers¹⁹³ mentioned that 14 independent parameters are necessary to apply this model. Among these 14 parameters 10 need to be evaluated in order to predict the self-diffusion coefficient. Furthermore, these parameters are not usually available in the literature for many polymers, especially new ones.

1.3.3.4. The model of Peppas and Reinhart

For the treatment of transport mechanism in cross-linked polymer networks, Peppas and Lustig¹⁹⁴ considered three different kinds of structures: (1) macroporous hydrogels defined by pore size greater than 0.1 μm where the mechanism of transport is mainly due to convection; (2) microporous hydrogels characterized by pore size in the range of 20-500 \AA (diffusants and pores have similar dimensions) where the mechanism of transport is due to both diffusion and convection; (3) nonporous hydrogels for which space between the macromolecular chains is limited and where the mechanism of transport is due to diffusion only.¹⁹⁴

In pharmaceutical applications such as drug releases, nonporous hydrogels seem to be more often used than macroporous or microporous gels.¹⁹⁴ The discussion here is focused on nonporous hydrogels. More information on convection and diffusion in macro- and microporous gels can be found in the paper by Peppas and Lustig.¹⁹⁴

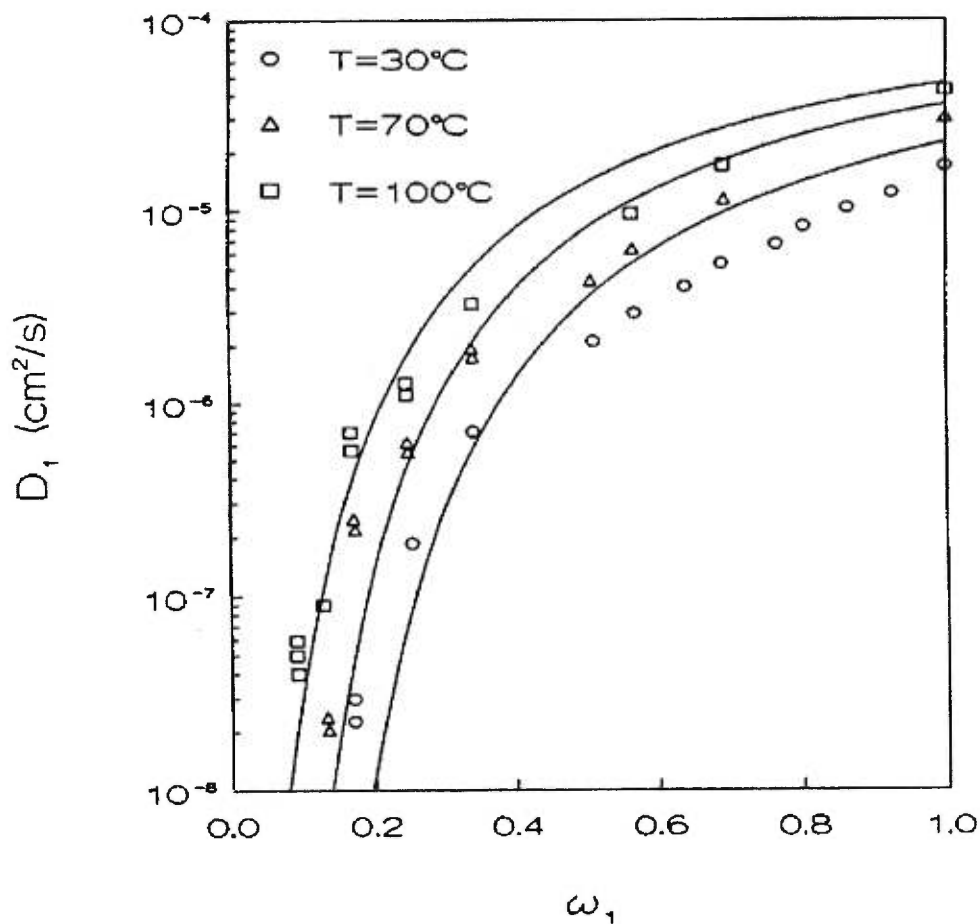


Figure 1.9. Semilogarithmic plot of the self-diffusion coefficient of ethylbenzene in polystyrene as a function of the mass fraction of the solvent, at different temperatures. The solid lines are the theoretical predictions of the solvent diffusion using the free volume theory of Vrentas and Duda (Section 2.3.3.). Reproduced with permission from American Institute of Chemical Engineers (Zielinski, J.M. and Duda, J.L., *AIChE J.* 1992, **38**, 405.).¹⁸⁵

The model of Peppas and Reinhart¹⁹⁵ was also based on the free volume concept.^{27,171} Diffusion is said to occur through the gel space not occupied by polymer chains. Thus, the self-diffusion coefficient of a diffusant is considered to be proportional to the probability of moving through the gel with mesh size ξ , P_ξ , but also proportional to the probability of finding the required free volume in the gel and solution, P'_0/P_0^+ , which is given by the following equation

$$\frac{D}{D_0} = P_\xi \frac{P'_0}{P_0^+} \quad (1.45)$$

where D is the solute diffusion coefficient in the hydrogel, D_0 is the solute diffusion coefficient in water.

The probability, P'_0/P_0^+ of finding the required free volume was analyzed by Peppas and Reinhart.¹⁹⁵ They also assumed that the free volume available for the solute diffusion was mainly due to water, and little from the polymer. The following expression was then obtained¹⁹⁵

$$\frac{D}{D_0} = P_\xi \exp\left(-\frac{Y}{Q-1}\right) \quad (1.46)$$

where $Y = k_2 R_h^2$, and Y is a structural parameter near unity and proportional to R_h^2 , k_2 a parameter of the polymer-water system, R_h the solute hydrodynamic radius, and Q the volume degree of swelling for the gel.

The probability, P_ξ , of moving through the mesh size ξ was studied later by Reinhart and Peppas,¹⁹⁶ who demonstrated that this quantity is related to a critical mesh size, M_c^* , below which the diffusion of a solute of size R_h could not occur:

$$P_\xi = \frac{M_c - M_c^*}{M_n - M_c^*} \quad (1.47)$$

where M_c is the number average molecular weight between cross-links and M_n the number average molecular weight of the uncross-linked polymer. In fact, M_c^* represents the minimal distance in monomer unit between two cross-link points for which diffusion is possible.

Combining Eqs 1.46 and 1.47, the diffusion coefficient in highly swollen membranes can be expressed by

$$\frac{D}{D_0} = k_1 \frac{M_c - M_c^*}{M_n - M_c^*} \exp\left(-\frac{k_2 R_n^2}{Q-1}\right) \quad (1.48)$$

where k_1 is a structural parameter of the polymer-water system.

To describe solute transport in moderately swollen networks,¹⁹⁷ they considered that the free volume was not equal to the total free volume of the solvent, and that diffusion jump length of the solute in solution was not equal to that of the solute in water. A new equation was derived:

$$\frac{D}{D_0} = \frac{\lambda^2}{\lambda_0^2} B(v^*) \exp\left[-v_s \left(\frac{1}{V} - \frac{1}{V_0}\right)\right] \quad (1.49)$$

where λ^2 and λ_0^2 are the diffusion jump lengths of the solute in the hydrogel and water, respectively, $B(v^*)$ is a term representing the characteristic size of the space available for diffusion in the membrane, v_s is the size of the diffusing solute, and where V and V_0 are the free volumes in the swollen membrane and water, respectively.¹⁹⁸

Peppas and coworkers have published several papers with diffusants of various sizes in various hydrogels which showed agreement with the model.¹⁹⁸⁻²⁰² Recently, they have also pointed out the limitations of this model. For example, Peppas and coworkers^{202,203} studied the diffusion of ionized diffusants in charged hydrogels and found that they were much more hindered than larger proteins because of their interactions with ionized carboxylic acid groups.²⁰³ Thus, a parameter relating the interactions between ionized diffusants and the network should be introduced. In addition, problems may also occur when the diffusant size is close to or larger than the mesh size in the network due to screening effects.

1.3.3.5. Summary

The free volume models have found various success in the description of diffusion in polymer systems. The advantages and constraints for each model described in this section are summarized in Table 1.6. The model of Vrentas and Duda^{175,176} seems to be the most useful as it is applicable over a large range of polymer concentrations and temperatures. However, obtaining the numerous

parameters required represent quite a task since these parameters are not always available in the literature. When these parameters are known, it is possible to predict solvent diffusion in certain binary systems.

The model of Peppas and Reinhart¹⁹⁵ describes specifically diffusion in cross-linked gels. Problems may arise when the size of the diffusant is close to or larger than the network mesh size, and when the diffusant is bound to the polymer network by ionic interactions. It does not seem to properly describe diffusion in polymer solutions where there is no cross-linking.

Manz and Callaghan,¹⁴⁷ and Xia and Wang¹⁶⁷ also suggested the use of William-Landel-Ferry²⁰⁴ (WLF) equation and Vogel-Fulcher-Tammann¹⁶⁷ (VFT) equation for the interpretation of diffusion data, but they cannot be used below T_g .^{147,167}

1.3.4. Other physical models of diffusion

Many of the diffusion models did not offer temperature dependence since most experiments were carried out at room temperature. Variable temperature diffusion data can be analyzed with physical models that can be considered as thermodynamic models. We also include here other models that do not fit to the descriptions in the previous categories.

1.3.4.1. Arrhenius' theory

Arrhenius equation describes the temperature dependence of a chemical reaction rate as illustrated by²⁰⁵

$$k = A \exp\left(-\frac{E_a}{RT}\right) \quad (1.50)$$

where k represents the kinetic rate of a chemical reaction, A a pre-exponential factor and E_a the activation energy. Eq 1.50 can be written in a logarithmic form

$$\log k = \log A - \frac{E_a}{RT} \quad (1.51)$$

which is useful to estimate E_a from a plot of logarithmic k versus $1/T$.

Table 1.6. Summary of the diffusion models based on the free volume theories (Section 1.3.3).

Author(s)	Ref(s).	Application(s)	Limitation(s)
Fujita	27	- Solvents and small-sized diffusants - Semi-dilute polymer solutions	- Large diffusants - Concentrated polymer solutions
Yasuda <i>et al.</i>	171	- Solvents and small-sized diffusants - Semi-dilute polymer solutions	- Large diffusants - Concentrated polymer solutions
Vrentas and Duda	175–178	- Various solutes and solvents - Both semi-dilute and concentrated polymer solutions	- Determination of the numerous parameters - Dilute polymer solutions
Peppas and Reinhart	195	- Various solutes and solvents - Chemically cross-linked gels and hydrogels	- Diffusants with size closer to or greater than the mesh size of the network - Diffusion in non cross-linked polymers

Some recent works reported diffusion experiments at different temperatures which led to the evaluation of the activation energy of diffusant in polymers systems with the Arrhenius equation.^{32,51,65,69}

$$D = A \exp\left(-\frac{E_a}{RT}\right) \quad (1.52)$$

Examples of E_a values found in the literature are given in Table 1.7. From the activation energy of a diffusant in a given system, we can obtain information of the network in which the diffusion takes place. In order to obtain complementary information, it is necessary to compare the E_a values in different systems for the same diffusant. However, the Arrhenius equation does not provide any correlation to the diffusant size or to the polymer networks.

The modified Enskog theory was recognized to provide a suitable description of gas and liquid diffusion in membranes.²⁰⁶ As shown by Waggoner *et al.*,³⁶ this model can also be employed to describe the diffusion of a diffusant in polymer networks. The diffusant particle was represented as a rigid sphere flowing through the polymer solution. The diffusion coefficient of such a tracer particle is given by

$$D_\alpha = \frac{1}{\frac{1}{D_{\alpha M}} + \frac{1}{D_{\alpha\beta}} \left[1 - x_\alpha \left(1 - \frac{D_{\beta M}}{D_{\alpha M}} \right) \right]} \quad (1.53)$$

where D_α represents the self-diffusion coefficient of the tracer, α , β and M represent the tracer, the solvent and the polymer, respectively, D_{ij} represents de mutual diffusion of component i with respect to component j and x_α is the molar fraction of the tracer. Consequently, $D_{\alpha M}$ is the mutual diffusion coefficient of the tracer with respect to the polymer, $D_{\alpha\beta}$ the mutual diffusion coefficient of the tracer with respect to the solvent, $D_{\beta M}$ the mutual diffusion coefficient of the solvent with respect to the polymer.

Table 1.7. Example of activation energy (E_a) studies based on Arrhenius equation found in the literature (Section 1.3.4.1). *o*-MR and *p*-MR stand for *ortho*- and *para*-methyl red, respectively.

	System	E_a (kJ/mol)
Sung and Chang ⁵¹	<i>o</i> -MR in toluene	11.9
Temperature: 15–55 °C	<i>p</i> -MR in toluene	12.6
Polymer concentration (PS and PVAc) 10 % weight	<i>o</i> -MR in toluene/PS	13.6
	<i>p</i> -MR in toluene/PS	15.1
	<i>o</i> -MR in toluene/PVAc	17.2
	<i>p</i> -MR in toluene/PVAc	21.7
Gao and Fagerness ³²	H ₂ O + 0.5% adinazolam	
Temperature: 10–50 °C	+ 2% glucose, or lactose, or HPMC	
	- Water diffusion	4.3–4.6
	- Adinazolam diffusion	5.0–5.3
Nyström <i>et al.</i> ⁶⁹	Cellulose/H ₂ O	23.3
Temperature: 14–44 °C	Cellulose/H ₂ O/ D ₂ O	17.0
Concentration: $\phi_p = 0.093$	Cellulose/H ₂ O/ D ₂ O/Dioxane	15.0
	Cellulose/H ₂ O/ D ₂ O/ <i>t</i> -Butanol	24.1
Pickup and Blum ⁶⁵	Toluene in PS	11-68
Temperature: 25–115 °C		
Concentration: $\phi_p = 0.04-0.90$		

In addition, Arrhenius model seems valid only in dilute and semi-dilute systems because *the diffusion rate is limited by the energy required for the diffusing species to escape its present surroundings and move into an adjacent environment. However, in moderate to high polymer concentration solutions, the diffusion process is limited by the polymer molecular motions.*³⁶

1.3.4.2. The modified Enskog theory

Further, if the tracer molecule is present in a small quantity and if both tracer and solvent have approximately the same mutual diffusion coefficient with respect to the polymer, Eq 1.53 can be rewritten as

$$\frac{1}{D_{\alpha}} = \frac{1}{D_{\alpha M}} + \frac{1}{D_{\alpha\beta}} \quad (1.54)$$

This equation offers a simple dependence on the tracer diffusion coefficient in a dilute solution. The respective mutual diffusion coefficient, $D_{\alpha\beta}$, can be expressed as²⁰⁶

$$D_{\alpha\beta} = \frac{3}{8n\sigma_{\alpha\beta}^2} \left(\frac{kT(m_{\alpha} + m_{\beta})}{2\pi m_{\alpha} m_{\beta}} \right)^{1/2} \frac{1}{g_{\alpha\beta}(\sigma_{\alpha\beta})} \quad (1.55)$$

where n the number of molecules per unit volume or the number density (mol/cm^3), $\sigma_{\alpha\beta}$ the hard sphere collision diameter of components α and β , m_i the molecular mass of component i , and $g_{\alpha\beta}(\sigma_{\alpha\beta})$ is the rigid sphere contact radial distribution function. This function was obtained from the scaled particle theory and depends on the molecular radius of the component and on the molecular friction coefficient.²⁰⁶

The modified Enskog theory was mainly employed for gas diffusion through membranes and not often used for polymer solutions. However, Waggoner *et al.*³⁶ used this model to draw up comparisons between the modified Enskog theory, the model of Vrentas and Duda and the model of Mackie and Meares in various polymer systems (PS and PMMA). They concluded that Enskog's model provided satisfactory correlation with the experimental data at lower polymer concentrations exclusively. At higher polymer concentrations the authors observed little correlation between theoretical predictions and experimental results (Figure 1.10). This conclusion is

consistent with the work of Pickup and Blum.⁶⁵ It should be noted that the modified Enskog theory does not provide a polymer concentration dependence.

1.3.4.3. The model of Petit *et al.*

Petit *et al.*³³ proposed a new physical model for the diffusion of solvents and solute molecules in polymer solutions and gels. This model considered the medium as a transient statistical network of an average mesh size ξ , as defined by de Gennes,¹²³ in which the diffusing molecules have to overcome energy barriers of equal magnitude (Figure 1.11). The transient network is considered to exist over the whole range of polymer concentrations including the dilute regime. A diffusing molecule is considered as residing temporarily in a cavity and diffusion occurs only when the particle has enough energy to jump over an energy barrier to move forward to the next cavity. Thus, diffusion is considered as a succession of jumps over energy barriers. Petit *et al.*³³ considered one-dimensional diffusion assuming that the energy potentials are equal in amplitude, ΔE , and spaced by equal intervals ξ , which corresponds to the correlation length. Introducing k as the solute jump frequency, Fick's first law of diffusion can be written as follow, according to Andreoli *et al.*²⁰⁷

$$D = \xi^2 k \quad (1.56)$$

where k , the jump frequency, is expected to depend on both temperature and size of the diffusant. The jump frequency can be written in an Arrhenius form, according to Kramer²⁰⁸ who studied the jump of Brownian particles over one potential barrier,

$$k = F_P \exp\left(-\frac{\Delta E}{k_B T}\right) \quad (1.57)$$

where F_P is a frequency pre-factor, ΔE the height of the potential barrier, k_B is the Boltzmann constant and T the temperature. Furthermore, dependence of ξ on the concentration was given by de Gennes' relation¹²²

$$\xi = R_g \left(\frac{c^*}{c}\right)^{\nu} = \beta c^{-\nu} \quad (1.58)$$

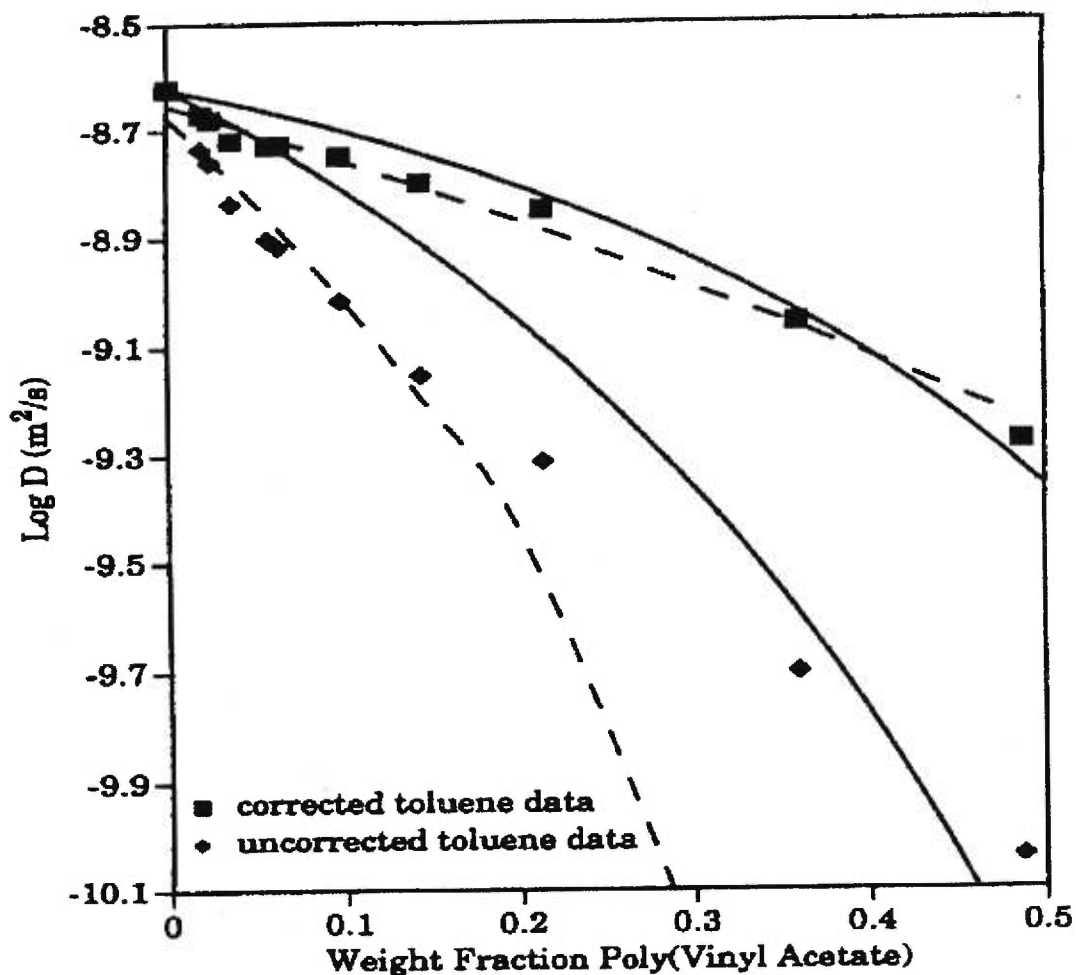


Figure 1.10. The self-diffusion coefficients of methyl red plotted as a function of PVAc concentration in toluene. Data displaying the hydrogen-bonding effect (diamonds) and data with the hydrogen-bonding effect removed (squares) are fitted with the free volume model of Vrentas and Duda (solid lines), Eq 1.41, and the modified Enskog theory (dotted lines), Eq 1.53. Reproduced with permission from ACS Publications (Waggoner, A. R. *et al.*, *Macromolecules* 1993, **26**, 6841).³⁶

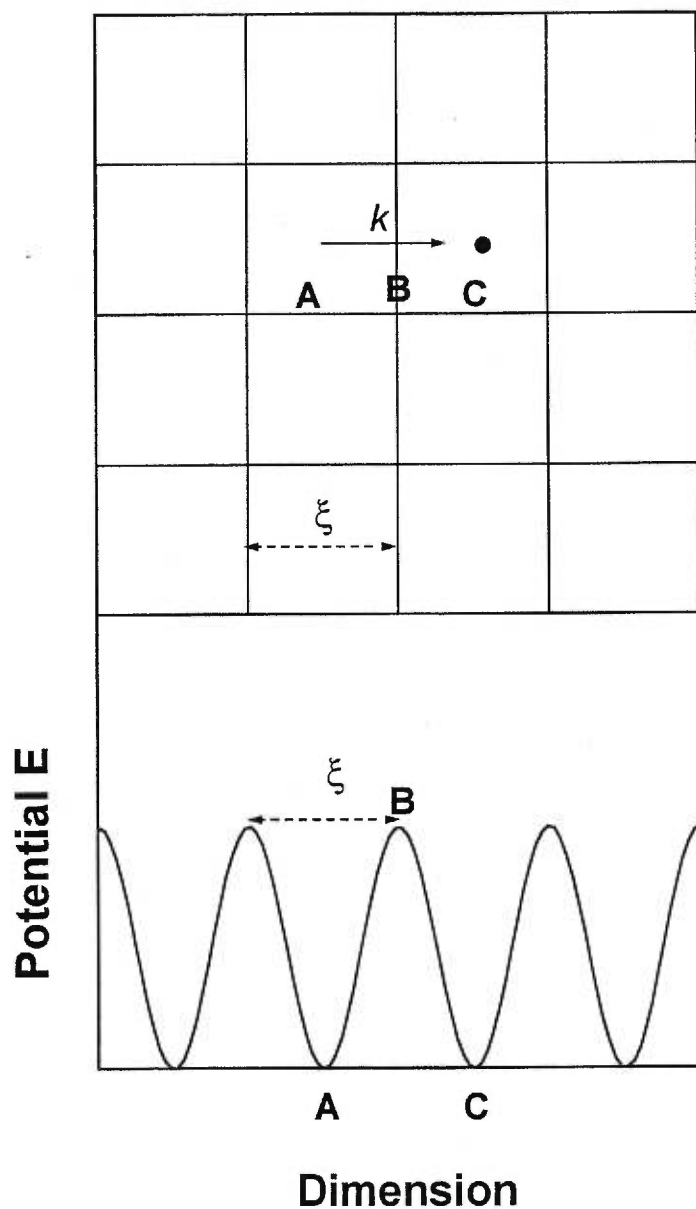


Figure 1.11. Representation of the polymer solution of a network of mesh size ξ , and potential E for the diffusion process of a diffusant in a polymer network. Reproduced with permission from ACS Publications (Petit, J.-M. *et al.*, *Macromolecules* 1996, **29**, 6031).³³

where R_g is the radius of gyration of the polymer, c^* the overlap concentration between the dilute and semi-dilute regimes, c the polymer concentration and ν is a parameter. In de Gennes' theory, ξ was said to depend on the polymer concentration but not on the molecular weight of the polymer when $c > c^*$.¹²³ Substituting Eq 1.58 into Eq 1.56 leads to the following equation

$$D = k\beta^2 c^{-2\nu} \quad (1.59)$$

This equation is suitable to describe the diffusion of a diffusant when the polymer concentration is greater than zero, but inappropriate at zero polymer concentration. Therefore Petit *et al.*³³ considered the friction coefficients of the diffusing molecules to formulate a better expression. It is generally assumed that the total friction coefficient, f , experienced by a diffusing molecules in a polymer solution results from an additive contribution of the background solvent, f_0 , and the polymer network, f_p .^{209,210}

$$f = f_0 + f_p \quad (1.60)$$

By the use of Stokes-Einstein relation, $D = k_B T/f$, and by the use of Eq 1.59, Eq 1.60 can be rewritten as

$$\frac{1}{D} = \frac{1}{D_0} + \frac{1}{k\beta^2 c^{-2\nu}} \quad (1.61)$$

where D_0 is the diffusion coefficient of the diffusant in absence of the polymer. Eq 1.61 can be rewritten as

$$\frac{D}{D_0} = \frac{1}{1 + a c^{2\nu}} \quad (1.62)$$

where $a = D_0/k\beta^2$ and ν is a characteristic parameter of the system that can be regarded as a constant. The value of k is not constant because F_P and ΔE (Eq 1.57) should both depend on the polymer concentration. Nevertheless, k can be approximated as a constant within a certain range of concentrations, although k may have a certain dependence on the mesh size of the network. The parameter β is expected to be constant for a given system so that $k\beta^2$ depends only on the solute size and on the temperature.

The model of Petit *et al.*³³ was employed to analyze the diffusion data of both solute molecules in ternary aqueous polymer (PVA) systems and solvents (esters and ketones) in binary polymer (PMMA) organic solutions over a wide range of concentrations.^{211,212} It has successfully described the effect of polymer concentration and the temperature dependence. Recently (*Chapitre 3*), this model was used to treat the diffusion data of both small and large diffusants varying from ethylene glycol ($M = 62$ g/mol) up to poly(ethylene glycol) with a molecular weight of 4000.²¹¹ This diffusion model provided good agreements with the experimental data. In addition, it was used to analyze variable temperature diffusion of solutes of various sizes. The activation energy calculated was found to increase with increasing size of the diffusant. Furthermore, an empirical relationship was found between the parameter $k\beta^2$ and the hydrodynamic radius of the linear PEG diffusants

$$\log k\beta^2 = -0.0356R_h - 10.45 \quad (1.63)$$

In order to further test the validity of this model, diffusion data can be gathered from the literature. For example, Wheeler and Lodge⁴⁵ studied the self-diffusion of linear PS ($M = 6.5 \times 10^4$, 1.79×10^5 , 4.22×10^5 , and 1.05×10^6) in *o*-fluorotoluene solutions of PVME ($M = 1.4 \times 10^5$, 6.3×10^5 , and 1.3×10^6) with concentrations increasing from 0 to 0.30 g/mL. In a companion paper, Lodge *et al.*¹¹¹ studied the self-diffusion of 3-arm ($M = 6.5 \times 10^4$, 1.79×10^5 , 4.22×10^5 , and 1.05×10^6) and 12-arm ($M = 6.5 \times 10^4$, 1.79×10^5 , 4.22×10^5 , and 1.05×10^6) star polystyrenes in the same system. These diffusion data were analyzed with the model of Petit *et al.*,³³ and the results are shown in Figure 1.12 for the linear and 12-arm star PS diffusants, respectively. It seems that the model of Petit *et al.*³³ is not accurate to describe diffusion of linear and star diffusant with molecular weight similar to the background polymer, in this organic solvent, despite its success with macromolecular diffusants in polymer gels.^{211,212}

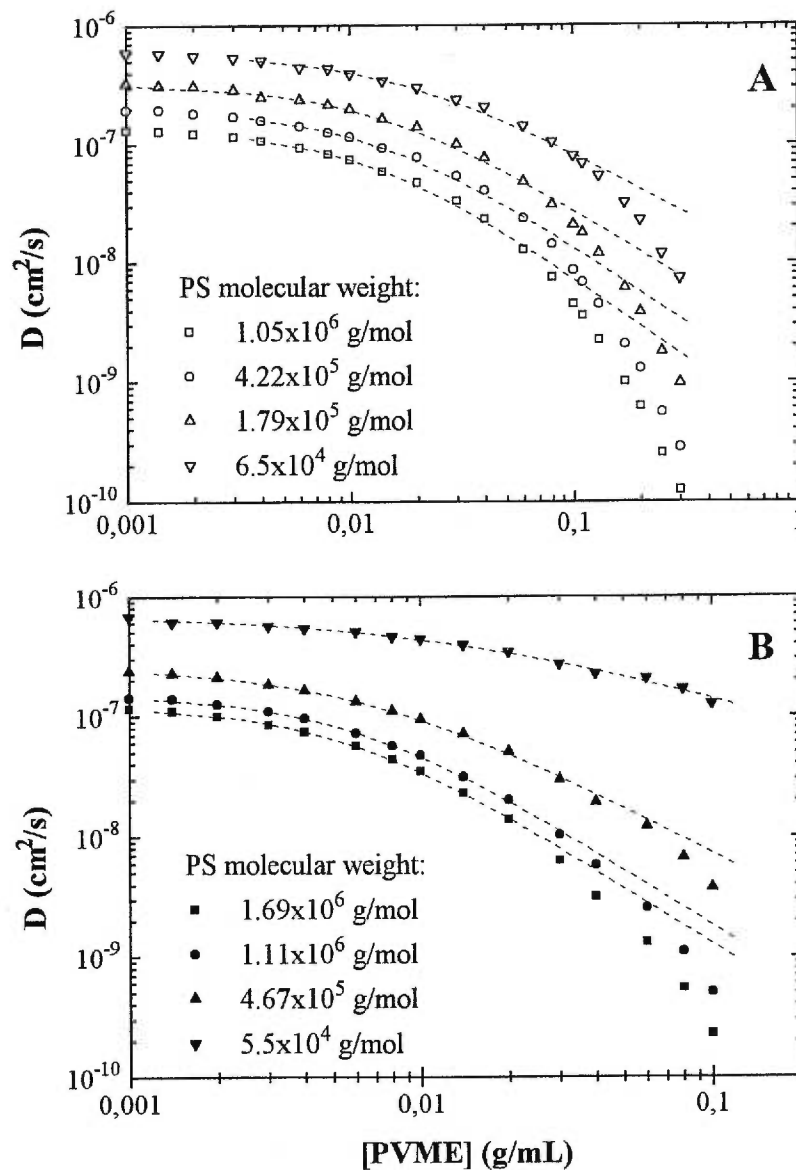


Figure 1.12. The logarithmic plots of the self-diffusion coefficients of a linear PS (A) and a 12-arm star PS (B) in PVME/*o*-fluorotoluene as a function of the PVME concentration, at 30 °C (data from the work of Lodge and coworkers^{45,111}). Dashed lines are fits to Eq 1.62.

1.3.4.4. Amsden' model

Recently, Amsden²⁸ published a brief review of several diffusion models including the models proposed by Yasuda *et al.*,¹⁷¹ Ogston *et al.*,⁷⁶ Johansson *et al.*,³¹ Altenberger *et al.*,⁹⁷ Cukier,²⁶ and Phillips.²¹³ The combined obstruction and hydrodynamic theories proposed by Brady²¹⁴ was also discussed in the review. In the author's opinion, the obstruction and hydrodynamic models cannot adequately describe the diffusion behavior of macromolecules within stiff-chained hydrogels, while the combined obstruction and hydrodynamic theories can provide a better approximation of the diffusion data but do not predict the effect of solute radius on its reduced diffusivity. Therefore, Amsden²⁸ proposed a new diffusion model which is based on the equation of Lustig and Peppas.¹⁹⁹ According to Amsden,²⁸ the transport of a molecule through a hydrogel is proportional to the probability of finding a succession of holes larger than the diffusant diameter. Therefore, the effective diffusivity of the diffusant, \bar{D}_e , is expressed as

$$\bar{D}_e = \bar{D}_m \int_{r^*}^{\infty} g(r) dr \quad (1.64)$$

where \bar{D}_m is the average mutual-diffusion coefficient of the solute, $g(r)$ the distribution of spherical holes within the hydrogel, and r^* the critical hole radius required for solute diffusion.

In the case of straight polymer fibers randomly dispersed in the hydrogel network, the distribution $g(r)$ can be expressed as

$$g(r) = \frac{\pi r}{2R^2} \exp\left[-\frac{\pi}{4}\left(\frac{r}{R}\right)^2\right] \quad (1.65)$$

where R is the mean radius of the distribution.

Substituting Eq 1.65 into Eq 1.64 and carrying out the integration, one can obtain

$$\frac{\bar{D}_e}{\bar{D}_m} = \exp\left[-\frac{\pi}{4}\left(\frac{r^*}{R}\right)^2\right] \quad (1.66)$$

To account for the specific polymer thickness, Amsden rewrote Eq 1.66 to include the average radius of space between the polymer chains, \bar{r} , and the radius of the polymer chain, r_f .

$$\frac{\bar{D}_e}{D_m} = \exp \left[-\frac{\pi \left(\frac{r_s + r_f}{\bar{r} + r_f} \right)^2}{4} \right] \quad (1.67)$$

\bar{r} can be approximated as the average end-to-end distance between the polymer chains, ξ . Further, from scaling concepts ξ was found dependent on the polymer volume fraction

$$\xi = k \phi^{-1/2} = k_1 r_f \phi^{-1/2} \quad (1.68)$$

where k is a constant for a given polymer-solvent system, dependent on the length of the monomer unit and the stiffness or flexibility of the polymer chain. k can be expressed as a function of the polymer chain radius, $k = k_1 r_f$. Substitution of Eq 1.68 into Eq 1.67 leads to the final form of Amsden's diffusion model²⁸

$$\frac{\bar{D}_e}{D_m} = \exp \left[-\pi \left(\frac{r_s + r_f}{r_f} \right)^2 \frac{\phi}{(k_1 + 2\phi^{1/2})^2} \right] \quad (1.69)$$

Thus, this model takes into account the polymer structural properties such as the polymer chain stiffness, the polymer chain radius, the polymer volume fraction as well as the size of the diffusant. According to Amsden, the model predicts a decrease of the solute diffusion when the polymer volume fraction increases, when the diffusant size increases, and when the radius of the polymer chain decreases.²⁸

Eq 1.69 was tested by studying protein (pepsin, ovalbumin, BSA and β -lactoglobulin) release from calcium alginate matrices. Amsden found that Eq 1.68 provided a good correlation with the experimental data over the entire range of the polymer volume fractions investigated ($\phi = 0-0.05$).²⁸ The dependence of the diffusion on the hydrodynamic radius of the solute was also predicted properly. Amsden²⁸ also reported the simulation data published by Johansson *et al.*^{31,77} showing that the model was capable of describing the effect of polymer chain radius and flexibility on the diffusion of solutes.

1.3.4.5. Summary

The theories presented in Sections 1.3.4.1 and 1.3.4.2 were not intended to describe diffusion in polymer solutions and gels, but they are useful in the description of the diffusion behavior, particularly the temperature effect. Other thermodynamic models such as Eyring's model²¹⁵ were not discussed here because of the limitations in their applicability.

The model of Petit *et al.*³³ describes the dependence of diffusion on the molecular size of the diffusant, polymer concentration, as well as temperature. This model was used successfully to link the diffusion of small and macromolecules in binary and ternary polymer systems. Nevertheless, the examination of certain diffusion data from the literature showed its limitations for diffusants of high molecular weights in concentrated polymer networks.

The new diffusion model proposed by Amsden²⁸ which combines the obstruction effect and the hydrodynamic interactions, seems to be an interesting approach. Further tests with more concentrated polymer networks need to be done to verify its usefulness.

1.4. Concluding remarks

Diffusion in polymer systems is a complicated process. It depends on the properties of the diffusants, the polymer network, and the solvents. The obstruction by the polymer network, the hydrodynamic interactions in the system, and the thermodynamic agitation should be all considered to understand the diffusion in polymer solutions, gels and even solids. Various models and theories have succeeded in describing the diffusion process under different circumstances. They all contribute to the understanding of diffusion phenomena. Enormous progress has been made in the field but controversies are not uncommon. It seems also fair to say that limitations exist for the application of each of these physical models and care should be taken in their use for the interpretation of the results obtained. It remains difficult, if not impossible, to estimate and predict the diffusion coefficient of a given diffusant in a given system under specific conditions. It is also important to establish a

correlation between the self-diffusion behavior in an equilibrated state and the diffusion in a real time non-equilibrated dynamic situations, where the swelling and the dissolution of the polymer matrix, the compatibility of the solvent, solute and polymer should all be considered.

The rapid development of various techniques such as NMR allows the study of more complicated systems to obtain further information on the properties of the diffusants and polymeric networks. For example, it is now possible to track the release of solutes such as drugs from a polymer matrix in real-time situations by NMR imaging.²¹⁶ Studies of this kind should generate more results, leading to a better understanding of the diffusion process in polymer systems.

1.5. Symbols and abbreviations

α	Parameter dependent on the diffusant size in Phillies' model, ^{52,101,102} and independent of the diffusant size in the model of Altenberger <i>et al.</i> ⁹⁷
β	Constant dependent on the solute size and on the temperature in the model of Petit <i>et al.</i> ³³
c	Concentration (g/mL)
c^*	Critical overlap concentration, or overlap concentration, at which the entanglement of polymer chains starts according to references 122 and 123.
c_e	Entanglement concentration, $c_e \approx c^*$ according to references 137 and 138.
ΔE	Energy barrier, kJ/mol
D	Diffusion coefficient, m ² /s (self- or tracer diffusion coefficient)
D_0	Diffusion coefficient in the absence of the polymer network, m ² /s
E_a	Activation energy, kJ/mol
ϕ_p	Volume fraction of polymer
ϕ_s	Volume fraction of solvent
HPC	Hydroxypropyl cellulose
HPMC	Hydroxypropyl methyl cellulose
κ	Screening parameter in Cukier's model ²⁶
k	Jump frequency in the model of Petit <i>et al.</i> , ³³ which depends on temperature and diffusant size
k_B	Boltzmann's constant ($1.380658 \times 10^{-23} \text{ JK}^{-1}$)
M	Polymer molecular weight
M_c	Number-average molecular weight between cross-links

M_c^*	Theoretical molecular weight between cross-links below which diffusion of a solute of size r_s could not occur, in the model of Peppas and Reinhart. ¹⁹⁵
M_n	Number-average molecular weight of uncross-linked polymer
ν	Scaling parameter characteristic of the system in Phillies' model, ^{52,101,102} and Parameter dependent on the system in the model of Petit <i>et al.</i> ³³
NMR	Nuclear magnetic resonance
P	Matrix polymer molecular weight in the model of de Gennes ¹²³
PA	Polyacrylamide
PEG	Poly(ethylene glycol)
PGSE	Pulsed-gradient spin-echo
PMA	Poly(methyl acrylate)
PMMA	Poly(methyl methacrylate)
PS	Polystyrene
PVA	Poly(vinyl alcohol)
PVAc	Poly(vinyl acetate)
PVME	Poly(vinyl methyl ether)
ρ	Radius of the polymer or fiber
R_h	Hydrodynamic radius of the diffusing molecule (Å)
R_g	Radius of gyration (Å)
T	Temperature (K)
T_g	Glass transition temperature
THF	Tetrahydrofurane
ξ	Correlation length or network mesh size as defined by de Gennes, ¹²³ and End-to end distance of a polymer chain in the model of Amsden ²⁸

1.6. Acknowledgment

Financial support from the Natural Sciences and Engineering Research Council (NSERC) of Canada and the Quebec Government (Fonds FCAR) is acknowledged. Helpful discussions with Professor P.M. Macdonald of University of Toronto, Professor B. Roux and Mr. J.-M. Petit of Université de Montréal are gratefully acknowledged. The authors also wish to thank the copyright owners, American Chemical Society, American Institute of Physics, American Institute of Chemical Engineers, and Plenum Publication Corporation, for their permission to use some of the illustrations in this review.

1.7. References

- 1 Crank, J., *The Mathematics of Diffusion*, 2nd Ed., Clarendon Press, Oxford (1975)
- 2 Cussler, E. L., *Diffusion, Mass Transfert in Fluids Systems*, 2nd Ed., Cambridge University Press, Cambridge (1997).
- 3 Fick, A., *Annln Phys.* 1855, **170**, 59.
- 4 Alfrey Jr., T., Gurnee, E. F. and Lloyd, W. G., *J. Polym. Sci., Part C* 1966, **12**, 249.
- 5 Grinsted, R. A., Clark L. and Koenig, J. L., *Macromolecules* 1992, **25**, 1235.
- 6 Qin, W., Shen, Y. and Fei, L., *Chin. J. Polym. Sci.* 1993, **11**, 358.
- 7 Ercken, M., Adriaensens, P., Reggers, G., Carleer, R., Vanderzande, D. and Gelan, J., *Macromolecules*, 1996, **29**, 5671.
- 8 Weisenberger, L. A. and Koenig, J. L., *Macromolecules* 1990, **23**, 2445.
- 9 Thomas, N.L. and Windle, A.H., *Polymer* 1982, **23**, 529.
- 10 Thomas, N.L. and Windle, A.H., *Polymer* 1978, **23**, 255.
- 11 Thomas, N.L. and Windle, A.H., *Polymer* 1977, **23**, 1195.
- 12 Thomas, N.L. and Windle, A.H., *Polymer* 1981, **23**, 627.
- 13 Thomas, N.L. and Windle, A.H., *J. Membr. Sci.* 1978, **3**, 337.
- 14 Weisenberger, L. A. and Koenig, J. L., *Macromolecules* 1990, **23**, 2454.
- 15 Ilg, M., Pfeleiderer, B., Albert, K., Rapp, W. and Bayer, E., *Macromolecules* 1994, **27**, 2778.
- 16 Perry, K. L., McDonald, P. J., Randall, E. W. and Zick, K., *Polymer* 1994, **35**, 2744.
- 17 Crank, J. and Park, G. S., *Diffusion in polymers*, Academic Press, London (1968).
- 18 Hu, D. S.-G. and Chou, K. J.-N., *Polymer* 1996, **37**, 1019.
- 19 Smith, B. A. H. and Sefton, M. V., *J. Biomed. Mater. Res.* 1988, **22**, 673.
- 20 Wisnudel, M. B. and Torkelson, J. M., *Macromolecules* 1996, **29**, 6193.
- 21 van Asten, A. C., Kok, W. T., Tilssen R. and Poppe, H., *J. Polym. Sci., Polym. Phys. Ed.* 1996, **34**, 283.

- 22 Kosmeyer, R. W. and Peppas, N. A., *J. Membr. Sci.* 1981, **9**, 211.
- 23 Hariharan, D. and Peppas, N. A., *J. Contr. Release* 1993, **23**, 123.
- 24 Peppas, N. A. and Scott, J. E., *J. Contr. Release* 1992, **18**, 95.
- 25 Fricke, H., *Phys. Rev.* 1924, **24**, 575.
- 26 Cukier, R. I., *Macromolecules* 1984, **17**, 252.
- 27 Fujita, H., *Adv. Polym. Sci.* 1961, **3**, 1.
- 28 Amsden, B. *Polym. Gels Networks* 1998, **6**, 14.
- 29 Stilbs, P. *Progr. NMR Spectrosc.* 1987, **19**, 1.
- 30 Westrin, B. A., Axelsson, A. and Zacchi, G., *J. Contr. Release* 1994, **30**, 189.
- 31 Johansson, L., Elvingson, C. and Löfroth, J.-E., *Macromolecules* 1991, **24**, 6024.
- 32 Gao, P. and Fagerness, P. E., *Pharm. Res.* 1995, **12**, 955.
- 33 Petit, J.-M., Roux, B., Zhu, X. X. and Macdonald, P. M., *Macromolecules* 1996, **29**, 6031.
- 34 Petit, J.-M., Zhu, X. X. and Macdonald, P. M., *Macromolecules* 1996, **29**, 70.
- 35 Mustafa, M. B., Tipton, D. L., Barkley, M. D., Russo, P. S. and Blum, F. D., *Macromolecules* 1993, **26**, 370.
- 36 Waggoner, A. R., Blum, F. D. and MacElroy, J. M. D., *Macromolecules* 1993, **26**, 6841.
- 37 Griffiths, P. C., Stilbs, P., Chowdhry, B. Z and Snowden, M. J., *Colloid Polym. Sci.* 1995, **273**, 405.
- 38 Viovy, J.-L., *Mol. Biotech.* 1996, **6**, 31.
- 39 Bu, Z. and Russo, P. S., *Macromolecules* 1994, **27**, 1187.
- 40 Park, I. H., Johnson Jr., C. S. and Gabriel, D. A., *Macromolecules* 1990, **23**, 1548.
- 41 Rotstein, N. A. and Lodge, T. P., *Macromolecules* 1992, **25**, 1316.
- 42 Won, J. and Lodge, T. P., *J. Polym. Sci., Part B* 1993, **31**, 1897.
- 43 Chang, T., Kim, H. and Yu, H., *Macromolecules* 1987, **72**, 4186.
- 44 Walderhaug, H., Hansen, F. K., Abrahmsén, S., Persson, K. and Stilbs, P., *J. Phys. Chem.* 1993, **97**, 8336

- 45 Wheeler, L. M. and Lodge, T. P., *Macromolecules* 1989, **22**, 3399.
- 46 Furukawa, R., Arauz-Lara, J. L. and Ware, B. R., *Macromolecules* 1991, **24**, 599.
- 47 De Smedt, S. C., Lauwers, A., Demeester, J., Engelborghs, Y., De Mey, G. and Du, M., *Macromolecules* 1994, **27**, 141.
- 48 Uemura, Y., McNulty, J., Macdonald, P. M., *Macromolecules* 1995, **28**, 4150.
- 49 Won, J., Oryenemezu, C., Miller, W., Lodge, T. P., *Macromolecules* 1994, **27**, 7389.
- 50 Cush, R., Russo, P. S., Kucukyavuz, Z., Bu, Z., Neau, D., Shih, D., Kucukyavus, S., Ricks, H., *Macromolecules*, 1997, **30**, 4920.
- 51 Sung, J. and Chang, T., *Polymer* 1993, **34**, 3741.
- 52 Phillies, G. D. J., *Macromolecules* 1986, **19**, 2367.
- 53 Cosgrove, T., Turner, M. J., Griffiths, P. C., Hollingshurst, J., Shenton, M. and Semlyen, J. A., *Polymer* 1996, **37**, 1535.
- 54 Cosgrove, T. and Griffiths, P. C., *Polymer* 1994, **35**, 509.
- 55 Nemoto, N., Kojima, T., Inoue, T., Kishine, M., Hirayama, T. and Kuruto, M., *Macromolecules* 1989, **22**, 3793.
- 56 Wesson, J. A., Noh, I., Kitano, T. and Yu, H., *Macromolecules* 1984, **17**, 782.
- 57 Kim, H., Chang, T., Yohanan, J. M., Wang, L. and Yu, H., *Macromolecules* 1986, **19**, 2737.
- 58 Hennink, W. E., Talsma, H., Borchert, J. C. H., De Smedt, S. C. and Demeester, J., *J. Contr. Release* 1996, **39**, 47.
- 59 Guo, C. J., De Kee, D., Harrison, B., *J. Appl. Polym. Sci.* 1995, **56**, 817.
- 60 Muhr, A. H. and Blanshard, M. V., *Polymer* 1982, **23**, 1012.
- 61 von Meerwall, E. D., *Adv. Polym. Sci.* 1983, **54**, 1.
- 62 von Meerwall, E. D., *Rubber Chem. Techn.* 1985, **58**, 527.
- 63 Tirrell, M., *Rubber Chem. Techn.* 1984, **57**, 523.
- 64 Cheever, E., Blum, F. D., Foster, K. R. and Mackay, R. A., *J. Colloid Interface Sci.* 1985, **104**, 121.
- 65 Pickup, S. and Blum, F. D., *Macromolecules* 1989, **22**, 3961.

- 66 Langdon, A. G. and Thomas, H. C., *J. Phys. Chem.* 1971, **75**, 1821.
- 67 Masaro, L. and Zhu X.X., unpublished results.
- 68 Mackie, J. S. and Meares, P., *Proc. R. Soc. Lond. A* 1955, **232**, 498.
- 69 Nyström, B., Moseley, M. E.; Brown, W. and Roots, J., *J. Appl. Polym. Sci.* 1981, **26**, 3385.
- 70 Brown, W. and Johnsen, R. M., *J. Appl. Polym. Sci.* 1981, **26**, 4135.
- 71 Brown, W.; Stilbs, P. and Lindström, T., *J. Appl. Polym. Sci.* 1984, **29**, 823.
- 72 Wang, J. H., *J. Am. Chem. Soc.* 1954, **76**, 4755.
- 73 Nilsson, G. and Lindman, B., *J. Phys. Chem.* 1983, **87**, 4756.
- 74 Laurent, T. C., Pietruszkiewicz, A. and Persson, H., *Biochim. Biophys. Acta* 1963, **78**, 351.
- 75 Laurent, T. C., *Biochem. J.* 1963, **89**, 249.
- 76 Ogston, A. G., Preston, B. N. and Wells, J. D., *Proc. R. Soc. Lond., A* 1973, **333**, 297.
- 77 Johansson, L., Skantze, U. and Löfroth, J.-E., *Macromolecules* 1991, **24**, 6019.
- 78 Petit, J.-M., Mémoire de M.Sc., Université de Montréal, April 1995.
- 79 Löfroth, J.-E., Elvingson, C. and Johansson, L., *Proceed. Intern. Symp. Control. Rel. Bioact. Mater.* 1991, **18**, 146.
- 80 Foye, W. O., *Principle of Medicinal Chemistry*, 3rd Ed., Lea & Febiger Editions, Philadelphia (1990).
- 81 Johansson, L. and Löfroth, J.-E., *J. Phys. Chem.* 1993, **98**, 7471.
- 82 Johansson, L., Hedberg, P. and Löfroth, J.-E., *J. Phys. Chem.* 1993, **97**, 747 .
- 83 Johansson, L., Skantze, U. and Löfroth, J.-E., *J. Phys. Chem.* 1993, **97**, 9817.
- 84 Zhang, K. and Lindman, B., *J. Phys. Chem.* 1994, **98**, 2459.
- 85 Li, C. Y., Zimmerman, C. L., and Wiedmann, T. S. *Pharm. Res.* 1996, **13**, 535.
- 86 Laurent, T. C., Bjork, I., Pietroszkiewicz, A. and Persson, H., *Biochim. Biophys. Acta* 1963, **78**, 351.
- 87 Jönsson, B., Wennerstrom, H., Nilsson, P. G. and Linse, P., *Colloid Polym. Sci.* 1986, **264**, 77.
- 88 Hanai, T., *Kolloid Z.* 1961, **171**, 23.

- 89 Phillips, C. G. and Janssons, K. M., *Macromolecules* 1990, **23**, 1717.
- 90 Lonnqvist, I., Hikarissan, B., Balinov, B., and Söderman, O., *J. Colloid Interface Sci.* 1977, **192**, 66.
- 91 Mel'nichenko, Y. B., Klepko, V. V. and Shilov, V. V., *Polymer* 1993, **34**, 1019.
- 92 Klepko, V., Mel'nichenko, Y. and Shilov, V., *Polym. Gels Networks* 1996, **4**, 351.
- 93 Freed, K. F. and Edwards, S. F., *J. Chem. Phys.* 1974, **61**, 3626.
- 94 de Gennes, P. G., *Macromolecules* 1976, **9**, 587.
- 95 Laurent, T. C., Preston, B. N., Pertoft, H., Gustafsson, B. and McCabe, M., *Eur. J. Biochem.* 1975, **53**, 129.
- 96 Brown, W. and Stilbs, P., *Polymer* 1983, **24**, 189.
- 97 Altenberger, A. R., Tirrell, M. and Dahler, J. S., *J. Chem. Phys.* 1986, **84**, 5122.
- 98 Matsukawa, S. and Ando, I., *Macromolecules* 1996, **29**, 7136.
- 99 Altenberger, A. R. and Tirrell, M., *J. Chem. Phys.* 1984, **80**, 2208.
- 100 Kosar, T. F. and Phillips, R. J., *AIChE J.* 1995, **41**, 701.
- 101 Phillies, G. D. J., *Macromolecules* 1987, **20**, 558.
- 102 Phillies, G. D. J., *J. Phys. Chem.* 1989, **93**, 5029.
- 103 Kirkwood, J. G. and Riseman, J., *J. Chem. Phys.* 1948, **16**, 565.
- 104 Phillies, G. D. J., *Macromolecules* 1988, **21**, 3101.
- 105 Phillies, G. D. J., Richardson, C., Quinlan, C. A. and Ren, S. Z., *Macromolecules* 1993, **26**, 6849.
- 106 Daoud, M., Cotton, J. P., Farnoux, B., Jannink, G., Sarma, G., Benoit, H., Duplessix, R., Picot, C. and de Gennes, P. G., *Macromolecules* 1975, **8**, 804.
- 107 Langevin, D. and Rondelez, F., *Polymer* 1978, **19**, 875.
- 108 Adler, R. S. and Freed, K. F., *J. Chem. Phys.* 1980, **72**, 4186.
- 109 Phillies, G. D. J., Gong, J., Li, L., Rau, A., Zhang, K., Yu, L.-P. and Rollings, J., *J. Phys. Chem.* 1989, **93**, 6219.
- 110 Phillies, G. D. J., Ahmed, S., Li, L., Xu, Y., Rostcheck, D., Cobb, M. and Tanaka, T., *Macromolecules* 1991, **24**, 5299.
- 111 Lodge, T. P., Markland, P. and Wheeler, L. M., *Macromolecules* 1989, **22**,

- 3409.
- 112 Rao, B., Uemura, Y., Dyke, L., Macdonald, P. M., *Macromolecules* 1995, **28**, 531.
- 113 Gibbs, S. J. and Johnson, C. S., *Macromolecules* 1991, **24**, 6110.
- 114 Russo, P. S., Mustafa, M., Cao, T. and Stephen, L. K., *J. Colloid Interface Sci.* 1988, **122**, 120.
- 115 Yang, T. and Jamieson, A. M., *J. Colloid Interface Sci.* 1988, **126**, 220.
- 116 Masaro, L., Zhu, X. X. and Macdonald, P. M., unpublished results.
- 117 Phillis, G. D. J., *J. Phys. Chem.* 1992, **96**, 10061.
- 118 de Gennes, P. G., *J. Chem. Phys.* 1971, **55**, 572.
- 119 Rouse, P. E., *J. Chem. Phys.* 1953, **21**, 1272.
- 120 Zimm, B. H., *J. Chem. Phys.* 1956, **24**, 269.
- 121 Léger, L., Hervet, H., Auroy, P., Boucher, E. and Massey, G., *Rheology for Polymer Melt Processing*, Elsevier Sciences, B.V., 1 (1996).
- 122 de Gennes, P. G., *Macromolecules* 1976, **9**, 594.
- 123 de Gennes, P. G., *Scaling Concepts in Polymer Physics*; Cornell University Press: Ithaca, New York (1979).
- 124 Gent, A. N. and Kaang, S. Y., *J. Polym Sci., Polym. Phys. Ed.* 1989, **27**, 893.
- 125 Gent, A. N. and Liu, G. L., *J. Polym Sci., Polym. Phys. Ed.* 1991, **29**, 1313.
- 126 Antonietti, M.; Sillescu, H., *Macromolecules* 1985, **18**, 1162.
- 127 Léger, L., Hervet, H. and Rondelez, F., *Macromolecules* 1981, **14**, 1732.
- 128 Kim, E., Kramer, E. J., Garrett, P. D., Mendelson, R. A. and Wu, W. C., *J. Mat. Sci.* 1995, **30**, 1709.
- 129 Pajevic, S., Bansil, R. and Konak, C., *Macromolecules* 1995, **28**, 7536.
- 130 von Meerwall, E. D., Amis, E. J. and Ferry, J. D., *Macromolecules* 1985, **18**, 260.
- 131 Narasimhan, B. and Peppas, N. A., *Macromolecules* 1996, **29**, 3283.
- 132 Narasimhan, B. and Peppas, N. A., *J. Polym. Sci., Polym. Phys. Ed.* 1996, **34**, 947.
- 133 Alon, U. and Mutamel, D., *Phys. Rev. E* 1997, **55**, 1783.

- 134 Akerman, B., *Phys. Rev. E* 1996, **54**, 6697.
- 135 Smith, D. E., Perkins, T. T. and Chu, S., *Phys. Rev. Lett.* 1995, **75**, 4146.
- 136 Schlick, S., Pilar, J., Kweon, S. C., Vacik, J., Gao, Z., Labsky, J., *Macromolecules* 1995, **28**, 578.
- 137 Kavassalis, T. A. and Noolandi, J., *Phys. Rev. Lett.* 1987, **59**, 2674.
- 138 Kavassalis, T. A. and Noolandi, J., *Macromolecules* 1988, **21**, 2869.
- 139 Klein, J., *Nature* 1978, **48**, 1410.
- 140 Bartels, C. R., Graessley, W. W., Crist, B., *J. Polym. Sci., Polym. Lett. Ed.* 1983, **21**, 495.
- 141 Fleischer, G., *Polym. Bull.* 1983, **9**, 152.
- 142 Kumagai, Y., Watanabe, H., Miyasaka, K., Hata, T., *J. Chem. Eng. Jpn.* 1979, **13**, 1.
- 143 Smith, B. A., Samulski, E. T., Yu, L.-P., Winnik, M. A., *Bull. Am. Phys. Soc.* 1983, **28**, 546.
- 144 Antonietti, M., Coutandin, J., Grütter, R., Sillescu, H., *Macromolecules* 1984, **17**, 798.
- 145 Schaefer, D. W., Joanny, J. F. and Pincus, P., *Macromolecules* 1980, **13**, 1280.
- 146 Callaghan, P. T. and Pinder, D. N., *Macromolecules* 1984, **17**, 431.
- 147 Manz, B. and Callaghan, P. T., *Macromolecules* 1997, **30**, 3309.
- 148 Marmonier, M. F. and Léger, L., *Phys. Rev. Lett.* 1985, **55**, 1078.
- 149 Cheng, S. Z. D., Barley, J. S. and von Meerwall, E. D., *J. Polym. Sci., B* 1991, **29**, 515.
- 150 Lodge, T. P., Rotstein, N. A. and Prager, S., *Adv. Chem. Phys.* 1990, **79**, 1.
- 151 Gao, P., Nixon P. R. and Skoug, J. W., *Pharm. Res.* 1995, **12**, 965.
- 152 Higuchi, T., *J. Pharm. Sci.* 1963, **52**, 1145.
- 153 Phillies, G. D. J., Rostcheck, D. and Ahmed, S., *Macromolecules* 1992, **25**, 3689.
- 154 Phillies, G. D. J. and Quinlan, C. A., *Macromolecules* 1992, **25**, 3110.
- 155 Phillies, G. D. J., and Clomenil, D., *Macromolecules* 1993, **26**, 167.
- 156 Phillies, G. D. J., Brown, W. and Zhou, P., *Macromolecules* 1992, **25**, 4948.

- 157 Phillies, G. D. J., *Macromolecules* 1990, **23**, 2742.
- 158 Phillies, G. D. J., *J. Chem. Phys.* 1997, **101**, 4226.
- 159 Phillies, G. D. J., Lacroix, M., Yambert, J., *J. Chem. Phys.* 1997, **101**, 5124.
- 160 Phillies, G. D. J., *Macromolecules* 1998, **31**, 2317.
- 161 Cohen, M. H. and Turnbull, D., *J. Chem. Phys.* 1959, **31**, 1164.
- 162 Hedenqvist, M. and Gedde, U. W., *Progr. Polym. Sci.* 1996, **21**, 299.
- 163 Stern, S. A., Sampat, S. R. and Kulkarni, S. S., *J. Polym. Sci., Polym. Phys. Ed.* 1986, **24**, 2149.
- 164 Kulkarni, S. S. and Stern, S. A., *J. Polym. Sci., Polym. Phys. Ed.* 1983, **21**, 441.
- 165 Zhu, X. X. and Macdonald, P. M., *Macromolecules* 1992, **25**, 4345.
- 166 Zhu, X. X., Wang, F., Nivaggioli, T., Winnik, M. A. and Macdonald, P. M., *Macromolecules* 1993, **26**, 6397.
- 167 Xia, J. and Wang, C. H., *J. Polym. Sci., Polym. Phys. Ed.* 1995, **33**, 899.
- 168 Kim, D., Caruthers, J. M., Peppas, N. A., von Meerwall, E. D., *J. Appl. Polym. Sci.* 1994, **51**, 661.
- 169 Bandis, A., Inglefield, P. T., Jones, A. A. and Wen, W.-Y., *J. Polym. Sci., Polym. Phys. Ed.* 1995, **33**, 1495.
- 170 Fujita, H. and Kishimoto, A., *J. Polym. Sci.* 1958, **28**, 547.
- 171 Yasuda, H., Lamaze, C. E. and Ikenberry, L. D., *Die Makro. Chem.* 1968, **118**, 19.
- 172 Matsukawa, S. and Ando, I., *Macromolecules* 1997, **30**, 8310.
- 173 Chen, S. X. and Lostritto, R. T., *J. Contr. Release* 1996, **38**, 185.
- 174 Gilbert, D. L., Okano, T., Miyata, T. and Kim, S. W., *Int. J. Pharm.* 1988, **47**, 79.
- 175 Vrentas, J. S. and Duda, J. L., *J. Polym. Sci., Polym. Phys. Ed.* 1977, **15**, 403.
- 176 Vrentas, J. S. and Duda, J. L., *J. Polym. Sci., Polym. Phys. Ed.* 1977, **15**, 417.
- 177 Vrentas, J. S., Duda, J. L. and Ling, H. C., *J. Polym. Sci., Polym. Phys. Ed.* 1985, **22**, 459.
- 178 Vrentas, J. S., Duda, J. L. and Ling, H. C., *J. Polym. Sci., Polym. Phys. Ed.* 1985, **23**, 275.

- 179 Vrentas, J. S., Duda, J. L., Ling, H. C. and Hou, A.-C., *J. Polym. Sci, Polym. Phys. Ed.* 1985, **23**, 289.
- 180 Vrentas, J. S. and Vrentas, C. M., *J. Appl. Polym. Sci.* 1991, **42**, 1931.
- 181 Vrentas, J. S. and Vrentas, C. M., *Macromolecules* 1993, **26**, 6129.
- 182 Vrentas, J. S., Vrentas, C. M. and Duda, J. L., *Polym. J.* 1993, **25**, 99.
- 183 Vrentas, J. S. and Vrentas, C. M., *Macromolecules* 1994, **27**, 4684.
- 184 Faldi, A., Tirrell, M., Lodge, T. P. and von Meerwall, E. D., *Macromolecules* 1994, **27**, 4184.
- 185 Zielinski, J. M., Duda, J. L., *AIChE J.* 1992, **38**, 409.
- 186 Lodge, T. P., Lee, J. A. and Frick, T. S., *J. Polym. Sci., Polym. Phys. Ed.* 1990, **28**, 2607.
- 187 Zielinski, J. M., Sillescu, H. and Romdhane, I. H., *J. Polym. Sci., Polym. Phys. Ed.* 1996, **34**, 121.
- 188 Hang, S. U., Duda, J. L., *J. Appl. Polym. Sci.* 1997, **65**, 51.
- 189 Bandi, A., Inglefield, P. T., Jones, A. A. and Wen, W.-Y., *J. Polym. Sci., Polym. Phys. Ed.* 1995, **33**, 1504.
- 190 Vrentas, J. S. and Vrentas, C. M., *Macromolecules* 1994, **27**, 5570.
- 191 Hong, S. U., Barbari, T. A. and Sloan, J. M., *J. Polym. Sci., Polym. Phys. Ed.* 1997, **35**, 1261.
- 192 Landry, M., Gu, Q.-J. and Yu, H., *Macromolecules* 1989, **21**, 1159.
- 193 Su, H., Benesi, A. J. and Duda, J. L., *Polym. Int.* 1996, **39**, 243.
- 194 Peppas, N. A. and Lustig, S. R., *Hydrogels in Medecine and Pharmacy, Vol. I*, CRC Press, Boca Raton, p. 57 (1987).
- 195 Peppas, N. A. and Reinhart, C. T., *J. Membr. Sci.* 1983, **15**, 275.
- 196 Reinhart, C. T. and Peppas, N. A., *J. Membr. Sci.* 1984, **18**, 227.
- 197 Peppas, N. A. and Moynihan, H. J., *J. Appl. Polym. Sci.* 1985, **30**, 2589.
- 198 Bell, C. L. and Peppas, N. A., *Adv. Polym. Sci., Biopolymers II* 1995, **122**, 125.
- 199 Lustig, S. R. and Peppas, N. A., *J. Appl. Polym. Sci.* 1988, **36**, 735.
- 200 Bell, C. L. and Peppas, N. A., *Biomaterials* 1996, **17**, 1203.
- 201 Peppas, N. A. and Wright, S. L., *Macromolecules* 1996, **29**, 8798.

- 202 Mallapragada, S. K. and Peppas, N. A., *J. Contr. Release* 1997, **45**, 87.
- 203 am Ende, M. T. and Peppas, N. A., *J. Contr. Release* 1997, **48**, 47.
- 204 Williams, M. L., Landel, R. F., Ferry, J. D., *J. Am. Chem. Soc.* 1955, **77**, 3701.
- 205 Barrow, G. M., *Physical Chemistry*, 5th Ed., McGraw-Hill, New-York (1988).
- 206 MacElroy, J. M. D. and Kelly, J. J., *AIChE J.* 1985, **31**, 35.
- 207 Macey, R.I., *Membrane Physiology*, Andreoli, T.E., Hoffman, J.F., and Fanestil, D.D., Eds.; Plenum, New-York; Chap. 7, p. 125 (1980).
- 208 Kramer, H.A., *Physica* 1940, **7**, 284.
- 209 Golden, K., Goldstein, S., and Lebowitz, J.L., *Phys. Rev. Lett.* 1985, **55**, 2629.
- 210 Zwanzig, R.W., *Proc. Natl. Acad. Sci. U.S.A.* 1988, **85**, 2029.
- 211 Masaro, L., Zhu, X. X. and Macdonald, P. M., *Macromolecules* 1998, **31**, 3880.
- 212 Zhu, X. X., Masaro, L., Petit, J.-M., Roux, B. and Macdonald, P. M., *Materials for Controlled Release Applications*; McCulloch, I., Shalaby, S. W. Eds.; ACS Publ., Washington, D.C.; Chap. 18, p. 223 (1998).
- 213 Phillips, R. J., Deen, W. M. and Brady, J. F., *AIChE J.* 1989, **35**, 1761.
- 214 Brady, J. F., *AIChE Annual Meeting, San Francisco, CA* 1994, p. 320.
- 215 Eyring, H., *J. Chem. Phys.* 1936, **4**, 283.
- 216 Reisfeld, B.; Blackband, S.; Calhoun, V.; Grossman, S.; Eller, S. and Leong K., *Magn. Reson. Imaging* 1993, **11**, 247.

Chapitre 2

Pulsed Field Gradient NMR Spectroscopy in the Study of Self-Diffusion in Polymer Systems

Masaro, L.; Zhu, X.X.

Canadian Journal of Analytical Science and Spectroscopy

1998, 43, 81–89.

2.1. Abstract

The pulsed field gradient NMR spectroscopy has become an important analytical technique to measure the self-diffusion coefficients in polymer solutions, gels, and melts. In the pulsed-gradient spin-echo (PGSE) technique, the displacement of the spins is related to the attenuation of the NMR echo height as a function of the gradient strength and duration used. The echo height attenuation versus the gradient strength is usually described by a mono-exponential function for classical Brownian diffusion. In complex systems this dependence is not mono-exponential. Important information about the diffusant, network or both can be obtained from the non-mono-exponential dependence. This article reviews primarily the PGSE experiment used in the study of diffusion in various systems, particularly polymer solutions and gels. The principle and the experimental procedures including the pulse sequence, gradient and temperature calibration, etc., are presented. The limitations of the techniques in its applications and the information which can be extracted from complex systems are also discussed.

2.2. Introduction

The number of diffusion studies of polymer solutions, gels, and melts has considerably increased during the last decades. Diffusion measurements in polymer systems help in the understanding of polymer network structures [1], transport phenomena [2], and the controlled release of drugs [3]. The study of diffusion is important in the research on polymers, chemistry, and chemical engineering, as well as biochemical and pharmaceutical science.

Various analytical techniques are available to study the diffusion in polymer solutions and gels. These techniques include nuclear magnetic resonance (NMR) spectroscopy [4], fluorescence [5], gravimetry [6], diaphragm cell [7], dynamic light scattering [8], and holographic relaxation spectroscopy [9]. The capacities, limitations, and specific requirements of these analytical techniques were reviewed recently by Westrin *et al.* [10]. They concluded that the Diaphragm cell and the PGSE-NMR methods were very accurate and precise. Although the diaphragm cell

allows the characterization of an effective diffusion coefficient that implies the need of a gradient concentration in the system, no information can be obtained for the diffusion into the polymer membranes or networks. The pulsed-gradient spin-echo (PGSE) technique is often employed to measure a self-diffusion coefficient. The main advantages of the PGSE NMR technique reside in the fact that this technique is non-destructive, less time-consuming and capable of measuring self-diffusion coefficients in multi-components systems. Furthermore, this technique can provide information on both the diffusant and the diffusant-polymer matrix behavior in addition to the measured self-diffusion coefficient. For example, unusual echo attenuation behavior due to the network structure or due to the diffusant physical characteristics were observed in restricted systems [11] and complex systems [12].

This article reviews the PGSE NMR technique, including the calibration of the gradient strength and temperature, the applications and the limitations, and the use of the technique to obtain important information on the network structure and on the diffusant behavior.

2.3. The PGSE NMR Technique

A magnetic field with a temporary or steady field gradient is needed in the measurement of self-diffusion coefficient by NMR. As shown in Figure 2.1., if we introduce two NMR tubes with the same compound in a uniform magnetic field, the same nuclear spins present in each of the tubes will resonate at the same frequency. Thus, only one NMR signal is obtained (Figure 2.1A). If we place the same NMR tubes into a non-uniform magnetic field or a magnetic field with gradients, the same spins in each tube will resonate at different frequencies (Figure 2.1B). Consequently, two NMR signals will be observed on the spectrum. Each signal is proportional to the quantity of component present within the tube. Such a magnet design allows to localize the spins in the magnet geometry. When the spins are displaced, it will be possible to measure their self-diffusion coefficient by monitoring the change of the intensity of NMR signals as a function of time. At the present time, magnet with a steady gradient is still limited by technical difficulties. Nevertheless, a uniform

magnetic field with pulsed gradient can be easily obtained. The gradient pulses create a temporary inhomogeneity in the magnetic field.

The PGSE sequence developed by Stejskal and Tanner [13] consists of a spin-echo sequence in which two gradients are added on both sides of the 180° r.f. pulse. The spin echo sequence is made up by a 90° r.f. pulse and a 180° r.f. pulse separated by time τ . An echo is formed at time 2τ (Figure 2.2A). A 180° r.f. pulse inverts the magnetization precession so that spins precessing in the xOy plane will focus toward y. The first gradient located between the 90° and the 180° r.f. pulses (Figure 2.2A) labels or encodes the spins by producing a rapid precessional phase shift. The second gradient can be considered as a phase compensation gradient (or refocussing) due to the 180° r.f. pulse. Thus, if diffusion occurs during the interval Δ , i.e., if the spins change their environment, the spin contribution to the echo will be reduced. In other words, the echo intensity, I , is proportional to the molecular motion in solution. In absence of any molecular diffusion, the 180° r.f. pulse and the refocussing gradient, will focus the magnetization as shown in Figure 2.2B. When diffusion occurs, the attenuation on the NMR signal depends on the self-diffusion coefficient D and is given by the following equation

$$I_{(\delta)} = I_{(0)} \exp\left(\frac{-2\tau}{T_2}\right) \exp\left[-\gamma^2 \delta^2 G^2 D \left(\Delta - \frac{\delta}{3}\right)\right] \quad (2.1)$$

where γ is the magnetogyric ratio of the nucleus under observation, G the gradient strength, δ the length of the gradient pulse, Δ the time interval between two gradients, τ the interval between r.f. pulses (90° – 180°) and between the 180° pulse and the echo, $I_{(0)}$ the intensity of the NMR signal without applied gradient pulses and $I_{(\delta)}$ defines the NMR signal with applied gradient. Basically, the PGSE sequence and the others pulsed field gradient (PFG) sequences are used to measure Brownian displacement which occurs between the period Δ , or time between the two gradient pulses. Detailed theoretical approaches of the PGSE technique can be found in the articles of Stilbs [14], Callaghan [11] and Price [15].

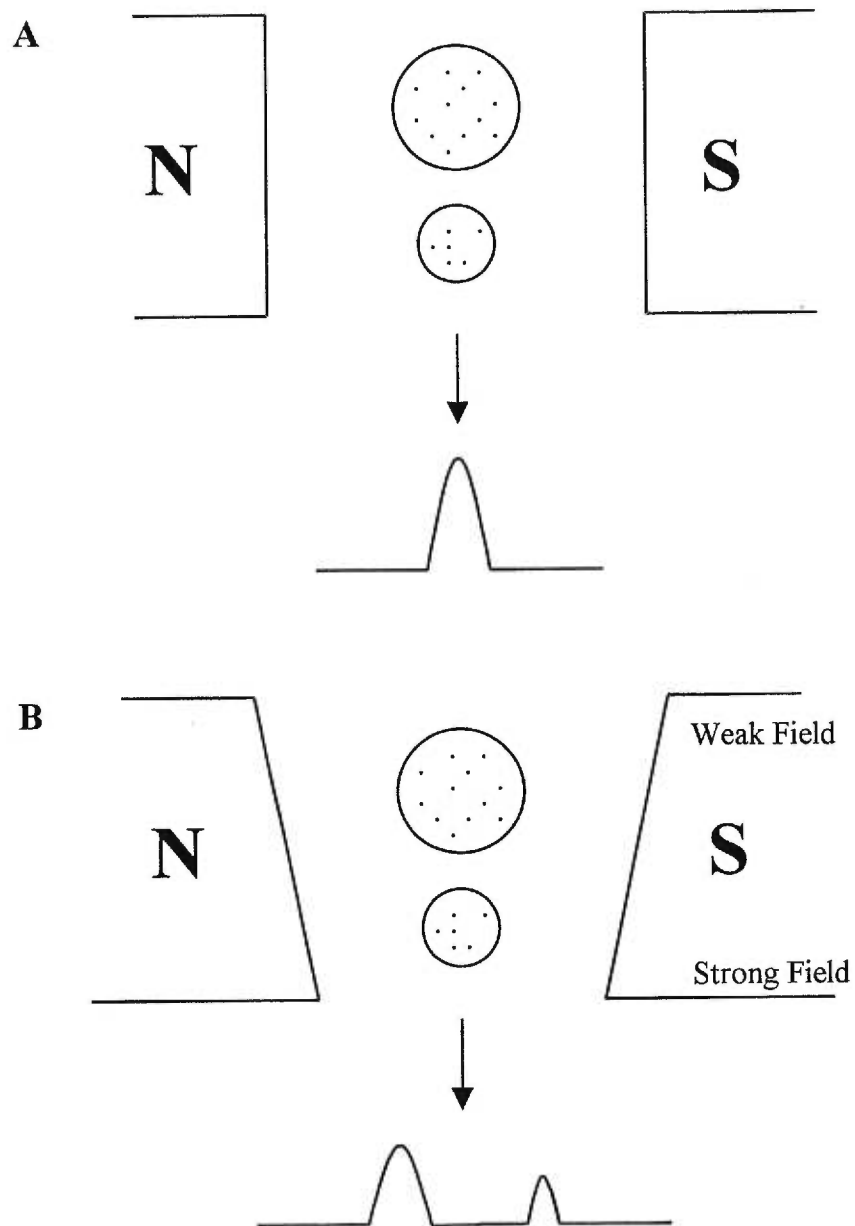


Figure 2.1. Illustrations of a uniform magnetic field (A), and of a magnetic field with gradient (B). Two NMR tubes containing the same spins provide one NMR signal in a uniform magnetic field but two NMR signals in a magnetic field with gradient. Displacements of the spins can be monitored by the change in the NMR signal integrations as a function of time.

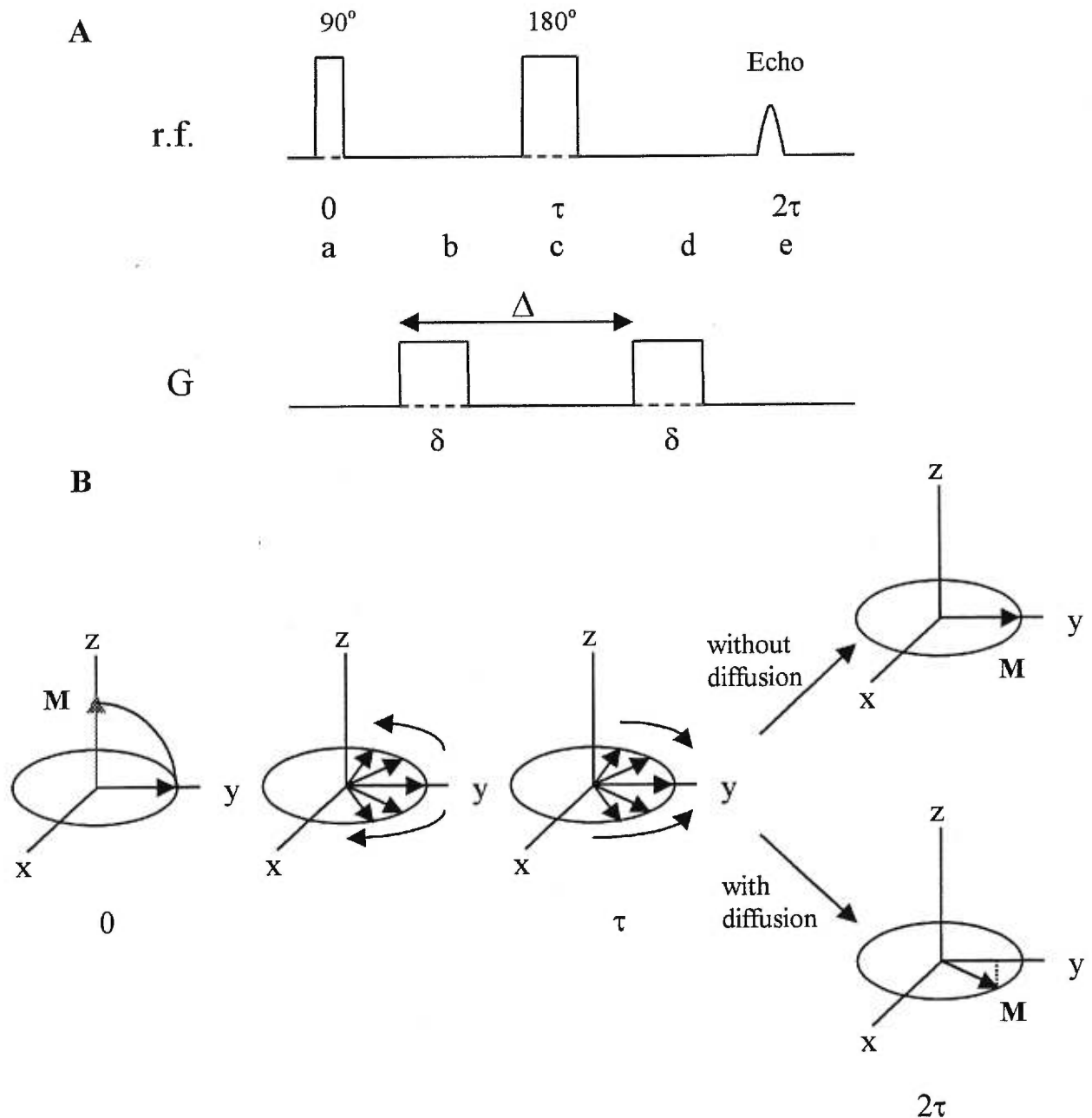


Figure 2.2. Pulsed-gradient spin-echo (PGSE) NMR sequence (A) and representation of the motion of the spins with respect to the r.f. pulses and gradient pulses (B). The self-diffusion coefficient is obtained by monitoring the intensity of the NMR signal(s) as a function of the strength and duration of the gradient pulse, as described in equation 2.1.

In PGSE experiments the parameters Δ and τ are kept constant in order to eliminate the dependence on the transverse relaxation time (T_2). A constant gradient strength can be used while the duration of the gradient pulse can be varied. Hence, the semi-logarithmic plot of $I(\delta)$ versus $\delta^2(\Delta-\delta/3)$ will be a straight line and from the slope the self-diffusion coefficient can be calculated once the gradient strength is known.

Figure 2.3. provides an example of poly(ethylene glycol) (PEG), diffusion determination in poly(vinyl alcohol)-water network. The plot represents a typical PGSE NMR experiment with varying δ and constant G . The highest signal on the first spectrum ($\delta = 1$ ms) is attributed to the PEG whereas the signal upfield is due to the CH_2 group of the polymer main chain, i.e., poly(vinyl alcohol) (PVA) and the signal downfield corresponds to the water resonance. The PVA signal intensity changes very little since the self-diffusion coefficient of the polymer is lower compared to the PEG signal. The water signal disappears rapidly since its self-diffusion coefficient is much higher.

2.4. Calibration of the gradient strength

Before running experiments the temperature and the gradient strength need to be calibrated. Samples with known self-diffusion coefficients such as water or glycerol can be used as standards to calibrate the gradient field strength. The self-diffusion coefficients of selected molecules at various temperature are listed in Table 2.1.

The most common standard is water in deuterated water [16,17], which is used to calibrate relatively low gradient strength. To study slow diffusion, stronger gradient strengths should be used, which are calibrated with more viscous standards such as dried glycerol [18] or polymer solutions [19]. A second standard is usually needed for the verification of possible evolution of the gradient strength with time. The calibration of the gradient should be verified daily by the use of a sample with a known self-diffusion coefficient. Moreover, since the gradient strength varies slightly with the temperature, calibration should be done as a function of the temperature.

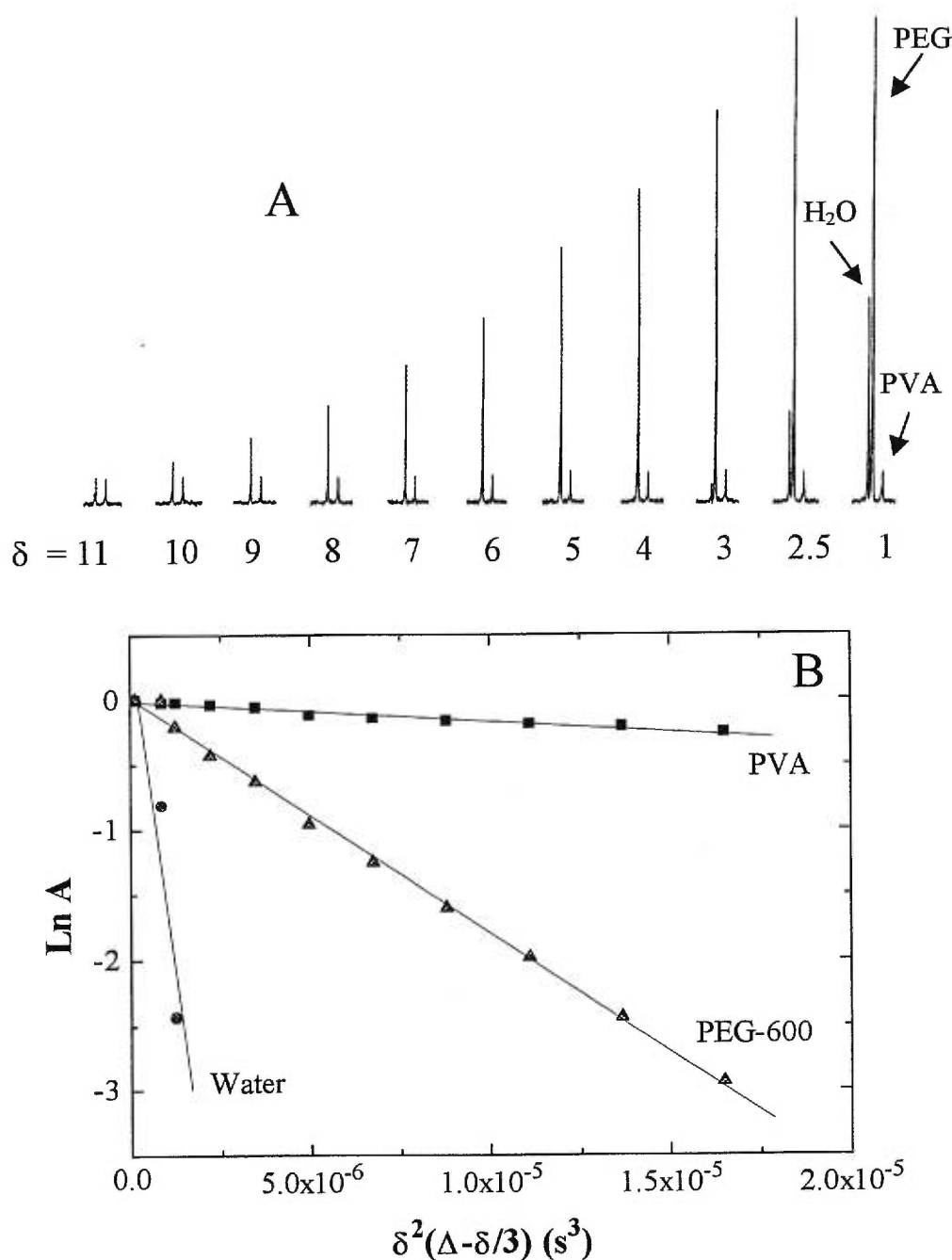


Figure 2.3. (A) Example of ^1H PGSE NMR spectra of PEG-600 in a PVA-water binary mixture at 43 °C, showing proton signal attenuation with increasing gradient pulse durations (δ). [PVA] = 0.03 g/mL, $G = 0.491$ T/m, interval between gradient pulses $\Delta = 140$ ms, and the recycle delay was 14 s. (B) The corresponding semi-logarithmic plot of the signal intensities as a function of $\delta^2(\Delta - \delta/3)$ for PVA, PEG-600 and water protons signals. The self-diffusion coefficients are calculated from the slope of the lines: $D_{\text{PVA}} = 3.64 \times 10^{-11}$ m^2/s , $D_{\text{PEG-600}} = 4.14 \times 10^{-10}$ m^2/s , and $D_{\text{water}} = 4.68 \times 10^{-9}$ m^2/s .

Table 2.1. List of standards with known self-diffusion coefficients that can be used for the gradient strength calibration.

Standard	Temperature (°C)	Self-diffusion coefficient (10^{-9} m ² /s)	Reference
pure H ₂ O	5	1.313	16
-	25	2.299	16
-	25	2.35	17
-	45	3.575	16
pure D ₂ O	5	1.015	16
-	25	1.872	16
-	45	2.979	16
trace of H ₂ O in D ₂ O	5	1.034	16
	25	1.902	16
	45	3.027	16
50 % DMSO-50 % H ₂ O	25	$D_{\text{water}} = 0.83$	17
		$D_{\text{DMSO}} = 0.50$	17
Pure glycerine	25	0.0173	18
	31	0.0323	18
	40	0.0614	18
10 g/L PEO in HDO	23	0.023	19

NMR instruments equipped with imaging probes usually allow the application of gradient pulses in the three directions (x, y, z). Calibrations can be achieved more easily by the use of one dimensional image along each direction [20]. This technique requires a sample with a predefined geometry immersed in a spin-rich liquid such as water doped with 1 wt% CuSO₄. The calibration is achieved by acquiring an image of the sample. An image profile is obtained and the width of the image can be correlated with the width of the sample. While performing the calibration, the image profile is measured in Hz thus voxel approximations from the reconstructed image are avoided.

2.5. Temperature calibration

Since the self-diffusion coefficient is strongly dependent on the temperature, temperature calibration inside the NMR probe is also very important. The temperature calibration can be achieved by using pure methanol or ethylene glycol and measuring the chemical shift difference in ppm, or in Hz, between the NMR signals of the solvent versus temperature changes [21]. Table 2.2 lists the values in ppm and Hz for the chemical shift difference between the CH₃ and OH groups for methanol and CH₂ and OH groups for ethylene glycol. This method is easy and rapid but can be erroneous. A small variation in the chemical shift due to an incorrect shimming procedure can induce a large error in the temperature calibration. Care should be taken when preparing the sample and when measuring the chemical shift difference. This method allows the measurement of the average temperature of the sample, but it is not easy to be used to detect any temperature gradient along the NMR tube.

The temperature calibration can be achieved also with a thermocouple which is not sensitive to the magnetic field. A thermocouple with a constantan copper-nickel extension (T) meets this requirement. The linearity of the thermocouple from 0 to 100 °C can be verified easily and rapidly by measuring the temperature of a water-ice mixture and the temperature of boiling water. Possible temperature gradient inside the NMR probe can be detected by moving the thermocouple inside the NMR probe.

Another way to calibrate the temperature in the NMR probe is to reproduce the self-diffusion coefficient values of standards measured at various temperatures by other

methods. The self-diffusion coefficients of several standards are listed in Table 2.1. with corresponding temperatures. This method can only be used to measure an average temperature, and the gradient strength has to be calibrated first.

Table 2.2. Example of chemical shift difference, for proton resonating at 300.13 MHz, between the CH₂ and OH groups for ethylene glycol and the CH₃ and OH groups for methanol at 29, 30 and 31 °C.

Temperature (°C)	Ethylene Glycol		Methanol	
	ppm	Hz	ppm	Hz
29	1.6113	483.6	1.528	458.6
30	1.6015	480.6	1.5183	455.7
31	1.5917	477.7	1.5082	452.8

2.6. The study of diffusion in polymers systems

The PGSE NMR technique can be easily used to study diffusion behavior of small molecules and large diffusants with NMR relaxation times long enough for the spin echo experiment. This applies to systems such as polymer solutions [22], gels [23] and melts [24]. The PGSE NMR technique can also be used to study the diffusion in a variety of chemical and even biochemical systems. For example, Lönnqvist *et al.* [25] determined the diffusion behavior of the different components in a water-oil-water double emulsion system. Schonhoff and Soderman [26] studied the equilibrium adsorption dynamics of surfactants at the solid/liquid interface. Stanisiz *et al.* [27] measured water diffusion in bovine optic nerve. Li *et al.* [28] studied the diffusion of drug-solubilizing bile salt/phosphatidylcholine aggregates in mucin mucous layer. Clericuzio *et al.* [29] studied mass transfer in the amorphous phase, i.e., ionic motion of ⁷Li, ²³Na, and ¹⁹F in polymer electrolytes. In addition, motion of

plastizers was also studied [29]. Callaghan and coworkers [30] studied the flow and diffusion in porous media and the convection in capillary [31].

We have used the PGSE technique to measure self-diffusion coefficients of diffusants in binary and ternary polymer-solvent systems [32-35]. These studies cover the diffusion of solvent, small and macromolecular diffusants, having different chemical function groups, various sizes and various geometries in both aqueous and organic solutions containing polymers such as poly(vinyl alcohol) and poly(methyl methacrylate). Recently, we have proposed a new physical model of diffusion for the interpretation of the data [36]. An example of an NMR experiment is shown in Figure 2.3. The gradient calibration was carried out with a sample of a known self-diffusion coefficient (1 wt% HDO in D₂O, $D = 1.9 \times 10^{-10}$ m²/s) as described in the previous section.

2.7. *J*-modulation effect

The study of homonuclear or heteronuclear diffusant can be perturbed by an artefact due to first and second order spin-spin coupling. This perturbation is commonly named *J*-modulation effect [14, 37]. The origin of this effect resides in the fact that spins precession frequencies have different rates, thus spins vectors will not refocus on the y axis at the same time [38]. As a result, distortion of the NMR spectrum appears. Distortions are characterized by negative signal and/or loss of some NMR signals in the spectrum. The *J*-modulation depends strongly on the gradient pulse time interval Δ . A first order *J*-modulation effect is present and persistent for a Δ period duration inferior to $1/J$, whereas this effect is less consistent for a Δ period duration superior to $1/J$. Another way to remove the phase distortion is to use a magnitude mode spectrum [39]. However, this method enlarges the NMR signal, especially at the base.

2.8. Spin-Spin relaxation time and eddy currents problems

The largest limitations of the PGSE technique concern the spin-spin relaxation time (T_2) and the eddy currents problems, particularly for polymer systems.

In the PGSE sequence, T_2 has to be long enough (namely, $T_2 \gg \tau$) for the application of the gradient pulses (Figure 2.2A.). Macromolecules are characterized by low self-diffusion coefficients and short T_2 values. One possible solution to overcome T_2 problems and/or slow diffusion is to shorten the gradient pulses while increasing the gradient strength. However, a strong gradient pulse can induce eddy currents in the probe that can persist for a considerable period of time after the gradient pulse is turned off. In severe cases the eddy currents can perturb the second pulse and lead to distortion or even complete loss of the NMR signal. Various methods can be used to compensate or correct the eddy currents effect in the PGSE NMR experiments. Hardware modifications such as the use of actively shielded gradient coils [40], compensation for the gradient coil [41] and application of a decay current to the Z_0 shim coil [42] can be useful in solving the eddy currents problems. Software methods were also reported. For example, a correction can be added to the second gradient pulse in order to compensate for any mismatch of the effective field gradient of the experiment [43], as shown in Figure 2.4. This empirical compensation function has been used successfully in the self-diffusion measurements of various solvents in different polymer systems [44,45]. Recent NMR spectrometers allow the detection and compensation of eddy currents by pulse preemphasis adjustments [20].

When the spin-lattice relaxation time (T_1) is much longer than the spin-spin relaxation time (T_2), the T_2 limitation can be avoided by the use of the stimulated echo (STE) sequence [46,47]. This sequence consists of a succession of three 90° pulses that lead to a stimulated echo after the third r.f. pulse, as illustrated in Figure 2.5A. In this sequence the spin attenuation depends mainly on T_1 instead of T_2 . The signal attenuation dependence on T_1 provides numerous advantages. For example, STE can be used to study diffusion over a larger Δ interval thereby reducing eddy current effect. In addition, STE was used for samples with $T_2 \ll T_1$, and samples with small self-diffusion coefficients for which no significant attenuation can be observed with PGSE sequence.

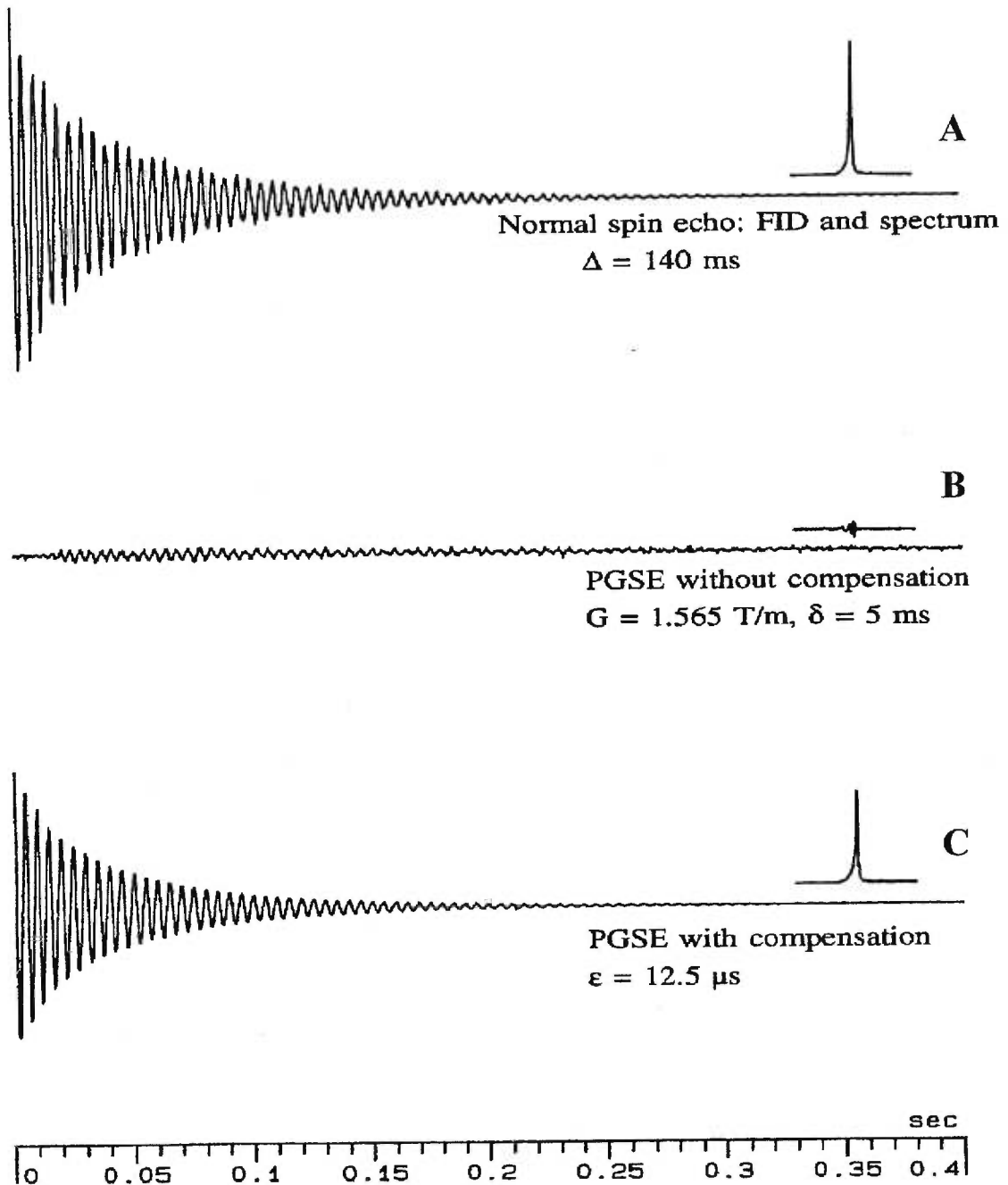


Figure 2.4. The compensation of the eddy current effect caused by the first gradient pulse (δ) by the addition of a correction (ϵ) to the second gradient pulse as measured with a sample consisting of 50 wt % of a PEG solution in D_2O ($\tau = 140 \text{ ms}$). (A) normal spin-echo FID and the corresponding spectrum. (B) PGSE FID in the presence of eddy currents (no compensation) and the distorted spectrum. (C) FID of the same PGSE experiment with eddy current compensation and the restored spectrum.

Eddy current problems can also be solved by the use of the longitudinal eddy-current delay (LED) sequence [48]. This sequence was created to overcome large eddy current fields. It consists of four 90° train pulses as illustrated in Figure 2.5B. After each gradient pulse a 90° r.f. pulse inverts the magnetization in the longitudinal plane where relaxation is mainly due to T_1 . The advantage of this sequence is obvious. The delay between the second gradient pulse and the acquisition is larger than in the stimulated echo sequence. Thus, if eddy-currents are induced by gradient pulses, their impact at the acquisition time will be much more attenuated in the LED experiment than in the STE and PGSE sequences as demonstrated by Gibbs *et al.* [48].

2.9. Signal overlapping

When two distinct NMR signals are overlapped it induces complications in the spectrum and therefore its analysis. As a result, equation 2.1 remains no longer valid and a bi-exponential fit to the data using a sum of two exponential functions should be employed [25]. Lönnqvist *et al.* [25] have performed a bi-exponential fitting to their data of water and oil diffusion in water-oil-water emulsion. According to the authors, the appropriate weight factor of each sample is key to successful determination of each independent self-diffusion coefficient. We have also encountered signal overlapping problems in our study of *tert*-butanol diffusion in poly(*N,N*-diethyl acrylamide)-water system. The signal of the methyl groups of the *tert*-butanol overlaps with that of the methyl groups of the polymer. Therefore, the overlapped NMR signals for the diffusant and the polymer were analyzed with a bi-exponential function. However, accurate results cannot be obtained when the proportion of each compound is unknown, as numerous mathematical solutions can result from a bi-exponential equation.

If a slow diffusion component overlaps with a fast diffusion one, it is easy to suppress the fast diffusing component by applying a gradient with sufficient strength. In fact, this is also one way to suppress NMR signals of solvents in high resolution NMR.

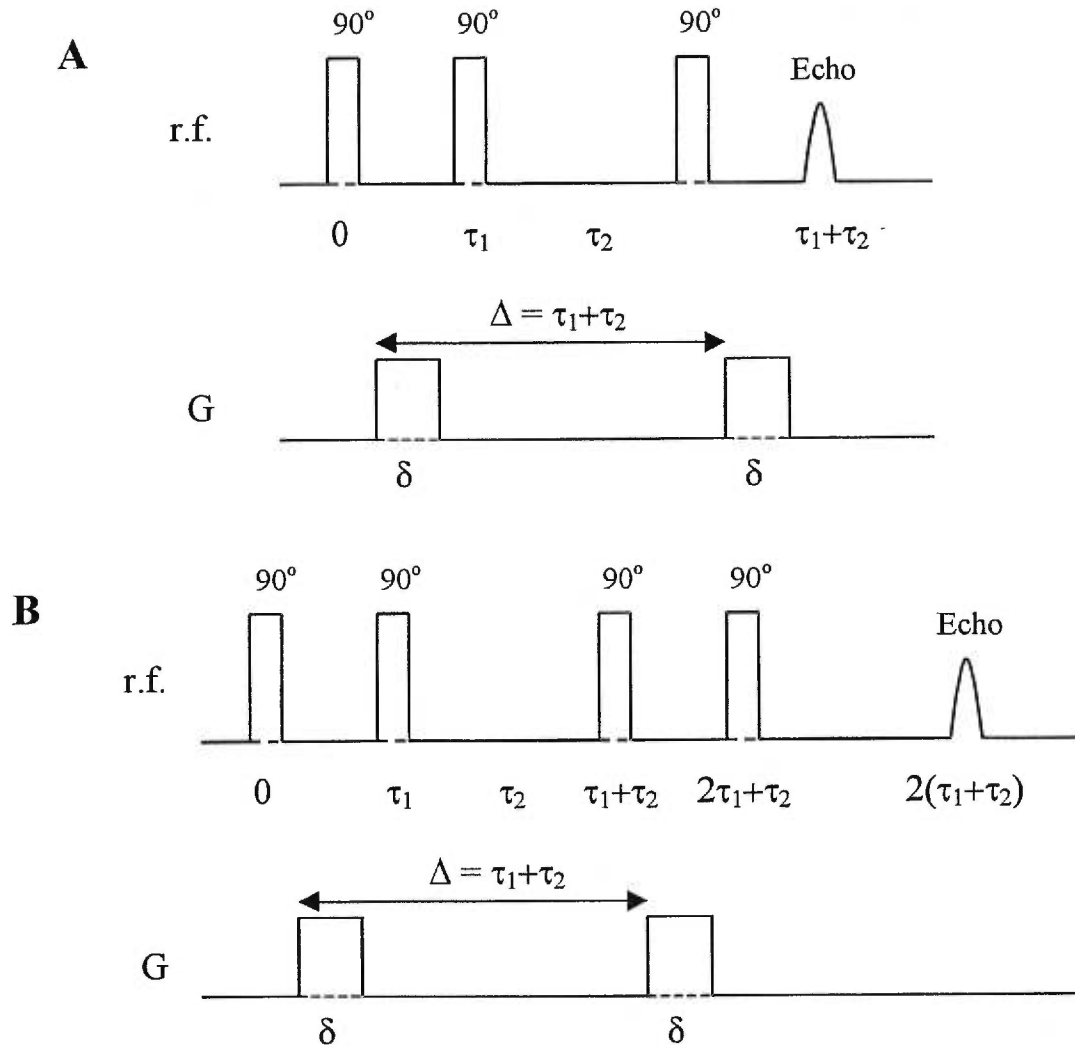


Figure 2.5. (A) The stimulated echo (STE) NMR sequence, and (B) the longitudinal eddy-current delay (LED) NMR sequence used to overcome T_2 and eddy-current problems in diffusion measurements.

2.10. Non-homogenous or anomalous diffusion

Non-homogenous or anomalous diffusion is characterized by a non-mono-exponential dependence of the echo height attenuation versus the experimental parameters, $(\gamma G \delta)^2 (\Delta - \delta/3)$. A non-mono-exponential dependence can be also attributed to restricted diffusion. Non-homogenous or anomalous diffusion corresponds to anisotropic Brownian motion while restricted diffusion is caused by the physical boundaries of the polymer matrix. This distinction is very important, and implies that for non-homogenous or anomalous diffusion the echo height attenuation is mainly due to the behavior of the diffusant. Examples of non-homogenous or anomalous diffusion are numerous in the literature. Walderhaug *et al.* [49] reported the study of the diffusion of associative polymers in water. The self-diffusion coefficients of the polymers showed an increasing distribution with increasing concentration. This increasing distribution of the self-diffusion coefficients resulted in a curvature in the semi-logarithmic plot of the NMR signal intensity as a function of the experimental parameters. Walderhaug *et al.* [49] demonstrated that the non-homogenous diffusion was due to the polymer polydispersity. The authors used a stretched exponential equation to extract their data,

$$I_{(\delta)} = I_{(0)} \exp\left[-(X D_{SE})^\beta\right] \quad (2.2)$$

where $I_{(\delta)}$ and $I_{(0)}$ have been defined previously, β ($0 < \beta \leq 1$) is a parameter describing the width of the distribution of the self-diffusion coefficients ($\beta = 1$ for monodisperse self-diffusion coefficient), $X = (\gamma G \delta)^2 (\Delta - \delta/3)$ and D_{SE} is used to calculate the mean self-diffusion coefficient, D , by

$$\frac{1}{D} = \int_0^\infty \exp\left[-(X D_{SE})^\beta\right] dX = \left(\frac{1}{\beta}\right) \Gamma\left(\frac{1}{\beta}\right) \left(\frac{1}{D_{SE}}\right) \quad (2.3)$$

where Γ denotes the gamma function.

Equation 2.2 has been used successfully in the literature, especially in the studies of associative polymers based on poly(ethylene oxide) [50], hydrophobic ethoxylated urethane [12] and hydrophobically modified poly(*N,N*-dimethylacrylamide) [19].

Recently, Walderhaug and Nyström [51] reported on anomalous diffusion. They studied triblock copolymer [poly(ethylene oxide)-poly(propylene oxide)-poly(ethylene oxide)] diffusion in aqueous systems during gelation as a function of temperature. When the temperature of gelation was reached, the decay of the spin echo attenuation exhibits an increasing non-exponentially behavior. The authors suggested that this polydispersity effect was due to the formation of intermolecular association between the polymer chains. Watanabe *et al.* [52] studied water diffusion in dextran gels. They found two types of water with different diffusion coefficients. The faster diffusion coefficient was assigned to bulk water, whereas the slower diffusion coefficient was assigned to trapped water.

We have studied the self-diffusion coefficient for a series of oligo- and poly(ethylene glycol) samples in poly(vinyl alcohol)-water systems [32]. The diffusants were monodispersed as demonstrated by size exclusion chromatography, and poly(vinyl alcohol) (PVA) used in these experiments was completely hydrolyzed. Ethylene glycol and some of its oligomers used in this study showed signs of anomalous diffusion. Echo attenuation of the ethylene glycol NMR signal is shown in Figure 2.6. Since it is a small molecule, there is no polydispersity problems as in the case of polymers. Moreover, this behavior cannot be attributed to the self-association of ethylene glycol since this compound is present in small quantity in the system (1 wt% in D₂O). We have also noticed that this behavior increases when the polymer concentration is increased. Thus, we believe that this behavior can only be explained by the presence of two different ethylene glycols in the system. Free ethylene glycol molecules with echo attenuation corresponding to the first part of the plot in Figure 2.6. ($D = 4.75 \times 10^{-10} \text{ m}^2/\text{s}$), and bound ethylene glycol molecules with echo attenuation corresponding to the second part of the plot ($D = 1.77 \times 10^{-10} \text{ m}^2/\text{s}$).

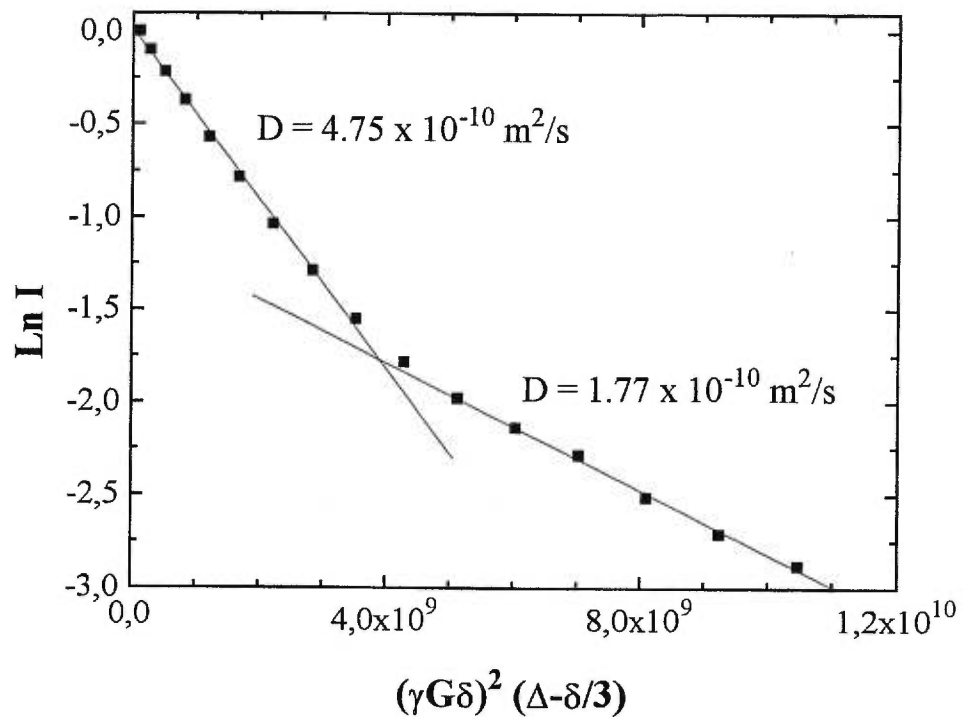


Figure 2.6. Plot of the echo attenuation versus $X = (\gamma\delta G)^2(\Delta - \delta/3)$ for ethylene glycol in poly(vinyl alcohol)-water system. Experimental conditions: [PVA] = 0.12 g/mL, $G = 10$ to 100 G/cm, gradient duration $\delta = 2.25$ ms, interval between gradient pulses $\Delta = 30$ ms, the recycle delay 16 s, and $T = 23$ °C. The curvature is due to the presence of two different types of ethylene glycol, one free ($D = 4.75 \times 10^{-10} \text{ m}^2/\text{s}$) and one bound to PVA ($D = 1.77 \times 10^{-10} \text{ m}^2/\text{s}$).

2.11. Restricted diffusion

The diffusion of diffusants is considered restricted when the Brownian motion of the studied molecule is hindered by physical boundaries. The physical boundaries can be due to macromolecules (polymer and proteins) or micelles. The physical boundaries exist in liquid crystals, lipid bilayers and porous materials. As specified above, the PFG NMR technique provides information on the diffusant mean square displacement, $\langle z^2 \rangle$, that occurs during the time Δ , or time between the two gradient pulses:

$$\langle z^2 \rangle = 2D\Delta \quad (2.4)$$

To be detected by PFG NMR, the length of the restricted geometry has to be smaller than the displacement of the diffusant. Thus, restricted diffusion is evidenced by a dependence of the self-diffusion coefficient on the time of diffusion Δ . Restricted diffusion is detected especially for long Δ , i.e., when the particle can travel far enough to feel the effect of the restricted geometry. When the displacement of a diffusant is restricted during the analysis time, Δ , the echo attenuation does not have a mono-exponential dependence on the experimental parameters X . Examples of restricted diffusion are numerous in the literature. For example, Callaghan and Pinder [53] have demonstrated that diffusion in entangled polystyrene solution of sufficiently high molecular weight is restricted. Similar results were obtained by Callaghan and Soderman [54] for AOT/water solutions.

Pavesi and coworkers [55,56] have used the STE sequence with increasing Δ to study water diffusion in chemically crosslinked gels. In their case, the restricted diffusion is due to the network microstructure. These experiments allowed the characterization of the diffusion in a polymer network (Fickian or non-Fickian diffusion) as well as the characterization of the polymer pore radius [55,56]. Such studies can be done also with the PGSE sequence as demonstrated by von Meerwall and Fergusson [57] when the diffusant has a long enough T_2 .

2.12. Concluding Remarks

With the recent development of the PGSE technique, many technical difficulties have been overcome. The PGSE NMR technique has been shown to be a very powerful technique in the study of polymer and other complex systems as it can provide information usually difficult to obtain. The determination of self-diffusion coefficient by PGSE NMR is a study of the motion of nuclear spins, which provides interesting and important information not only on anisotropic diffusion in chemical systems, but also on isotropic diffusion in ordered systems such as liquid crystals and lipid bilayers, non-homogenous diffusion due to the diffusant polydispersity, anomalous diffusion resulted from various interactions in the polymer-diffusant system, and restricted diffusion due to physical boundaries. The interpretation of the echo height attenuation in the latter cases remains more complicated than for the classical Brownian diffusion, but at the same time provides an interesting challenge to NMR spectroscopists to obtain information that is otherwise unavailable to researchers.

2.13. Acknowledgments

The financial support from the Natural Sciences and Engineering Research Council (NSERC) of Canada and the Quebec Government (Fonds FCAR) is gratefully acknowledged. The authors also thank Professor P.M. Macdonald of University of Toronto for helpful discussions.

2.14. References

- [1] S.Z.D. Cheng, J.S. Barley and E.D. von Meerwall, *J. Polym. Sci., Part B*, 29, 515 (1991).
- [2] D. Hariharan and N.A. Peppas, *J. Contr. Release*, 23, 123 (1993).
- [3] N.A. Peppas and J.E. Scott, *J. Contr. Release*, 18, 95 (1992).
- [4] R.A. Waggoner, F.D. Blum and J.C. Lang, *Macromolecules*, 28, 2658 (1995).
- [5] M.B. Wisnudel and J.M. Torkelson, *Macromolecules*, 29, 6193 (1996).
- [6] D. Shiaw-Guang Hu and K. Jiunn-Nan Chou, *Polymer*, 37, 1019 (1996).

- [7] B.A.H. Smith and M.V. Sefton, *J. Biomed. Mater. Res.*, **22**, 673 (1988).
- [8] A.C. van Asten, W.T. Kok, R. Tijssen and H. Poppe, *J. Polym. Sci., Part B*, **34**, 283 (1996)
- [9] I.H. Park, C.S. Johnson Jr. and D.A. Gabriel, *Macromolecules*, **23**, 1548 (1990).
- [10] B.A. Westrin, A. Axelsson and G. Zacchi, *J. Contr. Release*, **30**, 189 (1994).
- [11] P.T. Callaghan, *Aust. J. Phys.*, **37**, 359 (1984).
- [12] B. Rao, Y. Uemura, L. Dyke and P.M. Macdonald, *Macromolecules*, **28**, 531 (1995).
- [13] E.O. Stejskal and J.E. Tanner, *J. Chem. Phys.*, **42**, 288 (1965).
- [14] P. Stilbs, *Progr. NMR Spectrosc.*, **19**, 1 (1987).
- [15] W.S. Price, *Concepts Magn. Reson.*, **9**, 299 (1997).
- [16] R. Mills, *J. Phys. Chem.*, **77**, 685 (1973).
- [17] T.L. James and G.G. McDonald, *J. Magn. Reson.*, **11**, 58 (1973).
- [18] M. I. Hrovat and C. G. Wade, *J. Magn. Reson.*, **44**, 62 (1981).
- [19] Y. Uemura, J. McNulty and P.M. Macdonald, *Macromolecules*, **28**, 4150 (1995).
- [20] Bruker User Manual, "Microimaging: Avance Manual, Installation and User Manual", version 001, Bruker Analytische Messtechnik, Rheinstetten, Germany (1996).
- [21] C. Amman, P. Meier and A.E. Merbach, *J. Magn. Reson.*, **46**, 319 (1982).
- [22] R.A. Waggoner, F.D. Blum and J.C. Lang, *Macromolecules*, **28**, 2658 (1995).
- [23] S. Matsukawa and I. Ando, *Macromolecules*, **29**, 7136 (1996).
- [24] E.D. von Meerwal, T. Pryor and V. Galiatsatos, *Macromolecules*, **31**, 669 (1998).
- [25] I. Lönnqvist, B. Hakansson, B. Balinov and O. Soderman, *J. Colloid Int. Sci.*, **192**, 66 (1997).
- [26] M. Schonhoff and O. Soderman, *J. Phys. Chem. B*, **101**, 8237 (1997).
- [27] G.J. Stanisz, A. Szafer, G.A. Wright and R.M. Henkelman, *Magn. Reson. Med.*, **37**, 103 (1997).
- [28] C.Z. Li, C.L. Zimmerman and T.S. Wiedmann, *Pharm. Res.*, **13**, 535 (1996).
- [29] M. Clericuzio, W.O. Parker, M. Soprani and M. Andrei, *Solid State Ionic*, **82**,

- 179 (1995).
- [30] J.D. Seymour and P.T. Callaghan, *AIChE J.*, 43, 2096 (1997).
- [31] B. Manz, J.D. Seymour and P.T. Callaghan, *J. Magn. Reson.*, 125, 153 (1997).
- [32] L. Masaro, X.X. Zhu and P.M. Macdonald, *Macromolecules*, 31, 3880 (1998).
- [33] J.M. Petit, X.X. Zhu and P.M. Macdonald, *Macromolecules*, 29, 70 (1996).
- [34] X.X. Zhu, L. Masaro and P.M. Macdonald, *Polymer Preprints*, 38, 594 (1997).
- [35] X.X. Zhu, L. Masaro, J.-M. Petit, B. Roux and P.M. Macdonald, *Advances in Chemistry Series*, in press (1998).
- [36] J.M. Petit, B. Roux, X.X. Zhu and P.M. Macdonald, *Macromolecules*, 29, 6031 (1996).
- [37] E.L. Hahn and D.E. Maxwell, *Phys. Rev.*, 88, 1070 (1952).
- [38] R.J. Abraham, J. Fisher and P. Loftus, *Introduction to NMR spectroscopy*, John Wiley and Sons Ed. (1988).
- [39] L. Mahi, J.C. Duplan and B. Fenet, *Chem. Phys. Letters*, 211, 27 (1993).
- [40] P. Mansfield and B. Chapman, *J. Magn. Reson.*, 72, 211 (1987).
- [41] D.J. Jensen, W.W. Brey, J.L. Delayre and P.A. Narayana, *Med. Phys.*, 14, 859 (1987).
- [42] I.M. Brereton, J. Field, L.N. Moxon, M.G. Irving and D.M. Doddrell, *Magn. Reson. Med.*, 9, 118 (1989).
- [43] X.X. Zhu and P.M. Macdonald, *Solid State Nuclear Magnetic Resonance*, 4, 217 (1995).
- [44] X.X. Zhu and P.M. Macdonald, *Macromolecules*, 25, 4345 (1992).
- [45] X.X. Zhu, F. Wang, T. Nivaggioli, M.A. Winnik and P.M. Macdonald., *Macromolecules*, 26, 6397 (1993).
- [46] E.L. Hahn, *Phys. Rev.*, 80, 580 (1950).
- [47] J.E. Tanner, *J. Chem. Phys.*, 52, 2523 (1970).
- [48] S.J. Gibbs and C. S. Johnson Jr., *J. Magn. Reson.*, 93, 395 (1991).
- [49] H. Walderhaug, F.K. Hansen, S. Abrahmsén, K. Persson and P. Stilbs, *J. Phys. Chem.*, 97, 8336 (1993).
- [50] A. Abrahmsén-Alami, K. Persson, P. Stilbs and E. Alami, *J. Phys. Chem.*, 100,

4598 (1996).

[51]H. Walderhaug and B. Nyström, *J. Phys. Chem. B*, 101, 1524 (1997).

[52]T. Watanabe, A. Ohtsuka, N. Murase, P. Barth and K. Gersonde, *Magn. Reson. Med.*, 35, 697 (1996).

[53]P.T. Callaghan and D.N. Pinder, *Macromolecules*, 13, 1085 (1980).

[54]P.T. Callaghan and O. Soderman, *J. Phys.Chem.*, 87, 1737 (1987).

[55]L. Pavesi and M. Balzarini, *Mag. Res. Imaging*, 14, 985 (1996).

[56]L. Pavesi and A. Rigamonti, *Phys. Rev. E*, 51, 3318 (1995).

[57]E.D. von Meerwall and R.D. Fergusson, *J. Chem. Phys.*, 74, 6956 (1981).

Partie II

L'influence de la taille du soluté sur la diffusion

Chapitre 3

Self-diffusion of Oligo- and Poly(ethylene glycol)s in Poly(vinyl alcohol) Aqueous Solutions as Studied by Pulsed-Gradient NMR Spectroscopy

Masaro, L.; Zhu, X.X.; Macdonald, P.M.

Macromolecules **1998**, *31*, 3880–3885

3.1. Abstract

We have measured the self-diffusion coefficients of a series of solute probes, including ethylene glycol and its oligomers and polymers (PEG) in aqueous solutions and gels of poly(vinyl alcohol) (PVA) using pulsed-gradient spin-echo NMR techniques. In an effort to link the diffusion properties of small and large molecules in polymer systems, we have selected this group of diffusant probes with various molecular weights, ranging from 62 to 4000 g/mol. The self-diffusion coefficients of the solute probes decrease with increasing PVA concentrations (from 0 to 0.38 g/ml) and with increasing molecular size of the probes. The temperature dependence of the self-diffusion coefficients has also been studied for ethylene glycol and poly(ethylene glycol)s of molecular weights 600 and 2000 g/mol. Energy barriers of 30.0, 36.5 and 39.0 kJ/mol have been calculated respectively for the probes, in the temperature range of 23–53 °C. The experimental data are used to fit a new physical model of diffusion (Petit *et al.*, *Macromolecules*, **1996**, *29*, 6031), which is shown to be successful in describing the effects of polymer concentration, temperature and molecular size of the diffusants on the self-diffusion coefficients of small and large molecular probes in polymer systems.

3.2. Introduction

The study of diffusion of solute molecules in polymers is important to the application of the materials. The addition of plasticizers in polymers, the permeability through polymer membranes, the miscibility of polymers and the release of drugs and other molecules from polymers are all related to the diffusion in polymer matrices [1-3]. With the development of pulsed field-gradient NMR spectroscopic methods [4,5], self-diffusion of various diffusants in polymer systems can be much more easily determined. The diffusion of solute molecules in polymer gels is influenced by many factors: polymer concentration, size and shape of the diffusant, temperature and any specific interactions in the polymer networks. Physical models describing the self-diffusion of a solute in polymer systems are needed to understand the diffusion phenomena in polymers and to describe and estimate the mobility and diffusion rates of a component in a given polymer mixture. A number of physical models of diffusion for polymer systems have already been proposed,

including those based on the concepts of free-volume theory [6-9], obstruction effects [10,11] and hydrodynamic interactions [12-14]. The free-volume model introduced by Fujita [6] and its modified version for aqueous systems by Yasuda *et al.* [7] showed significant deviation when used to describe diffusion of large probes, such as poly(ethylene glycol)s [15]. The model of Vrentas and Duda [8,9] seems more adequate to describe the diffusion of solvents or polymers in polymer systems [16,17]. The use of this model, however, requires the knowledge of many free-volume parameters [17,18]. Some of these parameters have been reported in the literature for some solvents as well as polymers such as polystyrene [17] and poly(methyl methacrylate) [19], but some of these parameters are not readily available for many other polymers, solvents and solutes and would need to be determined by various physico-chemical experiments. The application of the models based on obstruction effect by Mackie and Meares [10] and Ogston *et al.* [11] is limited to very small diffusants or dilute systems [15,16]. Won and Lodge [20] reported similar problems with the models of Cukier [12] and Altenberger and Tirrell [13] based on hydrodynamic interactions. The “universal equation” proposed by Phillies intends to describe the diffusion of macromolecular probes over a wide range of polymer concentrations and demonstrated good agreement between the experimental data and the model [14]. We have used this model to fit the self-diffusion data of selected solute probes in poly(vinyl alcohol) (PVA) aqueous systems [15], but questions were raised as to the applicability of the model for small diffusants and the interpretation of the fitting parameters. We have shown previously the limitations encountered in the application of selected models in the treatment of the diffusion data obtained in aqueous solutions of PVA [15,21]. It seems fair to say that the physical models of diffusion are useful in many circumstances but are limited in others. It was our wish to find a physical model that can be used to describe the self-diffusion data of both small or large diffusants, including small molecules and polymers, in dilute and concentrated polymer systems.

We have proposed a new physical model for the interpretation of the diffusion of some solvent and solute molecules in selected polymer solutions and gels [21]. In this model, the polymer matrix is represented by a transient statistical network with a certain mesh size. The diffusing molecule is considered as a particle residing temporarily in a

cavity and the diffusion occurs when the particle has enough energy to overcome a certain potential barrier. The self-diffusion coefficient, D , is related to the concentration of the polymer, c , and temperature, T , by the following equation:

$$\frac{D}{D_0} = \frac{1}{1 + \alpha c^{2\nu}} \quad (3.1)$$

where D_0 is the self-diffusion coefficient of the solute probe in the absence of the polymer matrix, $\alpha = D_0 / k\beta^2$, β and ν can be regarded as constants which are characteristic of the system, and k represents the jump frequency over the energy barriers and is given by

$$k = F_p \exp\left(-\frac{\Delta E}{k_B T}\right) \quad (3.2)$$

where F_p can be considered as a constant, ΔE is the energy barrier of diffusion, and k_B is the Boltzmann constant.

This model has been used successfully [21] to reproduce the polymer concentration dependence of the self-diffusion of various solvents and solute molecules in binary and ternary polymer solutions [15,21-23]. The diffusant probes used previously were generally small molecules. In order to make a link between the diffusion of small molecules and that of larger diffusants such as oligomers and polymers, we selected a series of solute probes including ethylene glycol and its oligomers and polymers and measured their self-diffusion coefficients in aqueous solutions and gels of poly(vinyl alcohol) using the pulsed-gradient spin-echo (PGSE) NMR techniques. Poly(ethylene glycol)s were selected since (1) they are soluble in water and miscible with aqueous PVA gels; (2) they have distinct NMR signals which do not overlap with the PVA and water signals, and their NMR relaxation times (mainly T_2) are long enough so that their diffusion is easily studied by the PGSE NMR method; and (3) PEG samples are readily available with a variety of molecular weights and with narrow molecular weight distributions (nearly monodisperse). By examining the effects of polymer concentration, probe size and temperature on the self-diffusion of these probe molecules, we can test the validity of the new model of diffusion for the case of larger diffusant molecules such as oligomers and polymers.

3.3. Experimental

Ethylene glycol (EG) and its oligomers (OEG) and polymers (PEG) as well as the poly(vinyl alcohol) (PVA) sample used ($M = 50,000$ g/mol, 99% hydrolyzed) were all purchased from Aldrich (Milwaukee, WI) and used as received. Size exclusion chromatography (SEC) of the oligo- and poly(ethylene glycol)s were carried out to determine their molecular weights (M) on a Waters SEC system, equipped with three Ultrastyrigel columns of nominal porosities of 1000, 500 and 100 Å, respectively. The molecular weights (M_n and M_w) of each of the OEG and PEG samples are quite narrowly distributed, as shown in Table 3.1 ($M_w/M_n < 1.1$). The OEG and PEG samples include tri-, tetra-, penta- and hexa(ethylene glycol)s as well as PEG-200, PEG-400, PEG-600, PEG-1000, PEG-2000 and PEG-4000. The molecular weight of PEG is represented by the number following PEG.

The preparation of the samples for NMR experiments have been described previously [15]. PVA was dissolved in D_2O containing 1 wt% solute probe. The concentration of PVA ranged from 0.03 to 0.38 g/ml. D_2O (99.9%) was purchased from C.I.L. (Andover, MA). The NMR tubes containing the samples were sealed to avoid evaporation of the solvent and then heated at 100–110 °C. The heating of the samples is necessary to help in the mixing of the sample and also to prevent gelation effects. The NMR measurements were made within the three following days.

The self-diffusion coefficients were measured by the use of the pulsed-gradient spin-echo (PGSE) NMR technique developed by Stejskal and Tanner ($90^\circ_x - \tau - 180^\circ_y - \tau - \text{echo}$, with gradient pulses during the half echo time τ) [24] on a Chemagnetics CMX-300 NMR spectrometer operating at 300 MHz for protons. A magnetic resonance imaging probe with actively-shielded gradients coils (Doty Scientific, Columbia, SC) and a Techtron gradient amplifier were used. Gradient was applied only in the z direction. The gradient strengths used in this study were between 0.3 and 0.6 T/m, calibrated with a sample of known self-diffusion coefficient, i.e., 1 vol% HDO in D_2O with $D_{\text{HDO}} = 1.9 \times 10^{-9}$ m²/s [25]. Variable temperature NMR experiments were performed at 23, 33, 43 and 53 °C. These temperatures were calibrated while the gradient pulses were applied with a thermocouple having a constantan copper-nickel extension (T), which is not sensitive to

Table 3.1. Number- and weight-average molecular weights (M_n and M_w) of OEG and PEG samples used in the diffusion studies as determined by SEC.

Sample	Theoretical	Average M_w (g/mol)		M_w/M_n
	M_w (g/mol)	M_n	M_w	
EG	62	–	–	–
(EG) ₃	150	182	182	1.00
(EG) ₄	194	196	197	1.00
(EG) ₅	238	198	199	1.00
(EG) ₆	282	221	222	1.00
PEG-200	200	205	209	1.02
PEG-400	400	341	368	1.08
PEG-600	600	538	578	1.07
PEG-1000	1000	976	1038	1.06
PEG-1500	1500	1461	1532	1.04
PEG-2000	2000	2148	2246	1.04
PEG-4000	4000	4439	4626	1.04

the magnetic field. Given the slight fluctuation of the temperature (± 0.5 °C), no temperature gradient was detected along the sample position in the coil. The self-diffusion coefficient D can be extracted from the attenuation of the NMR signals due to the application of the gradient pulse of various durations [4] as given in the following expression:

$$A_{2\tau} = A_{2\tau}^* \exp \left[-(\gamma G \delta)^2 \left(\Delta - \frac{\delta}{3} \right) D \right] \quad (3.3)$$

where $A_{2\tau}$ is the echo amplitude, γ is the magnetogyric ratio of ^1H , G is the pulsed gradient strength, δ the duration of the gradient pulse and Δ the interval between the gradient pulses. The effect of T_2 (spin-spin relaxation time) is constant when τ is kept constant and is

contained in $A^*_{2\tau}$, the amplitude of the echo in the absence of gradient pulses. The self-diffusion coefficient can be obtained from the relationship between the amplitude of the NMR signal and the other NMR parameters as shown in eq 3.3. The error of the measured self-diffusion coefficients was estimated as less than 5%. In the NMR experiments, the gradient pulse duration δ varied from 0.1 ms to 60 ms, the other parameters were kept constant and their values are those noted in the parentheses: half spin echo time τ (120–140 ms); gradient pulse interval Δ (the same as τ), recycle delay (8–60 s), number of acquisitions (4–8), 90° pulse length (22–35 μ s), spectral width (10 kHz), and line broadening (5–10 Hz).

A nonlinear least-square fitting method was used to fit the experimental data to the diffusion model (eq 3.1) and the errors listed in Table 3.2. are expressed as the root-mean-square (RMS) fractional errors.

3.4. Results and Discussion

Figure 3.1A represents a series of typical ^1H NMR spectra of a PVA-water-PEG system from a PGSE experiment with varying gradient pulse duration δ and constant gradient strength. The NMR signals of all components in the system are very well resolved. Even though D_2O was used as the solvent, the peak of the residual water (resulting from exchange with the protons of the hydroxyl groups in the system) was observable only when shorter gradient pulses were used. This signal rapidly disappears as the duration of the gradient pulses increases, indicating a faster self-diffusion of the molecule. Only one proton signal was observed for PVA under the experimental conditions used. This signal is attributed to the CH_2 group on the main chain of PVA. It is little affected by the duration of the gradient pulses, indicating a much slower diffusion rate. The most intense signal in this case belongs to PEG-2000. It is of note that the signal intensities here are not indications of the abundance of the protons, but rather the effects of the spin-spin relaxation times and diffusion rates of the individual molecules. Figure 3.1B shows the logarithms of the NMR signal intensities plotted as a function of the NMR parameter $\delta^2(\Delta - \delta/3)$. According to eq 3.3, this relationship is linear and the slope of the line equals $-\gamma^2 G^2 D$.

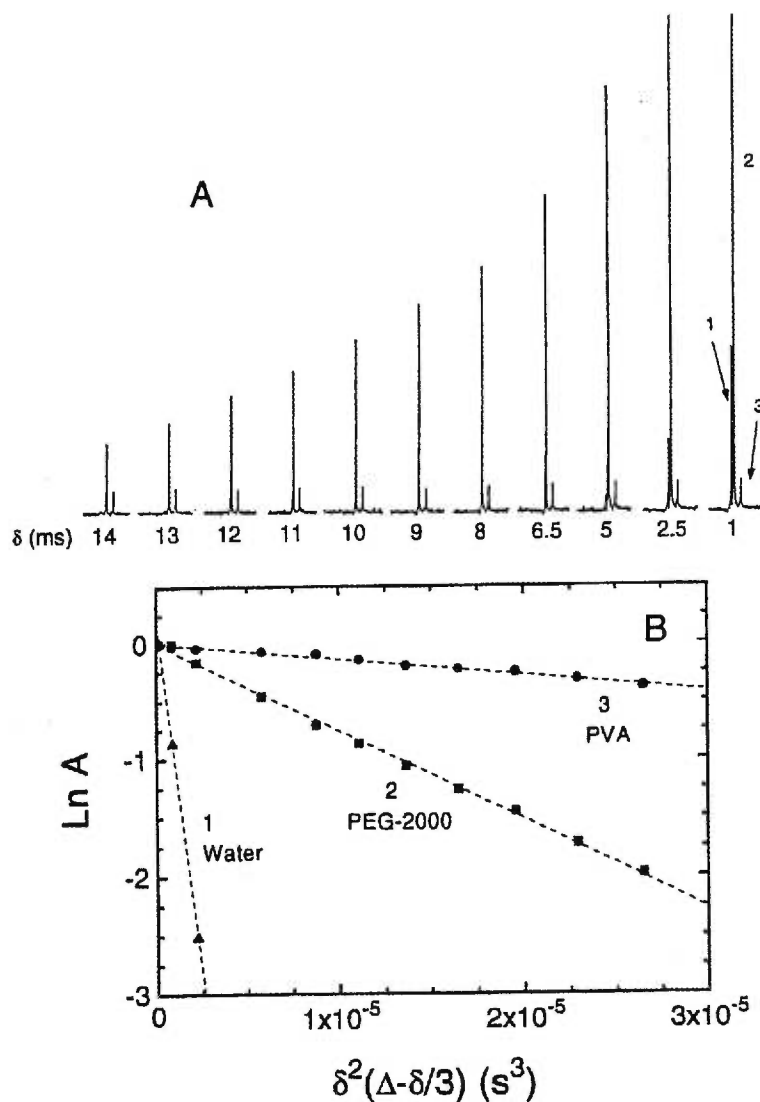


Figure 3.1. (A) ^1H PGSE-NMR spectra of the PVA-water-PEG-2000 system at 43 °C, showing proton signal attenuation with increasing gradient pulse durations (δ). [PVA] = 0.03 g/ml, $G = 0.491$ T/m, interval between gradient pulses $\Delta = 120$ ms, and recycle delay was 12 s. (B) Semilogarithmic plot of the signal intensities as a function of $\delta^2(\Delta - \delta/3)$ (eq 3.3) for PVA, PEG-2000 and water proton signals. From the slope of these lines, the self-diffusion coefficients can be calculated. In this particular case, $D_{\text{PVA}} = 3.18 \times 10^{-11}$ m²/s, $D_{\text{PEG-2000}} = 1.73 \times 10^{-10}$ m²/s, and $D_{\text{water}} = 2.77 \times 10^{-9}$ m²/s.

When G is already known from calibration, D can be easily calculated from the slopes. For the diffusants investigated in this study, in general, monoexponential decays were observed, indicating that the samples were homogeneous and that the self-diffusion coefficients are monodisperse. We have also noticed some curvature of the line, particularly in the case of ethylene glycol, where the linear part with shorter gradient pulses were used for the calculation of the self-diffusion coefficients. The curvature might be due to the fact that ethylene glycol, being a small molecule with two hydroxyl groups, can form hydrogen bonds much more easily than the larger OEG and PEG molecules. However, further experimental evidence is needed to confirm such a hypothesis.

3.4.1. Effect of Polymer Concentration

The measured self-diffusion coefficients of EG, OEG and PEG as a function of PVA concentration are shown in Figure 3.2. It is evident that there is a decrease of the values of D with increasing PVA concentration for each of the solute probes. The PVA concentration ranged from 0 to 0.38 g/ml, close to which the solutions became viscous gels. The difference of the self-diffusion coefficients of the solute probes at lower PVA concentrations are greater and it appears that all of the measured D values approach a common low value at high PVA concentrations.

In a recent work, Matsukuwa and Ando studied the diffusion of PEG in water and poly(N,N-dimethylacrylamide) gels by ^1H PGSE NMR spectroscopy [26]. The D value for PEG-4250 (ca. $1.2 \times 10^{-10} \text{ m}^2/\text{s}$, for 1 wt% aqueous solution at 303 K) is comparable with the D_0 value determined for PEG-4000 ($0.95 \times 10^{-10} \text{ m}^2/\text{s}$) at 23 °C in this report. Their experimental temperature is about 7 °C higher, and their PEG samples seemed more polydisperse ($M_w/M_n < 1.19$) than the sample used in this study. They have also observed decreases in D values as the degree of swelling of the gels decreased, which corresponds to a higher concentration of the polymer matrix [26].

3.4.2. Effect of Molecular Size of the Diffusant

In Figure 3.2, we can observe the dependence of the measured D values of the solute probes on their molecular sizes. In general, the D values decrease as the molecular size of the diffusant increases for the entire PVA concentration range studied. The self-diffusion coefficients of EG measured at different concentrations of PVA are significantly higher than the oligomers and polymers (Figure 3.2A). As the molecular weight (M_w) or the molecular size of the diffusant increases, the measured D value decreases. The difference in D values of PEGs with different M_w becomes less significant as the M_w of PEG increases, especially at higher PVA concentrations (Figure 3.2B). The hydrodynamic radii of the diffusants, R_h , can be calculated from the D_0 value by the use of the Stokes-Einstein equation (Table 3.2) and give an indication of the relative size of the diffusants. The effect of the molecular size of the diffusant on self-diffusion observed here is similar to those observed in other types of gels and solutions by the radioactive tracer method [27] and the results of another study in cellulose gels and membranes [28]. It is to be noted that the D values measured by PGSE NMR methods here and in the study of Matsukuwa and Ando [26] are in the same order of magnitude with results obtained by other methods [27,28], but they seem to be consistently lower in values. As shown in Table 3.2, R_h of the probes increases in a non-linear fashion as a function of the molecular weight of the PEG samples. The use of R_h as an indication of the molecular size is justified in this case since all the probes used are linear oligo- and poly(ethylene glycol)s. However, the R_h value does not take into account the effect of molecular shape. The study by Won and Lodge showed that the diffusion behavior of linear and star-shaped polystyrene probes in poly(vinyl methyl ether)-toluene systems are different since the freedom of motion of the linear polymer is much higher than that of the star-shaped molecules [20]. The same is true for the diffusion of polystyrene latex spheres [29]. Therefore, precautions should be taken when R_h is used to indicate the molecular size of the diffusant probes having various molecular shapes. The Stokes-Einstein equation may even fail at higher concentrations of polymers [30]. The hydrodynamic radius of the diffusants may also change as a function of polymer concentration since the diffusion coefficient and viscosity are independent

parameters [29,30]. R_h values in Table 3.2 are calculated from D_0 and are regarded as a molecular size parameter in our discussion.

Table 3.2. Hydrodynamic radii, self-diffusion coefficients and fitting parameters $k\beta^2$ and ν obtained for the diffusants (EG, OEG and PEG) in aqueous PVA systems, at $T = 23$ °C.

Sample	R_h (Å)	D_0 (10^{-10} m ² /s)		$K\beta^2$ (10^{-10} m ² /s)	ν	RMS Error
		Measured	calculated			
EG	2.43	9.37	9.56	0.28	0.76	0.13
(EG) ₃	3.91	5.95	5.95	0.23	0.60	0.08
(EG) ₄	4.32	5.38	5.42	0.24	0.59	0.05
(EG) ₅	5.08	4.58	4.85	0.25	0.60	0.04
(EG) ₆	5.70	4.08	4.08	0.21	0.63	0.06
PEG-200	4.81	4.84	4.85	0.24	0.60	0.08
PEG-400	7.00	3.31	3.34	0.23	0.56	0.04
PEG-600	12.48	1.86	1.87	0.12	0.58	0.002
PEG-1000	13.99	1.66	1.66	0.12	0.49	0.02
PEG-1500	20.59	1.13	1.13	0.068	0.54	0.02
PEG-2000	22.69	1.07	1.02	0.053	0.53	0.001
PEG-4000	24.35	0.958	0.96	0.047	0.50	0.01

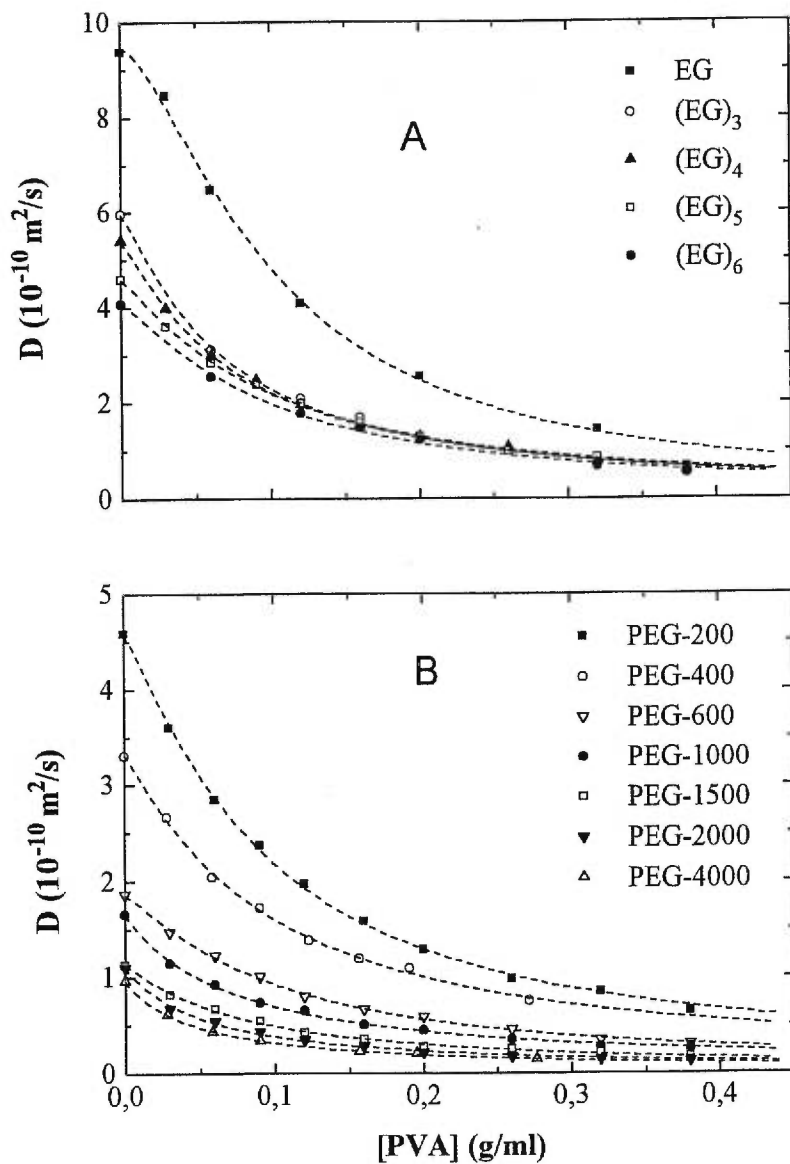


Figure 3.2. Self-diffusion coefficients of the solute probes, (A) EG and OEG and (B) OEG and PEG, plotted as a function of PVA concentration at 23°C . Dashed lines are fits to eq 3.1.

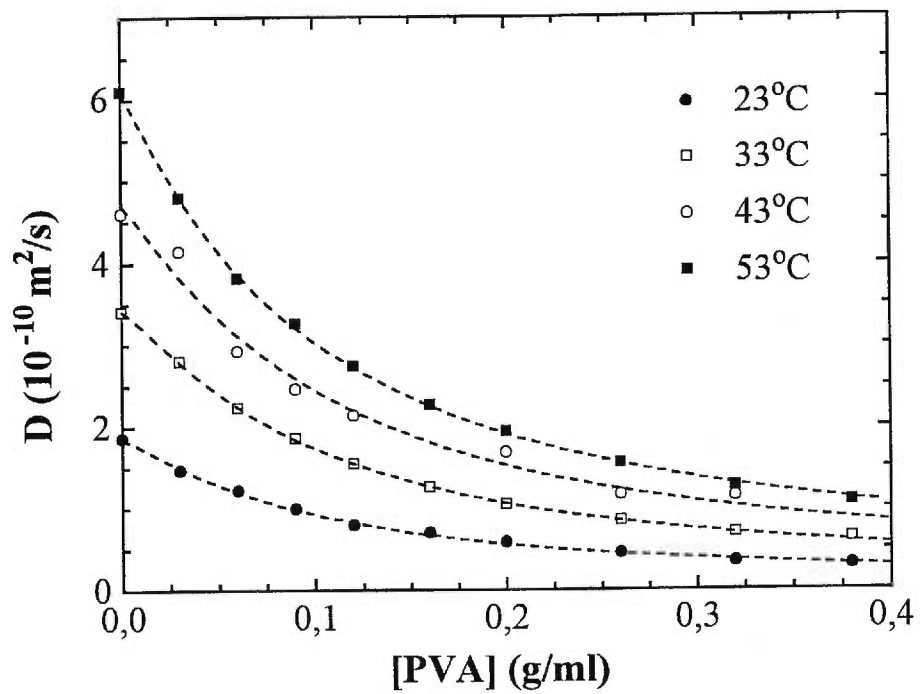


Figure 3.3. Self-diffusion coefficients of PEG-600 plotted as a function of PVA concentration at four different temperatures. Dashed lines are fits to eq 3.1.

3.4.3. Effect of Temperature

We have studied the variable temperature effect on the self-diffusion coefficients of selected solute probes such as EG, PEG-600 and PEG-2000. As one may expect, the D values increase for a given diffusant as the temperature rises. An example of the plots of D values as a function of PVA concentration at different temperatures (PEG-600) is shown in Figure 3.3. The experimental data can be fitted very well to eq 3.1 for each of the temperatures studied and for all the probes used, including EG and PEG-2000.

3.4.4. Correspondence with the New Diffusion Model

As shown in Figures 3.2 and 3.3, the experimental data can be fitted very well with the new model of diffusion as expressed in eq 3.1. In order to use the model to estimate and eventually to predict the diffusion behavior in polymer systems, it is necessary to obtain values of the fitting parameters in eqs 3.1 and 3.2. The quantity of $k\beta^2$ is related to the jump frequency k of the diffusant while β is a characteristic constant. Clearly, the jump frequency should be related inversely to the molecular size of the diffusant. Values of $k\beta^2$ can be obtained from fit the experimental data to eq 3.1, but a separate value for k cannot be extracted since the value of the constant β is not known. They can be related to the hydrodynamic radii of the diffusants, R_h . The logarithm of the parameter $k\beta^2$ as a function of R_h has more or less a linear relationship (Figure 3.4A), which confirms that an increase in the molecular size of the diffusant leads to a lower jump frequency, k . The following empirical expression can be obtained for this series of probe molecules:

$$\log k\beta^2 = -0.0356R_h - 10.45 \quad (3.4)$$

which provides a rough estimate of the $k\beta^2$ value at 23 °C for a given OEG or PEG diffusant with a known R_h , which can be calculated from the D_0 value as shown above.

The second fitting parameter, ν , should remain more or less a constant for a given polymer system. Figure 3.4B shows that indeed ν can be regarded to be characteristic of the PVA-water system since the variation of ν is small for the series of OEG and PEG studied. The average value of ν obtained in this study (*ca.* 0.58) is similar to that obtained previously for the same system [21]. A certain deviation was observed for the very small molecules such as ethylene glycol itself ($\nu = 0.76$), probably as a result of the curvature in

the measurement of the diffusion coefficient as discussed previously. In addition, we can also notice a slight decrease in v as a function of the hydrodynamic size of the diffusants in this series. This decreasing trend, however, is very small and may be regarded as negligible when the RMS errors of the fits (Table 3.2) are taken into account.

As shown in eq 3.2, the jump frequency k for a given diffusant is expected to be dependent on the temperature. The $k\beta^2$ values can be obtained from fits to eq 3.1 at each temperature. Since we assume that β is a constant within the temperature range studied here, the relationships between $k\beta^2$ and T shown in Figure 3.5 can be regarded as the relationship between k and T . The Arrhenius plots ($\log k\beta^2$ vs $1/T$, as in eq 3.2) in Figure 3.5 show excellent linear relationships. The energy barrier ΔE can be calculated from the slopes of the linear plots. We have obtained ΔE values of 30, 36.5 and 39 kJ/mol, respectively, for selected diffusants EG, PEG-600 and PEG-2000. Previously, we have calculated the energy barrier for *tert*-butanol (*t*BuOH) to be 21 kJ/mol in the same system over the same temperature range [21]. The data points are also plotted in Figure 3.5. The molecular weight of *t*BuOH is higher than that of EG, but the energy barrier for the diffusion of *t*BuOH is lower. The higher facility of EG in forming hydrogen bonds with the polymer matrix and with the aqueous environment is probably the reason for its higher energy barrier of diffusion than that of *t*BuOH. The effect of hydrogen bonds on diffusion of small molecules was also evidenced when trimethylamine was compared with tetramethylammonium cation [15]. Since PEG is a flexible linear polymer, the increase in molecular weight of PEG does not seem to increase the energy barrier of diffusion to a great extent. There is a clear trend that the energy barrier of diffusion increases with increasing molecular size of the diffusant, which leads to smaller self-diffusion coefficients.

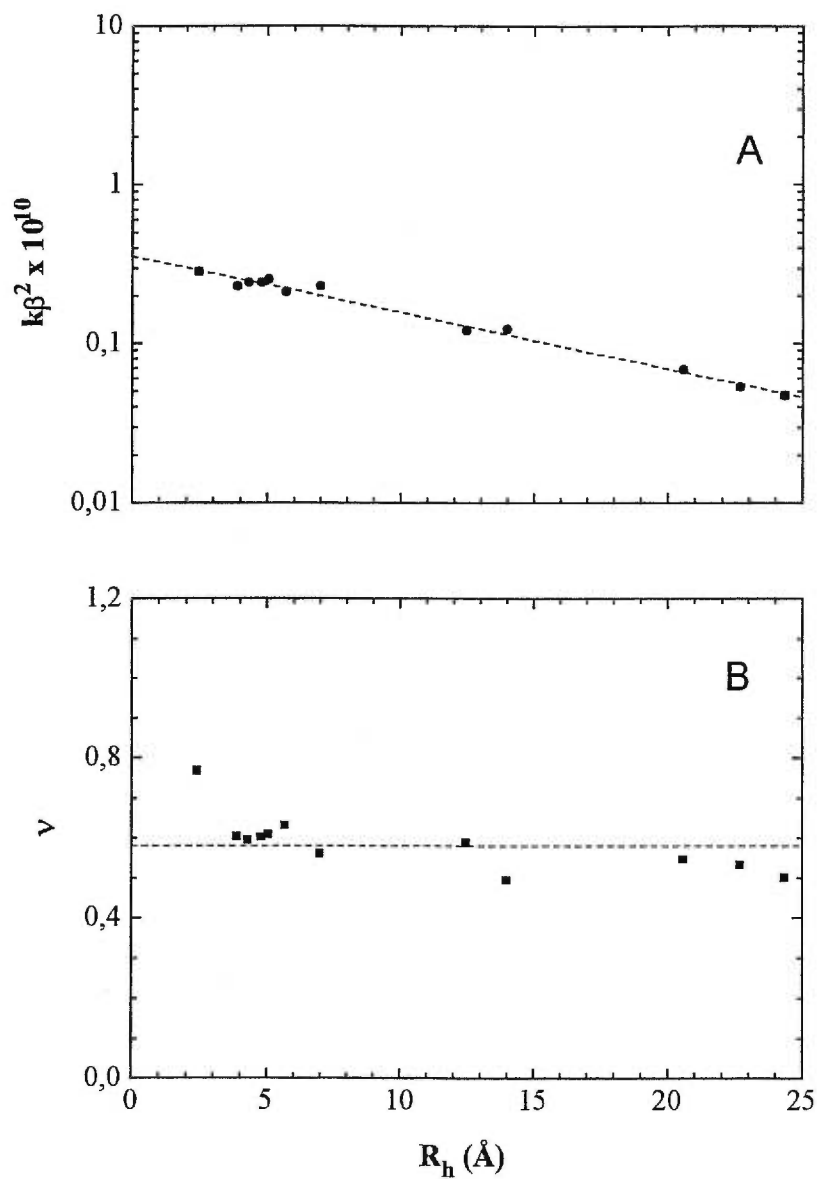


Figure 3.4. (A) Semilogarithmic plot of $k\beta^2$ and (B) plot of the parameter ν , as a function of the hydrodynamic radius, R_h , of this series of diffusants in PVA-water systems at 23 °C.

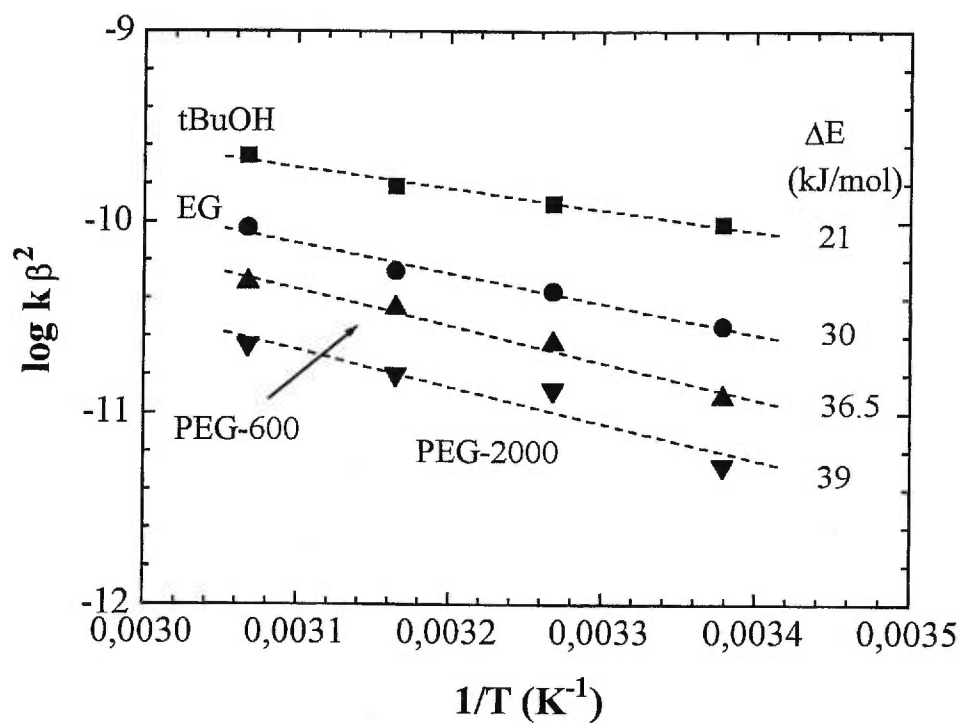


Figure 3.5. Logarithm of the parameter $k\beta^2$ plotted as a function of reciprocal temperature for selected diffusants. The potential energy barriers can be calculated from the slopes of these lines.

3.5. Concluding Remarks

We have measured the self-diffusion coefficients of a series of diffusant probes based on ethylene glycol in PVA aqueous solutions and gels. These diffusants ranged from the monomer EG, to oligomers and to polymers with a molecular weight up to 4000 g/mol, which enabled us to link the diffusion behavior of small to large molecules in the polymer system. The newly proposed physical model of diffusion is used successfully in the treatment of the self-diffusion data of these molecules. The effects of polymer concentration, molecular size of the diffusants and temperature can be described by the model. The jump frequency k , a physical parameter defined in the model, is shown to depend on the size of the diffusant as well as on temperature, while the parameter v in the model remains more or less a constant of the given system. In this study, the hydrodynamic radii of the diffusants have been used to account for the changes of molecular size of the diffusants. The energy barriers of diffusion have been obtained from the variable temperature studies for selected diffusants of different sizes. Further studies are under way in an effort to elucidate the effect of molecular shape of the diffusant as well as the effects of hydrogen-bonding and other interactions in the diffusion of solutes in polymer systems.

3.6. Acknowledgments

Financial support from Natural Sciences and Engineering Research Council (NSERC) of Canada and from the Quebec Government (Fonds FCAR and a Quebec-Ontario collaboration travel grant) is gratefully acknowledged. The authors also thank Professor J. Prud'homme of Université de Montréal for the use of SEC in his laboratory.

3.7. References and notes

- [1] Kosmeyer, R.W.; von Meerwall, E.D.; Peppas, N.A. *J. Polym. Sci., Polym. Phys. Ed.* **1986**, *24*, 409.
- [2] Waggoner, A.; Blum, F.D. *J. Coatings Technol.* **1989**, *61*, 768.
- [3] Clericuzio, M.; Parker, W.O.; Soprani, M.; Andrei, M. *Solid State Ionic* **1995**,

- 77, 685.
- [4] Stilbs, P. *Prog. Nucl. Magn. Reson. Spectrosc.* **1987**, *19*, 1.
- [5] Price, W.S. *Annual Reports on NMR Spectroscopy* **1996**, *32*, 51.
- [6] Fujita, H. *Adv. Polym. Sci.* **1961**, *3*, 1.
- [7] Yasuda, H.; Lamaze, C.E.; Ikenberry, L.D. *Makromol. Chem.* **1968**, *118*, 19.
- [8] Vrentas, J.S.; Duda, J.L. *J. Polym. Sci., Polym. Phys. Ed.* **1977**, *15*, 403.
- [9] Vrentas, J.S.; Duda, J.L. *J. Polym. Sci., Polym. Phys. Ed.* **1977**, *15*, 417.
- [10] Mackie, J.S.; Meares, P. *Proc. R. Soc. Lond., A* **1955**, *232*, 498.
- [11] Ogston, A.G.; Preston, B.N.; Wells, J.D. *Proc. R. Soc. Lond., A* **1973**, *333*, 297.
- [12] Cukier, R.I. *Macromolecules* **1984**, *17*, 252.
- [13] Altenberger, A.R.; Tirrell, M. *J. Chem. Phys.* **1984**, *80*, 2208.
- [14] Phillies, G.D.J. *Macromolecules* **1986**, *19*, 2367.
- [15] Petit, J.-M.; Zhu, X.X.; Macdonald, P.M. *Macromolecules* **1996**, *29*, 70.
- [16] Waggoner, R.A.; Blum, F.D.; MacElroy, J.M.D. *Macromolecules* **1993**, *26*, 6848.
- [17] Su, H.; Benesi, A.J.; Duda, J.L. *Polym. Int.*, **1996**, *39*, 243.
- [18] Vrentas, J.S.; Vrentas, C.M. *Macromolecules* **1994**, *27*, 5570.
- [19] Faldi, A.; Tirrell, M.; Lodge, T.P.; von Meerwall, E. *Macromolecules* **1994**, *27*, 4184.
- [20] Won, J.; Lodge, T.P. *J. Polym. Sci. B. Polym. Phys.* **1993**, *31*, 1897.
- [21] Petit, J.-M.; Roux, B.; Zhu, X.X.; Macdonald, P.M. *Macromolecules* **1996**, *29*, 6031.
- [22] Zhu, X.X.; Macdonald, P.M. *Macromolecules* **1992**, *25*, 4345.
- [23] Zhu, X.X.; Wang, F.; Nivaggioli, T.; Winnik, M.A.; Macdonald, P.M. *Macromolecules* **1993**, *26*, 6397.
- [24] Stejskal, E.O.; Tanner, J.E. *J. Chem. Phys.* **1965**, *42*, 288.
- [25] Mills, R. *J. Phys. Chem.* **1973**, *77*, 685.
- [26] Matsukawa, S.; Ando, I. *Macromolecules* **1996**, *29*, 7136.
- [27] Johansson, L.; Skantze, U.; Löfroth, J.-E. *Macromolecules* **1991**, *24*, 6019.

- [28] Brown, W.; Honsen, R.M. *J. Appl. Polym. Sci.* **1981**, *26*, 4135.
- [29] Won, J.; Onyenemezu, C.; Miller, W.G.; Lodge, T.P. *Macromolecules* **1994**, *27*, 7389.
- [30] Phillis, G.D.J. *J. Phys. Chem.* **1989**, *93*, 5029.

Chapitre 4

Study of the self-diffusion of poly- (ethylene glycol)s in poly(vinyl alcohol) aqueous systems

Masaro, L.; Zhu, X.X.; Macdonald, P.M.

Journal of Polymer Science, Part B, Polymer Physics Edition

1999, accepté

4.1. Abstract

We have measured the self-diffusion coefficients of a series of oligo- and poly(ethylene glycol)s with molecular weights ranging from 150 to 10000, in aqueous solutions and gels of poly(vinyl alcohol) (PVA), using the pulsed-gradient spin-echo NMR technique. The PVA concentrations varied from 0 to 0.38 g/mL which ranged from dilute solutions to polymer gels. Effects of the diffusant size and polymer concentration on the self-diffusion coefficients have been investigated. The temperature dependence of the self-diffusion coefficients has also been studied for poly(ethylene glycol)s with molecular weights of 600 and 2000. Several theoretical models based on different physical concepts are used to fit the experimental data. The suitability of these models in the interpretation of the self-diffusion data is discussed.

4.2. Introduction

Diffusion of various solutes and solvents in polymer solutions and gels has drawn much research attention in recent years because of the growing theoretical and practical interests in the subject. The diffusion of plasticizers [1], the miscibility of polymers [2], the permeability through membranes [3], and the controlled release of drugs [4] are all related to the diffusion process in polymer systems. The study of diffusion can provide important information regarding the applications of the materials.

With the availability of more experimental data, physical models of diffusion are needed for the interpretation of the results. Various physical models of diffusion have been proposed over the years [5–18]. These models are generally divided into three categories based on considerations of the obstruction effect [5–8], the free volume effect [14–18] and the hydrodynamic interactions [9–13] in polymer systems. In addition, new models of diffusion have been proposed recently which combine the different physical concepts [19,20]. The usefulness and limitations of many of the existing models have been documented [20–23]. Therefore, it is important to test the existing diffusion models with data obtained for a better understanding of the diffusion process and to verify the applicability of the models.

We have studied the self-diffusion coefficients of a series of linear poly(ethylene glycol)s in poly(vinyl alcohol) aqueous solutions and gels by ^1H pulsed-gradient spin-echo NMR spectroscopy. The selected diffusants include oligo- and poly(ethylene glycol)s in an effort to make a link between the diffusion of small and large diffusants. The polymer concentrations in this study cover the dilute, semidilute, and concentrated regimes as defined by de Gennes [12]. Effects of the diffusant size, polymer concentration and temperature have been studied. We have used the diffusion model of Petit *et al.* [24] for the treatment of the data in a previous paper [25]. The model of Petit *et al.* seems adequate in the description and interpretation of the self-diffusion of diffusants of various sizes over a large range of polymer concentrations [23]. The interpretation of the effects of diffusant size, polymer concentration, and temperature was also successful. However, it seems that interest has mounted and it was requested to use some of the other models for the interpretation of the data. Questions were raised concerning the applicability of the other models in the literature, particularly the suitability for ternary systems. We report here the analysis of the data with several pertinent diffusion models. Agreements between the diffusion data and the theoretical fits are verified and the physical meanings of the parameters in the models are discussed.

4.3. Theoretical models of diffusion

4.3.1. Models based on obstruction effects.

The polymer chains of the network are considered here as motionless and impenetrable. Consequently, the diffusion of a solute in the system is hindered due to the obstruction by the polymer chains. The root-mean-square displacement of the solute is increased when the polymer matrix concentration is increased, which leads to a decrease of the diffusion coefficient of the diffusing molecule.

Mackie and Meares [6] developed an expression for the diffusion inside a gel. They considered the gel as a solvent-polymer lattice model that blocks a fraction of the sites. The diffusion inside the lattice is possible for a solute of a size equal to or smaller

than that of the monomer units of the polymer. The diffusion is predicted to decrease with the volume fraction of the polymer, ϕ , following the equation

$$\frac{D}{D_0} = \left(\frac{1-\phi}{1+\phi} \right)^2 \quad (4.1)$$

where D and D_0 are the self-diffusion coefficients of the diffusant in the presence and in the absence of the polymer matrix.

A more phenomenological approach was proposed by Ogston *et al.* [7] based on a lattice model for the solvent-polymer gel system. They considered the polymer as randomly oriented fibers, whereas the solute was considered as a hard sphere. The diffusion behavior was assumed to correspond to the average displacement of a sphere in a solution of long fibers of negligible width

$$\frac{D}{D_0} = \exp \left[- \frac{r_s + r_f}{r_f} \phi^{1/2} \right] \quad (4.2)$$

where r_s is the hydrodynamic radius of the solute, and r_f the hydrodynamic radius of the fiber, i.e., polymer network. [L'équation 4.2 est identique à l'équation 1.12, page 20, et les paramètres utilisés dans les deux équations ont la même signification physique malgré la notation différente].

4.3.2. Free volume models

In these models the diffusion process is considered as a succession of jumps into voids created by the thermal motion of all the molecules present in the system. The voids are also due to the redistribution of the free volume within the liquid [26]. The contribution to the free volume is assumed to be mainly from the solvent. Therefore, solute or solvent diffusion decreases with increasing polymer concentration. The diffusion of a solute is a function of the probability to find a void large enough to allow the diffusion of the solute. The free volume models of Fujita cannot be used to describe diffusion in aqueous systems because of the numerous interactions between the solvent molecules [14]. The model of Vrentas-Duda [16,17] and Vrentas-Vrentas [18] can be used for the diffusion in binary polymer-solvent systems. Because of the numerous physical parameters needed, it is difficult to apply this model to ternary

systems. Yasuda *et al.* [15] proposed a free volume model that can be used for ternary aqueous systems when the solute probe is present in low concentrations, i.e., the total free volume is mainly contributed by the solvent. It was assumed that there are no interactions between the solute and the polymer. Yasuda *et al.* [15] successfully analyzed electrolyte diffusion in organic and aqueous systems by using the following equation

$$D = D_0 \exp \left[\frac{B_s}{f_v^*} \left(1 - \frac{1}{1 - \phi} \right) \right] \quad (4.3)$$

where B_s is the minimum hole size required for diffusant displacement and f_v^* is the free volume of the solvent in the system.

4.3.3. Hydrodynamic models

In these models, the hydrodynamic interactions between the diffusants (solvent or solute) and the polymer are taken into account and the polymer chains are considered to be mobile. Phillies proposed a model to describe the self-diffusion of one macromolecule (polymers and proteins) in another over a wide range of polymer concentrations [13]. The polymer chains are considered to be mobile and can be described by spheres joined by rods that can rotate as defined by Kirkwood and Riseman [27]. The universal equation proposed by Phillies takes the form

$$D = D_0 \exp(-\alpha c^\nu) \quad (4.4)$$

where c is the polymer concentration, α and ν are scaling parameters. According to Phillies, α depends strongly on the molecular weight ($\alpha \sim M^{0.9 \pm 0.1}$) for macromolecular diffusants, whereas it depends on the hydrodynamic radius ($\alpha \sim R_h$) for smaller diffusants [28–31]. The scaling parameter ν should range between 1 for low molecular weight diffusants and 0.5 for high molecular weight diffusants [30]. Between these limits, it scales according to $\nu \sim M^{-1/4}$. Eq 4.4 provides good fits to the experimental data in many polymer systems [13]. However, the dependence of the parameters α and ν remains a source of disagreement [32,33]. Several authors argued that the scaling parameters lack

physical significance and that the good fits obtained with eq 4.4 reflect more the flexibility of the equation than its physical significance [34–36].

The reptation theory was introduced by de Gennes [11], who studied the self-diffusion coefficient of a polymer chain M , trapped inside a three-dimensional network P , with P and M of similar molecular weights. The diffusing polymer chain is considered to be surrounded by fixed obstacles represented by the gel. Therefore, the leading displacement of the polymer chain corresponds to a “tubular” or reptational behavior. The self-diffusion coefficient of a large polymer is predicted to scale with its molecular weight according to: $D \sim M^{-2}$. The diffusion of the same polymer chain in an unentangled system, i.e., dilute system, is described by the Rouse model [37]: $D \sim M^{-1}$. The original reptation model was later extended by de Gennes to the diffusion of a polymer in a polymer network with a higher molecular weight than the diffusant, $P > M$ [12]. This new reptation plus scaling concept takes into account the dependence on the matrix concentration, c . The scaling arguments led to the following predictions: $D \sim M^{-2}c^{-3}$ under θ -solvent condition, and $D \sim M^{-2}c^{-1.75}$ in a good solvent.

4.3.4. Combined theory

Recently, Amsden [20] proposed a new diffusion model by combining the free volume theory with the obstruction and scaling concepts. This model takes into account factors concerning the chain stiffness, the chain radius and the volume fraction of the polymer as well as the size of the diffusant [20]. The transport of a molecule through a hydrogel matrix depends on the probability of finding holes larger than the diffusant diameter (free volume concept). The distribution of the holes, or the openings between the polymer fibers, is described by the expression given by Ogston *et al.* (eq 4.2). Amsden evaluated the distance between polymer chains, or the openings, with the help of scaling concepts and the following expression is obtained

$$\frac{D}{D_0} = \exp \left[-\pi \left(\frac{r_s + r_f}{r_f} \right)^2 \frac{\phi}{(k_1 + 2\phi^{1/2})^2} \right] \quad (4.5)$$

where r_s is the hydrodynamic radius of the solute, r_f the radius of the polymer chain, and k_1 a constant for a given polymer-solvent system [l'équation 4.5 est identique à l'équation 1.68 page 69 malgré la notation différente: D/D_0 au lieu de $\overline{D}_e / \overline{D}_m$]. This model was used successfully in the treatment of the diffusion of proteins (pepsin, ovalbumin, bovine serum albumin and β -lactoglobulin) in sodium alginate gels for diluted regimes ($\varphi = 0.005$ – 0.05) [20].

4.4. Experimental

The characteristics of the polymers, i.e., oligo- and poly(ethylene glycol)s (OEG and PEG) as well as poly(vinyl alcohol) (PVA), used in this study have been reported previously [25]. PVA was dissolved in D_2O containing 1 wt % of an OEG or PEG solute. The PVA concentration ranged from 0 to 0.38 g/mL. The experimental details on the NMR instrumentation used for the diffusion studies, the pulsed-gradient spin-echo NMR sequence used, as well as the calibration of the gradient pulses have been described previously [23,25]. In the present study, PEG with a higher molecular weight (PEG-10000), purchased from Aldrich (Milwaukee, WI), was also used as a solute probe. Its molecular weight was determined by size exclusion chromatography (SEC) as described previously [25]. The number and weight average molecular weights (M_n and M_w) of PEG-10000 were found to be 10 158 and 11 445, respectively, with a polydispersity of 1.12.

To measure the molecular weight of the PVA used, the solutions were prepared with sodium thiocyanate in a salt/polymer weight ratio of 1.5 to 1 to prevent the aggregation of PVA [38]. SEC experiments were also performed on a Waters 600 controller system, equipped with a Waters 410 differential refractometer and two Ultrahydrogel columns of nominal porosity of 10 and 6 μm (Ultrahydrogel 500 and 120), respectively, with water as the eluent. The M_w of PVA was found equal to 52 800 with a polydispersity of 2.09. Static light scattering measurements were performed on a Dawn-B instrument (Wyatt Technology Corp., Santa Barbara, CA) in combination with a helium-neon laser operating at 632.8 nm at room temperature. An incremental refractive index of 0.159 mL/g was used. PVA molecular weight was found to be $(52 \pm 4) \times 10^3$ g/mol. The M_w values determined by the two techniques are quite similar.

4.5. Results and discussion

The diffusion data of the series of oligo- and poly(ethylene glycol)s in PVA are examined to demonstrate the effect of the concentration (c) or volume fraction (ϕ) of the polymer matrix (PVA), the temperature (T) and the size (R_h) or molecular weight (M) of the diffusant. The effect of the molecular weight of the polymer matrix (P) was not examined in this study. Note that D should be independent of P when the molecular weight of the diffusant is lower than P [35].

4.5.1. The obstruction models

Figure 4.1 shows the normalized self-diffusion coefficient of selected diffusants as a function of the volume fraction of the polymer matrix. The selected diffusants include an oligomer, PEG-200 whose major components are tetra(ethylene glycol) and penta(ethylene glycol) according to SEC analysis, and a polymer, PEG-2000. The self-diffusion coefficient decreases when the volume fraction of the polymer is increased and the self-diffusion coefficient decreases also with increasing size of the diffusant. The dashed line represents the prediction with the model of Mackie-Meares [6]. The correlation between the model and the data is quite poor since the model of Mackie-Meares does not take into account the properties (size, molecular weight, etc.) of the diffusant. Waggoner *et al.* [22] have shown that eq 4.1 can be used relatively successfully to describe organic solvent diffusion in polymer systems. But the model of Mackie-Meares cannot be used to describe the diffusion of larger diffusants.

The dotted lines in Figure 4.1 are fits with the model of Ogston *et al.* [7] for PEG-200 and PEG-2000, respectively. Eq 4.2 appears to provide improved correlation to the data as the physical properties of the diffusant are taken into consideration, but the fits still deviate significantly from the data. Fits to the experimental data with r_s and r_f as free parameters provided a larger hydrodynamic radius (r_s) for PEG-200 (10.4 Å) than for PEG-2000 (9.27 Å), while different values for r_f were obtained (5.58 and 3.37 Å) for the two systems. This does not seem reasonable. When, the r_s values were fixed to the R_h values calculated from the Stokes-Einstein equation (Table 4.1), different values of r_f (2.57 and 8.25 Å) were obtained for PEG-200 and PEG-2000, respectively. But these fits did

not show any perceivable changes when compared to the fits obtained with free parameters. Previously, Amsden [20] reported studies of protein diffusion in alginate gels and found that the model of Ogston *et al.* failed to describe the results. Johanson *et al.* [39] also reported a failure of this model for the diffusion of albumin in solutions of hyaluronic acid and dextran.

Table 4.1. Hydrodynamic radii calculated from the Stokes-Einstein equation, measured self-diffusion coefficients (D_0) and fitting parameters D_0 , α and ν obtained for the diffusants (OEGs and PEGs) in aqueous PVA systems according to eq 4.4.

Sample	R_h (Å)	D_0 (10^{-10} m ² /s)		α	ν
		Experimental	Fitted		
(EG) ₃	3.91	5.95	5.96	4.72	0.70
(EG) ₄	4.32	5.38	5.42	4.78	0.74
(EG) ₅	5.08	4.58	4.62	4.47	0.79
(EG) ₆	5.70	4.08	4.08	4.45	0.80
PEG-200	4.81	4.84	4.85	4.81	0.80
PEG-400	7.00	3.31	3.34	4.32	0.79
PEG-600	12.48	1.86	1.87	4.16	0.78
PEG-1000	13.99	1.66	1.66	3.64	0.64
PEG-1500	20.59	1.13	1.13	4.10	0.70
PEG-2000	22.69	1.07	1.02	4.33	0.66
PEG-4000	24.35	0.96	0.96	4.42	0.61
PEG-10000	50.62	0.45	0.45	10.95	0.84

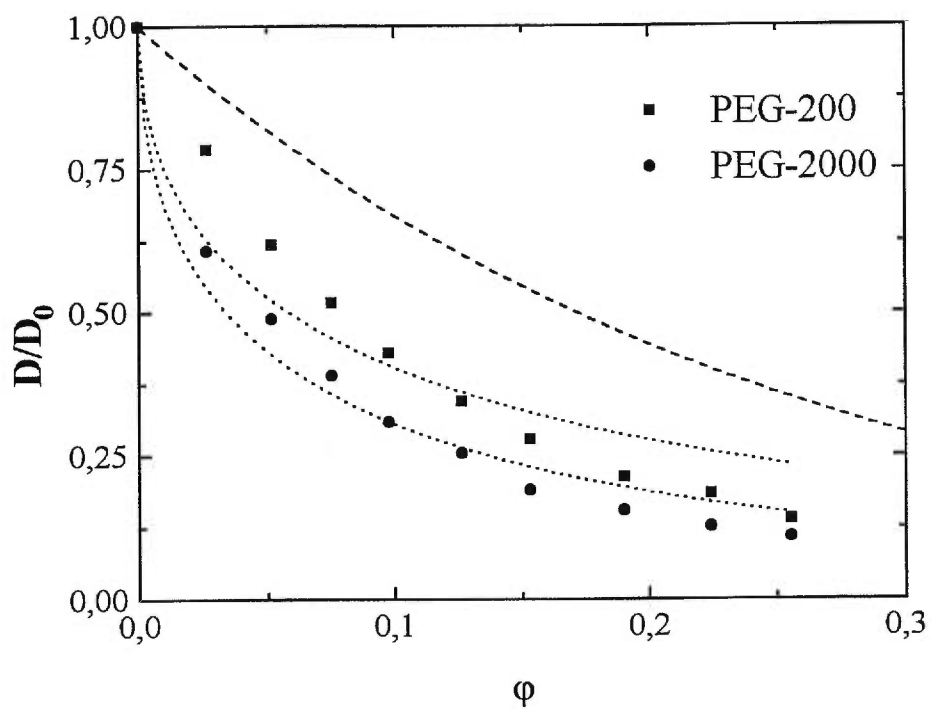


Figure 4.1. Plot of the normalized self-diffusion coefficient of selected diffusants as a function of the volume fraction of the PVA. Dashed line is fit to eq 4.1. The two dotted lines are fits to eq 4.2 for PEG-200 and PEG-2000.

4.5.2. The free volume model

A semi-logarithmic plot of the normalized self-diffusion coefficient as a function of $1/(1-\phi)$ is shown in Figure 4.2. The dashed lines are fits to eq 4.3 and should be straight lines. Linear fits are only observed for low volume fractions of the polymer. In addition, a gradual deterioration of the fits to the data is observed as the size of the diffusant is increased. This free volume model provides good agreement with the data for low polymer concentrations and for smaller diffusants, but fails for high polymer concentration where the hydrodynamic interactions are not negligible. Hennink *et al.* [40], Petit *et al.* [23] and Amsden [20] pointed out the limitations of this model. It seems that it is not suitable to describe probe diffusion when the diffusant size is close to the hydrogel mesh size where screening effects started to occur [23,40].

4.5.3. The hydrodynamic models

Phillies' universal equation was used for the treatment of the diffusion data. The self-diffusion coefficients of PEGs are plotted as a function of PVA concentration in Figure 4.3A. Dashed lines are fits to eq 4.4 with floating parameters, including α , ν and D_0 . Fixing D_0 to the measured value does not induce significant variations of the results. The fitting parameters for OEGs and PEGs are listed in Table 4.1. The measured values of D_0 and those obtained from fits to eq 4 are very close. Lodge and co-workers [34–36] studied the self-diffusion of linear and star polystyrenes in poly(vinyl methyl ether)/*o*-fluorotoluene systems by dynamic light scattering. They reported systematic difference between the measured and calculated D_0 values by as much as a factor of 2, and the difference was attributed to the polymer coil contraction with increasing matrix concentration [35]. In our case, such a deviation is not observed for OEG and PEG, as shown in Table 4.1 and Figure 4.3, even at high PVA concentrations that correspond to highly viscous gels.

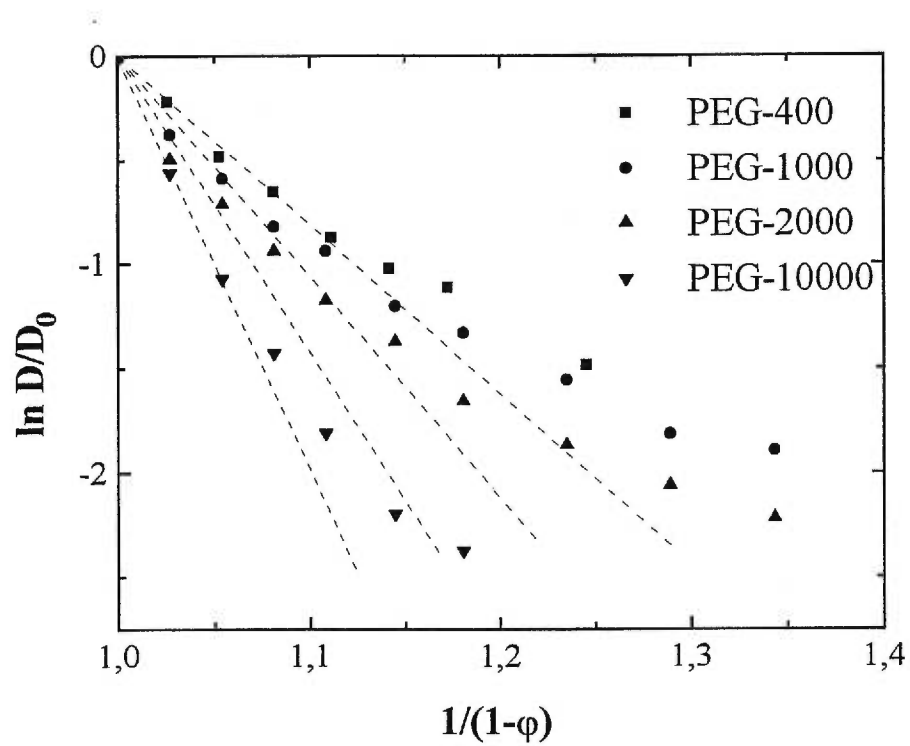


Figure 4.2. Semi-logarithmic plot of the normalized self-diffusion coefficient of selected diffusants as a function of $1/(1-\phi)$ (ϕ = volume fraction of PVA), at 25°C. Dashed lines are fits to eq 4.3.

Phillies related the parameters α and ν to the molecular weight of the diffusants (M) [31]. Figure 4.4 shows the variation of R_h calculated with the Stokes-Einstein equation as a function of M of the diffusants (PEGs). As expected, R_h increases as a function of M . The α values obtained by fitting the diffusion data in Figure 4.3A are reported in Table 4.1. With the exception of PEG-10000 ($\alpha = 10.95$), the parameter α seems to remain quite constant. A linear dependence between α and R_h was suggested by Russo *et al.* [41], but Park *et al.* [42] and Gibbs and Johnson [43] reported α being equal to $3.03 R_h^{0.59}$ and $3.2 R_h^{0.53}$, respectively, which is not observed in this study. The parameter ν is found also to be more or less constant with an average value of 0.74 for the present diffusants (Table 4.1). According to Phillies, ν should be equal to 1 for small-sized diffusants and 0.5 for macromolecules [30]. To further evaluate the parameters, we have fixed ν to the average value of 0.74 to fit the data again, leaving α and D_0 as free parameters. The fitting curves are reasonably good except for the high polymer concentration end, where the best fits deviate somewhat from the experimental data (results not shown). The values of D_0 were very close to the experimental values and the parameter α was found to vary between 3.91 and 5.83 (with the exception of PEG-10000 for which $\alpha = 8.31$).

We have studied the temperature effect on the self-diffusion coefficients of selected solute probes: *t*BuOH, PEG-600, and PEG-2000, an example of which is shown in Figure 4.3B (PEG-600). It is clear that the diffusion data can be fitted quite well to eq 4.4 over the whole concentration range at all temperatures. Phillies indicated that α decreases while ν increases with increasing temperature [31]. Within the temperature range between 23 and 53 °C for each diffusant studied here, no significant change is observed for the scaling parameters α and ν with varying temperatures. However, the variation with temperature is evidenced by the Arrhenius behavior of D_0 , as shown in Figure 4.5. The activation energies of the selected diffusants can be estimated from the slopes of the lines. Values of 18.4 ± 2.0 , 31.0 ± 3.9 , and 27.1 ± 7.0 kJ/mol are obtained for *t*BuOH, PEG-600, and PEG-2000, respectively. The lower activation energy for PEG-2000 as compared to PEG-600 may reflect the errors of the estimates. The activation energy obtained with the model of

Petit *et al.* provided increasing activation energies with increasing size of the diffusant (30.0, 36.5 and 39.0 kJ/mol, respectively), based on the same experimental data [25].

De Gennes' reptation model [11] can also be used to describe the diffusion of one polymer in another. Tests have shown that de Gennes' model is not suitable to describe the diffusion of these molecules. Although the PEG diffusant used in this study have molecular weights as high as 10000, it is considered that they are too small for reptation to take place.

4.5.4. Amsden's model

Figure 4.6 shows the normalized self-diffusion coefficient of selected probes as a function of the volume fraction of the polymer. In general, eq 4.5 with floating parameters (r_s , r_f and k_1) provided good fits to the experimental data as shown by the examples in Figure 4.6. PEG-10000 was not studied over the same polymer concentration range due to solubility problems of this PEG at higher PVA concentrations. However, the fitting parameters of r_s and r_f obtained are far from any reasonable values (even negative values were obtained). Therefore, we have tried to fix r_s to the R_h values listed in Table 4.1 during the fittings, but negative values of r_f were obtained in each case while k_1 was not found to be a constant either. The fitting curves, however, overlap nicely with the data points. Therefore, the physical meaning of the parameters needs to be clarify with further studies.

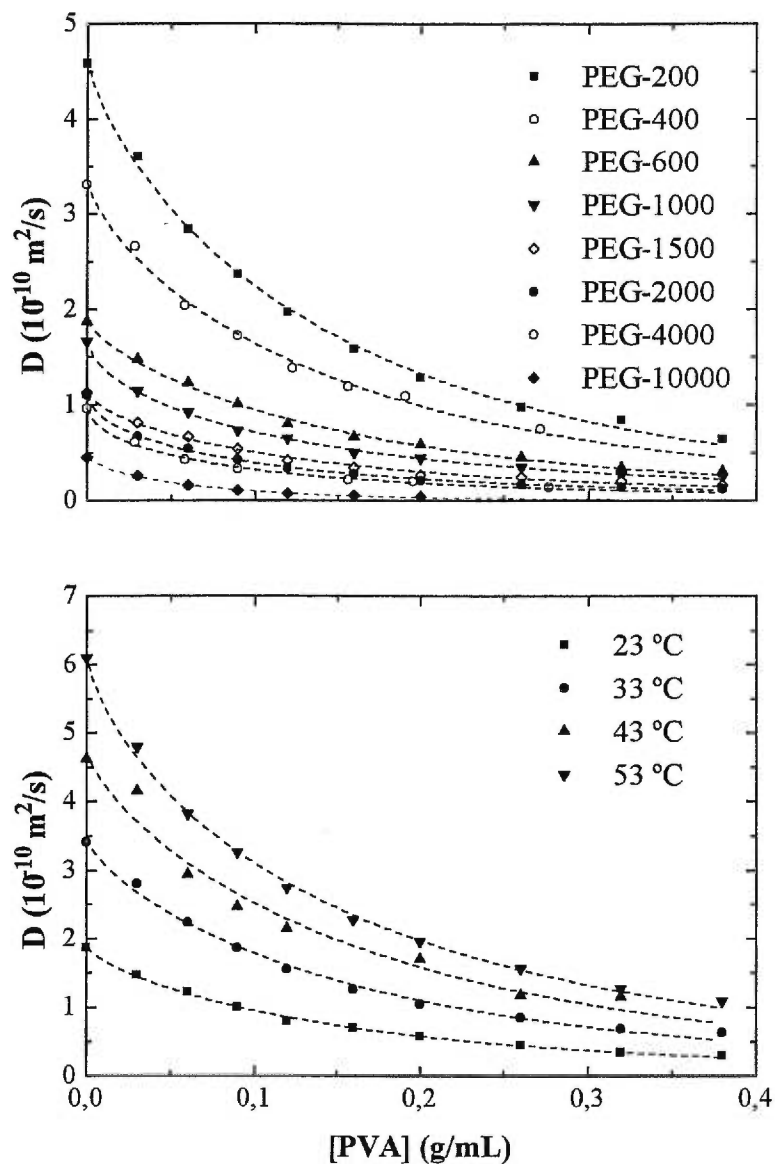


Figure 4.3. (A) Self-diffusion coefficients of selected PEGs plotted as a function of PVA concentration at 23 °C. (B) Self-diffusion coefficients of PEG-600 plotted as a function of the PVA concentration at four temperatures: 23, 33, 43, and 53 °C. Dashed lines are fits to eq 4.4.

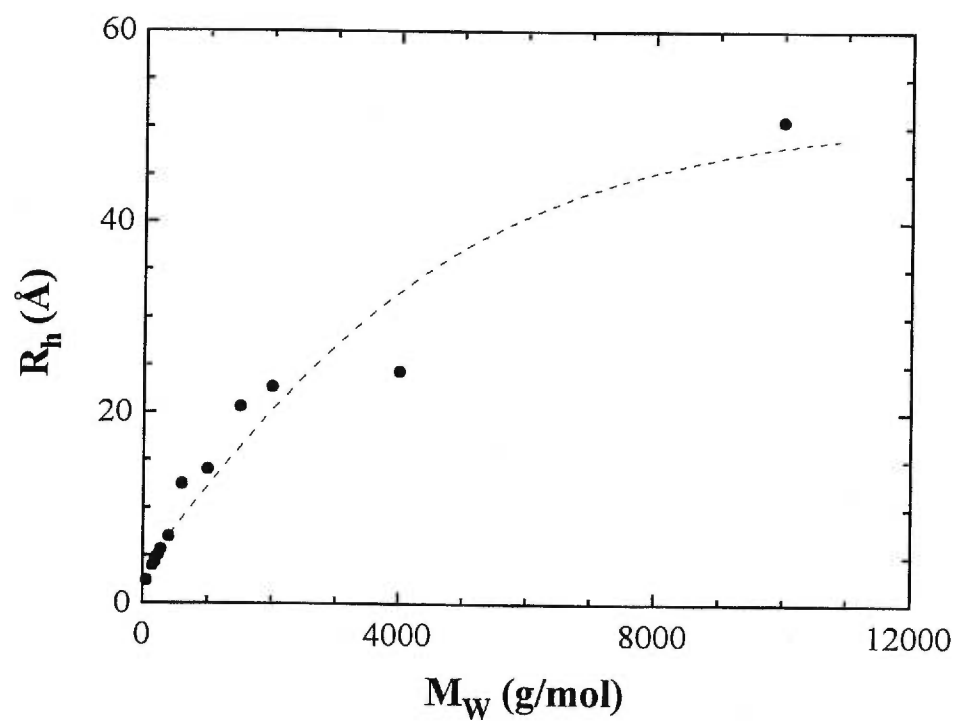


Figure 4.4. Plot of the hydrodynamic radius, R_h , as a function of molecular weight M of the PEG diffusants. Dashed lines are drawn to indicate the general trend of the variation.

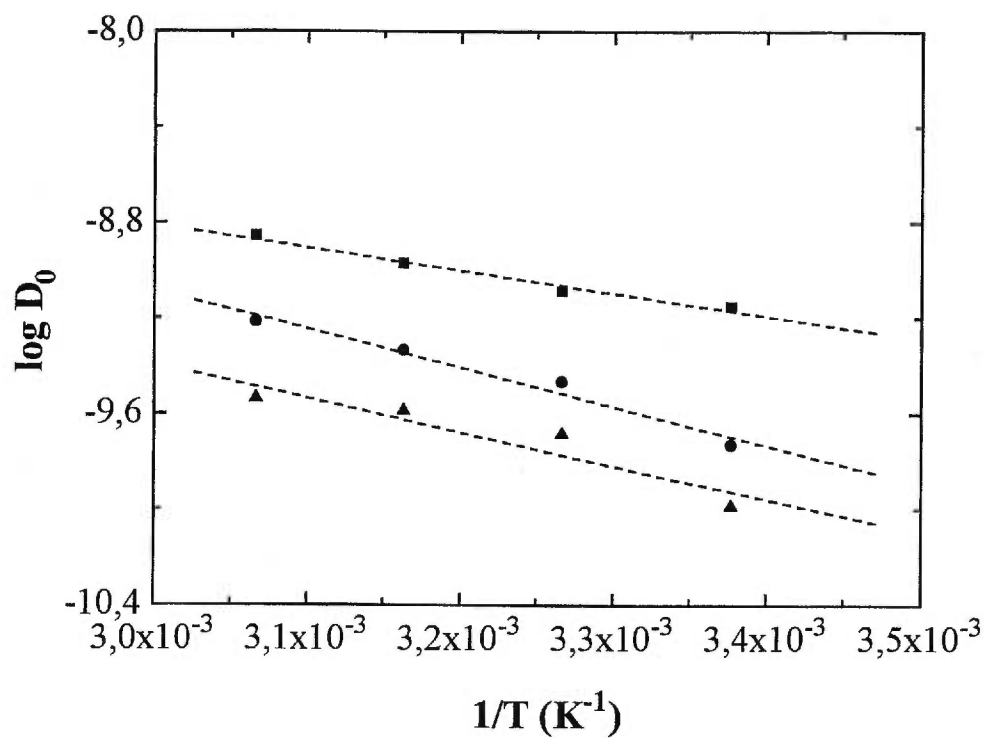


Figure 4.5. Semilogarithmic plot of the self-diffusion coefficients D_0 as a function of the reciprocal temperature for selected diffusants. Dashed lines are drawn to indicate the general trend of the variations.

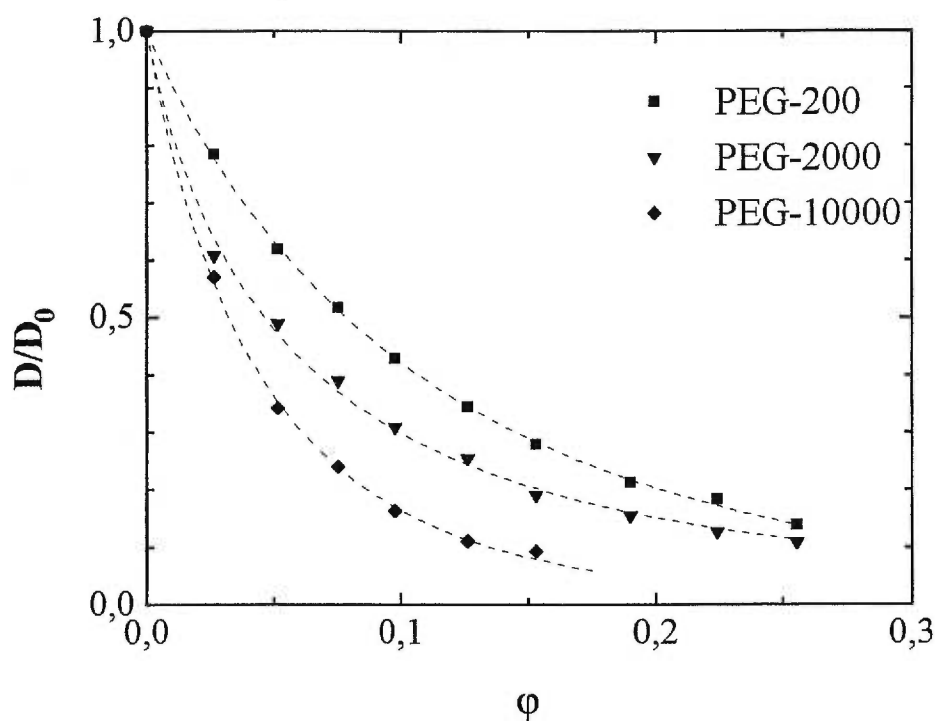


Figure 4.6. Plot of the normalized self-diffusion coefficient of selected diffusants as a function of the volume fraction of PVA. Dashed lines are fits to eq 4.5 for PEG-200, PEG-2000 and PEG-10000, respectively, with r_s , r_f and k_l as floating parameters.

4.6. Concluding remarks

Complementary to the analysis of the diffusion data [25] with the model of Petit *et al.* [24], we have used various pertinent physical models of diffusion in the treatment of the diffusion data obtained for poly(ethylene glycol)s in PVA ternary aqueous solutions and gels in an effort to verify the applicability of these models in the interpretation of the diffusion data in such systems. It is obvious that the models based on the obstruction effect are not suitable for such a purpose. The free volume model of Yasuda *et al.* can be used for the description of the diffusion in the dilute samples of the series, but cannot be used for the concentrated samples. Because of the low molecular weights of the diffusants used, the scaling relationships in the reptation models of de Gennes were not found with these diffusants.

The universal equation proposed by Phillies provided good fits to the diffusion data over the whole range of polymer concentrations for the diffusants and temperatures studied. The scaling parameter ν seems to be a constant for the system, while the variation of α cannot be correlated to the property of the diffusants. But the flexibility of this equation (eq 4.4) is clearly confirmed. The variable temperature effect was shown mainly by the Arrhenius behavior of the self-diffusion coefficient of the solutes in the absence of polymer, D_0 , from which the activation energy of diffusion can be estimated. It should be noted that the molecular weights of the PEG diffusants used here are still much lower than that of the matrix polymer.

The idea of combining different concepts to describe the diffusion in polymer systems is interesting. The new model proposed by Amsden is a good example in this effort. This model was shown to be quite flexible and provided good fits to the experimental data, but the physical significance of the parameters used in the model cannot be confirmed by the results.

4.7. Acknowledgments

Financial support from Natural Sciences and Engineering Research Council (NSERC) of Canada and from the Quebec Government (Fonds FCAR and a Quebec-Ontario collaboration travel grant) is gratefully acknowledged. The authors also thank Dr.

J. Roovers of the National Research Council of Canada for his constructive comments, and Dr. M. Ousalem and Mr. W.E. Baille for their help in the determination of the molecular weight of the PVA.

4.8. References

- [1] M. Clericuzio, W.O. Parker, M. Soprani and M. Andrei, *Solid State Ionic*, **77**, 685 (1995).
- [2] P. Hoerner, G. Riess, F. Rittig and G. Fleischer, *Macromol. Chem. Phys.*, **199**, 343 (1998).
- [3] D. Hariharan and N.A. Peppas, *J. Contr. Release*, **23**, 123 (1993).
- [4] P. Gao and P.E. Fagerness, *Pharm. Res.*, **12**, 955 (1995).
- [5] H. Fricke, *Phys. Rev.*, **24**, 575 (1924).
- [6] J.S. Mackie and P. Meares, *Proc. R. Soc. Lond., A*, **232**, 498 (1955).
- [7] A.G. Ogston, B.N. Preston and J.D. Wells, *Proc. R. Soc. Lond., A*, **333**, 297 (1973).
- [8] J.F. Douglas and D. Leporini, *J. Non-Cryst. Solids*, **137**, 235 (1998).
- [9] R.I. Cukier, *Macromolecules*, **17**, 252 (1984).
- [10] A.R. Altenberger and M. Tirrell, *J. Chem. Phys.*, **80**, 2208 (1984).
- [11] P.G. de Gennes, *J. Phys. Chem.*, **55**, 572 (1971).
- [12] P.G. de Gennes, in *Scaling Concepts in Polymer Physics*, Cornell University Press: Ithaca, New-York, 1979.
- [13] G.D.J. Phillies, *Macromolecules*, **19**, 2367 (1986).
- [14] H. Fujita, *Adv. Polym. Sci.*, **3**, 1 (1961).
- [15] H. Yasuda, C.E. Lamaze and L.D. Ikenberry, *Makromol. Chem.*, **118**, 19 (1968).
- [16] J.S. Vrentas and J.L. Duda, *J. Polym. Sci., Polym. Phys. Ed.*, **15**, 403 (1977).
- [17] J.S. Vrentas and J.L. Duda, *J. Polym. Sci., Polym. Phys. Ed.*, **15**, 417 (1977).
- [18] J.S. Vrentas and C.M. Vrentas, *Macromolecules*, **27**, 4684 (1994).
- [19] J. Brady, *AIChE Ann. Meet.*, 320 (1994).
- [20] B. Amsden, *Polym. Gels Networks*, **6**, 13 (1998).

- [21] A.H. Muhr and M.V. Blanshard, *Polymer*, **23**, 1012 (1982).
- [22] R.A. Waggoner, F.D. Blum and J.M.D. MacElroy, *Macromolecules*, **26**, 6848 (1993).
- [23] J.-M. Petit, X.X. Zhu and P.M. Macdonald, *Macromolecules*, **29**, 70 (1996).
- [24] J.-M. Petit, B. Roux, X.X. Zhu and P.M. Macdonald, *Macromolecules*, **29**, 6031 (1996).
- [25] L. Masaro, X.X. Zhu and P.M. Macdonald, *Macromolecules*, **31**, 3880 (1998).
- [26] M. H. Cohen and D. Turnbull, *J. Chem. Phys.*, **31**, 1164 (1959).
- [27] J.G. Kirkwood and J. Riseman, *J. Chem. Phys.*, **16**, 565 (1948).
- [28] G.D.J. Phillies, *Macromolecules*, **20**, 558 (1987).
- [29] G.D.J. Phillies, *Macromolecules*, **21**, 3101 (1988).
- [30] G.D.J. Phillies, *J. Phys. Chem.*, **93**, 5029 (1989).
- [31] G.D.J. Phillies, C. Richardson, C.A. Quinlan and S.Z. Ren, *Macromolecules*, **26**, 6849 (1993).
- [32] R. Furukawa, J.L. Arauz-Lara and B. R. Ware, *Macromolecules*, **24**, 599 (1991).
- [33] J. Sung and T. Chang, *Polymer*, **34**, 3741 (1993).
- [34] L.M. Wheeler, T.P. Lodge, B. Hanley and M. Tirrell, *Macromolecules*, **20**, 1120 (1987).
- [35] L.M. Wheeler and T.P. Lodge, *Macromolecules*, **22**, 3399 (1989).
- [36] T.P. Lodge, P. Markland and L.M. Wheeler, *Macromolecules*, **22**, 3409 (1989).
- [37] P.E. Rouse, *J. Phys. Chem.*, **21**, 1272 (1953).
- [38] T. Okaya, in *Polyvinyl Alcohol-Developments*, Finch, C.A. Ed.; John Wiley, London, 1992; Chap. 1, p. 1.
- [39] L. Johansson, U. Skantze and J.-E. Löfroth, *Macromolecules*, **24**, 6024 (1991).
- [40] W. E. Hennink, H. Talsma, J. C. H. Borchert, S. C. De Smedt and J. Demeester, *J. Contr. Release*, **39**, 47 (1996).
- [41] P.S. Russo, M. Mustafa, T. Cao and L.K. Stephen, *J. Colloid. Interface Sci.*, **122**, 120 (1988).
- [42] I.H. Park, C.S. Johnson Jr. and D.A. Gabriel, *Macromolecules*, **23**, 158 (1990).
- [43] S.J Gibbs and C.S. Johnson Jr., *Macromolecules*, **24**, 6110 (1991).

Partie III

L'influence de la géométrie du soluté sur la diffusion

Chapitre 5

Self-Diffusion of End-Capped Oligo- (ethylene glycol)s in Poly(vinyl alcohol) Aqueous Solutions and Gels

Masaro, L.; Zhu, X.X.

Macromolecules, **1999**, soumis

5.1. Abstract

We have studied the self-diffusion of a series of end-capped ethylene glycol and oligo(ethylene glycol)s in poly(vinyl alcohol) aqueous solutions and gels by pulsed-gradient spin-echo NMR spectroscopy. The end groups of the diffusants include small flexible groups (methyl, ethyl, hexyl) and bulky rigid groups (*tert*-butyl and aromatic groups). The effect of the size and geometry of the end groups on the self-diffusion coefficients of the derivatives of ethylene glycol and of oligo(ethylene glycol)s is investigated. The diffusion data are analyzed with several physical models of diffusion based on different physical concepts to test their applicabilities. The variation of the parameters used in these diffusion models with the size and geometry of the diffusants is also discussed.

5.2. Introduction

The diffusion of small molecules in polymer solutions and gels has been a subject of increasing research interest in the last decade [1–10]. The understanding of the diffusion of small molecules in polymers is useful and important for the processes involving the devolatilization of monomer and solvent from polymer products [11], controlled release of drugs [12], membrane permeation [13], transport in porous medium [14,15], electrophoresis and gel filtration [16,17], etc. With the development of more convenient experimental techniques such as pulsed field gradient NMR spectroscopy [18,19], more diffusion data have become available [1,2,4,12]. The interpretation of the results has not been always easy [4,20–22] even with the availability of numerous physical models of diffusion in the literature [23–34]. In fact there remains disagreement regarding the applicability of the models for various polymer systems. Due to the origin of the physical concepts considered, including the obstruction effect [23,24], the free volume effect [28–32], or hydrodynamic interactions [25–27], limitations of the models to the different circumstances are bound to occur. It would be useful to verify the applicability of some pertinent diffusion models in the analysis of the diffusion results of relatively small molecules in polymer systems.

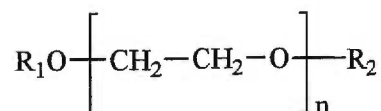
The diffusion in polymers may be influenced by various factors such as the concentration or the cross-linking of the polymer matrix, the temperature, and the size of the diffusants [19-21,35,36]. We have studied the effect of the size of the diffusant on its self-diffusion in poly(vinyl alcohol) (PVA) aqueous solutions and gels by using a series of linear diffusants based on ethylene glycol with increasing molecular weights [36]. It was found that at a given concentration of the polymer the size of the diffusant has the most significant effect on its diffusion [36]. However, the hydroxyl groups of ethylene glycol (EG) in these diffusants were found to interact strongly with the polymer system by the formation of hydrogen bonds. This was clearly shown in another report where the interaction of EG with PVA was studied by monitoring the changes in chemical shifts, self-diffusion coefficients and relaxation times [37]. Therefore, we would like to examine the effect of molecular size and geometry of the diffusant by the use of end-capped ethylene glycol and derivatives. To do this, we have studied the self-diffusion coefficients of a series of ethylene glycol derivatives as well as a crown ether in PVA-aqueous systems by pulsed-gradient spin-echo (PGSE) NMR spectroscopy. Several pertinent models of diffusion are used in the analysis of the diffusion data and the physical significance of the parameters used in these models is evaluated as well. The results are also compared with those obtained with oligo- and poly(ethylene glycol) diffusants in the same system.

5.3. Experimental

5.3.1. Materials

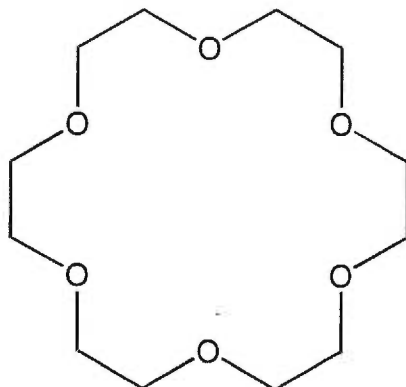
The diffusants used in this study are shown in Table 5.1 and Figure 5.1. These diffusants include ethylene glycol, oligo(ethylene glycol)s and their end-capped derivatives, a crown ether (18-crown-6) and 2-[3-(6-Methyl-2-pyridyl)-propoxy] ethanol (MPPE). These compounds and poly(vinyl alcohol) ($M_w = 52\ 000$, $M_w/M_n = 2.09$, degree of hydrolysis 99 %) were all purchased from Aldrich (Milwaukee, WI) and used as received. D_2O (99.9 %) was purchased from C.I.L. (Andover, MA).

Table 5.1. The structure and molecular weight (M) of the end-capped oligo(ethylene glycol)s used in this study.

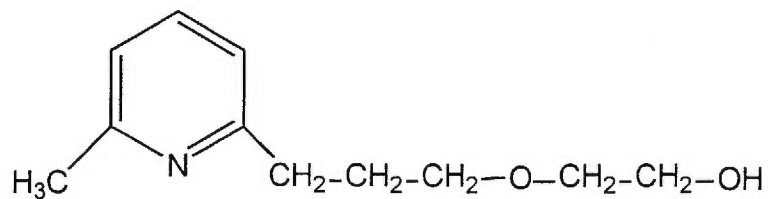


Diffusant	Abbreviation	n	R ₁	R ₂	M (g/mol)
Ethylene glycol	EG	1	-H	-H	62
Ethylene glycol methyl ether (2-Methoxyethanol)	EG-Me	1	-H	-CH ₃	76
Ethylene glycol dimethyl ether	EG-Me ₂	1	-CH ₃	-CH ₃	90
Ethylene glycol <i>tert</i> -butyl methyl ether (1- <i>tert</i> -Butoxy-2-methoxyethane)	EG- <i>t</i> BuMe	1	-CH ₃	- C(CH ₃) ₃	132
Di(ethylene glycol) methyl ether	DEG-Me	2	-H	-CH ₃	120
Di(ethylene glycol) ethyl ether	DEG-Et	2	-H	-C ₂ H ₅	134
Di(ethylene glycol) hexyl ether	DEG-He	2	-H	-C ₆ H ₁₃	190
Diethylene glycol <i>tert</i> -butyl methyl ether	DEG- <i>t</i> BuMe	2	-CH ₃	- C(CH ₃) ₃	176
Tri(ethylene glycol) methyl ether	TEG-Me	3	-H	-CH ₃	164
Tri(ethylene glycol) dimethyl ether	TEG-Me ₂	3	-CH ₃	-CH ₃	178

Remarque: Le triéthylène glycol (TEG) ne figure pas dans cette étude car son profil de diffusion en fonction de la concentration en PVA comparé au TEG-Me et TEG-Me₂ montre l'existence de certains problèmes d'association. Une étude exhaustive est en préparation (c.f. annexe).



18-crown-6



2-[3-(6-Methyl-2-pyridyl)-propoxyl]ethanol (MPPE)

Figure 5.1. Chemical structure of the diffusants 18-crown-6 and 2-[3-(6-Methyl-2-pyridyl)-propoxyl]ethanol (MPPE) used in this study.

5.3.2. NMR measurements.

The samples were prepared as described previously [22,36]. The measurements of the self-diffusion coefficients were carried out on a Bruker Avance AMX-300 NMR spectrometer operating at 300.13 MHz for protons. The temperature was set at 25 °C. The PGSE pulse sequence developed by Stejskal and Tanner [38] was used. A Bruker magnetic resonance imaging probe, Micro 2.5 Probe, was used in conjunction with a gradient amplifier (BAFPA-40). Gradient pulses were applied only in the z direction. The calibration of the gradient strength and the temperature was described elsewhere [18,19,39]. The gradient strengths, G , used in this study ranged between 0.1 and 1 T/m. The other parameters were kept constant and their values are those noted in the parentheses depending on the experiments: gradient pulse duration (1-4 ms), gradient pulse interval (30-80 ms), recycle delay (10-25 s), number of acquisitions (1-8), 90° pulse (23-29 μ s), spectral width (3-8 kHz), line broadening (5-10 Hz).

The fitting procedure of the experimental diffusion data to the physical models of diffusion was the chi-square (χ^2) minimization procedure available with Microcal Origin 3.5 (Northampton, MA) and the χ^2 values are listed in the tables.

5.3.3. Rheological measurements

Rheological experiments were carried out in order to characterize the PVA solutions and gels. A Bohlin VOR rheometer equipped with a couette for dilute solutions and with a cone for more concentrated solutions was used. Calibration of the rheometer was achieved with poly(dimethyl siloxane) standards. PVA concentrations were similar to those of the samples used for NMR measurements ($[PVA] = 0-0.38$ g/mL) but without the diffusant.

5.4. Results and discussion

The rheological experiments of the PVA samples have shown that the PVA-water systems are Newtonian solutions for a PVA concentration between 0 and 0.12 g/mL. But for samples with PVA concentrations above 0.26 g/mL, the elastic

modulus (G') was higher than the viscous modulus (G''), which is characteristic of a gel. The samples of intermediate PVA concentrations lie in between these two cases.

The measured self-diffusion coefficients of the solutes molecules in the PVA systems have been analyzed with several physical models with varying degree of success. The self-diffusion coefficient values, D , are those of the free diffusant (especially in the case of EG).

5.4.1. The model of Petit *et al.* [35]

In this model, the polymer network is considered as a transient statistical network characterized by a mesh size, ξ . The diffusant is considered to reside temporarily inside a cavity until it has enough energy to diffuse to the next one. Therefore, the diffusion process is a succession of jumps over equal potential barrier [35]. The self-diffusion coefficient D is given as

$$D = \frac{D_0}{1 + a c^{2\nu}} \quad (5.1)$$

where D is the self-diffusion coefficient, D_0 the self-diffusion coefficient without the matrix polymer, a and ν are the parameters of the model. The parameter ν depends on the solvent quality and should be a constant for a given system. In a previous study [36], ν was found to be equal to 0.58 in PVA aqueous systems. The parameter a is given by

$$a = \frac{D_0}{k\beta^2} \quad (5.2)$$

where k is the jump frequency of the diffusant and β can be regarded as a constant for a given system. The parameter $k\beta^2$ depends on the size of the diffusant, such as the hydrodynamic radius (R_h), and on the temperature [36]. R_h can be calculated with the Stokes-Einstein equation from the D_0 values listed in Table 5.2:

$$R_h = \frac{k_B T}{6\pi\eta_0 D_0} \quad (5.3)$$

where k_B is Boltzmann constant, T the temperature, η_0 is approximated as the viscosity of the solvent without the polymer. The Stokes-Einstein equation is

applicable to spherical diffusants. R_h is used as an indication of the relative size of the diffusants, but the R_h value calculated from eq 5.3 does not necessarily take into account the effect of the molecular shape. Therefore, precautions should be taken when R_h is used to indicate the molecular size of the diffusants, as discussed previously [36].

Figure 5.2 shows the self-diffusion coefficients of EG and its end-capped derivatives as a function of PVA concentration with fits to eq 5.1. The modification of the hydroxyl groups of EG by the addition of one or two methyl group(s) does not change to any significant extent the self-diffusion coefficients at a given PVA concentration (Figure 5.2A). The most important difference is that for the end-capped EG derivatives mono-exponential decrease of the spin-echo attenuation was observed, unlike in the case of EG, where both free and bound molecules were clearly evidenced [37]. This indicates that the methyl groups reduced or prevented the binding of EG to PVA. A bulky *tert*-butyl end group, however, affects much more the diffusion behavior of EG over the entire range of polymer concentrations. For the end-capped di(ethylene glycol) derivatives, the data are shown in Figure 5.2B. At a given PVA concentration D decreases with increasing size of the end alkyl group ($D_{\text{methyl}} > D_{\text{ethyl}} > D_{\text{hexyl}}$). A large linear hydrophobic end group such as a hexyl group seems to have a greater effect than a more spherical end group such as a *tert*-butyl. For the derivatives of tri(ethylene glycol), D values for TEG-Me and TEG-Me₂ are quite the same over the entire range of PVA concentrations, which is similar to the results observed for EG, EG-Me, and EG-Me₂ in concentrated PVA solutions. If the self-diffusion coefficients of EG-*t*BuMe ($M = 132$ g/mol) and DEG-Et ($M = 134$ g/mol) are compared, we notice that the diffusant with a bulkier end group (*tert*-butyl) diffuses less rapidly than the diffusant with a linear end group (ethyl) over the entire range of polymer concentrations. Similar differences can also be observed between DEG-*t*BuMe and TEG-Me₂. Obviously, the geometry of the diffusant seems to be quite important in the diffusion process. Similarly, the self-diffusion coefficient of TEG-Me₂ is always higher than that of MPPE (Figure 5.2C). The difference can be explained by the fact that MPPE has a bulky aromatic end group. The cyclic molecule

18-crown-6 behaves similarly as MPPE in the concentration range studied (Figure 5.2C).

Good fits are obtained for all the diffusants in Figure 5.2 over the entire range of polymer concentrations. The fitting parameters are listed in Table 5.2. When the data are fitted with free parameters of D_0 , $k\beta^2$ and ν , the average value obtained for ν is equal to 0.59 (Table 5.2) which is almost identical to the average value of 0.58 reported previously for the same polymer-water system [36]. This confirms that the parameter ν is an indication of the quality of the solvent [35]. Table 5.2 also lists the values obtained for the parameters D_0 and $k\beta^2$ when ν is fixed to 0.58. D_0 is found in good agreement with the experimental values. The $k\beta^2$ values are similar to those obtained with free ν values.

In Figure 5.3A, the logarithm of the parameter $k\beta^2$ (obtained with floating ν) is plotted as a function of R_h of the diffusants. The data are combined with the data obtained previously with a series of linear poly(ethylene glycol)s [36]. For both series, the jump frequency k decreases when the size of the diffusant is increased. Some of the linear PEG diffusants, especially the oligomers, were found to interact strongly with PVA via hydrogen bonding as mentioned previously. In the presence of hydrogen bonds in the PEG series, the jump frequency k is lower because of the hindrance caused by the interaction, and the decrease of the jump frequency with R_h is also more gradual as shown by the slope of the line ($k\beta^2 \sim R_h^{-0.036}$). With end-capped EG derivatives, even when the molecular size are similar to the PEGs, the jump frequency is still higher since the interactions are not as strong because of the capped ends that screen the interaction with PVA. The decrease of the jump frequency with R_h is also more abrupt as shown by the steeper slope ($k\beta^2 \sim R_h^{-0.19}$). When the PEG chain is sufficiently long, the effect of the end-group are no longer as significant and may even be negligible. In Figure 5.3B, the parameter $k\beta^2$ is plotted as a function of the molecular weight (M) of the diffusants. The general trend of the data is similar, i.e., the jump frequency decreases when the size of the diffusant is increased. Too distinct regions can be identify also corresponding to low molecular weight diffusant and high molecular weight diffusant, with an inflexion point approximately around $M =$

500. The first part of the line seems quite linear the decrease becomes much less abrupt in the second part.

Table 5.2. Measured D_0 values and the D_0 , $k\beta^2$ and ν values obtained as free parameters from fits to eq 5.1 and the D_0 and $k\beta^2$ values obtained from fits to eq 5.1 with ν fixed to 0.58, at $T = 25$ °C.

Diffusant	R_h	$D_0 \times 10^{-10}$	$D_0 \times 10^{-10}$	$k\beta^2$	$\nu^{(b)}$	$\chi^2^{(b)}$	$D_0 \times 10^{-10}$	$k\beta^2$	$\chi^2^{(c)}$
	(Å)	(m ² /s) ^(a)	(m ² /s) ^(b)	$\times 10^{10}$			(m ² /s) ^(c)	$\times 10^{10}$	
				(b)				(c)	
EG	2.79	8.59	8.48	0.93	0.65	0.020	8.68	1.16	0.033
EG-Me	3.07	7.88	7.83	1.16	0.60	0.004	7.89	1.24	0.005
EG-Me ₂	3.24	7.56	7.55	1.27	0.55	0.008	7.49	1.18	0.009
EG-tBuMe	4.38	5.58	5.52	0.65	0.59	0.009	5.54	0.67	0.008
DEG-Me	3.83	6.46	6.32	0.87	0.59	0.025	6.33	0.89	0.022
DEG-Et	4.18	5.77	5.72	0.66	0.62	0.010	5.80	0.76	0.011
DEG-He	5.45	4.43	4.42	0.38	0.60	0.003	4.45	0.41	0.003
DEG-tBuMe	5.05	4.80	4.74	0.48	0.62	0.009	4.80	0.55	0.013
TEG-Me	4.65	5.23	5.21	0.65	0.58	0.003	5.21	0.65	0.002
TEG-Me ₂	4.75	5.15	5.10	0.64	0.58	0.004	5.10	0.63	0.005
18-crown-6	5.54	4.37	4.37	0.36	0.58	0.005	4.37	0.35	0.004
MPPE	5.55	4.39	4.40	0.40	0.56	0.005	4.38	0.38	0.004

(a) Measured experimentally.

(b) Obtained from fits to eq 5.1 with free parameters

(c) Obtained from fits to eq 5.1 with $\nu = 0.58$

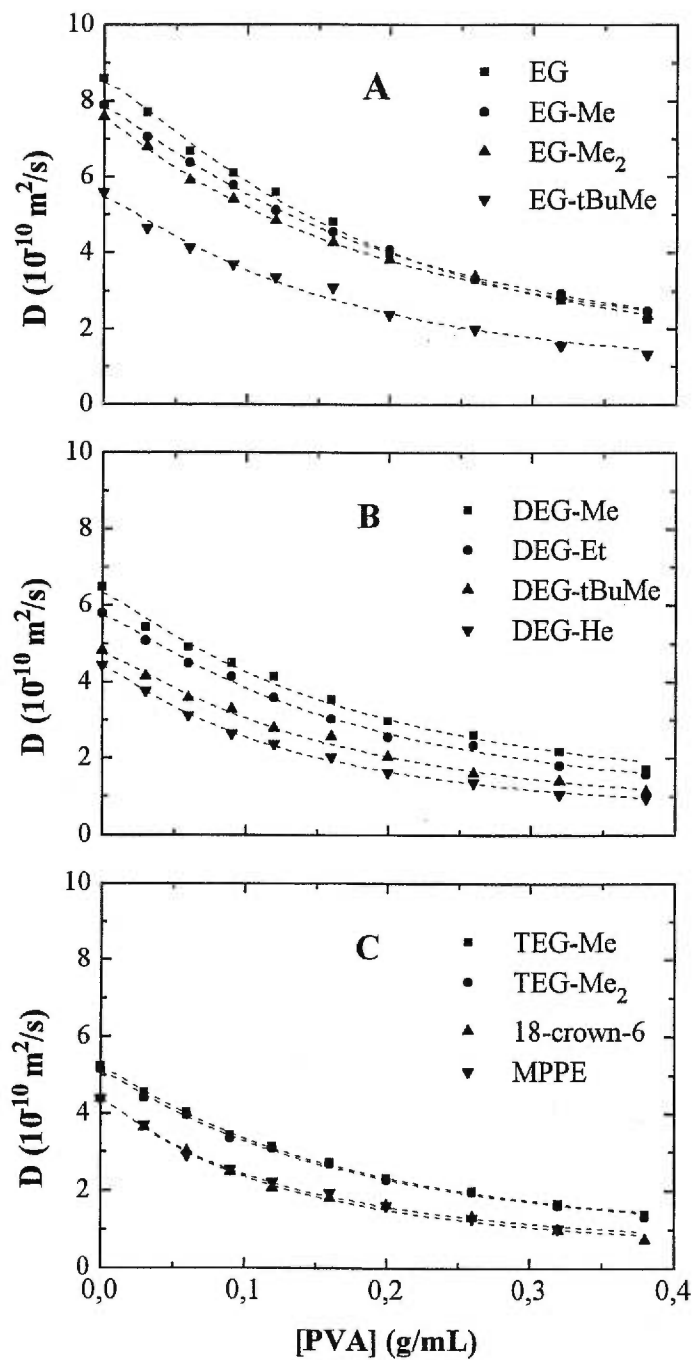


Figure 5.2. Plot of the self-diffusion coefficient of (A) ethylene glycol and its end-capped derivatives, (B) end-capped di(ethylene glycol)s, and (C) other end-capped oligo(ethylene glycol)s as a function of the PVA concentration at 25 °C. Dashed lines are fit to eq 5.1.

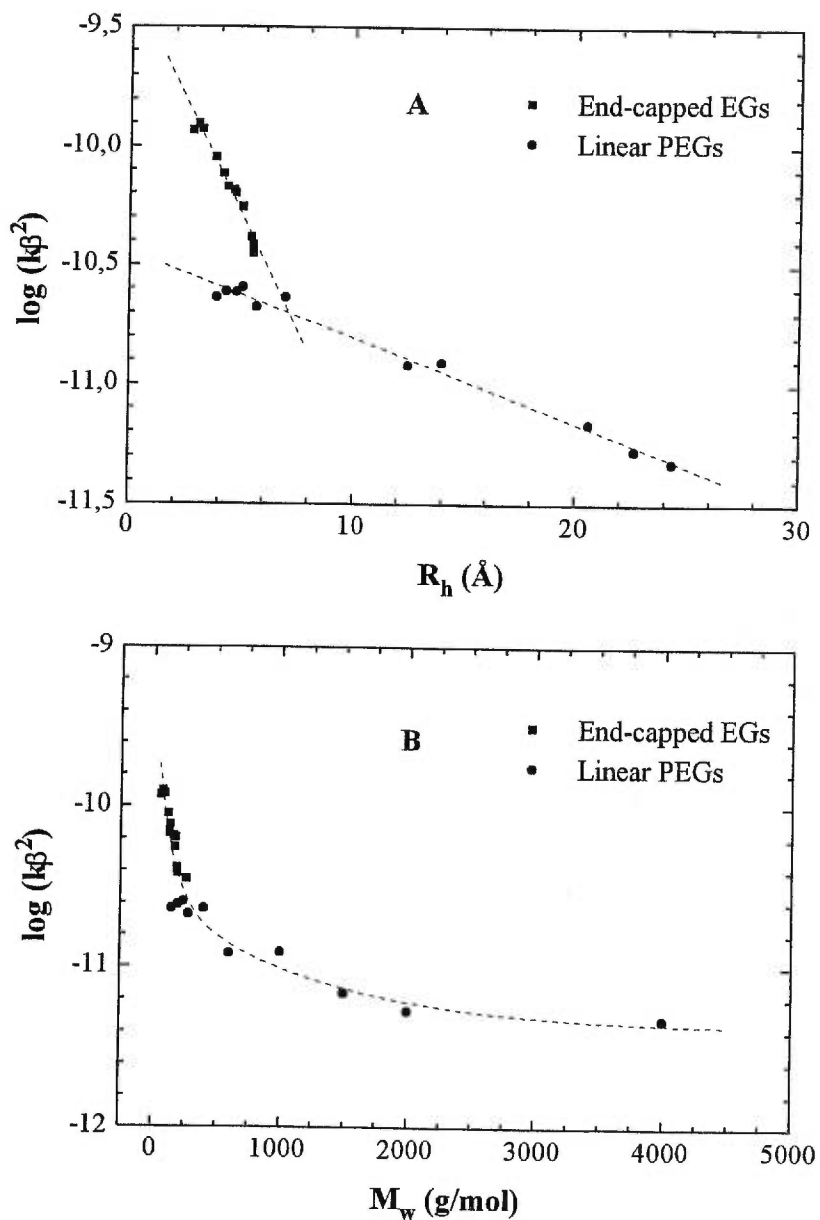


Figure 5.3. Semi-logarithmic plot of the parameter $k\beta^2$ as a function of (A) the hydrodynamic radius and (B) the molecular weight of the diffusants.

Remarque: la valeur de D_0 pour EG donnée au chapitre 3 est légèrement différente de celle indiquée dans le tableau 5.2. Cette différence s'explique par le fait qu'il existe une certaine erreur expérimentale lors des mesures de diffusion, et que les mesures n'aient pas été faites aux mêmes températures. De plus, ces mesures ont été réalisées avec deux appareils différents (Varian à Toronto et Bruker à Montréal) et deux méthodes différentes (variation de δ et de G , respectivement) dont les fiabilités ne sont pas comparables. Les mesures faites à Montréal sont considérées plus précises et plus fiables.

5.4.2. The model of Phillies [27]

Phillies proposed a universal equation to describe the self-diffusion of one macromolecule in another over a wide range of concentrations [27]. In this model, the hydrodynamic interactions between the diffusants (solvent or solute) and the polymer are taken into account and the polymer chains are considered to be mobile. This approach provided good fits to the experimental data in many polymer systems [40–42]. It also provided good results in the treatment of the diffusion data of small molecules [22,43,44]. The equation is given as

$$D = D_0 \exp(-\alpha c^{\nu}) \quad (5.4)$$

where α and ν are scaling parameters. The scaling parameter α is predicted to depend strongly on the hydrodynamic radius ($\alpha \sim R_h$) for small diffusants [45], as proposed by Mustafa *et al.* [46].

Eq 5.4 was used to fit the diffusion data of EG and its end-capped derivatives as a function of PVA concentration in Figure 5.4. The fitting parameters are listed in Table 5.3. A very good correlation is observed between the fits and the experimental data for all the diffusants over the entire range of polymer concentrations.

Park *et al.* [47] and Gibbs and Johnson [48] reported $\alpha = 3.03 R_H^{0.59}$ and $\alpha = 3.2 R_H^{0.53}$, respectively, for small probes (water, tetramethylammonium iodide, tetramethylethylenediamine, tetrahexylammonium, benzospiropyran and bovine serum albumin) in polyacrylamide gels. In the present study, the estimates obtained from these

empirical relationships tend to be higher than the α values obtained from the fits. However, the parameter α listed in Table 5.3 seems to depend somewhat on the hydrodynamic radius of the diffusant as shown in Figure 5.5A. A more or less linear relationship is observed ($\alpha \sim 0.28 R_h$).

Table 5.3. Measured D_0 values, calculated hydrodynamic radius (R_h) and D_0 , α and ν obtained as free parameters from fits to eq 5.4.

Diffusant	$D_0 \times 10^{10}$ (m ² /s)		α	ν	χ^2
	Experimental	Fitted			
EG	8.59	8.60	3.40	0.95	0.010
EG-Me	7.88	7.92	2.83	0.90	0.006
EG-Me ₂	7.56	7.61	2.60	0.83	0.009
EG-tBuMe	5.58	5.52	3.32	0.88	0.013
DEG-Me	6.46	6.40	2.94	0.86	0.010
DEG-Et	5.77	5.80	3.22	0.90	0.010
DEG-He	4.43	4.81	3.53	0.89	0.006
DEG-tBuMe	4.80	4.47	3.67	0.83	0.005
TEG-Me	5.23	5.27	3.06	0.84	0.004
TEG-Me ₂	5.15	5.16	3.06	0.84	0.003
18-crown-6	4.37	4.41	3.84	0.80	0.088
MPPE	4.39	4.42	3.69	0.80	0.007

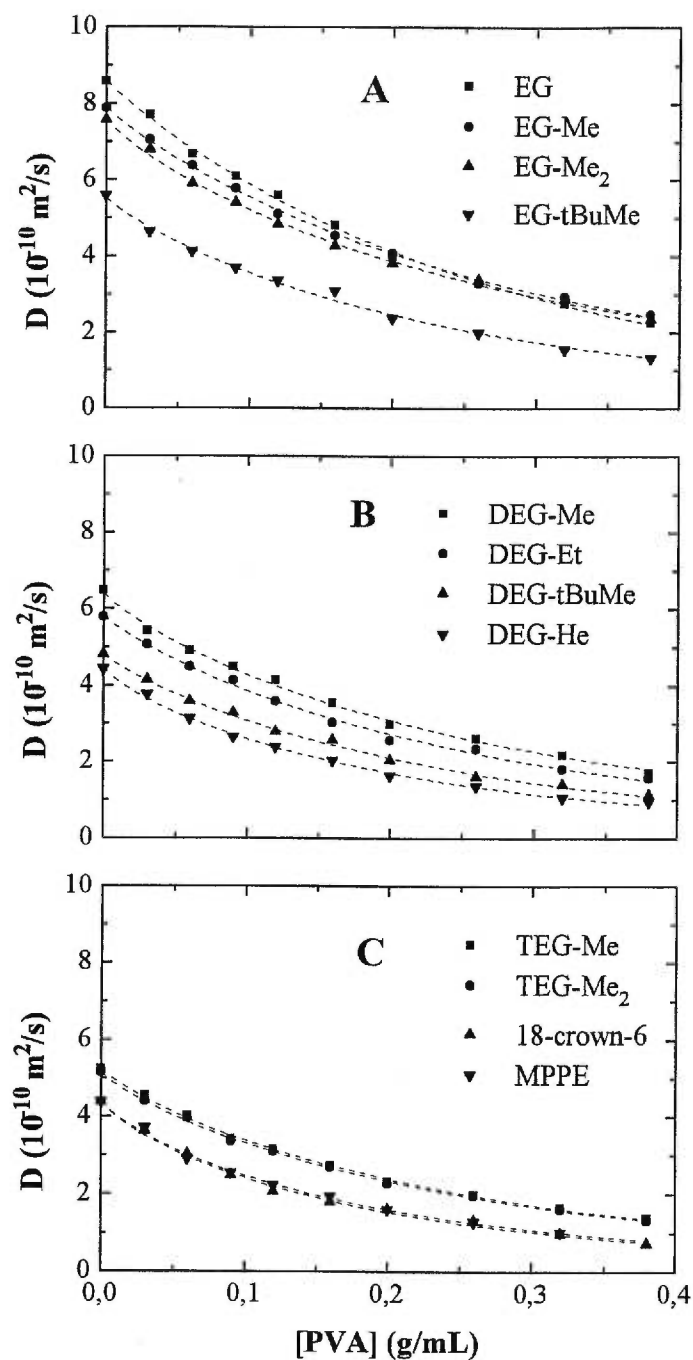


Figure 5.4. Plot of the self-diffusion coefficient of (A) ethylene glycol and its end-capped derivatives, (B) end-capped di(ethylene glycol), and (C) other end-capped oligo(ethylene glycol)s as a function of the PVA concentration at 25 °C. Dashed lines are fits to eq 5.4.

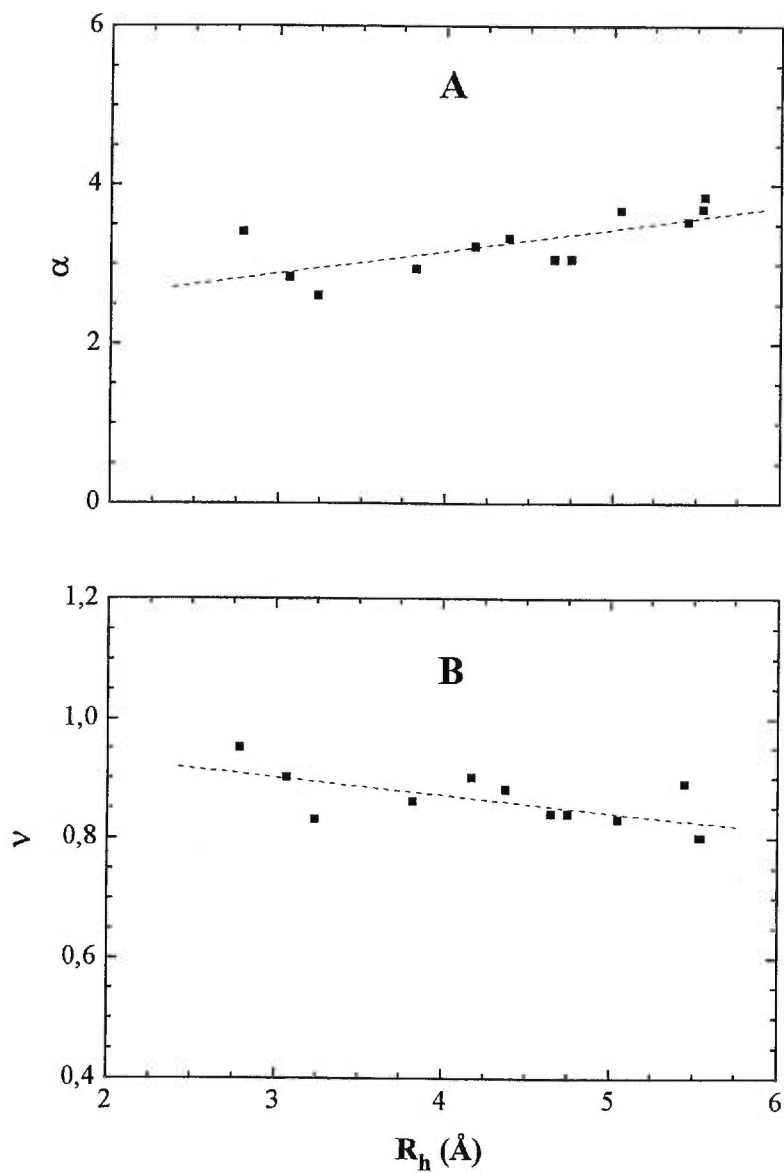


Figure 5.5. (A) Plot of the parameter α as a function of the hydrodynamic radius of the diffusants, and (B) plot of ν as a function of the molecular weight of the diffusants.

According to Phillies, ν should scale between 1 for low molecular weight diffusants and 0.5 for high molecular weight diffusants [40–42]. Inside these limits the scaling follows $\nu \sim M^{-1/4}$. The ν values listed in Table 5.3 are found to be more or less a constant and always less than 1. These values are plotted as a function of the hydrodynamic radius of the diffusants (Figure 5.5B). An average value of 0.86 is found. Gibbs and Johnson [48] reported values for the parameter ν between 0.89 and 1.13, slightly higher than the values obtained here.

5.3.3. The model of Yasuda *et al.* [29]

The free volume models consider the diffusion process as a succession of jumps into voids created by the thermal motion of the molecules. The diffusion of a solute is a function of the probability to find a void large enough to allow the diffusion of the solute. The free volume model of Fujita [28] is not suitable to describe diffusion in aqueous systems. The model of Vrentas-Duda [30,31] can be used for the diffusion in binary polymer-solvent systems. Because of the numerous physical parameters needed, it is difficult to use it in the more complicated ternary systems. Yasuda *et al.* [29] assumed that the contribution to the free volume is mainly contributed by the solvent in binary and ternary systems when the solute probe is present in low concentration (pseudo binary system). The following expression was obtained

$$\ln D = \ln D_0 - \frac{B_f}{f_w} \left(\frac{\phi}{1-\phi} \right) \quad (5.5)$$

where B_s is the minimum hole size required for the diffusant displacement, f_w is the free volume of water in the polymer-water system.

The semi-logarithmic of the normalized self-diffusion coefficient of selected solutes as a function of $\phi/(1-\phi)$ is shown in Figure 5.6A. The dashed lines are fits to eq 5.5, which seems to be linear for EG-Me and DEG-tBuMe at lower PVA concentrations, but deviations are observed at higher PVA concentrations, where the free volume contribution by the polymer may no longer be negligible. The deviation of the diffusion data of a larger diffusant such as MPPE from linearity is much more

significant, which clearly shows that the use of the model is limited to relatively small diffusants in relatively dilute solutions. This is consistent with the previous studies with similar systems [22,34,49]. We tried to use D_0 and B_s/f_w as free parameters in the fitting to eq 5.5. The D_0 values obtained for the diffusants from the fits are similar to the measured D_0 . If the parameter f_w is a constant as assumed by Yasuda *et al.* [30], B_s/f_w should reflect the variation of the minimum hole size (B_s) required for diffusant displacement to take place. The values obtained for B_s/f_w from the fits of the linear part of the curves are plotted as a function of the hydrodynamic radii of the diffusants in Figure 5.6B. B_s/f_w is found to be quite constant for the smaller diffusants and increases for the large ones in this series. The minimum hole size required for diffusant displacement should increase with increasing size of the diffusant.

5.4.4. The model of Mackie and Meares [23]

In this model, the polymer chains are regarded as motionless relative to the diffusing molecules. Therefore, they impose a tortuosity or an increase in the path length for the molecules in motion. The self-diffusion coefficient of the diffusants is related to the volume fraction of the polymer according to the following equation

$$\frac{D}{D_0} = \left[\frac{1-\phi}{1+\phi} \right]^2 \quad (5.6)$$

where ϕ the volume fraction of the matrix polymer.

Figure 5.7 shows the normalized self-diffusion coefficient of selected diffusants (EG-Me, EG-Me₂, EG-tBuMe and 18-crown-6) as a function of the volume fraction of the polymer matrix. The self-diffusion coefficient decreases with increasing volume fraction of the polymer and with increasing size of the diffusant. This is consistent with the results reported in previous studies [22,36]. The dotted line in Figure 5.7 represents the fit to eq 5.6. The fit can be regarded as acceptable for the diffusion data of EG-Me and EG-Me₂ especially at low PVA concentrations, but the deviation becomes obvious for higher polymer concentrations. The deviation between eq 5.6 and the data is more pronounced for the larger diffusants such as EG-tBuMe and 18-crown-6. Petit *et al.* [22] studied the self-diffusion of solvents and solute

probes in PVA-water systems and found that this model can only be used for the description of the diffusion data of water and methanol, whereas the fits for larger diffusants significantly deviate from the experimental data. Waggoner *et al.* [4] also studied the self-diffusion coefficients of different solvents (toluene, ethylbenzene, cumene, *tert*-butyl acetate, chloroform, and methyl ethyl ketone) in polystyrene (PS) and in poly(methyl methacrylate). They found that the model of Mackie-Mearns described fairly well the data, but they noticed that the subtle differences between the various systems were not taken into account by the model.

5.4.5. The model of Ogston *et al.* [24]

In this model the diffusing particle is considered as a hard sphere and the polymer as randomly oriented fibers. The diffusion process is assumed to correspond to the average displacement of a hard sphere in a lattice of long fibers of negligible width according to

$$\frac{D}{D_0} = \exp\left[-\frac{r_s + r_f}{r_f} \phi^{1/2}\right] \quad (5.7)$$

where r_s is the hydrodynamic radius of the diffusant and r_f the hydrodynamic radius of the fiber.

Dashed lines in Figure 5.7 are fits to eq 5.7. The model of Ogston *et al.* [24] takes into account the volume fraction of the polymer matrix, the hydrodynamic radius of the polymer fiber as well as the hydrodynamic radius of the diffusant. Therefore, the model provides different fits for each diffusant, which seems to be an improvement compared with the model of Mackie and Meares [24]. However, the fits to eq 5.7 still deviate significantly from the experimental data, indicating the limitation of this model in handling the diffusion data in such a system.

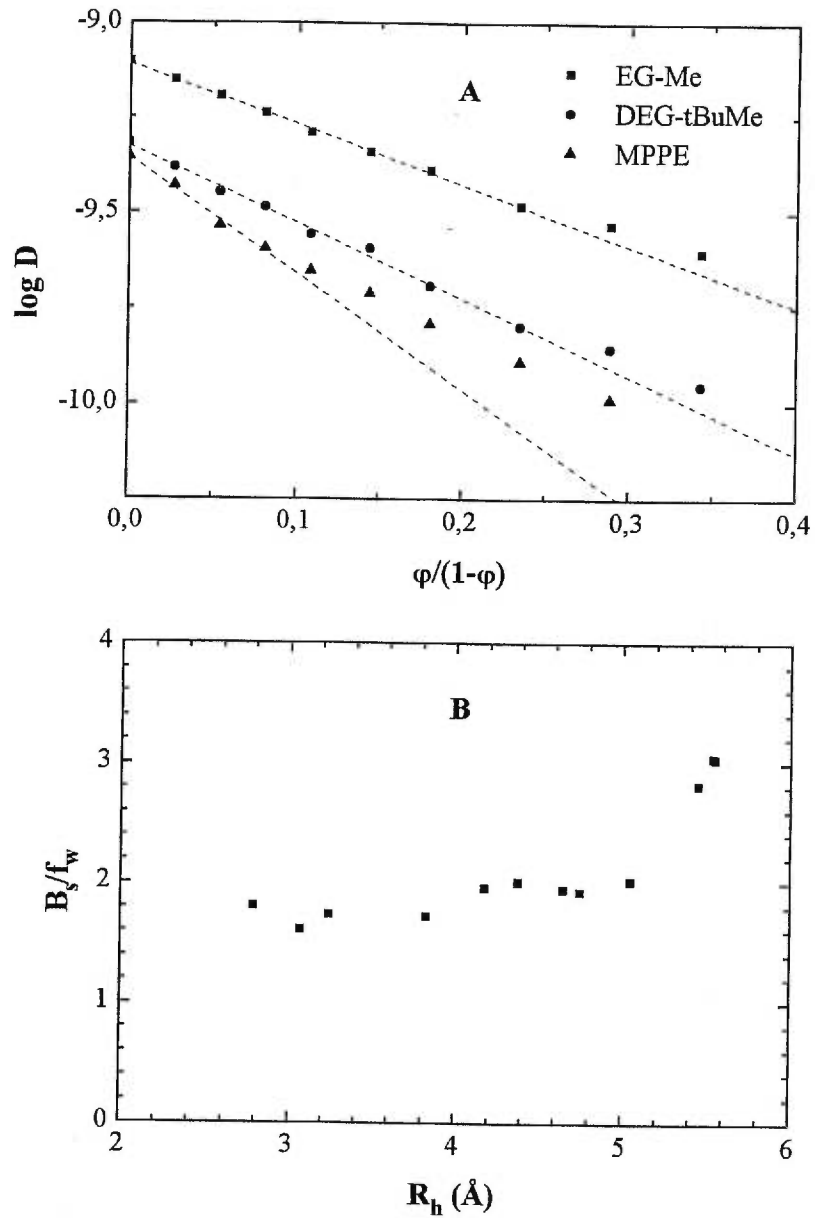


Figure 5.6. (A) Plot of the logarithmic self-diffusion coefficient of selected diffusants as a function of $\phi/(1-\phi)$ at 25 °C, (B) plot of the parameter B_s/f_w as a function of the hydrodynamic radius of the diffusants. Dashed lines are fits to eq 5.5.

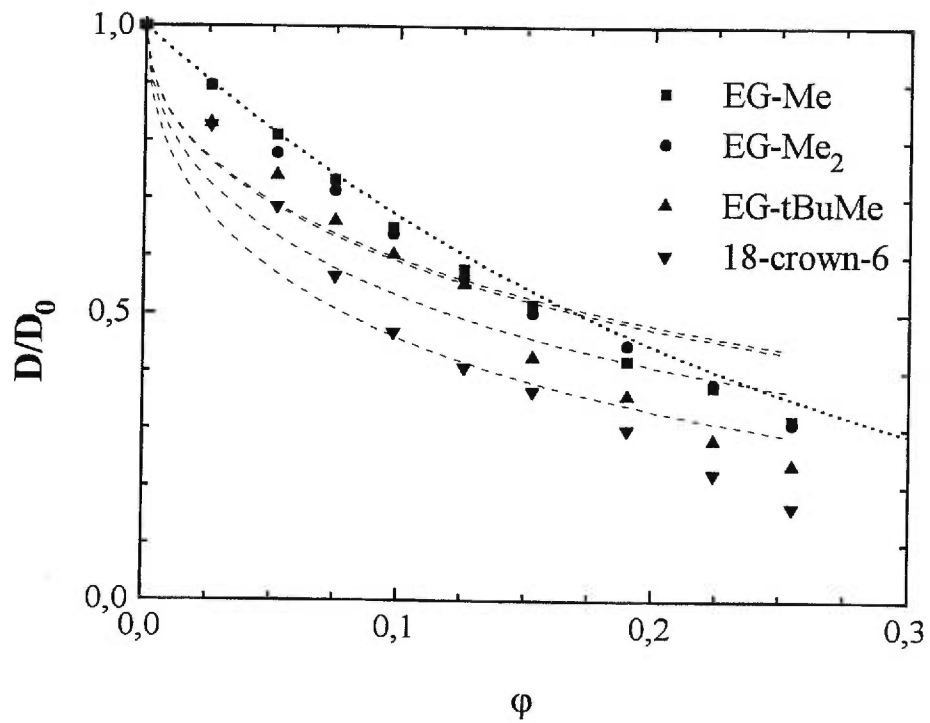


Figure 5.7. Plot of the normalized self-diffusion coefficient of selected diffusants as a function of the volume fraction of PVA at 25 °C. Dotted line and dashed lines are fits to eq 5.6 and eq 5.7, respectively.

5.4.6. The model of Amsden [34]

This diffusion model combines the free volume theory with the obstruction and scaling concepts. It takes into account several structural properties of the polymer such as the polymer chain stiffness, the chain radius, the volume fraction as well as the size of the diffusant [34]. The motion of a molecule through a hydrogel matrix depends on the probability of finding holes larger than the diffusant diameter. The distribution of the holes is described by the expression given by Ogston *et al.* [24]. Amsden evaluated the distance between polymer chains with the help of scaling concepts, and the following equation was given

$$\frac{D}{D_0} = \exp \left[-\pi \left(\frac{r_s + r_f}{r_f} \right)^2 \frac{\phi}{(k_1 + 2\phi^{1/2})^2} \right] \quad (5.8)$$

where r_s and r_f are the same as in eq 5.7, and k_1 a constant for a given polymer-solvent system.

The normalized self-diffusion coefficient D/D_0 of selected diffusants is plotted as a function of the volume fraction of the PVA in Figure 5.8. Dashed lines are fits to eq 5.8 with floating parameters, including r_s , r_f and k_1 . Eq 5.8 provides relatively good fits to the data. Similar results are observed with the other diffusants. The fits provided values of r_s of 3.99, 5.42, 3.02, 284.0 and values of r_f of 0.033, 0.050, 0.031, 2.29 for EG-Me₂, EG-tBuMe, and 18-crown-6, respectively, which does not seem to be coherent. Therefore, we have fixed r_s to the R_h values listed in Table 5.2 during the fittings, but systematically lower values of r_f were obtained for each diffusant, while k_1 was found negative as shown in Table 5.4. The various r_f values obtained can be hardly related to the hydrodynamic radius of the polymer chain. The physical significance of k_1 remains unclear.

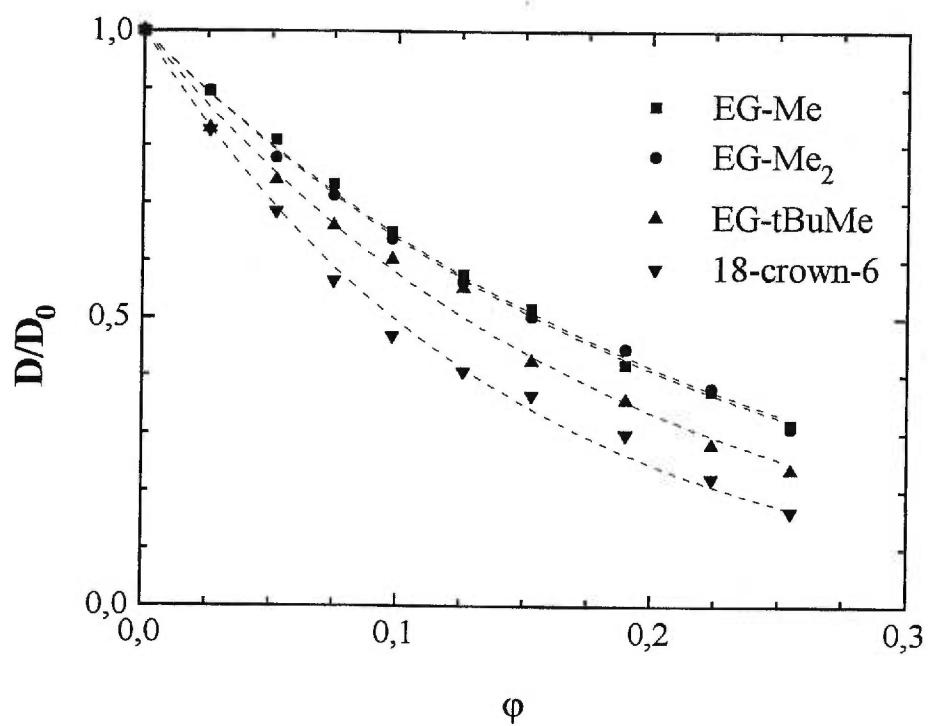


Figure 5.8. Plot of the normalized self-diffusion coefficient of selected diffusants as a function of the volume fraction of PVA at 25 °C. Dashed lines are fits to eq 5.8.

Table 5.4. The parameters D_0 , r_f and k_1 obtained by fitting the diffusion data to eq 5.8 while fixing r_s to the R_h values reported in Table 5.2.

Diffusant	$D_0 \times 10^{-10}$ (m ² /s)	r_f (Å)	k_1	χ^2
EG	8.56	0.404	-7.14	0.015
EG-Me	7.93	0.051	-51.68	0.013
EG-Me ₂	7.53	0.019	-137.95	0.013
EG-tBuMe	5.46	0.264	-14.35	0.007
DEG-Me	6.32	0.160	-21.00	0.009
DEG-Et	5.77	0.225	-16.26	0.006
DEG-He	4.39	0.017	-217.67	0.008
DEG-tBuMe	4.77	0.269	-15.73	0.007
TEG-Me	5.20	0.020	-178.82	0.004
TEG-Me ₂	5.09	0.026	-144.53	0.007
MPPE	4.30	0.010	-196.17	0.004
18-crown-6	4.31	0.019	-367.43	0.005

5.5 Conclusion

This study confirms that the self-diffusion coefficient depends on the size and geometry of the diffusant, evidenced by the effect of bulky end groups. Diffusants with a bulkier end group diffuse less rapidly than those with a smaller linear end group even though the molecular weights of the molecules are comparable. A hydrophobic hexyl group also restrains the diffusion more than the shorter alkyl groups.

The diffusion model of Mackie-Mearns is strictly limited to very small diffusants since it does not take into account the differences of the diffusants. The diffusion model of Ogston *et al.* improved in this regard, but still deviates significantly from the experimental data. The model of Amsden solved this problem by combining

this obstruction model with other concepts such as the free volume concept, but the numerical values of the parameters are inconsistent with their original physical significance. The free volume model of Yasuda *et al.* is limited to the diffusion of small-sized diffusants and in dilute polymer solutions. The experimental data for this group of relatively small diffusants all fitted very well to the diffusion model of Phillies. The parameter α was found to increase as a function of the hydrodynamic radius of the diffusants, while a slight decrease is observed for the parameter ν .

The model of Petit *et al.* was used successfully in the fitting of the experimental data of all the diffusants over the entire range of polymer concentrations. As predicted, the parameter ν was found related to the solvent quality and remained a constant for the PVA-water system. The parameter $k\beta^2$ reflects the jump frequency of the diffusants and was found to decrease with increasing size of the diffusing molecules. By comparing these parameters with those obtained for oligo- and poly(ethylene glycol) diffusants, we are able to confirm the usefulness of this model in the analysis of both small and large diffusants in the PVA-water systems.

5.6 Acknowledgment

The financial support from the Natural Sciences and Engineering Research Council (NSERC) of Canada and the Quebec Government (Fonds FCAR) is gratefully acknowledged.

5.7. References and Notes

- [1] Zhu, X.X.; Macdonald, P.M. *Macromolecules* **1992**, *25*, 4345.
- [2] Zhu, X.X.; Wang, F.; Nivaggioli, T.; Winnik, M.A.; Macdonald, P.M. *Macromolecules* **1993**, *26*, 6397.
- [3] Wisnudel, M.B.; Torkelson, J.M. *Macromolecules* **1996**, *29*, 6193.
- [4] Waggoner, R.A.; Blum, F.D.; MacElroy, J.M.D. *Macromolecules* **1993**, *26*, 6841.
- [5] Pickup, S.; Blum, F.D. *Macromolecules* **1989**, *22*, 3961
- [6] Zielinski, J.M.; Duda, J.L. *AIChE J.* **1992**, *38*, 405.

- [7] Faldi, A.; Tirrell, M.; Lodge, T.P. *Macromolecules* **1994**, *27*, 4176.
- [8] Faldi, A.; Tirrell, M.; Lodge, T.P.; von Meerwall, E.D. *Macromolecules* **1994**, *27*, 4184.
- [9] Bandis, A.; Inglefield, P. T.; Jones, A. A.; Wen, W.-Y. *J. Polym. Sci., Polym Phys. Ed.* **1995**, *33*, 1495.
- [10] Lodge, T.P.; Lee, J. A.; Frick, T. S. *J. Polym. Sci., Polym Phys. Ed.* **1990**, *28*, 2607.
- [11] Duda, J.L. *Pure Appl. Chem.* **1985**, *57*, 1681.
- [12] Gao, P.; Fagerness, P.E. *Pharm. Res.* **1995**, *12*, 955.
- [13] Sakai, K. *J. Membr. Sci.* **1994**, *96*, 91.
- [14] Dvoyashkin, N.K.; Maklakov, A.I. *Colloid J.* **1996**, *58*, 595.
- [15] Krause, C.; Klain, S.; Kärger, J.; Maeir, W.F. *Adv. Materials* **1996**, *8*, 912.
- [16] Lee, J.; Park, K.; Chang, T.; Jung, J.C. *Macromolecules* **1992**, *25*, 6977.
- [17] Park, H.S.; Sung, J.; Chang, T. *Macromolecules* **1996**, *29*, 3216.
- [18] Callaghan, P.T. *Aust. J. Phys.* **1984**, *37*, 359.
- [19] Price, W.S. *Concepts Magn. Reson.* **1997**, *9*, 299.
- [20] Wheeler, L.M.; Lodge, T.P. *Macromolecules* **1989**, *22*, 3399.
- [21] Lodge, T.P.; Markland, P.; Wheeler, L.M. *Macromolecules* **1989**, *22*, 3409.
- [22] Petit, J.-M.; Zhu, X.X.; Macdonald, P.M. *Macromolecules* **1996**, *29*, 70.
- [23] Mackie, J.S.; Meares, P. *Proc. R. Soc. Lond., A* **1955**, 232,498.
- [24] Ogston, A.G.; Preston, B.N.; Wells, J.D. *Proc. R. Soc. Lond., A* **1973**, 333, 297.
- [25] Cukier, R.I. *Macromolecules* **1984**, *17*, 252.
- [26] Altenberger, A.R.; Tirrell, M. *J. Chem. Phys.* **1984**, *80*, 2208.
- [27] Phillis, G.D.J. *Macromolecules* **1986**, *19*, 2367.
- [28] Fujita, H. *Adv. Polym. Sci.* **1961**, *3*, 1.
- [29] Yasuda, H.; Lamaze, C.E.; Ikenberry, L.D. *Makromol. Chem.* **1968**, *118*, 19.
- [30] Vrentas, J.S.; Duda, J.L. *J. Polym. Sci., Polym. Phys. Ed.* **1977**, *15*, 403.
- [31] Vrentas, J.S.; Duda, J.L. *J. Polym. Sci., Polym. Phys. Ed.* **1977**, *15*, 417.
- [32] Peppas, N. A.; Reinhart, C. T., *J. Membr. Sci.* **1983**, *15*, 275.

- [33] Brady, J. *AIChE Ann. Meet.* **1994**, 320.
- [34] Amsden, B. *Polym. Gels Networks* **1998**, *6*, 13.
- [35] Petit, J.-M.; Roux, B.; Zhu, X.X.; Macdonald, P.M. *Macromolecules* **1996**, *29*, 6031.
- [36] Masaro, L.; Zhu, X.X.; Macdonald, P.M. *Macromolecules* **1998**, *31*, 3880.
- [37] Masaro, L.; Zhu, X.X. *Langmuir* **1999**, submitted.
- [38] Stejskal, E.O.; Tanner, J.E. *J. Chem. Phys.* **1965**, *42*, 288.
- [39] Masaro, L.; Zhu, X.X. *Can. J. Anal. Sci. Spectro.* **1998**, *43*, 81.
- [40] Phillies, G.D.J. *J. Phys. Chem.* **1989**, *93*, 5029.
- [41] Phillies, G.D.J. *Macromolecules* **1988**, *21*, 3101.
- [42] Phillies, G.D.J. *Macromolecules* **1987**, *20*, 558.
- [43] Furukawa, R.; Arauz-Lara, J.L. Ware, B. R. *Macromolecules* **1991**, *24*, 599.
- [44] Park, H.S.; Sung, J.; Chang, T. *Macromolecules* **1996**, *29*, 3216.
- [45] Phillies, G.D.J.; Richardson, C.; Quinlan, C.A.; Ren, S.Z. *Macromolecules* **1993**, *26*, 6849.
- [46] Mustafa, M.; Tipton, D.L.; Barkley, M.D.; Russo, P.S.; Blum, F.D. *Macromolecules* **1993**, *26*, 370.
- [47] Park, I.H.; Johnson Jr., C.S.; Gabriel, D.A. *Macromolecules* **1990**, *23*, 158.
- [48] Gibbs, S.J.; Johnson Jr., C.S. *Macromolecules* **1991**, *24*, 6110.
- [49] Hennink, W. E.; Talsma, H.; Borchert, J. C. H.; De Smedt, S. C.; Demeester, J. *J. Contr. Release* **1996**, *39*, 47.

Partie IV

L'influence du réseau polymère sur la diffusion

Chapitre 6

Self-Diffusion Studies of Water and Poly- (ethylene glycol) in Solutions and Gels of Selected Hydrophilic Polymers

Masaro, L.; Ousalem, M.; Baille, W.E.; Lessard, D. and Zhu, X.X.

Macromolecules, 1999, accepté

6.1. Abstract

To test the effect of the matrix polymer on diffusion, we have measured the self-diffusion coefficients of water and poly(ethylene glycol) of a molecular weight of 600 (PEG-600) in aqueous systems of selected polymers using the pulsed-gradient spin-echo NMR technique. The polymers used in this study include poly(vinyl alcohol) (PVA), hydroxypropyl methyl cellulose (HPMC), poly(*N,N*-diethylacrylamide) (PNNDEA), and poly(*N*-isopropylacrylamide) (PNIPA). The polymer concentrations varied from 0 to 0.38 g/mL. The effect of the polymer network on the self-diffusion coefficients of the solvent (water) and a solute (PEG-600) was investigated by analyzing the diffusion data with the use of the free volume model of Yasuda *et al.* [Yasuda, H.; Lamaze, C.E.; Ikenberry, L.D. *Makromol. Chem.* **1968**, *118*, 19], the diffusion model proposed by Phillis [Phillis, G.D.J. *Macromolecules* **1986**, *19*, 2367], and the model of Petit *et al.* [Petit, J.-M.; Roux, B.; Zhu, X.X.; Macdonald, P.M. *Macromolecules* **1996**, *29*, 6031]. The results obtained with PVA, HPMC, PNNDEA, and PNIPA are used to evaluate the applicability of these models in polymer-water-solute ternary systems. The physical significance of the parameters used in the models is discussed.

6.2. Introduction

The study of the diffusion of solvents and solutes in polymer solutions and gels has attracted much research interest because of its importance related to the use of polymer materials. For example, diffusion studies can be used to obtain information on the mixing of polymers [1], the diffusion of a plasticizer in a polyelectrolyte [2], the characterization of polymer microstructures [3,4], intermolecular interactions [5], and more recently the controlled release of drugs in biomedical and pharmaceutical applications of polymers [6]. The polymer carriers used for the controlled release of drugs are usually hydrophilic and can swell in water. They include poly(vinyl alcohol) (PVA) and hydroxypropyl methyl cellulose (HPMC) [7]. PVA is also used in many other applications [8], and the degree of hydrolysis of the acetic groups of poly(vinyl acetate) determines the solubility of PVA in water [9]. Recently, the use of thermosensitive polymers in biomedical fields has also been studied [10].

We have already studied the self-diffusion of diffusants of various sizes in PVA aqueous solutions and gels [11–13]. In the study of self-diffusion of solutes probes with different functional groups (alcohol, amine, ammonium salt, amide, acid) in PVA solutions and gels, we found that the diffusion behavior is primarily influenced by the size of the diffusant and secondarily by the chemical functions [11]. The self-diffusion of a series of linear oligo- and poly(ethylene glycol)s in PVA solutions and gels was also studied [13]. It was found that the molecular size of the diffusant plays the most important part in the diffusion process [11, 13]. In the present study, we would like to examine the effect of different polymer matrices on the diffusion of the solvent, water, and a solute, poly(ethylene glycol) (PEG), in different ternary polymer-water-PEG systems. The polymers used include PVA, HPMC, poly(*N,N*-diethyl acrylamide) (PNNDEA), and poly(*N*-isopropyl acrylamide) (PNIPA). PVAs with various molecular weights and degrees of hydrolysis were selected in order to investigate the effect of the chain length and structure of the matrix polymer on the self-diffusion of the solvent and the solute. For a better understanding of the diffusion in polymers, we have used the pertinent physical models of diffusion in the analysis of the experimental data obtained.

6.3. Theoretical background

A number of physical models of diffusion have been proposed [14–26]. They are based on different physical concepts, such as the obstruction effect, the hydrodynamic interactions and the free volume concept in polymers. Recently, Amsden [27] reviewed some of these models and indicated their usefulness and limitations (*voir également le Chapitre 1*).

In the diffusion models based on the obstruction effect, the polymer chains are considered as motionless and impenetrable objects that increase the root-mean-square displacement of the diffusants. These models usually work well in the treatment of self-diffusion data of small diffusants, but not for those of large diffusants [11,17,19,27–29]

The free volume theory considers the diffusion process as a succession of jumps in voids created by the thermal motion of the species present in solution [22].

In a binary system (solvent-polymer), or in a ternary system (solvent-polymer-solute) where the solute is present in low concentration, the contribution to the free volume is mainly from the solvent. The diffusion of all the species in the system would slow down with increasing polymer concentration. The free volume model of Fujita [22] does not apply to aqueous systems and the model of Vrentas-Duda [25,26] is difficult to be used in ternary systems because of the numerous physical parameters needed. The model of Yasuda *et al.* [23], however, can be used to describe diffusion in aqueous systems

$$D = D_0 \exp\left[\frac{B_s}{f_w} \left(1 - \frac{1}{1-\phi}\right)\right] \quad (6.1)$$

where D is the self-diffusion coefficient of the solute, D_0 the self-diffusion coefficient of the solute in the same solvent but in the absence of the polymer, B_s is the minimum hole size required for diffusant displacement, f_w is the free volume of the solvent in the polymer-water system, and ϕ the volume fraction of the matrix polymer.

The hydrodynamic models take into account the interactions between the solvent and the polymer [17]. Among them, the model proposed by Phillies [30] is often used since it provides generally good fits to the experimental data. This model was proposed to describe the self-diffusion of one macromolecule (polymers and proteins) in another over a wide range of concentrations [30]. The polymer chains are considered mobile and can be described by spheres joined by rods that can rotate as defined by Kirkwood [31]. The stretched exponential equation proposed by Phillies is written as

$$D = D_0 \exp(-\alpha c^\nu) \quad (6.2)$$

where c is the polymer concentration, α and ν are the scaling parameters. Phillies also developed theoretical arguments for eq 6.2 [32,33] and provided physical interpretations of the parameters α and ν . According to Phillies, α depends strongly on the molecular weight ($\alpha \sim M^{0.9 \pm 0.1}$) for macromolecular diffusants, whereas it depends on the hydrodynamic radius ($\alpha \sim R_h/a_0$, where a_0 is defined as the distance of closest approach) for smaller diffusants [32–35]. Park *et al.* [36] and Gibbs and Johnsson [37] reported empirical relationships of $\alpha = 3.03 \times R_h^{0.59}$ and $\alpha = 3.2 \times R_h^{0.53}$, respectively. The parameter ν

should scale between 1 for low molecular weight diffusants and 0.5 for high molecular weight diffusants and inside these limits it scales according to $\nu \sim M^{-1/4}$ [34]. Eq 6.2 can provide good fits to the experimental data in many polymer systems [30,32–34]. However, disagreements still remain on the dependence and physical meaning of the parameters [38,39].

The diffusion model of Petit *et al.* [12] was elaborated in the treatment of the diffusion data of molecules with various sizes and functional groups in ternary PVA-aqueous-solute systems and binary poly(methyl methacrylate)-organic solvent systems [12,13,40]. The diffusion is considered to be a succession of jumps of the diffusant from one cavity to another in the polymer matrix. The following equation was given to describe the self-diffusion coefficient

$$D = \frac{D_0}{1 + ac^{2\nu}} \quad (6.3)$$

where $a = D_0/k\beta^2$, and $k\beta^2$ and ν are the parameters of the model. The parameter ν depends on the quality of the solvent and should be a constant for a given system. β should be a constant and independent of the concentration or molecular weight of the matrix [12]. k is the jump frequency, which varies with the molecular weight or size of the diffusant, temperature as well as the concentration of the matrix polymer. However, k is considered as a constant within a certain polymer concentration range, even though the polymer concentration influences the size of the cavity [12]. In the treatment of the diffusion data of both small and macromolecular probes, the parameters of the model were determined [13]. The parameter ν , which depends on the solvent quality, was found to be a constant equal to 0.58 for the PVA-water system. $k\beta^2$ was found to depend on the hydrodynamic radius (R_h) of the diffusant [13].

6.4. Experimental section

6.4.1. Materials

PEG with a molecular weight of 600 (PEG-600), PVA and HPMC (see Table 6.1 for more details) as well as *N*-isopropylacrylamide, 2,2'-azobis(isobutyronitrile) (AIBN)

and sodium thiocyanate (NaSCN) used in this study were purchased from Aldrich (Milwaukee, WI). D₂O was purchased from C.I.L. (Andover, MA). PNNDEA and PNIPA were synthesized in this laboratory.

6.4.2. Synthesis of polymers [41].

The monomer *N,N*-diethylacrylamide was synthesized by reacting acryloyl chloride with diethylamine in dichloromethane in an ice bath under a flow of dry nitrogen. After the removal of diethylammonium chloride salt and the evaporation of the solvent, the product was purified by vacuum distillation (b.p. 30–35 °C at 0.01 mm of Hg). *N,N*-diethylacrylamide was then polymerized in toluene with AIBN as the initiator. The starting temperature at 40 °C was gradually raised to 70 °C during one hour and maintained for *ca.* 3 hours. After removing toluene on a rotary evaporator, poly(*N,N*-diethylacrylamide) was re-dissolved in acetone, precipitated by adding hexane and dried. Poly(*N*-isopropylacrylamide) was synthesized similarly [41].

6.4.3. Molecular weight determination.

Size exclusion chromatography (SEC) was carried out on a Waters 600 controller system equipped with a Waters 410 differential refractometer and two Ultrahydrogel columns of nominal porosity of 10 and 6 μm (Ultrahydrogel 500 and 120), respectively. Poly(ethylene glycol)s and poly(ethylene oxide) (PEO) standards (Polymer Standards Service-USA, Inc., MD) were used for the calibration. The polymers were solubilized in deionized water (Milli-Q), and sodium thiocyanate was added in a salt/polymer mass ratio of 1.5 to 1 to avoid the aggregation of the polymers [8]. The polymer solutions (5 mg/mL) were filtered through 0.45-μm filters (Sarstedt, NJ) before injection. The flow rate of the eluent was at 0.6 mL/min. The columns and detector were equilibrated at 32 °C and 35 °C, respectively.

For light scattering measurements, sets of five concentrations (0.3–3 wt %) were obtained by dilution of the stock solutions (3 wt %) containing 0.5 M of NaSCN. The dilute solutions were filtered five times through 0.2-μm Anotop 25 filters (Whatman, NJ) directly in scintillation vials, which were previously treated with

sulfochromic acid and washed thoroughly with distilled water and methanol to prevent spurious scatterers in the solutions. Static light scattering measurements were performed on Dawn-B instrument (Wyatt Technology Corp., Santa Barbara, CA) [42] with a helium-neon laser operating at 632.8 nm at room temperature. An incremental refractive index of 0.159 mL/g was used. The weight-average molecular weights of our samples were derived by the Zimm double extrapolation method using the Aurora routine [43,44].

6.4.4. Pulsed-gradient spin-echo (PGSE) NMR measurements

The samples were prepared as described previously [11–13]. The measurements of the self-diffusion coefficients were carried out on a Bruker Avance AMX-300 NMR spectrometer operating at 300,13 MHz for protons. The temperature was set at 25 °C. The PGSE pulse sequence developed by Stejskal and Tanner [45] was used. A Bruker magnetic resonance imaging probe (Micro 2.5 Probe) coupled with a gradient amplifier (BAFPA-40) was used. Gradient pulses were applied only in the z-direction. The gradient strength was calibrated by doing one-dimensional imaging experiment along the axis, using a solution of doped water (with CuSO₄) in a 10-mm NMR tube in which a well-defined object was contained. The NMR image profile was compared to the dimension of the object. The daily calibration was accomplished with a sample of known self-diffusion coefficient such as 1 vol % HDO in D₂O ($D_{\text{HDO}} = 1.9 \times 10^{-9} \text{ m}^2/\text{s}$) [46]. The gradient strengths, G , used in this study ranged between 0.1 and 1 T/m. The other parameters were kept constant and their values are those noted in the parentheses depending on the experiments: δ (1-5 ms), Δ (40-150 ms), recycle delay (15-60 s), number of acquisitions (1-16), 90° pulse (23-29 μs), spectral width (3-8 kHz), line broadening (5-10 Hz).

6.5. Results and discussion

6.5.1. Characterization of the polymers

The polymers (PVA, HPMC, PNNDEA, and PNIPA) used as the matrix were analyzed by SEC and light scattering experiments to determine their molecular weights and polydispersity and the results are listed in Table 6.1.

The first SEC experiments were carried out three days after sample preparation, which corresponds to the same delay for the PGSE NMR measurements. SEC measurements of PVA and HPMC can be significantly affected by the formation of aggregates in water. The aggregation of PVA in solutions and gels is due to inter- and intramolecular hydrogen-bonding [9]. In fact, the PVA aggregates appear as separated peaks corresponding to higher molar masses on the chromatograms (Figure 6.1). In the case of PVA-1, no such aggregation was observed for the freshly prepared solution. The same solutions were injected four days later, the peaks of the aggregated PVAs became more intense (Figure 6.1), and the aggregation for PVA-1 also became apparent. Therefore, the aggregation of PVA is time dependent and is affected by the degree of hydrolysis of PVA. PVA-1 has the lowest molecular weight and lowest degree of hydrolysis among all the PVA samples. Stephans and Foster [9] showed by magnetization-transfer NMR technique that completely hydrolyzed PVA chains form a gel more rapidly than PVA with a lower degree of hydrolysis, which seems to confirm the difference between PVA-1 and other PVAs observed in this study. To overcome this problem, we have prepared polymer solutions with NaSCN [8]. Addition of the salt prevented the aggregation as shown in Figure 6.1A. The molecular weights reported in Table 6.1 are obtained from SEC measurements with added NaSCN. Very broad peaks were observed with HPMCs as a result of aggregation, but the addition of sodium thiocyanate did not change the appearance of the peaks.

The aggregation of PVAs and HPMCs in water caused saturation of the detectors in the light scattering experiments. The weight-average molecular weights of PVAs were determined with PVA solutions in water in the presence of NaSCN, and the results are reported in Table 6.1. These values are mostly comparable with those determined by SEC. Due to the presence of aggregates, light scattering measurements of HPMC solutions were not possible even after the addition of NaSCN.

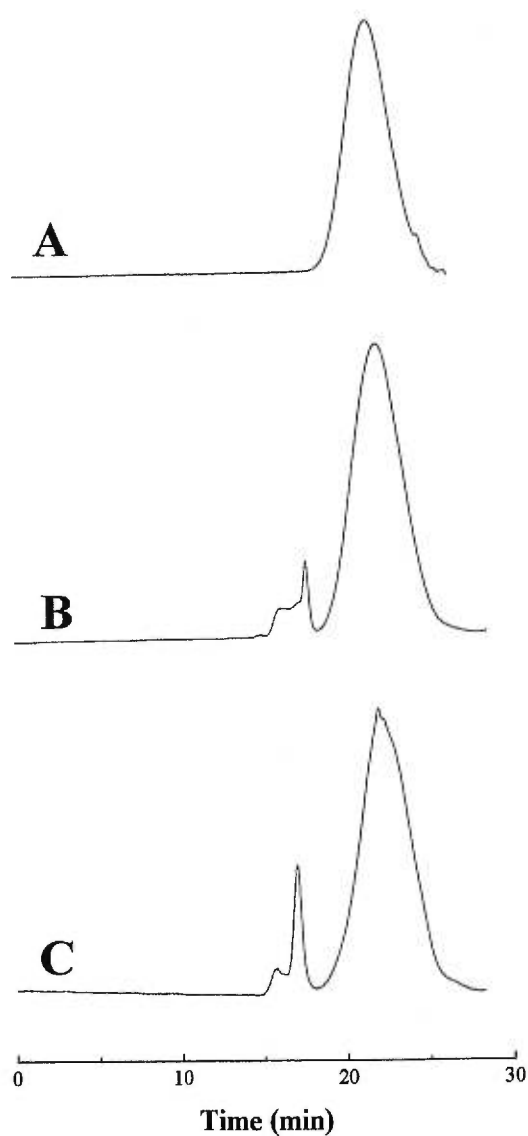


Figure 6.1. Size exclusion chromatograms obtained for PVA-4 (A) dissolved in an aqueous solution of NaSCN (salt/polymer weight ratio = 1.5:1), (B) dissolved in water and injected three days after preparation, and (C) the same water solution as B but injected after seven days. Chromatogram A shows that the salt NaSCN can prevent the aggregation of PVA. Comparison of chromatograms B and C indicates that the aggregation of PVA is time dependent.

Table 6.1. The physical characteristics of the polymers used.

Sample	Degree of Hydrolysis ^(a) (%)	M _w ^(b) (10 ³ g/mol)	M _w /M _n ^(b)	M _w ^(c) (10 ³ g/mol)
PVA-1	80	8.4	1.42	18 ± 1
PVA-2	88	15.4	1.76	21 ± 1
PVA-3	99	20.3	1.63	17 ± 2
PVA-4	99	52.8	2.09	52 ± 4
PVA-5	88	124.7	2.46	130 ± 9
PVA-6	99	131.5	2.26	136 ± 9
HPMC-1	—	10.7	4.14	—
HPMC-2	—	231.0	2.98	—
PNIPA	—	105.0	2.95	—
PNNDEA	—	69.8	3.13	—

(a) given by the supplier (Aldrich)

(b) determined by SEC

(c) determined by static light scattering

6.5.2. Analysis of the diffusion data with the model of Yasuda *et al.*

Eq 6.1 can be rewritten as

$$\ln D = \ln D_0 - \frac{B_f}{f_w} \left(\frac{\phi}{1-\phi} \right) \quad (6.4)$$

Therefore, the free volume parameters can be obtained by linear regression of the data. The logarithms of the self-diffusion coefficients of water and PEG-600 are plotted as a function of $\phi/(1-\phi)$ as shown in Figure 6.2 for PVA-2. The dashed lines are fits to the linear parts of the data to eq 6.4. The fitting parameters are listed in Table 6.2. For small molecules, such as water, a very good fit can be obtained. For larger molecules such

as PEG-600 the linearity over the entire range is rather poor. Petit *et al.* [11] observed a gradual deterioration of the fits with increasing diffusant size. The same observation can be made here which illustrates the limitation of the model. Similar results and limitations were obtained for the diffusion of water and PEG-600 in the other hydrophilic polymers (PVA, HPMC, PNNDEA and PNIPA). The deviations at higher polymer volume fractions are due to the approximation that the total free volume of the system is only contributed by the solvent (water), i.e., $f_{total} = f_w$ [23]. This approximation is no longer valid in concentrated polymer systems where the free volume contribution from the polymer is no longer negligible. We have attempted to fit the diffusion data of PEG-600 only for the low polymer concentrations as shown in Figure 6.2.

The measured D_0 values for PEG-600 and water are 2.56×10^{-10} and 1.73×10^{-9} m²/s, respectively. We tried to use D_0 and B_s/f_w all as free parameters in the fitting to eq 6.4. The D_0 values obtained for PEG-600 and water from the fittings are systematically lower than the measured D_0 values in all the polymer matrices studied here (Table 6.2). The parameter B_s/f_w obtained for PEG-600 is more or less a constant for a given polymer system. Average values of 6.59, 7.87 and 5.64 were found for PVA, HPMC and PNNDEA-PNIPA, respectively. When the diffusant (only 1 wt % solution in water) does not affect the properties of the solvent, f_w should remain constant. Consequently, the variation of the parameter B_s/f_w should reflect the variation of the minimum hole size required for diffusant displacement, B_s . The average value obtained for B_s/f_w increases from PNNDEA-PNIPA to PVA and HPMC. This suggests that the minimum hole size required for diffusant displacement increases with the ease of formation of hydrogen bonds in the polymer matrix. The values of B_s/f_w obtained for water are similar for all polymer systems, which indicates that the minimum hole size required for solvent displacement remains a constant. This is logical and agrees with the results of Gao and Fagerness [6] who studied water self-diffusion in HPMC solutions and gels. They reported that the degree of polymerization of the polymer matrix does not affect the diffusion of the solvent [6]. We have also fitted the experimental data after fixing D_0 to the experimental value. In this case, the B_s/f_w values are generally higher.

Table 6.2. D_0 and B_s/f_w as free parameters obtained from fits to eq 6.4 with the experimental diffusion data obtained for PVA, HPMC, PNNDEA and PNIPA aqueous systems.

Polymer	Parameters for PEG-600		Parameters for water	
	$D_0 \times 10^{10}$ (m ² /s)	B_s/f_w	$D_0 \times 10^9$ (m ² /s)	B_s/f_w
PVA-1	2.49	6.81	1.69	2.66
PVA-2	2.46	6.48	1.64	2.50
PVA-3	2.48	6.48	1.63	2.88
PVA-4	2.40	6.76	1.65	2.42
PVA-5	2.43	6.49	1.66	2.59
PVA-6	2.42	6.55	1.64	2.52
HPMC-1	2.42	7.53	1.63	2.29
HPMC-2	2.43	8.21	1.62	3.02
PNNDEA	2.50	5.21	1.70	2.31
PNIPA	2.52	6.08	1.64	2.78

6.5.3. Analysis of the diffusion data with the model of Phillies.

Figure 6.3 shows the self-diffusion coefficient of water and PEG-600 plotted as a function of PVA concentration for PVA-water-PEG ternary systems. Good agreement is observed between the fits to eq 6.2 and the experimental data for both water and PEG-600 over the entire range of polymer concentrations. Very good agreements are also obtained for the other hydrophilic polymers (HPMC, PNNDEA and PNIPA). The fitting parameters are listed in Table 6.3. Even when D_0 is allowed to vary freely in all the fittings, it remained a constant for a given diffusant in all the polymer systems.

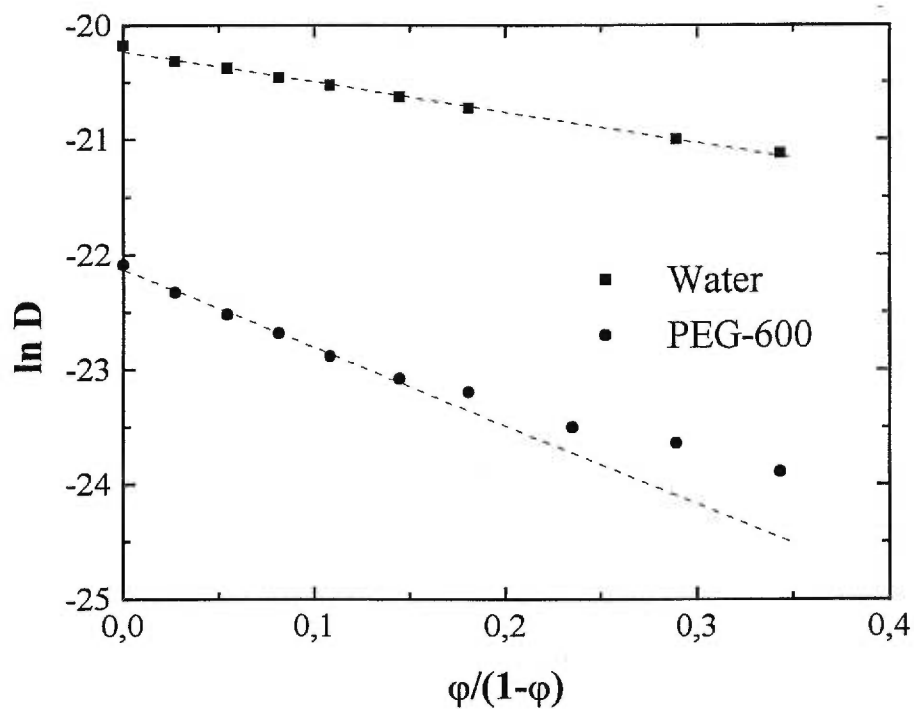


Figure 6.2. Semi-logarithmic plot of the self-diffusion coefficient of water and PEG-600 in PVA-2 as a function of $\phi/(1-\phi)$. Dashed lines are the best fits to eq 6.4. For PEG-600, the deviation from the linearity at high polymer concentrations is shown.

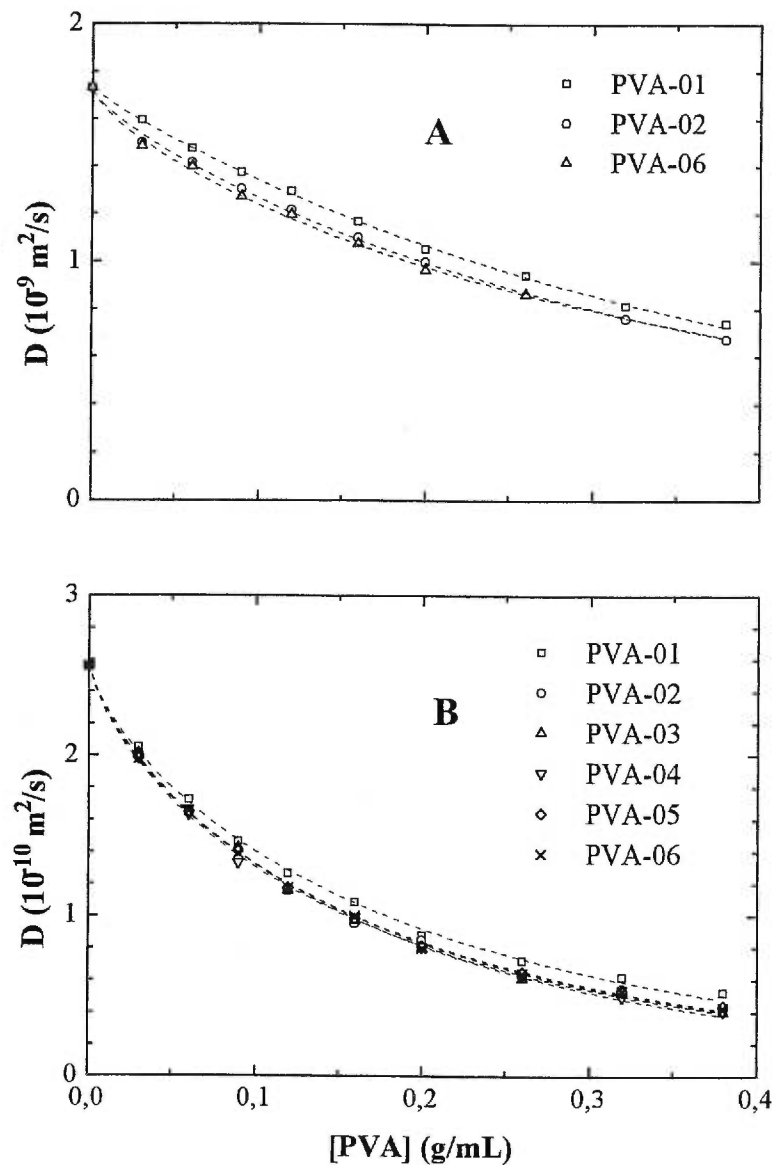


Figure 6.3. Plot of the self-diffusion coefficient of water (A) and PEG-600 (B) as a function of the PVA concentration for various PVA matrices at 25 °C. Dashed lines are fits to eq 6.2.

Table 6.3. D_0 , α and ν as free parameters obtained from fits to eq 6.2 with the experimental diffusion data obtained for PVA, HPMC, PNNDEA and PNIPA aqueous systems.

Polymer	Parameters for PEG-600			Parameters for water		
	$D_0 \times 10^{10}$ (m ² /s)	α	ν	$D_0 \times 10^9$ (m ² /s)	α	ν
PVA-1	2.57	3.51	0.76	1.73	2.10	0.91
PVA-2	2.57	3.92	0.77	1.72	2.08	0.83
PVA-3	2.57	4.13	0.79	1.73	1.82	0.78
PVA-4	2.57	3.91	0.76	1.72	2.00	0.83
PVA-5	2.57	3.80	0.76	1.73	2.00	0.85
PVA-6	2.57	3.85	0.76	1.72	2.04	0.79
HPMC-1	2.56	3.75	0.71	1.71	1.71	0.78
HPMC-2	2.56	3.96	0.71	1.72	1.93	0.72
PNNDEA	2.57	3.83	0.88	1.73	1.95	0.91
PNIPA	2.56	4.48	0.89	1.73	2.06	0.79

According to Phillies, the scaling parameter ν should scale between 0.5 for high molecular weight diffusant and 1 for low molecular weight diffusants [34]. All the ν values obtained (Table 6.3) lie between these limits. In this study, the diffusant is kept constant and the matrix is changed. The ν values obtained for PEG-600 are found to be unique for a given polymer-water system. Average values of 0.77, 0.71 and 0.89 are found for the diffusion of PEG-600 in PVA, HPMC and PNNDEA-PNIPA, respectively. Therefore, the results tend to indicate that the scaling parameter ν is a constant for a given polymer system, independent of the molecular weight of the polymer matrix. Distinct average ν values are also observed for water, *ca.* 0.83, 0.75 and 0.85 for PVA, HPMC and PNNDEA-PNIPA, respectively. Therefore, the scaling parameter ν may reflect the

quality of the solvent for a given polymer. No significant dependence on the molecular weight of the matrix polymer was observed.

The scaling parameter α is found to be more or less a constant for water and PEG-600 as shown in Table 6.3. Average α values of 3.85 and 3.86 are found for PEG-600 diffusion in PVA and HPMC, respectively. But the α values in PNNDEA and PNIPA are quite different. Average α values of 2.00, 1.82 and 2.00 are found for water diffusion in PVA, HPMC, and PNNDEA-PNIPA, respectively. The hydrodynamic radii of water and PEG-600 can be calculated from the self-diffusion coefficients with the Stokes-Einstein equation, corresponding to 13.95 Å and 1.30 Å for PEG-600 and water, respectively. With these values, the relationship of Park *et al.* [36] would give α values of 14.4 and 3.54 for PEG-600 and water, respectively, and the relationship of Gibbs and Johnson [37] would provide α values of 13.0 and 3.68 for PEG-600 and water, respectively. These α values are higher than the values obtained from the fits (Table 6.3). In a previous work [13], we have studied the self-diffusion of a series of oligo- and poly(ethylene glycol)s in PVA solutions and gels by PGSE NMR spectroscopy. The dependence of the parameter α and the molecular weight of the diffusants did not show any simple mathematical dependence. The parameter α seems to depend on the size of the diffusant but no significant dependence is observed in these hydrophilic systems.

6.5.4. Analysis of the diffusion data with the model of Petit *et al.*

Diffusion data of water and PEG-600 in PVA solutions and gels and the fits to eq 6.3 are shown in Figure 6.4. The fits for both water and PEG-600 are very good in all the PVA systems over the entire range of polymer concentrations. The fitting parameters are listed in Table 6.4. D_0 , as a free fitting parameter, remained a constant for both diffusants, close to the experimental value. The ν values obtained for PEG-600 are found to be close to the value of 0.58 as reported previously [13]. This result confirms that ν depends on the solvent quality, which should be similar for the PVA-water systems. $k\beta^2$ remains also more or less a constant for a diffusant in the PVA systems as shown in Table 6.4. This implies that the jump frequency of a given diffusant is similar for all the PVA systems used here. The ν values obtained for the solvent water as diffusant are also quite constant

(0.53) and slightly lower than the ν value for the solute (*ca.* 0.58). $k\beta^2$ remains also quite constant, but the values are much higher than those determined for PEG-600. This is reasonable since the jump frequency of water should be higher than that of PEG-600. This result is in good agreement with the prediction of the model of Petit *et al.* that considers k dependent on the molecular weight or the size of the diffusant [12,13,40].

For the PVA systems, the measured self-diffusion coefficients for a given diffusant, either water or PEG-600, are quite similar over the entire range of polymer concentrations. The diffusion data are almost superposed as shown in Figure 6.4, which indicate that the microstructures (porosity and mesh size) of the PVAs are rather similar. At a given PVA concentration, the diffusion of PEG-600 does not seem to vary to any significant extent with the molecular weight or degree of hydrolysis of PVA. However, the self-diffusion coefficients of PEG-600 are slightly but systematically higher in PVA-1 than in the other PVA solutions, indicating less obstruction in this polymer network. The PVA microstructure in water depends mainly on the intra- and intermolecular associations via hydrogen bonds, which should be related to the degree of hydrolysis of the polymer [9]. Therefore, PVA-1 may differ as a result of its lower degree of hydrolysis. This is also seen in the $k\beta^2$ values for PEG-600 which are quite constant for the PVAs, with the exception of PVA-1. A small difference is also observed for the self-diffusion coefficients of water in PVA-1 and in the other PVAs (Figure 6.4A). PVA-1 may be less hydrated than the other PVAs due to its lower degree of hydrolysis. Therefore, the solvent molecules on average are freer to diffuse in PVA-1 than in the other PVAs. The existence of several states of water in PVA solutions and gels due to interactions was often noted in the literature [47–49]. The intermolecular interactions between PVA and solvent may also depend on the microtacticity of PVA. The PVAs used in this study, however, are atactic polymers as shown in the NMR characterization of the polymer in water. The results of an example of PVAs (PVA-4) has been reported earlier [50].

Matsukawa and Ando [5] showed that PEG-4250 can form complexes with poly(acrylic acid) (PAA) through intermolecular hydrogen bonds. The self-diffusion coefficient of PEG-4250 was found to be lower in PAA gels than in PNNDEA gels. Furthermore, the authors have also studied the self-diffusion coefficient of PEG-4250

in PAA-PNNDEA copolymers. The self-diffusion coefficient of PEG-4250 in a copolymer with a PAA molar fraction higher than 0.9 is much smaller than that in a copolymer with a PAA molar fraction lower than 0.5. We have found that PVA-4 can also form complexes with diffusants such as ethylene glycol and even poly(ethylene glycol)s by hydrogen bonding. In this study, PVA-1 has a lower degree of hydrolysis (*ca.* 80 %) thus fewer hydroxyl groups. Therefore, we can assume that this polymer will form fewer intra- or intermolecular hydrogen bonds than the other PVAs used, which may explain the higher D values observed.

Table 6.4. D_0 , $k\beta^2$ and ν as free parameters obtained from fits to eq 6.3 with the experimental diffusion data obtained for PVA, HPMC, PNNDEA and PNIPA aqueous systems.

Polymer	Parameters for PEG-600			Parameters for water		
	$D_0 \times 10^{10}$ (m ² /s)	$k\beta^2 \times 10^{10}$	ν	$D_0 \times 10^9$ (m ² /s)	$k\beta^2 \times 10^{10}$	ν
PVA-1	2.54	0.228	0.56	1.72	4.30	0.58
PVA-2	2.54	0.181	0.58	1.70	4.18	0.53
PVA-3	2.54	0.166	0.60	1.72	5.07	0.50
PVA-4	2.55	0.184	0.57	1.71	4.57	0.52
PVA-5	2.54	0.194	0.56	1.72	4.55	0.53
PVA-6	2.54	0.190	0.57	1.71	4.28	0.51
HPMC-1	2.54	0.192	0.53	1.71	5.64	0.48
HPMC-2	2.55	0.197	0.51	1.72	5.04	0.44
PNNDEA	2.53	0.211	0.63	1.73	4.83	0.56
PNIPA	2.54	0.170	0.64	1.73	4.47	0.50

Figure 6.5 shows the diffusion data for water and PEG-600 in HPMC solutions and gels and the fits to eq 6.3. The fitting parameters are listed in Table 6.4. The ν values determined from the fits of PEG-600 are similar for both HPMCs with an average value of 0.52. This value is somewhat lower than the average value determined for PVAs systems, indicating that it is characteristic of the system. The $k\beta^2$ values determined from the fittings are similar to those determined for PVAs, which indicates that the diffusant PEG-600 in HPMC solutions and gels may have similar jump frequencies as in PVAs. The ν values determined from the fittings for water seem to be lower than those obtained for PVAs, whereas the $k\beta^2$ values are higher. As shown in Figure 6.5B, the D values of PEG-600 decrease with increasing polymer concentration and the data are almost superimposed for both polymers. As in the case of PVA, the molecular weight of HPMC does not have any significant effect on the diffusion of PEG-600. Recently, Gao and Fagerness studied the self-diffusion of adinazolam in HPMC gels by PGSE NMR spectroscopy [6]. They used HPMCs with different viscosity grades (i.e., different molecular weights) and also found similar D values for adinazolam in all the HPMC used.

As shown in Figure 6.5A, the self-diffusion coefficient of water decreases when the molecular weight of the matrix is increased. This indicates that the root-mean-square displacements of water molecules in the two HPMC systems are not quite the same. Water molecules experienced a larger obstruction effect in HPMC-2. The existence of different states of water in HPMC is well known [51–53] and it depends on the methoxy/hydroxypropoxy substitution ratio [54,55]. HPMCs used in this study have the same percentage of methoxy and hydroxypropoxy groups but different molecular weights. Gao *et al.* have studied the effects of HPMC/lactose ratio and of HPMC molecular weight on solute release and swelling of HPMC matrix tablets [56]. They found that drug release rates observed with low viscosity grade HPMC are greater than those observed with high viscosity grade HPMC due to inhomogeneous gel swelling. The difference in D values of water may also be due to inhomogeneous gel swelling.

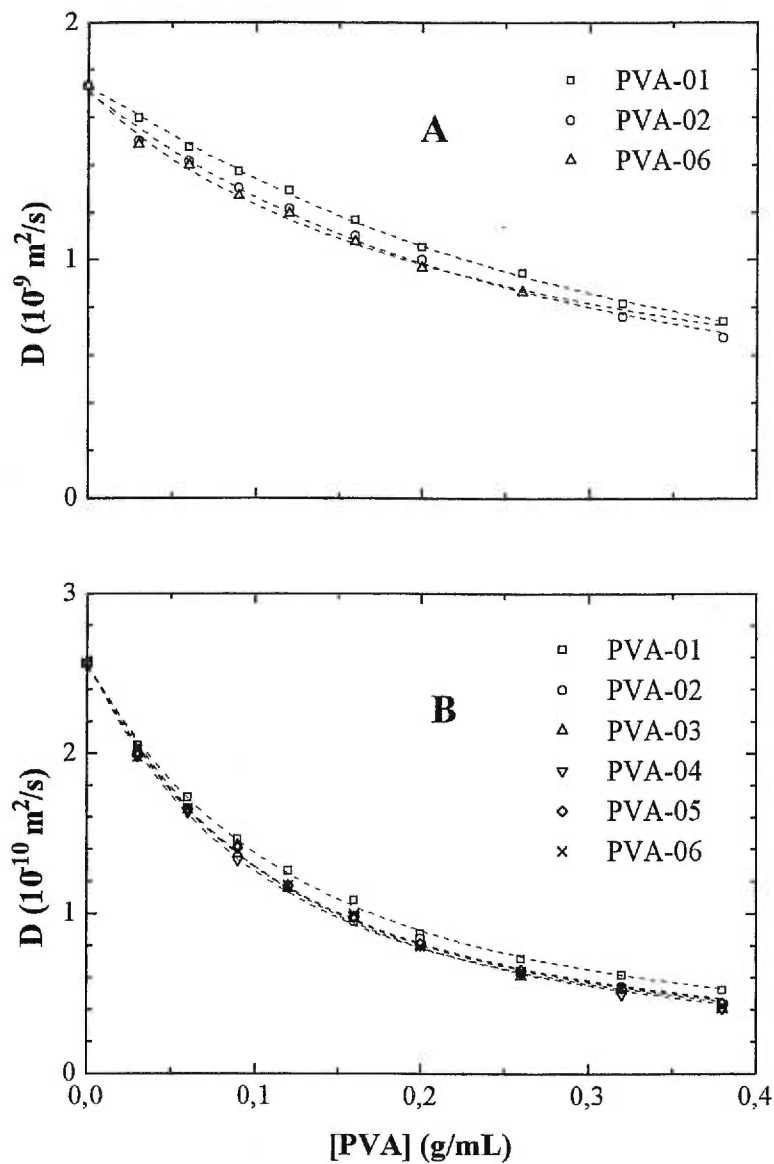


Figure 6.4. Plot of the self-diffusion coefficient of water (A) and PEG-600 (B) as a function of the PVA concentration for various PVA matrices at 25 °C. Dashed lines are fits to eq 6.3.

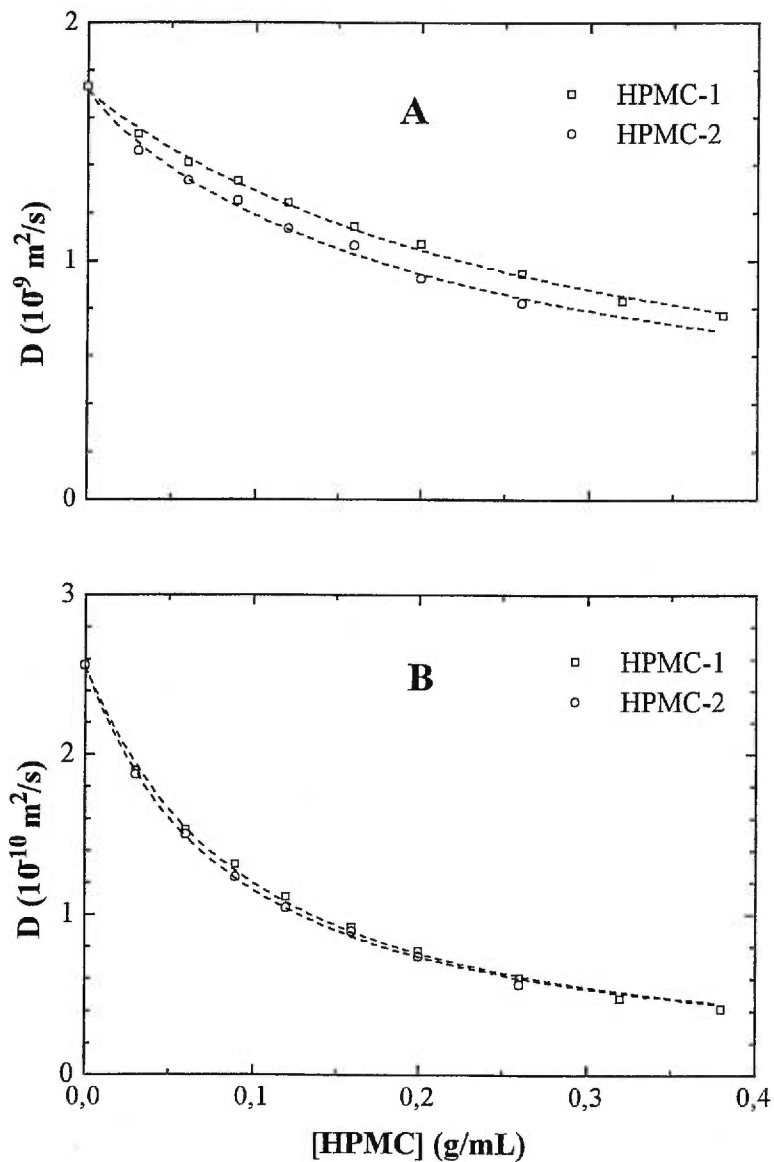


Figure 6.5. Plot of the self-diffusion coefficient of water (A) and PEG-600 (B) as a function of the HPMC concentration for the two HPMC matrices at 25 °C. Dashed lines are fits to eq 6.3.

Figure 6.6 shows the self-diffusion data of water and PEG-600 in PNNDEA and PNIPA systems. The fits of the experimental data to eq 6.3 are very good for water and PEG-600 in both polymers. Although the measured D values are different in PNIPA and PNNDEA for both water and PEG-600, the ν values obtained from the fittings of PEG-600 are very close. The average value, 0.64, is higher than the values obtained in PVAs and HPMCs. In PNIPA and PNNDEA, the formation of hydrogen bonds is not as easy as in PVAs and HPMCs. Therefore, the variations in the diffusion data should be attributed to the quality of the solvent. The $k\beta^2$ value obtained for PEG-600 in PNNDEA is higher than the $k\beta^2$ value obtained in PNIPA. This means that the jump frequency of PEG-600 is higher in PNNDEA than in PNIPA, which is in concordance with the relative D values. The difference observed for the self-diffusion of PEG-600 between the two polymers may be attributed to the hydration of the polymer chains. PNIPA should be more hydrated since its amide group is both a proton donor and acceptor in the formation of hydrogen bonds. The difference of the $k\beta^2$ values for water can be explained similarly. The diffusion of both water and PEG-600 in PNNDEA is faster than that in PNIPA.

6.6. Concluding remarks

We have studied the self-diffusion of water and PEG-600 in different hydrophilic polymer systems, including different polymers as well the same polymer with different molecular weight or different degree of hydrolysis. The diffusion of both water and PEG-600 in the same class of polymers is rather similar and does not vary significantly with the molecular weight or small variations in the degree of hydrolysis of the polymer matrix used. It seems that diffusion in these hydrophilic polymers is mostly affected by the facility in the formation of hydrogen bonds as exemplified by the differences observed for PNNDEA and PNIPA.

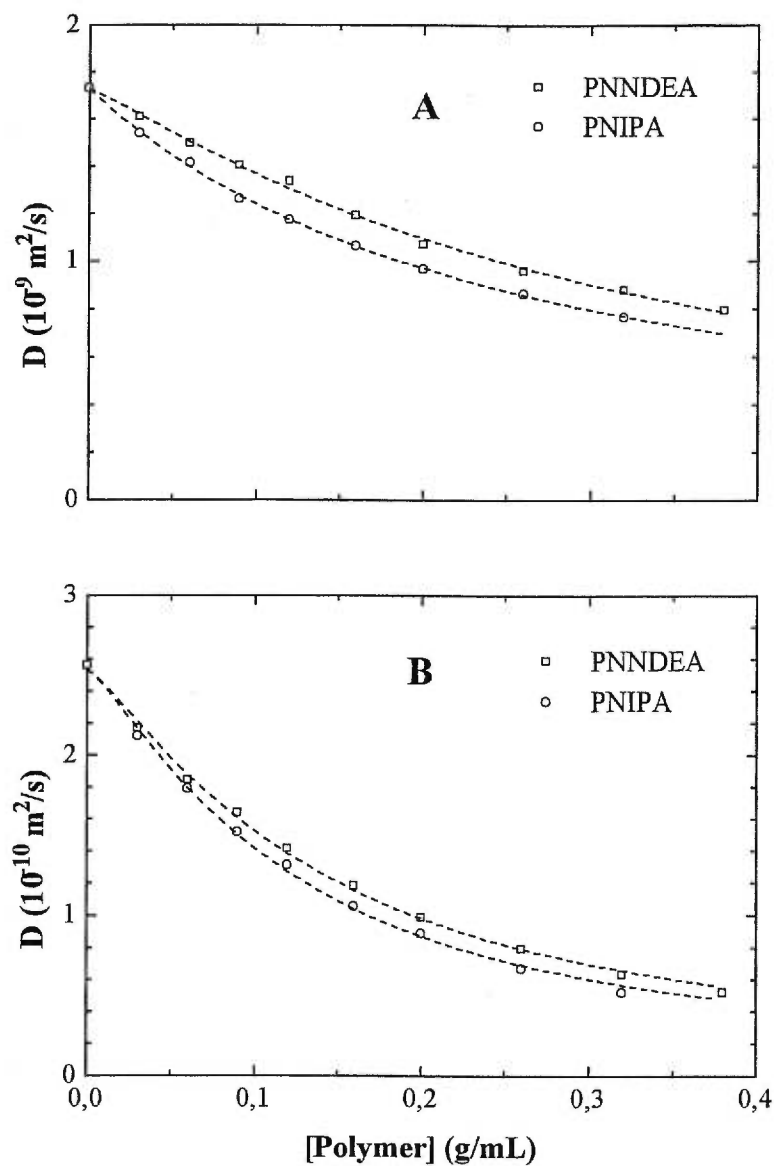


Figure 6.6. Plot of the self-diffusion coefficient of water (A) and PEG-600 (B) as a function of the polymer (PNNDEA and PNIPA) concentration for at 25 °C. Dashed lines are fits to eq 6.3.

The diffusion data have been also analyzed with several pertinent physical models in the literature. The free volume model of Yasuda *et al.* can be used in the description of the diffusion of small molecules, such as the solvent water in this case. Significant deviations from the model were observed for the diffusion data of larger diffusants in polymer solutions and gels. The universal equation proposed by Phillies provided good fits to the diffusion data over the whole range of polymer concentrations, for all the diffusants and matrix polymers. The parameter ν was found to be a constant for a given class of polymers and for a given diffusant. In general, the parameter α was also found to increase somewhat with increasing size of the diffusant (from water to PEG-600). The diffusion data of both water and PEG-600 in all these polymer systems all fitted very well to the diffusion model of Petit *et al.* The parameter ν was found to be constant for a given polymer system and depends on the quality of the solvent. The parameter $k\beta^2$ was found to be a measure of the jump frequency of the diffusant which depends mostly on the size of the diffusant. To a less extent, it also depends on the interaction of the diffusant with the matrix polymer as shown by the differences for PVA-1 and between PNNDEA and PNIPA.

6.7. Acknowledgments.

Financial support from Natural Sciences and Engineering Research Council (NSERC) of Canada and from the Quebec Government (Fonds FCAR) is gratefully acknowledged. The authors would like to thank Professor A. Eisenberg and Mr. C. Bartels of McGill University for their help in the light scattering experiments.

6.8. References and notes.

- [1] Hoerner, P.; Riess, G.; Rittig, F.; Fleischer, G. *Macromol. Chem. Phys.* **1998**, *199*, 343.
- [2] Clericuzio, M.; Parker, W.O.; Soprani, M.; Andrei, M. *Solid State Ionic* **1995**, *77*, 685.
- [3] Pavesi, L.; Rigamonti, A. *Phys. Rev. E* **1995**, *51*, 3318.
- [4] Pavesi, L.; Balzarini, M. *Magn. Res. Imag.* **1996**, *14*, 985.

- [5] Matsukawa, S.; Ando, I. *Macromolecules* **1997**, *30*, 8310.
- [6] Gao, P.; Fagerness, P.E. *Pharm. Res.* **1995**, *12*, 955.
- [7] Peppas, N. A. in *Hydrogels in Medicine and Pharmacy*, CRC Press, Boca Raton, FL, 1987.
- [8] Okaya, T. In *Polyvinyl Alcohol-Developments*, Finch, C.A. Ed.; John Wiley, London, 1992; Chap. 1, p. 1.
- [9] Stephans, L.E.; Foster, N. *Macromolecules* **1998**, *31*, 1644.
- [10] Allan, S.H. *J. Contr. Release* **1987**, *6*, 297.
- [11] Petit, J.-M.; Zhu, X.X.; Macdonald, P.M. *Macromolecules* **1996**, *29*, 70.
- [12] Petit, J.-M.; Roux, B.; Zhu, X.X.; Macdonald, P.M. *Macromolecules* **1996**, *29*, 6031.
- [13] Masaro, L.; Zhu, X.X.; Macdonald, P.M. *Macromolecules* **1998**, *31*, 3880.
- [14] Fricke, H. *Phys. Rev.* **1924**, *24*, 575.
- [15] Mackie, J.S.; Meares, P. *Proc. R. Soc. Lond., A* **1955**, *232*, 498.
- [16] Ogston, A.G.; Preston, B.N.; Wells, J.D. *Proc. R. Soc. Lond., A* **1973**, *333*, 297.
- [17] Cukier, R.I. *Macromolecules* **1984**, *17*, 252.
- [18] Altenberger, A.R.; Tirrell, M. *J. Chem. Phys.* **1984**, *80*, 2208.
- [19] Johansson, L.; Elvingson, C.; Löfroth, J.-E., *Macromolecules* **1991**, *24*, 6024.
- [20] De Gennes, P.G. *J. Phys. Chem.* **1971**, *55*, 572.
- [21] De Gennes, P.-G. *Scaling Concepts in Polymer Physics*, Cornell University Press: Ithaca, New-York, 1979.
- [22] Fujita, H. *Adv. Polym. Sci.* **1961**, *3*, 1.
- [23] Yasuda, H.; Lamaze, C.E.; Ikenberry, L.D. *Makromol. Chem.* **1968**, *118*, 19.
- [24] Peppas, N.A.; Lustig, S.R. *Hydrogels in medicine and pharmacy, Vol. I*, CRC Press, Boca Raton (1987).
- [25] Vrentas, J.S.; Duda, J.L. *J. Polym. Sci., Polym. Phys. Ed.* **1977**, *15*, 403.
- [26] Vrentas, J.S.; Duda, J.L. *J. Polym. Sci., Polym. Phys. Ed.* **1977**, *15*, 417.
- [27] Amsden, B. *Polym. Gels Networks* **1998**, *6*, 13.
- [28] Mustafa, M. B.; Tipton, D. L.; Barkley, M. D.; Russo, P. S.; Blum, F. D., *Macromolecules* **1993**, *26*, 370.

- [29] Waggoner, A. R.; Blum, F. D.; MacElroy, J. M. D., *Macromolecules* **1993**, *26*, 6841.
- [30] Phillies, G.D.J. *Macromolecules* **1986**, *19*, 2367.
- [31] Kirkwood, J. G.; Riseman, J. *J. Chem. Phys.* 1948, **16**, 565.
- [32] Phillies, G.D.J. *Macromolecules* **1987**, *20*, 558.
- [33] Phillies, G.D.J. *Macromolecules* **1988**, *21*, 3101.
- [34] Phillies, G.D.J. *J. Phys. Chem.* **1989**, *93*, 5029.
- [35] Phillies, G.D.J.; Richardson, C.; Quinlan, C.A.; Ren, S.Z. *Macromolecules* **1993**, *26*, 6849.
- [36] Park, I. H.; Johnson Jr., C. S.; Gabriel, D. A., *Macromolecules* **1990**, *23*, 1548.
- [37] Gibbs, S. J.; Johnson Jr., C. S., *Macromolecules* **1991**, *24*, 6110.
- [38] Furukawa, R.; Arauz-Lara, J.L.; Ware, B. R. *Macromolecules* **1991**, *24*, 599.
- [39] Sung, J.; Chang, T. *Polymer* **1993**, *34*, 3741.
- [40] Zhu, X.X.; Masaro, L.; Petit, J.-M.; Roux, B.; Macdonald, P.M. In *Materials for Controlled Release Applications*; McCulloch, I., Shalaby, S.W. Eds.; ACS Publ., Washington, D.C., 1998; Chap. 18.
- [41] Liu, H.Y.; Zhu, X.X. *Polymer* **1999**, *40*, in press.
- [42] Wyatt, P.J. *Anal. Chim. Acta* **1993**, *272*, 1.
- [43] Zimm, B.H. *J. Chem. Phys.* **1948**, *16*, 1093.
- [44] Wang, B.; Mukataka, S.; Kodama, M.; Kokufata, E. *Langmuir* **1997**, *13*, 6108.
- [45] Stejskal, E.O.; Tanner, J.E. *J. Chem. Phys.* **1965**, *42*, 288.
- [46] Mills, R. *J. Phys. Chem.* **1973**, *77*, 685.
- [47] Gusev, D.G.; Lozinsky, V.I.; Vainerman, E.S.; Bakhmutov, V.I. *Magn. Res. Chem.* **1990**, *28*, 651.
- [48] Shiga, T.; Fukumori, K.; Hirose, Y.; Okada, A.; Kurauchi, T. *J. Polym. Sci., Part B* **1994**, *32*, 85.
- [49] Nagura, M.; Takagi, N.; Katakami, H.; Gotoh, Y.; Ohkoshi, Y.; Koyano, T.; Minoura, N. *Polym. Gels Net.* **1997**, *5*, 455.
- [50] Petit, J.-M.; Zhu, X.X. *Macromolecules* **1996**, *29*, 2075.
- [51] Nokhodchi, A.; Ford, J.L.; Rubinstein, M.H. *J. Pharm. Sci.* **1997**, *86*, 608.

- [52] Radloff, D.; Boeffel, C.; Spiess, H.W. *Macromolecules* **1996**, *29*, 1528.
- [53] Maccrystal, C.B.; Ford, J.L.; Rajabisiahboomi, A.R. *Thermochimica Acta*, **1997**, *294*, 91.
- [54] Malamataris, S.; Karidas, T. *Int. J. Pharm.* **1994**, *104*, 115.
- [55] Malamataris, S.; Karidas, T.; Goidas, P. *Int. J. Pharm.* **1994**, *113*, 205.
- [56] Gao, P.; Skoug, J.W.; Nixon, P.R.; Ju, R.; Stemm, N.L.; Sung, K.-C. *J. Pharm. Sci.* **1996**, *85*, 732.

Partie V

L'influence des interactions soluté- polymère sur la diffusion

Chapitre 7

Interaction of Ethylene Glycol with Poly- (vinyl alcohol) in Aqueous Systems as Studied by NMR Spectroscopy

Masaro, L.; Zhu, X.X.

Langmuir, 1999 soumis

7.1. Abstract

The interaction of a diffusant with the polymer matrix may cause difficulties in the determination of its self-diffusion coefficient by the pulsed field gradient NMR technique. We report here the study of the interaction of ethylene glycol with poly(vinyl alcohol) (PVA) in aqueous solutions and gels by NMR spectroscopy and the elucidation of the diffusion coefficients of the free and bound ethylene glycol molecules which co-exist in PVA-water system. The fraction of bound ethylene glycol increases as a function of PVA concentration and a binding constant of *ca.* $1.7 \times 10^3 \text{ M}^{-1}$ was estimated. Various ^1H NMR parameters such as the chemical shifts, the self-diffusion coefficients as well as the spin-lattice and the spin-spin relaxation times have been determined to study the interactions. The free and bound ethylene glycol molecules have different chemical shifts, NMR relaxation times and self-diffusion coefficients at various polymer concentrations.

7.2. Introduction

The diffusion and interaction of solutes and solvents in polymers is of great research interest because of the importance in the application of the materials. For example, the retardation of the diffusion of small molecules in polymer solutions and gels has direct applications in analytical methods such as gel electrophoresis and gel filtration [1,2]. In the controlled release of drugs, Coulombic interactions or hydrogen bonding can retard the transport of drugs in polymer systems, which results in the deviation of the release profile from theoretical models [3,4]. The diffusion of solute probes in polymer solutions and gels is usually related to the concentration of the polymer matrix and the size of the diffusant [1,2,5–7]. However, the elucidation of the effect of molecular interactions on the diffusion process is not always straightforward since comparisons between different solutes in different polymer systems are often needed. Lee and Lodge [8] used the forced Rayleigh scattering technique to determine the retardation of the diffusion of methyl red in poly(vinyl acetate)-toluene solutions by comparing with the diffusion of the same diffusant in polystyrene-toluene at the same polymer concentrations. Further comparison with the

diffusion data of isomers and derivatives of methyl red showed that the retardation was due to hydrogen-bonding between the carboxylic acid group of methyl red and poly(vinyl acetate) [2].

The pulsed-gradient spin-echo (PGSE) NMR spectroscopy [9–12] has become one of the most commonly used technique in the study of self-diffusion in polymer systems, such as solvent and solute probe diffusion in polymer solutions and gels [13–15]. The self-diffusion coefficient is related to the signal intensity (A) in the presence of gradient pulses according to [9]

$$A_{2\tau} = A_{2\tau}^* \exp \left[-(\gamma G \delta)^2 \left(\Delta - \frac{\delta}{3} \right) D \right] \quad (7.1)$$

where $A_{2\tau}$ is the echo amplitude, $A_{2\tau}^*$ is the amplitude of the echo in the absence of gradient pulses, γ is the gyromagnetic ratio of ^1H , G is the pulsed gradient strength, δ is the duration of the gradient pulses, Δ is the interval between the gradient pulses, and D the self-diffusion coefficient. Usually, a mono-exponential decrease of $A_{2\tau}$ should be observed as a function of $(\gamma G \delta)^2 (\Delta - \delta/3)$. However, non-mono-exponential dependence can be often observed in polymer systems and this may render the determination of the diffusion coefficient difficult. The non-mono-exponential behavior can be due to the heterogeneity of the system, the specific interactions with the polymers, the polydispersity of macromolecular diffusants, or anomalous diffusion caused by intra- and intermolecular interactions in the systems [10–12,14,16]. PGSE NMR was also used to study the anomalous diffusion of a triblock copolymer during the temperature-induced sol-gel transition [17]. It was employed recently to investigate the binding between a probe polymer and the matrix polymer in a gel [18]. Watanabe *et al.* [19] studied water and polymer diffusion in dextran gels. They found two distinct self-diffusion coefficients for water. The faster diffusion corresponds to the bulk water ($D = 7.55 \times 10^{-6} \text{ cm}^2/\text{s}$) and the slower diffusion corresponds to the trapped water ($D = 6.7 \times 10^{-8} \text{ cm}^2/\text{s}$). By the use of PGSE NMR spectroscopy, Hansen *et al.* [20] found that both methine and methylene groups of poly(vinyl alcohol) (PVA) showed anomalous diffusion after gelation of PVA with glutaraldehyde in water.

In a previous work [7], we have studied the self-diffusion coefficients of a series of oligo- and poly(ethylene glycol)s in PVA solutions and gels by PGSE NMR and observed deviations from the mono-exponential variation of the NMR echo height attenuation as shown in eq 7.1. The deviation was quite significant with ethylene glycol (EG), but became less and less obvious with increasing molecular size of the diffusants, i.e., oligo(ethylene glycol)s. In the case of larger diffusants such as poly(ethylene glycol)s, the deviation was not obvious at all. The deviations may cause errors in the determination of the self-diffusion coefficient and the interpretation of the diffusion data obtained by the NMR technique. Because of the numerous applications of PVA [21,22] and its facility in the formation of inter- and intramolecular hydrogen bonds [21,23], it can serve as an ideal system to characterize the interactions and their effects on the diffusion measurements. We have studied the molecular interactions between EG and the PVA by monitoring the chemical shift, spin-lattice (T_1) and spin-spin (T_2) relaxation times and the self-diffusion coefficient of EG. The results all indicate the co-existence of free and bound EG molecules in the system. The validity of the determination of the diffusion coefficients of both free and bound EG by the PGSE NMR technique is also discussed.

7.3. Experimental section

Ethylene glycol (EG) and the poly(vinyl alcohol) ($M_w = 52\,800$, $M_n/M_w = 2.09$, degree of hydrolysis 99 %) used in this study were purchased from Aldrich (Milwaukee, WI) and used as received. D_2O (99.9%) was purchased from C.I.L. (Andover, MA).

The preparation of the NMR samples was described previously [5,7]. A certain amount of PVA was weighed directly inside the NMR tube. D_2O containing 1 wt % EG was then added into the tube to obtain the desired PVA concentration (0.03–0.38 g/mL). The NMR tubes were then sealed to avoid evaporation of the solvent and heated to help the mixing of the sample. During heating, the NMR tubes were periodically agitated to obtain homogeneous polymer solutions.

The self-diffusion coefficient was measured on a Bruker Avance AMX-300 NMR spectrometer operating at 300.13 MHz for protons. The PGSE NMR technique developed by Stejskal and Tanner [9] was used. A Bruker magnetic resonance imaging probe, Micro 2.5 Probe, was coupled with a gradient amplifier BAFPA-40. Gradient pulses were applied only in the z direction. The calibration of the gradient strength along each axis was achieved by one-dimensional imaging of an object contained in a 10 mm NMR tube filled with a solution of doped water (with CuSO_4). The dimension of the NMR profile was correlated to the real dimension of the object. The gradient strength, G , used in this study varied between 0.1 and 1 T/m. The gradient strength was also verified daily with a sample of known self-diffusion coefficient such as 1 vol % HDO in D_2O ($D_{\text{HDO}} = 1.9 \times 10^{-9} \text{ m}^2/\text{s}$) [24]. The other parameters were kept constant and their values are those noted in the parentheses: δ (1–3 ms), Δ (25–200 ms), recycle delay (15–60 s), number of acquisitions (1–16), 90° pulse length (23–29 μs), spectral width (3–8 kHz), line broadening (5–10 Hz).

The T_1 and T_2 relaxation times measurements were made on the same NMR instrument. The inversion recovery [25] and the Carr-Purcell [26] methods were used for T_1 and T_2 measurements, respectively. The chemical shift study was carried out on a Bruker ARX-400, resonating at 400 MHz for protons, equipped with a high resolution probe.

7.4. Results and discussion

7.4.1. Chemical shifts (δ)

Figure 7.1 shows ^1H NMR spectra of EG in PVA- D_2O solutions at different PVA concentrations. The NMR spectrum of EG without PVA (Figure 7.1A) contains only two signals, residual solvent water ($\delta = 4.8$ ppm) and EG ($\delta = 3.7$ ppm). When PVA is present at a concentration of 0.03 g/mL, three groups of additional NMR signals appear on the spectrum (Figure 7.1B). Two of them are attributed to PVA ($\delta_{\text{CH}} = 4\text{--}4.2$ ppm and $\delta_{\text{CH}_2} = 1.6\text{--}1.8$ ppm). The additional NMR signal at 3.8 ppm is assumed to correspond to EG bound to PVA. This signal was not observed in

the EG sample in the absence of PVA, nor in the PVA sample in the absence of EG. Therefore, it must be due to the EG bound to the polymer. In addition, the signal intensity of this peak increases and becomes more distinct with increasing PVA concentration (Figure 7.1C–D), while at the same time the other EG signal decreases in its intensity. This confirms that the new NMR signal belongs to the protons of EG bound to PVA. From the NMR spectrum, the proton signals were integrated to calculate the fractions of free and bound EG. The variation of the relative intensities of the free and bound EG signals as a function of PVA concentration is shown in Figure 7.2. For a higher PVA concentration of 0.38 g/mL, approximately half of EG in the system is found to be bound to the polymer. With the data in Figure 7.2, we are able to calculate the binding constant [27] for the interaction between PVA and EG and a value of *ca.* $1.7 \times 10^3 \text{ M}^{-1}$ was obtained. This value corresponds to a binding free energy change of *ca.* -18.5 kJ/mol at 25 °C.

The NMR samples need to be heated for the homogeneous mixing of the polymer solutions as described previously [5,7]. The ^1H NMR signal of bound EG was not observed immediately after the heating of the NMR samples. This signal only appeared after a certain period of time, which indicates that the binding is time-dependent. The spectra in Figure 7.1 were acquired 15 days after heating. This is in agreement with the work of Stephans and Foster [23] who studied by magnetization-transfer NMR technique the gelation process of PVA as a function of time and the degree of hydrolysis. They found that the intra- and intermolecular interactions of PVA depend mainly on time and also on the degree of hydrolysis of PVA. Completely hydrolyzed PVA chains can form a gel more rapidly than PVA with a lower degree of hydrolysis. The PVA used in our study has a degree of hydrolysis of 99 %. Therefore, the presence of a large number of hydroxyl groups on the polymer chain favors the formation of hydrogen bonds.

Matsukawa and Ando [18] reported studies of poly(ethylene glycol) (PEG) diffusion in poly(acrylic acid) (PAA) and in poly(*N,N*-dimethylacrylamide) (PDMAA) gels by ^1H PGSE NMR spectroscopy. They found that PEG was bound to the acid groups of PAA by forming hydrogen bonds, whereas no such interactions were

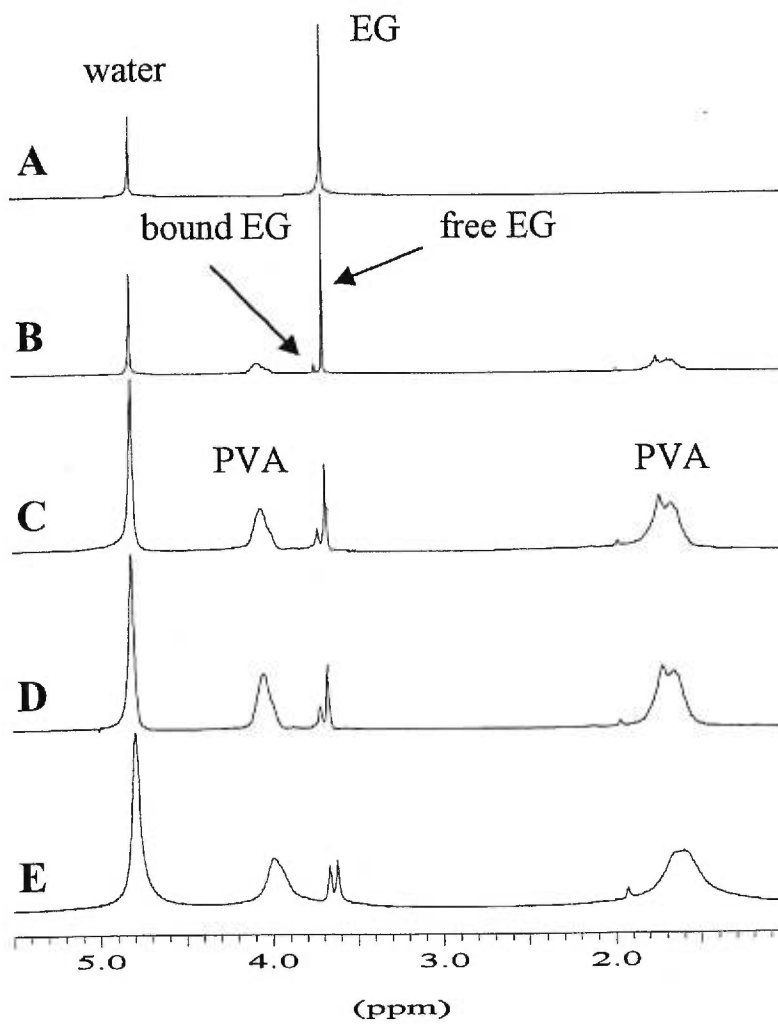


Figure 7.1. ^1H NMR spectra of EG in PVA- D_2O solution at different PVA concentrations. $T = 23\text{ }^\circ\text{C}$ and $[\text{PVA}] = 0$ (A), 0.03 (B), 0.09 (C), 0.16 (D), and 0.38 g/mL (E).

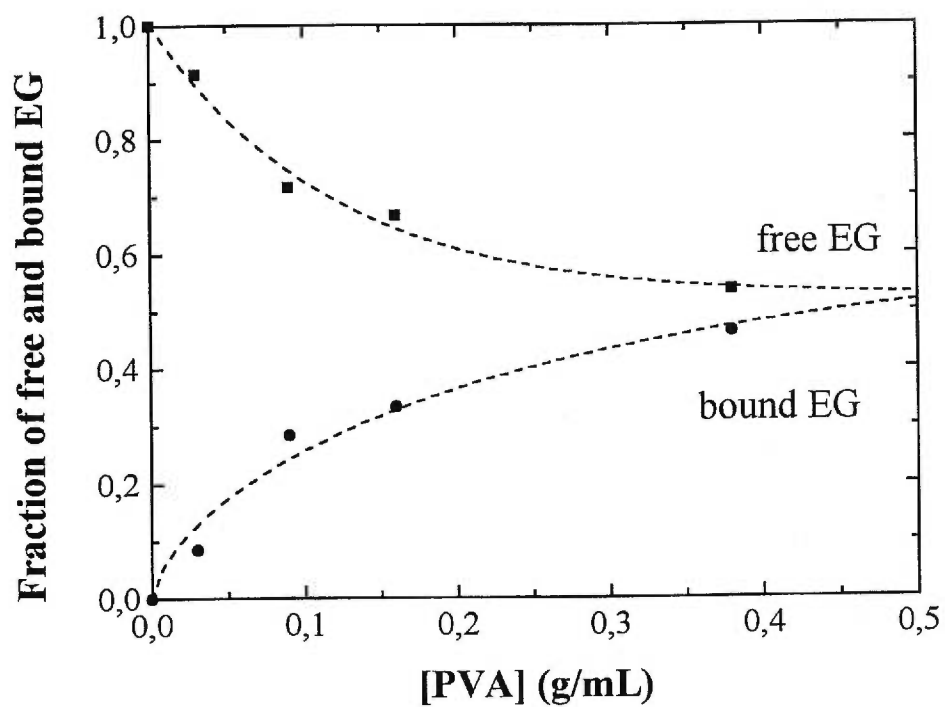


Figure 7.2. Plot of the fractions of free and bound EG as a function of the PVA concentration. Dashed lines are drawn to indicate the general trend of the variations. From the data shown here, a binding constant for PVA-EG is estimated to be equal to $1.7 \times 10^3 \text{ M}^{-1}$.

detectable with the less hydrophilic PDMAA. They did not observe any change in the chemical shift of PEG when it is bound to PAA gels, probably due to the fact that the NMR signal of PEG is much broader than that of EG.

7.4.2. PGSE NMR measurements.

Figure 7.3 shows that the self-diffusion coefficients of both free and bound EG molecules can be determined by the PGSE NMR experiment. For a given sample, all the experimental parameters (see eq 7.1) in the PGSE NMR pulse sequence were kept constant with the exception of G . Therefore, only G is varied in the spectra shown in Figure 7.3A and the plot shown in Figure 7.3B is in fact a plot of $\ln A$ as a function of G^2 . The water (HDO) signal at 4.8 ppm disappears rapidly as the gradient strength increases, which indicates a high self-diffusion coefficient. NMR signals of PVA did not attenuate very much since the diffusion of the polymer is slow (D in the order of 10^{-11} m²/s [7]). Both free and bound EG NMR signals decrease when the gradient strength is increased, but the signal intensity of bound EG decreases much less rapidly (Figure 7.3). Therefore, the free and bound fractions of EG have two distinct self-diffusion coefficients (6.20×10^{-10} and 1.54×10^{-10} m²/s, respectively, at a PVA concentration of 0.09 g/mL). The same behavior has been observed with other PVA concentrations as shown in Figure 7.4.

The self-diffusion coefficient of the bound EG (1.54×10^{-10} m²/s) at a PVA concentration of 0.09 g/mL is at least an order of magnitude greater than that of PVA ($D_{\text{PVA}} \sim 10^{-11}$ m²/s) [7]. This is an indication that the binding between EG and PVA is in a thermodynamic equilibrium. Since the hydrogen bonds are relatively weak (the strength of the bond is about 20 kJ/mol [28]), exchanges between the bound and free EG still exist and can be considered to be rapid on the NMR timescale. Therefore, the measured self-diffusion coefficient of the “bound” EG represents a weighted average of the diffusion coefficients of the free and bound EG molecules in this exchange process. But this value is significantly lower than the self-diffusion coefficient of PVA, which should correspond to the self-diffusion coefficient of the truly bound EG molecules.

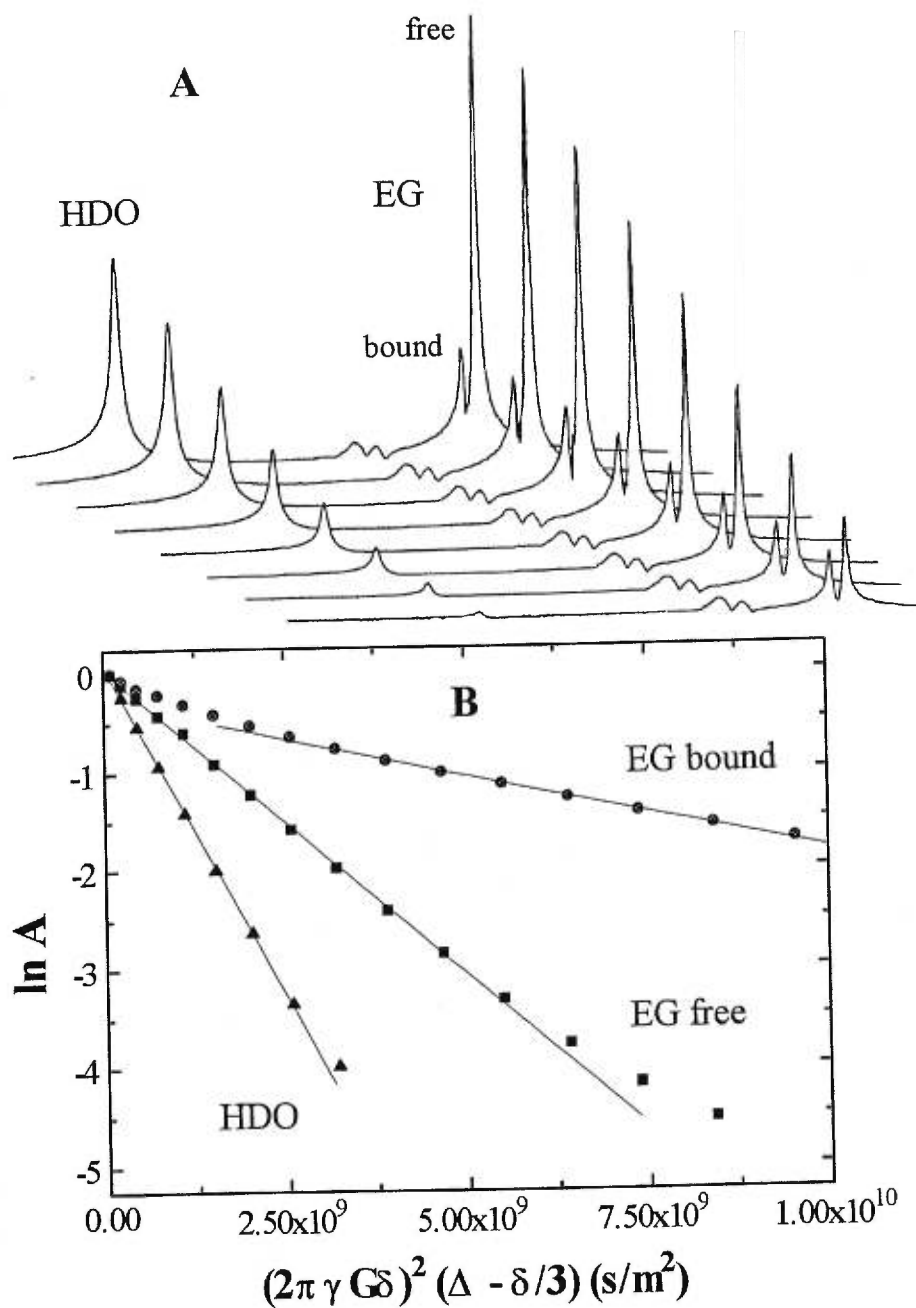


Figure 7.3. (A) ^1H PGSE NMR spectra of EG in PVA- D_2O solution at 23 °C with $[\text{PVA}] = 0.09$ g/mL. Gradient pulse strengths used are 0.10, 0.16, 0.22, 0.28, 0.34, 0.40, 0.46, and 0.52 T/m, respectively, for each spectrum from top to bottom. (B) The plot of the NMR signal intensity according to eq 7.1. The D values are calculated from the slopes of the lines and are equal to 1.54×10^{-10} , 6.20×10^{-10} , and 1.35×10^{-9} m 2 /s for bound EG, free EG and HDO, respectively.

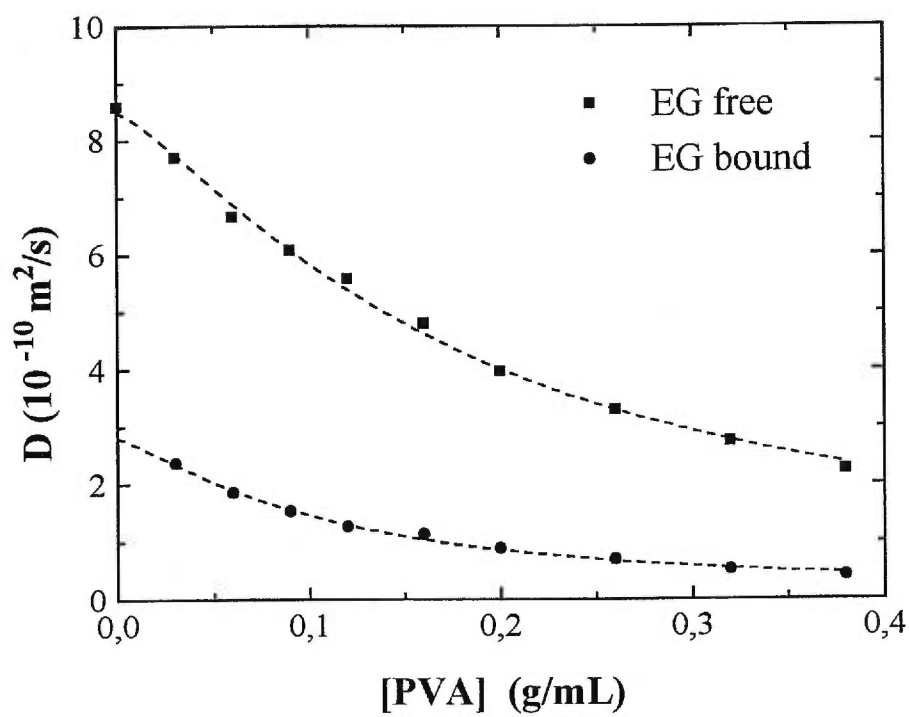


Figure 7.4. Plot of the self-diffusion coefficient for free and bound EG as a function of PVA concentration at 23 °C. Fits are obtained with the model of Petit *et al.* (eq 7.2) [15].

The binding between the polymer and the diffusant evolves with time. For the freshly prepared samples (within 3 days), only one EG signal was observed in the NMR spectra. When the diffusion coefficient is measured for the fresh samples, non-mono-exponential behavior of the NMR signal intensities (as discussed in the introduction) is clearly observed, as shown in Figure 7.5. Obviously, this can cause difficulties in the determination of the correct self-diffusion coefficient. After a certain period of time (e.g., 10 days), two distinct signals can be observed, as shown in Figures 7.1 and 7.3. The PGSE NMR echo attenuations of EG as a function of $(\gamma G \delta)^2 (\Delta - \delta/3)$ for the samples prepared within 3 days and after 10 days are all shown in Figure 7.5. Ten days after the sample preparation, free and bound EG showed up as two signals and both decayed mono-exponentially according to eq 7.1. The curvature observed at the very end of the data (with high G) for free EG is due to the influence of bound EG NMR signal which tends to overlap (Figure 7.1) and give error to the measured intensity of the free EG. The NMR signal of the bound EG attenuates more slowly than that of the free EG in the presence of strong gradient pulses. Similarly, the curvature observed for the data of bound EG corresponding to low G is due to the presence of the nearby free EG NMR signal which is much higher in intensity at low G (Figure 7.3). Mutual influence of the NMR signal intensities is due to the fact that the NMR signals for free and bound EG are very close ($\delta = 3.7$ and 3.8 ppm, respectively). In addition, the phase correction was carried out in magnitude mode, which helps to prevent the J -modulation effects but causes enlargement of the NMR signals at their bases [29]. The behavior of EG within 3 days of preparation seems to be a combination of the free and bound EG, for which no separate signals can be observed. The initial part of the curve, corresponding to low gradient strengths, is mainly due to the signal of free EG whereas the latter part of the curve was mainly due to the signal of the bound EG. In fact, as shown in Figure 7.5, the initial part of this curve within 3 days overlaps nicely with the data for free EG after 10 days, indicating very similar self-diffusion coefficients (4.57×10^{-10} and 4.95×10^{-10} m²/s, respectively). As seen in the same figure, the data corresponding to the bound EG within 3 days does not have exactly the same slope as the bound EG after

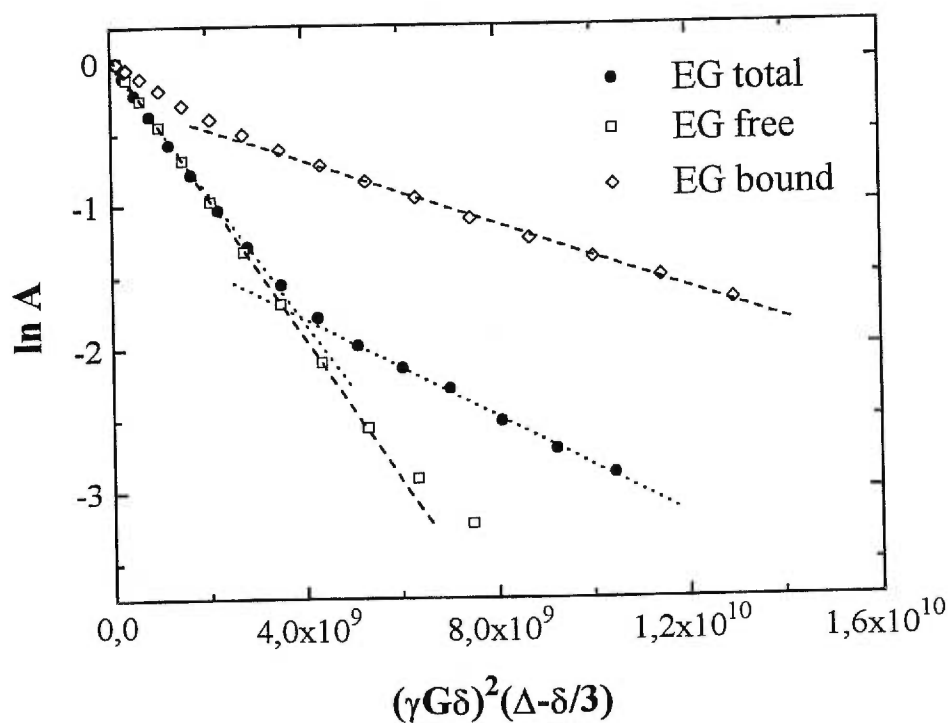


Figure 7.5. Semilogarithmic plot of the NMR signal intensity as a function of $(\gamma G \delta)^2 (\Delta - \delta/3)$ (eq 7.1) for ethylene glycol in PVA-water system. Data were acquired within 3 days (closed symbols) and after 10 days (open symbols) upon the heating of the samples. The self-diffusion coefficients calculated are 4.57×10^{-10} , 1.71×10^{-10} m²/s for free and bound EG within 3 days and 4.95×10^{-10} , 1.12×10^{-10} m²/s for free and bound EG after 10 days, respectively. T = 23 °C, [PVA] = 0.16 g/mL.

10 days, leading to a somewhat different D values (1.71×10^{-10} m²/s in comparison to 1.12×10^{-10} m²/s of the bound EG after 10 days). The difference is due to the fact that the middle portion of the curve for the sample within 3 days was still much influenced by the overlapping free EG NMR signal. Therefore, the data obtained within 3 days tend to over-estimate the D value for the bound EG as a result of the overlapping. The kinetic aspect of the binding may have also contributed to the larger D value (1.71×10^{-10} m²/s) at this stage, indicating the binding is still in progress.

Matsukawa and Ando [18] studied the diffusion of PEG in PAA, PDMAA, and copolymers of DMAA and AA. By comparison of the self-diffusion coefficient and T_2 of PEG in different polymer systems, they identified hydrogen bonding between PEG and the acrylic acid groups. They found that D and T_2 values of PEG were lower in a network where the fraction of acrylic acid was higher than 0.9. However, no different self-diffusion coefficients of free and bound PEG were reported for the system.

The data in the Figure 7.4 are fitted to the diffusion model of Petit *et al.* [6]

$$D = \frac{D_0}{1 + ac^{2\nu}} \quad (7.2)$$

where D_0 the self-diffusion coefficient of the diffusant in the absence of the polymer network, c the polymer concentration, a and ν are fitting parameters. The parameter ν depends on the quality of the solvent and should be a constant for a given system, while a is another parameter related to D_0 and the jump frequency of the diffusant [6]. This model was used to describe the diffusion of small molecules and macromolecules in polymer matrices, such as ternary PVA-aqueous systems, and the diffusion of small molecules in binary organic solutions of poly(methyl methacrylate) [6,7,30]. In general, the self-diffusion coefficients of both free and bound EG decreases with increasing concentration of PVA. However, this decrease is much more pronounced for the fraction of free EG. Table 7.1 shows the chemical shifts and all the other physical parameters related to eq 7.2. From Figure 7.4, we have found a value of 0.65 and 0.64 for the parameter ν of the free and bound EG, respectively. These values are almost identical and they are close to the average value of 0.58 obtained for the PVA

aqueous systems in a previous study [7]. As for the parameter α , a value of 9.08 and 17.44 was found for the free and bound EG, respectively. The hydrodynamic radius (R_h) for the free EG (2.71 Å) and bound EG (8.19 Å) (Table 7.1) were calculated with the Stokes-Einstein equation.

Table 7.1. Chemical shift, D_0 , α , ν , and R_h (calculated from the Stokes-Einstein equation) for free and bound EG.

	δ (ppm)	$D_0 \times 10^{-10}$ (m ² /s)	α	ν	R_h (Å)
Free EG	3.7	8.49	9.08	0.65	2.71
Bound EG	3.8	2.81	17.44	0.64	8.19

7.4.3. Measurements of NMR relaxation times (T_1 and T_2)

The relaxation times, T_1 and T_2 , reflect the freedom of motion of a molecule whereas the self-diffusion coefficient reflects more the displacement of the molecule [18]. Both T_1 and T_2 of the NMR signals of the free and bound EG (at 3.7 and 3.8 ppm, respectively), were measured for various PVA concentrations. T_1 and T_2 measured for free EG decrease with increasing PVA concentration, as shown in Figure 7.6. This variation of the relaxation times can be attributed to changes in the environment of the diffusant, due to an increased restriction in the freedom of motion at higher PVA concentrations. T_1 and T_2 measured for bound EG, however, are found to be more or less constant with increasing PVA concentration. Comparison of T_1 and T_2 values for free and bound EG showed restricted motions of bound EG at various PVA concentrations (Figure 7.6). This result is another clear evidence of interactions between EG and PVA.

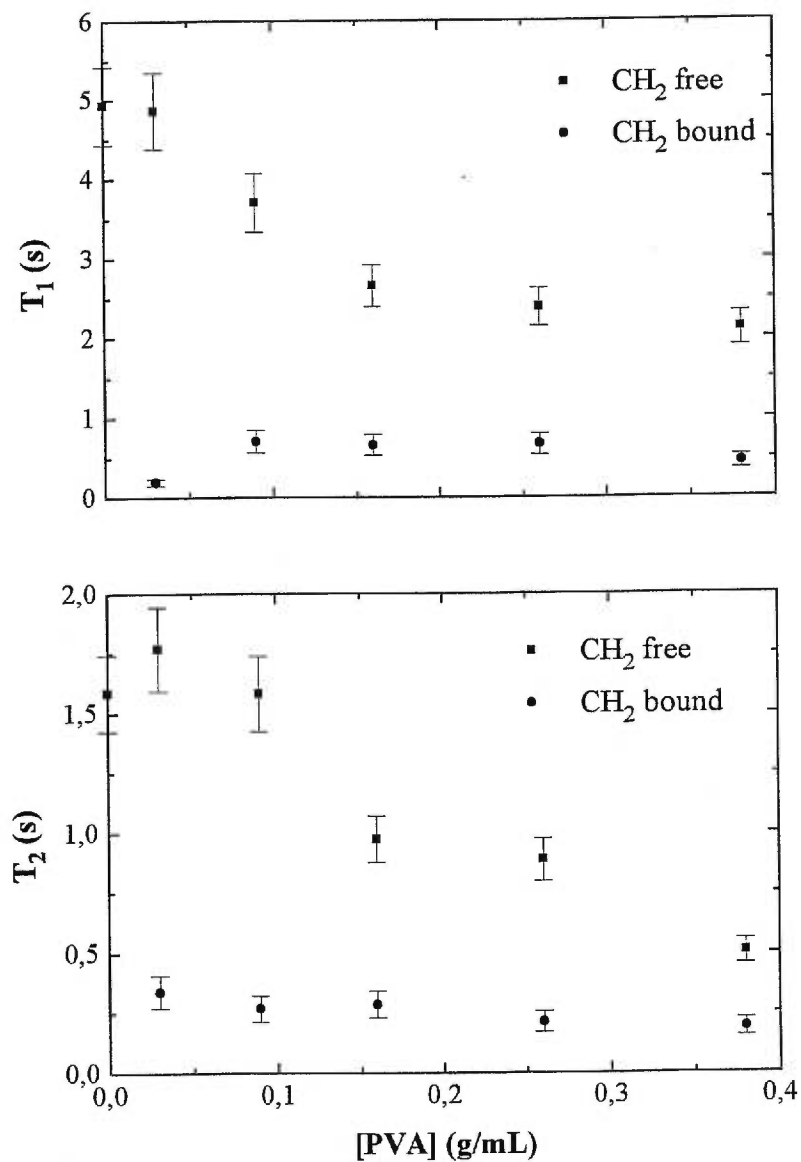


Figure 7.6. Plot of T_1 (A) and T_2 (B) relaxation times for free and bound EG as a function of PVA concentration. Large variations can be observed for free EG, but the variations for bound EG are much smaller.

7.5. Concluding remarks

The binding of a small diffusant such as ethylene glycol with a polymer (in this case PVA) is often a kinetic and dynamic process. The free and bound species may not always appear as separate NMR signals. As shown in this study, the co-existence of both free and bound molecules may cause difficulties in the correct determination of the self-diffusion coefficient when the NMR signals are not well separated and when the echo attenuation shows non-mono-exponential behavior (eq 7.1) as in the case of freshly prepared PVA-EG-water samples. We were able to characterize the interaction of EG with PVA in the aqueous solutions by measuring the different NMR parameters (chemical shift, relaxation times, etc.). In many other cases, such as the PVA-PEG systems, the evidence of interaction may not be as apparent, but similar problems may arise in the study of diffusion by the PGSE NMR technique, as mentioned in a previous work [7]. The self-diffusion of oligo(ethylene glycol)s and their derivatives in PVA solutions and gels is currently studied. In this report, we have shown how the diffusion coefficients of the free and bound diffusant can be measured or estimated and how the PGSE NMR technique can be used in the investigation of such interactions in a polymer system.

7.6. Acknowledgment

The financial support from the Natural Sciences and Engineering Research Council (NSERC) of Canada and the Quebec Government (Fonds FCAR) is gratefully acknowledged.

7.7 References and notes

- [1] Lee, J.; Park, K.; Chang, T.; Jung, J.C. *Macromolecules* **1992**, *25*, 6977.
- [2] Park, H.S.; Sung, J.; Chang, T. *Macromolecules* **1996**, *29*, 3216.
- [3] Peppas, N.A.; Wright, S.L. *Macromolecules* **1996**, *29*, 8798.
- [4] am Ende, M.T.; Peppas, N.A. *J. Contr. Release* **1997**, *48*, 47.
- [5] Petit, J.-M.; Zhu X.X.; Macdonald, P.M. *Macromolecules* **1996**, *29*, 70.
- [6] Petit, J.-M.; Roux B.; Zhu, X.X.; Macdonald, P.M. *Macromolecules* **1996**, *29*,

- 6031.
- [7] Masaro, L.; Zhu X.X.; Macdonald, P.M. *Macromolecules*, **1998**, *31*, 3880.
- [8] Lee, J.A.; Lodge, T.P. *J. Phys. Chem.* **1987**, *91*, 5546.
- [9] Stejskal, E.O.; Tanner, J.E. *J. Chem. Phys.* **1965**, *42*, 288.
- [10] Callaghan, P.T. *Aust. J. Phys.* **1984**, *37*, 359.
- [11] Price, W.S. *Concepts Magn. Reson.* **1997**, *9*, 299.
- [12] Masaro, L.; Zhu, X.X. *Can. J. Anal. Sci. Spectro.* **1998**, *43*, 81.
- [13] Griffiths, P.C.; Stilbs, P.; Chowdhry, B.Z.; Snowden, M.J. *Colloid Polym. Sci.* **1995**, *273*, 405.
- [14] Rao, B.; Uemura, Y.; Dyke, L.; Macdonald, P.M. *Macromolecules* **1995**, *28*, 531.
- [15] Zhu, X.X.; Wang, F.; Nivaggioli, T.; Winnik, M.A.; Macdonald, P.M. *Macromolecules* **1993**, *26*, 6397.
- [16] Walderhaug, H.; Hansen, F.K.; Abrahmsén, S.; Persson, K.; Stilbs, P. *J. Phys. Chem.* **1993**, *97*, 8336.
- [17] Walderhaug, H.; Nyström, B. *J. Phys. Chem. B* **1997**, *101*, 1524.
- [18] Matsukawa, S.; Ando, I. *Macromolecules* **1997**, *30*, 8310.
- [19] Watanabe, T.; Ohtsuka, A.; Murase, N.; Barth, P.; Gersonde, K. *Magn. Reson. Med.* **1996**, *35*, 697.
- [20] Hansen, E.W.; Olafsen, K.; Klaveness T.M.; Kvernberg P.O. *Polymer* **1998**, *39*, 1279.
- [21] Okaya, T. In *Polyvinyl Alcohol-Developments*; Finch, C.A. Ed.; John Wiley, London, 1992; Chap. 1, p. 1.
- [22] Peppas, N.A.; Korsmeyer, R.W. In *Hydrogels in Medecine and Pharmacy*; Peppas, N.A. Ed.; CRC Press, Boca Raton, 1987; Vol. II; Chap. 6, p. 109.
- [23] Stephans, L.E.; Foster, N. *Macromolecules* **1998**, *31*, 1644.
- [24] Mills, R. *J. Phys. Chem.* **1973**, *77*, 685.
- [25] Vold, R.L.; Waugh, J.S.; Klein, M.P.; Phelps, D.E. *J. Chem. Phys.* **1968**, *48*, 3831.
- [26] Carr, H.Y.; Purcell, E.M. *Phys. Rev.* **1954**, *94*, 630.

- [27] Zhu, X.X.; Brizard, F.; Wen, C.C.; Brown, G.R. *J. Macromol. Sci.* **1997**, *A34*, 335
- [28] Atkins, P. In *Physical Chemistry*, 5th Ed., W.H. Freeman and Company, New-York, 1994, p. 771.
- [29] Mahi, L.; Duplan, J.C.; Fenet, B. *Chem. Phys. Letters* **1993**, *211*, 27.
- [30] Zhu, X.X.; Masaro, L.; Petit, J.-M.; Roux, B.; Macdonald, P.M. In *Materials for Controlled Release Applications*; McCulloch, I., Shalaby, S.W. Eds.; ACS Publ., Washington, D.C., 1998; Chap. 18.

Partie VI

Conclusion générale

Nous avons étudié la diffusion dans les solutions et gels de polymères afin de mieux comprendre les procédés de diffusion dans ces systèmes. Les modèles théoriques de diffusion les plus pertinents ont été testés avec les données expérimentales, de manière à déterminer leur domaine d'application. La méthode RMN d'écho de spin à gradient de champ pulsé a été utilisée pour mesurer les coefficients d'auto-diffusion. Plusieurs systèmes ont été étudiés afin d'évaluer l'impact de certains paramètres physico-chimiques sur la diffusion.

8.1. L'effet de la taille et la géométrie du soluté

Deux séries de diffusants basées sur l'éthylène glycol ont été sélectionnées pour réaliser notre étude: une série de solutés linéaires, dont la taille varie, et une série de solutés ayant des géométries différentes, i.e., les groupes terminaux changent. Les mesures de diffusion ont montré que le coefficient d'auto-diffusion diminue lorsqu'on augmente la concentration du polymère ou la taille du soluté. L'effet de la taille du soluté est majeur dans les solutions diluées et semi-diluées de polymère. Nous avons observé des variations du coefficient d'auto-diffusion plus importantes avec les diffusants de petite taille qu'avec les macromolécules. Cependant, dans les régimes concentrés de polymère, les coefficients d'auto-diffusion ont tendance à converger vers une valeur commune. La géométrie du soluté joue aussi un rôle prépondérant dans le procédé de diffusion. Par exemple, un groupe hexyle restreint plus la diffusion qu'un groupe méthyle car il est plus volumineux. De même, un soluté ayant une fonction *tert*-butyle ou un groupe cyclique diffuse plus lentement qu'un soluté linéaire.

8.2. L'effet du réseau polymère

Nous avons étudié la diffusion du solvant (l'eau) et d'un soluté (PEG-600) dans différents systèmes polymères. Les systèmes étudiés sont des PVA avec différentes masses molaires et taux d'hydrolyse, des HPMC, un PNNDEA et un PNIPA. La diffusion de ces solutés ne varie pas de façon significative pour une série de polymère donnée, quel que soit la masse molaire ou le taux d'hydrolyse de la matrice de polymère. Ces résultats montrent que la diffusion dans les systèmes

polymères est gouvernée par la microstructure du polymère. La caractérisation des polymères par des études de diffusion de la lumière et de chromatographie d'exclusion stérique ont permis de montrer que les PVA et les HPMC forment de nombreuses liaisons hydrogène intra- et intermoléculaires. Dans le cas de PNNDEA et PNIPA, il n'y a peu de formation de liaison hydrogène intra- et intermoléculaire, cependant le taux d'hydratation des chaînes du polymère influence les procédés de diffusion.

8.3. L'effet de la température

Les expériences à température variable montrent qu'une augmentation de la température augmente les coefficients d'auto-diffusion. Cependant, l'effet de la taille du soluté et de la concentration en polymère persiste. La température est donc un paramètre important qui doit être pris en considération. Les énergies d'activation de *t*BuOH, EG, PEG-600 et PEG-2000 ont été calculées, des valeurs de 21.1, 30.0, 36.5 et 39.0 kJ/mol ont été obtenues, respectivement. Ces résultats montrent que l'énergie d'activation dépend principalement de la taille de la sonde. Les données expérimentales utilisées pour EG correspondent aux données de diffusion anormale. La première partie des courbes de $\ln I$ vs $\delta^2(\Delta-\delta/3)$ fût utilisée pour calculer les coefficients d'auto-diffusion. Cette procédure n'induit pas trop d'erreur selon l'étude faite au chapitre 7. Cependant, on peut constater que la valeur de ΔE pour EG semble élevée par rapport à la valeur de ΔE pour *t*BuOH, qui est aussi une petite molécule. On peut donc penser que cette valeur est moins fiable que les autres.

8.4. Les interactions dans les systèmes aqueux

L'interaction entre l'éthylène glycol et le PVA, observée lors de la première étude, chapitre 3, a été étudiée. Nous avons observé que l'éthylène glycol avait un profil de diffusion anormal dans un tel système. Cette diffusion anormale est due à la formation de ponts hydrogène entre le diffusant et le polymère. Un signal RMN, résultant de cette interaction, apparaît en fonction du temps. L'analyse de ce signal en RMN (coefficient d'auto-diffusion et temps de relaxation) montre qu'il s'agit bien d'une fraction d'éthylène glycol liée par pontage hydrogène (chapitre 7). Par

conséquent, l'atténuation progressive du phénomène de diffusion anormale avec l'augmentation de la taille du soluté, signalée dans le chapitre 3, peut être attribuée, en partie, au mode de préparation des échantillons. En effet, la concentration en soluté est toujours de 1% en poids. Ce qui implique que la proportion de fonction hydroxyle soit trois fois plus faible dans une solution de TEG comparée à une solution de EG, et approximativement dix fois plus faible pour une solution de PEG-600. Un tel phénomène (liens hydrogènes entre le PVA et les groupements hydroxyles du soluté) devrait également intervenir dans le cas des oligo(éthylènes glycol)s.

Par ailleurs, les travaux de Matsukawa et Ando ont permis de mettre en évidence que le PEG-4250 forme des interactions avec les fonctions acides de l'acide polyacrylique, tel que mentionné au chapitre 7. Ces résultats, combinés à nos travaux permettent de penser que les PEG forment des associations avec les polymères ayant des fonctions hydroxyles. Pour conclure, nous pouvons affirmer que nos travaux montrent que les systèmes aqueux PEG-PVA sont très complexes.

8.5. Les modèles physiques de diffusion

Parmi tous les modèles examinés, ceux de Petit *et al.*, Phillies et Amsden ont donné les meilleures corrélations avec les données expérimentales.

Le modèle de diffusion proposé par Petit *et al.* permet de décrire la diffusion du solvant, de solutés moléculaires de taille et de géométrie différentes, incluant les macromolécules, dans divers solutions et gels de polymères. De plus, les paramètres utilisés dans ce modèle ont une signification physique, ce qui est essentiel pour comprendre les procédés de diffusion. Ainsi, nous avons confirmé que le paramètre $k\beta^2$ décrit la fréquence de saut de la molécule diffusante. Ce paramètre dépend principalement de la taille du soluté, i.e., de son rayon hydrodynamique, et de la température. Nous avons également constaté que ce paramètre est influencé par la capacité de la matrice polymère à former des liaisons hydrogène. Le paramètre v relate la qualité du solvant. C'est une constante pour un système solvant-polymère donné. Nous avons établie cette valeur pour un système PVA-eau et pour trois autres systèmes polymère-eau sur la base de données obtenues pour le HPMC, PNNDEA et

PNIPA. L'application du modèle a été satisfaisante quelle que soit la taille et la géométrie du soluté étudiée dans les solutions et gels de polymères. Par conséquent, ce modèle permet de faire le lien entre la diffusion de molécules de petites tailles et de grandes tailles comme les macromolécules, ce que peu de modèles de diffusion permettent de faire. Ce modèle tient compte non seulement de la taille des molécules diffusantes, mais aussi de la concentration en polymère, de la température et des interactions soluté-polymère. Cependant, il semble que ce modèle ne puisse pas décrire correctement la diffusion de molécules de très haute masse molaire dans des solutions concentrées ou des gels de polymères d'après les données de diffusion tirées de la littérature.

Les modèles de diffusion de Phillies et de Amsden reproduisent de façon satisfaisante les données expérimentales pour toutes les études que nous avons effectuées. Cependant, suite à l'analyse des résultats, nous n'avons pas été en mesure de confirmer la signification physique des paramètres utilisés dans ces modèles. Toutefois, dans le cas du modèle de Phillies nous avons montré que le paramètre v reflète la qualité du solvant. Des études complémentaires sont nécessaires pour identifier la signification de ces paramètres.

Nous avons constaté que les modèles de diffusion décrits par Mackie-Meares, Ogston *et al.* et Yasuda *et al.* ne donnent pas de résultats satisfaisants. Le modèle de diffusion de Mackie-Meares ne reproduit pas les données expérimentales car il ne tient pas compte des propriétés physiques du diffusant. Ceux de Ogston *et al.* et Yasuda *et al.* produisent de meilleurs résultats sans toutefois donner une bonne corrélation avec les données expérimentales car ils ont été établis à partir d'hypothèses qui limitent leur domaine d'application.

8.6. Travaux futurs

Il serait très intéressant de continuer ce travail en étudiant la diffusion de molécules sphériques et rigides tels que les dendrimères. En effet, de telles molécules doivent diffuser dans des solutions et gels de polymères selon des procédés différents des oligo- et poly(éthylènes glycol)s qui sont des molécules très flexibles. En sélectionnant des

dendrimères de différentes grandeurs, on pourrait étudier la diffusion de molécules dont la taille est similaire et supérieure à la longueur de corrélation du réseau. Cela permettrait de mieux comprendre l'influence des chaînes du réseau polymère sur la diffusion. Dans le même ordre d'idée, il serait intéressant d'étudier la diffusion de molécules linéaires de hautes masses molaires dans des réseaux de polymères de hautes masses molaires afin de mieux caractériser le modèle de Petit *et al.*

Au niveau des polymères il pourrait être intéressant de faire des mesures de diffusion dans des gels réticulés chimiquement. La dynamique de tels systèmes est différente des solutions et gels de polymères reporté dans cette étude. Le coefficient d'auto-diffusion dans de tels systèmes ne peut pas être reliée à la concentration en polymère, mais est fonction du taux de gonflement du polymère. Par conséquent, une telle étude permettrait de savoir si le taux de gonflement est le principal paramètre qui permet de décrire la diffusion. De plus, un tel système peut être utilisé pour évaluer la pertinence du modèle de Petit *et al.* dans de telles circonstances.

Finalement, il est serait intéressant de faire des études de diffusion à partir de matrices de polymère à l'état sec (sous forme de tablettes) et renfermant un soluté, par imagerie RMN, afin de se rapprocher des systèmes exploités en pharmacie. De telles conditions impliquent deux phénomènes, à savoir le gonflement de la matrice polymère et la diffusion du soluté. Dans le cas particulier des polymères biodégradables, le phénomène d'érosion s'ajoutera aux deux phénomènes déjà mentionnés.

Partie VII

Annexe

Annexe A: Résultats expérimentaux

Figure 1.8.

1/(1-φ)	ln D/D ₀				
	tBuOH	MeOH	⁺ N(CH ₃) ₄	PEG-400	PEG-4000
1	0	0	0	0	0
1.022	-0.061	-0.056	-0.055	-0.095	-0.200
1.043	-0.108	-	-	-	-
1.046	-	-0.100	-0.103	-0.210	-0.349
1.071	-0.169	-	-	-0.284	-0.458
1.094	-	-0.164	-	-	-
1.097	-0.211	-	-0.194	-0.382	-
1.123	-	-	-	-0.444	-0.644
1.150	-0.319	-	-	-0.481	-
1.154	-	-0.221	-0.296	-	-0.678
1.214	-	-0.314	-	-0.645	-
1.215	-0.421	-	-	-	-
1.218	-	-	-0.389	-	-0.837
1.257	-0.510	-	-	-	-
1.278	-	-0.391	-	-	-
1.290	-	-	-0.471	-	-

Figure 1.12A.

[PVME] (g/mL)	$D_{PS} \times 10^{-7}$ (cm ² /s)			
	(a)	(b)	(c)	(d)
0.001	1.318	1.949	3.236	5.888
0.0014	1.288	1.949	3.090	5.754
0.002	1.230	1.819	3.020	5.495
0.003	1.148	1.698	2.818	5.248
0.004	1.071	1.584	2.454	5.011
0.006	0.933	1.412	2.344	4.365
0.008	0.831	1.259	2.138	4.265
0.01	0.741	1.148	1.949	3.890
0.014	0.588	0.933	1.621	3.388
0.02	0.467	0.776	1.380	2.951
0.03	0.331	0.537	1.000	2.344
0.04	0.229	0.407	0.758	2.041
0.06	0.126	0.234	0.478	1.412
0.08	0.074	0.141	0.302	1.047
0.1	0.045	0.085	0.204	0.794
0.11	0.035	0.068	0.173	0.692
0.13	0.022	0.045	0.117	0.537
0.17	0.010	0.020	0.060	0.316
0.20	0.006	0.013	0.038	0.224
0.25	0.002	0.005	0.017	0.117
0.30	0.001	0.002	0.095	0.072

(a) $M_{PS} = 1.05 \times 10^6$

(b) $M_{PS} = 4.22 \times 10^5$

(c) $M_{PS} = 1.79 \times 10^5$

(d) $M_{PS} = 6.5 \times 10^4$

Figure 1.12B.

[PVME] (g/mL)	$D_{PS} \times 10^{-7}$ (cm ² /s)			
	(a)	(b)	(c)	(d)
0.001	1.148	1.412	2.344	6.761
0.0014	1.096	1.380	2.238	6.025
0.002	1.000	1.259	2.089	6.025
0.003	0.851	1.096	1.819	5.623
0.004	0.741	0.955	1.621	5.370
0.006	0.562	0.724	1.318	5.012
0.008	0.436	0.562	1.096	4.571
0.01	0.346	0.467	0.933	4.365
0.014	0.229	0.309	0.708	3.890
0.02	0.138	0.199	0.501	3.388
0.03	0.063	0.102	0.295	2.691
0.04	0.032	0.057	0.190	2.238
0.06	0.013	0.025	0.120	2.042
0.08	0.005	0.011	0.066	1.659
0.1	0.002	0.005	0.037	1.259

(a) $M_{PS} = 1.69 \times 10^6$

(b) $M_{PS} = 4.11 \times 10^6$

(c) $M_{PS} = 4.67 \times 10^5$

(d) $M_{PS} = 5.5 \times 10^4$

Figure 2.3B.

$\delta^2(\Delta-\delta/3)$ (10^{-5} s^3)	ln A		
	H ₂ O	PEG-600	PVA
0.014	0	0	0
0.087	-0.81	-0.003	-0.02
0.12	-2.44	-0.21	-0.02
0.22	-	-0.43	-0.04
0.34	-	-0.63	-0.06
0.49	-	-0.96	-0.12
0.67	-	-1.25	-0.14
0.89	-	-1.60	-0.17
1.11	-	-1.98	-0.19
1.36	-	-2.44	-0.21
1.65	-	-2.94	-0.26

Figure 2.6.

$(\gamma G \delta)^2(\Delta-\delta/3)$ (10^9 s/m^2)	ln A
0.11	0
0.27	-0.10
0.51	-0.22
0.83	-0.37
1.22	-0.57
1.69	-0.78
2.24	-1.03
2.86	-1.29
3.56	-1.55
4.34	-1.78
5.20	-1.98
6.12	-2.14
7.12	-2.28
8.20	-2.51
9.36	-2.71
10.59	-2.88

Figure 3.1B.

$\delta^2(\Delta\delta/3)$ (10^{-5} s^3)	ln A		
	H ₂ O	PEG-2000	PVA
0.014	0	0	0
0.087	-0.87	-0.005	-0.023
0.22	-2.51	-0.16	-0.046
0.58	-	-0.46	-0.071
0.88	-	-0.71	-0.095
1.11	-	-0.87	-0.15
1.36	-	-1.07	-0.20
1.65	-	-1.27	-0.23
1.95	-	-1.46	-0.26
2.30	-	-1.72	-0.32
2.65	-	-1.98	-0.38

Figure 3.2A.

[PVA] (g/mL)	D ($10^{-10} \text{ m}^2/\text{s}$)					
	EG	(EG) ₃	(EG) ₄	PEG-200	(EG) ₅	(EG) ₆
0	9.37	5.96	5.39	4.84	4.58	4.08
0.03	8.45	-	3.97	3.69	3.60	-
0.06	6.47	3.11	2.98	2.98	2.84	2.54
0.09	-	-	2.46	2.39	2.37	-
0.12	4.07	2.08	1.95	2.00	1.97	1.77
0.16	-	1.67	1.53	1.54	1.58	1.47
0.20	2.55	1.21	1.26	1.30	1.28	1.22
0.26	-	-	1.05	1.01	0.97	-
0.32	1.42	0.70	0.76	0.73	0.84	0.66
0.38	-	0.61	0.58	0.58	0.64	0.51

Figure 3.2B.

[PVA] (g/mL)	D (10^{-10} m ² /s)					
	PEG-400	PEG-600	PEG-1000	PEG-1500	PEG-2000	PEG-4000
0	3.31	1.87	1.66	1.13	1.10	0.98
0.0284	2.66	–	–	–	–	0.60
0.03	–	1.47	1.14	0.81	0.67	–
0.0583	2.04	–	–	–	–	0.43
0.06	–	1.22	0.92	0.67	0.54	–
0.0898	–	–	–	–	–	–
0.09	–	0.99	0.73	0.54	0.43	–
0.12	–	0.79	0.65	0.42	0.34	–
0.123	1.38	–	–	–	–	–
0.1567	1.19	–	–	–	–	0.22
0.16	–	0.69	0.50	0.35	0.28	–
0.1908	1.09	–	–	–	–	–
0.1954	–	–	–	–	–	0.20
0.20	–	0.58	0.44	0.26	0.21	–
0.26	–	0.45	0.35	0.25	0.17	–
0.2716	0.75	–	–	–	–	–
0.2767	–	–	–	–	–	0.14
0.32	–	0.34	0.27	0.21	0.14	–
0.38	–	0.30	0.25	0.16	0.12	–

Figure 3.3.

[PVA] (g/mL)	D (10^{-10} m ² /s)			
	23 °C	33 °C	43 °C	53 °C
0	1.87	3.41	4.60	6.09
0.03	1.47	2.79	4.14	4.79
0.06	1.22	2.22	2.92	3.81
0.09	0.99	1.85	2.45	3.26
0.12	0.79	1.54	2.13	2.73
0.16	0.69	1.26	–	2.26
0.20	0.58	1.05	1.69	1.95
0.26	0.45	0.85	1.17	1.56
0.32	0.34	0.69	1.14	1.27
0.38	0.30	0.63	–	1.08

Figure 3.4.

Sample	R_H (Å)	$k\beta^2$	ν
EG	2.43	0.28	0.76
(EG) ₃	3.91	0.23	0.60
(EG) ₄	4.32	0.24	0.59
(EG) ₅	5.08	0.25	0.60
(EG) ₆	5.70	0.21	0.63
PEG-200	4.81	0.24	0.60
PEG-400	7.00	0.23	0.56
PEG-600	12.48	0.12	0.58
PEG-1000	13.99	0.12	0.49
PEG-1500	20.59	0.068	0.54
PEG-2000	22.69	0.053	0.53
PEG-4000	24.35	0.047	0.50

Figure 3.5.

$1/T$ (10^{-3} K^{-1})	$\log k\beta^2$			
	<i>t</i> BuOH	EG	PEG-600	PEG-2000
3.38	-10.01	-10.54	-10.91	-11.27
3.27	-9.90	-10.36	-10.54	-10.87
3.16	-9.81	-10.25	-10.45	-10.80
3.07	-9.65	-10.03	-10.32	-10.64

Figure 4.1.

φ	D/D_0		
	PEG-200	PEG-2000	PEG-10000 ^(a)
0	1	1	1
0.026	0.78	0.61	0.57
0.051	0.62	0.49	0.34
0.075	0.52	0.39	0.24
0.097	0.43	0.31	0.16

0.126	0.34	0.25	0.11
0.153	0.28	0.19	0.09
0.190	0.21	0.15	–
0.224	0.18	0.13	–
0.255	0.14	0.11	–

(a) données pour la Figure 4.8.

Figure 4.2.

$\varphi/(1-\varphi)$	$\ln D/D_0$			
	PEG-400	PEG-1000	PEG-2000	PEG-10000
1	0	0	0	0
1.025	-0.218	–	–	–
1.027	–	-0.375	-0.498	-0.561
1.052	-0.484	–	–	–
1.054	–	-0.590	-0.716	-1.071
1.081	-0.654	-0.821	-0.941	-1.426
1.108	–	-0.937	-1.176	-1.813
1.111	-0.875	–	–	–
1.141	-1.023	–	–	–
1.144	–	-1.199	-1.370	-2.196
1.172	-1.115	–	–	–
1.180	–	-1.328	-1.658	-2.373
1.235	–	-1.556	-1.869	–
1.245	-1.480	–	–	–
1.289	–	-1.812	-2.064	–
1.343	–	-1.893	-2.218	–

Figure 4.3A.

[PVA] (g/mL)	D (10^{-10} m ² /s) pour PEG							
	200	400	600	1000	1500	2000	4000	10000
0	4.59	3.31	1.87	1.66	1.13	1.10	0.96	0.45
0.0284	–	2.66	–	–	–	–	0.60	–
0.03	3.60	–	1.44	1.14	0.81	0.67	–	0.26
0.0583	–	2.04	–	–	–	–	0.43	–
0.06	2.84	–	1.22	0.92	0.67	0.54	–	0.16
0.0898	–	1.72	–	–	–	–	0.33	–
0.09	2.37	–	0.99	0.73	0.54	0.43	–	0.11
0.12	1.97	–	0.79	0.65	0.42	0.34	–	0.07
0.123	–	1.38	–	–	–	–	–	–
0.1567	–	1.19	–	–	–	–	0.22	–
0.16	1.58	–	0.66	0.50	0.35	0.28	–	0.05
0.1908	–	1.19	–	–	–	–	–	–
0.1954	–	–	–	–	–	–	0.20	–
0.20	1.28	–	0.58	0.44	0.27	0.21	–	0.04
0.26	0.97	–	0.45	0.35	0.25	0.17	–	–
0.2716	–	0.75	–	–	–	–	–	–
0.2767	–	–	–	–	–	–	0.14	–
0.32	0.84	–	0.34	0.27	0.21	0.14	–	–
0.38	0.64	–	0.30	0.25	0.16	0.12	–	–

Figure 4.3.B. (voir Figure 3.3.)

Figure 4.4.

M_w (g/mol)	R_h (Å)
150	3.91
194	4.32
200	4.81
238	5.08
282	5.7
400	7.00
600	12.48
1000	13.99
1500	20.59
2000	22.69
4000	24.35
10000	50.62

Figure 4.5.

R_h (Å)	α	ν
3.91	4.72	0.70
4.32	4.78	0.74
4.81	4.81	0.80
5.08	4.47	0.79
5.7	4.45	0.80
7.00	4.32	0.79
12.48	4.16	0.78
13.99	3.64	0.64
20.59	4.10	0.70
22.69	4.33	0.66

24.35	4.42	0.61
50.62	10.95	0.84

Figure 4.6(A, B et C).

$T \times 10^3$ (K ⁻¹)	α (A)			ν (B)			$\log D_0$ (C)		
	(a)	(b)	(c)	(a)	(b)	(c)	(a)	(b)	(c)
3.38	3.02	4.17	4.33	0.86	0.79	0.66	-9.15	-9.73	-9.99
3.27	3.17	4.07	4.81	0.92	0.79	0.70	-9.08	-9.47	-9.68
3.16	3.20	3.94	4.13	0.91	0.79	0.68	-8.97	-9.34	-9.59
3.07	3.09	3.72	4.21	0.93	0.74	0.68	-8.85	-9.21	-9.54

(a) tBuOH

(b) PEG-600

(c) PEG-2000

Figure 4.7(A et B).

M_w (g/mol)	$\log D$	[PVA] (g/mL)	puissance de M
400	-9.92	0	-0.62
600	-10.18	0.03	-0.64
1000	-10.30	0.06	-0.68
1500	-10.46	0.09	-0.74
2000	-10.55	0.12	-0.78
4000	-10.66	0.16	-0.89
10000	-11.30	0.20	-0.89
-	-	0.26	-0.89
-	-	0.32	-0.74
-	-	0.38	-0.71
-	-	0.38	-0.78

Figure 4.8. (voir Figure 4.1.)

Figure 5.2.

φ	$D (10^{-10} \text{ m}^2/\text{s})$			
	EG-Me	EG-Me ₂	EG-tBuMe	18-crown-6
0	7.88	7.56	5.58	4.37
0.026	7.05	6.78	4.63	3.62
0.052	6.37	5.88	4.12	2.99
0.075	5.76	5.39	3.68	2.47
0.098	5.11	4.82	3.35	2.05
0.126	4.53	4.26	3.08	1.78
0.153	4.06	3.80	2.37	1.60
0.190	3.29	3.37	1.98	1.31
0.224	2.93	2.86	1.56	0.97
0.253	2.47	2.33	1.31	0.72

Figure 5.3 (A et B)

$\varphi/(1-\varphi)$	$D (10^{-10} \text{ m}^2/\text{s})$			R_h (Å)	B_s/f_w
	EG-Me	DEG-tBuMe	MPPE		
0	-9.10	-9.32	-9.36	2.79	1.80
0.027	-9.15	-9.38	-9.43	3.07	1.60
0.054	-9.19	-9.45	-9.54	3.24	1.73
0.082	-9.24	-9.48	-9.60	4.38	2.00
0.108	-9.29	-9.56	-9.65	3.83	1.71
0.144	-9.34	-9.59	-9.71	4.18	1.95
0.181	-9.39	-9.69	-9.79	5.45	2.81
0.235	-9.48	-9.80	-9.89	5.05	2.01
0.289	-9.53	-9.86	-9.99	4.65	1.94

0.343	-9.61	-9.95	4.75	1.92
			5.54	3.04
			5.55	3.03

Figure 5.4A.

[PVA] (g/mL)	D (10^{-10} m ² /s)			
	EG	EG-Me	EG-Me ₂	EG-tBuMe
0	8.58	7.88	7.56	5.58
0.03	7.70	7.05	6.78	4.63
0.06	6.66	6.37	5.88	4.12
0.09	6.08	5.76	5.39	3.68
0.12	5.58	5.11	4.82	3.35
0.16	4.80	4.53	4.26	3.08
0.20	3.97	4.06	3.80	2.37
0.26	3.30	3.29	3.37	1.98
0.32	2.75	2.93	2.86	1.56
0.38	2.25	2.47	2.33	1.31

Figure 5.4B.

[PVA] (g/mL)	D (10^{-10} m ² /s)			
	DEG- Me	DEG-Et	DEG-tBuMe	DEG-He
0	6.46	5.77	4.80	4.43
0.03	5.41	5.07	4.14	3.77
0.06	4.90	4.48	3.57	3.12
0.09	4.48	4.13	3.27	2.63
0.12	4.13	3.59	2.76	2.37
0.16	3.53	3.02	2.54	2.01
0.20	2.96	2.54	2.02	1.62

0.26	2.61	2.33	1.59	1.36
0.32	2.16	1.80	1.39	1.05
0.38	1.71	1.57	1.11	0.94

Figure 5.4C.

[PVA] (g/mL)	D (10^{-10} m ² /s)			
	TEG- Me	TEG-Me ₂	18-crown-6	MPPE
0	5.23	5.14	4.37	4.39
0.03	4.55	4.40	3.62	3.70
0.06	4.01	3.94	2.99	2.91
0.09	3.41	3.34	2.47	2.53
0.12	3.12	3.08	2.05	2.21
0.16	2.72	2.69	1.78	1.93
0.20	2.31	2.26	1.60	1.61
0.26	1.98	1.94	1.31	1.28
0.32	1.64	1.61	0.97	1.02
0.38	1.39	1.32	0.72	—

Figure 5.5 (A et B).

R_h (Å)	α (Å)	ν (B)
2.79	3.40	0.95
3.07	2.83	0.90
3.24	2.60	0.83
4.38	3.32	0.88
3.83	2.94	0.86
4.18	3.22	0.90

5.45	3.53	0.89
5.05	3.67	0.83
4.65	3.06	0.84
4.75	3.06	0.84
5.54	3.84	0.80
5.55	3.69	0.80

Figure 5.6 (A, B et C). voir Figure 5.4 (A, B et C)

Figure 5.7 (A et B).

R_h (Å)	M_w (g/mol)	$\log k\beta^2$
2.79	62	-9.93
3.07	76	-9.91
3.24	90	-9.93
4.38	132	-10.17
3.83	120	-10.05
4.18	134	-10.12
5.45	190	-10.39
5.05	176	-10.26
4.65	164	-10.19
4.75	178	-10.20
5.54	264	-10.45
5.55	195	-10.42

Figure 5.8. voir Figure 5.1.

Figure 6.2.

$\phi/(1-\phi)$	$\ln D$	
	H ₂ O	PEG-600
0	-20.17	-22.08
0.027	-20.32	-22.33
0.054	-20.38	-22.52
0.081	-20.46	-22.68
0.108	-20.53	-22.88
0.144	-20.63	-23.08
0.181	-20.73	-23.19
0.235	–	-23.50
0.289	-20.90	-23.64
0.343	-21.12	-23.89

Figure 6.3A.

[PVA] (g/mL)	$D_{\text{HDO}} (10^{-9} \text{ m}^2/\text{s})$		
	PVA-1	PVA-2	PVA-6
0	1.73	1.73	1.73
0.03	1.59	1.50	1.48
0.06	1.47	1.41	1.39
0.09	1.37	1.30	1.27
0.12	1.29	1.21	1.19
0.16	1.17	1.10	1.07
0.20	1.05	0.99	0.96
0.26	0.94	–	0.86
0.32	0.81	0.76	–
0.38	0.74	0.67	–

Figure 6.3B.

[PVA] (g/mL)	$D_{\text{PEG-600}} (10^{-10} \text{ m}^2/\text{s})$					
	PVA-1	PVA-2	PVA-3	PVA-4	PVA-5	PVA-6
0	2.56	2.56	2.56	2.56	2.56	2.56
0.03	2.05	2.01	2.01	1.98	1.98	1.98
0.06	1.72	1.65	–	1.63	1.65	1.65
0.09	1.46	1.41	1.42	1.33	1.40	1.39
0.12	1.26	1.15	1.15	–	1.17	1.17
0.16	1.08	0.95	0.96	0.99	0.98	0.99
0.20	0.87	0.84	0.79	0.80	0.81	0.79
0.26	0.71	0.62	0.60	0.63	0.65	0.64
0.32	0.61	0.54	0.51	0.50	0.53	0.53
0.38	0.52	0.42	0.40	0.41	0.44	0.43

Figure 6.4 (A et B). voir Figure 6.3A. et 6.3B.**Figure 6.5 (A et B).**

[HPMC] (g/mL)	$D_{\text{HDO}} (10^{-9} \text{ m}^2/\text{s})$ (A)		$D_{\text{PEG-600}} (10^{-10} \text{ m}^2/\text{s})$ (B)	
	HPMC-1	HPMC-2	HPMC-1	HPMC-2
0	1.73	1.73	2.56	2.56
0.03	1.53	1.46	1.89	1.87
0.06	1.41	1.33	1.53	1.50
0.09	1.33	1.25	1.31	1.23
0.12	1.24	1.13	1.11	1.04
0.16	1.14	1.06	0.92	0.89
0.20	1.07	0.93	0.77	0.74

0.26	0.95	0.82	0.60	0.56
0.32	0.83	–	0.48	–
0.38	0.77	–	0.41	–

Figure 6.6 (A et B).

[polymère] (g/mL)	$D_{\text{HDO}} (10^{-9} \text{ m}^2/\text{s})$ (A)		$D_{\text{PEG-600}} (10^{-10} \text{ m}^2/\text{s})$ (B)	
	PNNDEA	PNIPA	PNNDEA	PNIPA
0	1.73	1.73	2.56	2.56
0.03	1.61	1.54	2.17	2.12
0.06	1.49	1.41	1.84	1.79
0.09	1.40	1.26	1.63	1.51
0.12	1.34	1.17	1.41	1.31
0.16	1.19	1.06	1.18	1.05
0.20	1.07	0.96	0.99	0.89
0.26	0.96	0.86	0.79	0.67
0.32	0.88	0.76	0.63	0.52
0.38	0.79	–	0.52	–

Figure 7.2.

[PVA] (g/mL)	Fraction d'éthylène glycol	
	libre	lié
0	1	0
0.03	0.91	0.09
0.09	0.72	0.28
0.16	0.66	0.33
0.38	0.54	0.46

Figure 7.3B.

$(\gamma G \delta)^2 (\Delta - \delta/3)$ (10^9 s/m ²)	Ln A		
	H ₂ O	EG libre	EG lié
0.09	0	0	0
0.24	-0.24	-0.10	-0.06
0.46	-0.54	-0.24	-0.14
0.75	-0.94	-0.42	-0.21
1.10	-1.42	-0.60	-0.31
1.52	-1.99	-0.92	-0.41
2.02	-2.63	-1.23	-0.52
2.58	-3.35	-1.59	-0.64
3.21	-	-1.98	-0.77
3.91	-	-2.41	-0.88
4.67	-	-2.85	-1.02
5.51	-	-3.32	-1.14
6.41	-	-3.77	-1.28
7.39	-	-4.18	-1.42
8.42	-	-4.54	-1.57
9.54	-	-	-1.72

Figure 7.4.

[PVA] (g/mL)	D (10^{-10} m ² /s)	
	EG libre	EG lié
0	8.58	-
0.03	7.70	2.37
0.06	6.66	1.86
0.09	6.08	1.54
0.12	5.58	1.27
0.16	4.80	1.14
0.20	3.97	0.89
0.26	3.30	0.70
0.32	2.75	0.52
0.38	2.25	0.41

Figure 7.5.

$(\gamma G \delta)^2 (\Delta - \delta/3)$ (10^9 s/m ²)	Ln A		Ln A	
	EG		EG libre	EG lié
0.10	0	0.13	0	0
0.27	-0.10	0.33	-0.12	-0.04
0.51	-0.22	0.63	-0.26	-0.11
0.82	-0.37	1.02	-0.45	-0.19
1.21	-0.57	1.50	-0.68	-0.30
1.67	-0.79	2.07	-0.97	-0.39
2.21	-1.03	2.74	-1.33	-0.520
2.83	-1.29	3.50	-1.69	-0.61
3.52	-1.55	4.36	-2.10	-0.72
4.28	-1.78	5.31	-2.56	-0.84
5.12	-1.98	6.35	-2.91	-0.95
6.04	-2.14	7.48	-3.23	-1.10
7.03	-2.29	8.71	-	-1.24
8.10	-2.51	10.03	-	-1.37
9.24	-2.71	11.44	-	-1.51
10.04	-2.88	12.95	-	-1.67

Figure 7.6.

[PVA] (g/mL)	T_1 (s)		T_2 (s)	
	EG libre	EG lié	EG libre	EG lié
0	4.93	-	1.58	-
0.03	4.86	0.19	1.76	0.34
0.09	3.70	0.70	1.58	0.27
0.16	2.65	0.66	0.97	0.28
0.26	2.38	0.67	0.88	0.21
0.38	2.11	0.44	0.50	0.19

Annexe B. Autres articles publiés ou en préparation

Deux articles concernant ces travaux, mais non inclus dans la thèse, ont été publiés

Self-diffusion of Molecular Probes in Polymer Gels:

The Test of a New Physical Model of Diffusion

Zhu, X.X.; Masaro, L.; Macdonald, P.M.

Polymer Preprints **1997**, *38* (2), 594-595.

Self-diffusion of Solvents and Solute Probes in Polymer Solutions and Gels:

The Use of a New Physical Model of Diffusion

Zhu, X.X.; Masaro, L.; Petit J.-M.; Roux B.; Macdonald, P.M.

Material for Controlled Release Applications

McCulloch, I., Shalaby, S.W. Eds., ACS Publ.; Washington, D.C.; 1998, Chap. 18, p

Deux articles sont en préparation, un sur la caractérisation des polymères (PVA, HPMC, PNNDEA et PNIPA):

(titre non disponible)

Ousalem, M.; Baille, W.E.; Masaro, L.; Zhu, X.X.

L'autre sur l'association entre les oligo(éthylène glycol)s et le PVA:

(titre non disponible)

Masaro, L.; Zhu, X.X.